

# **REMOVAL OF HEAVY METALS FROM BIOWASTE**

Modelling of heavy metal behaviour and development of removal technologies

**Adrie Veeken**

Promotor:

dr. ir. W.H. Rulkens  
hoogleraar in de milieutechnologie

A.H.M. Veeken

NNOB201,2449

**Removal of heavy metals from biowaste Modelling of heavy metal  
behaviour and development of removal technologies**

**Proefschrift**

ter verkrijging van de graad van doctor  
op gezag van de rector magnificus  
van de Landbouwniversiteit Wageningen,  
dr. C.M. Karssen,  
in het openbaar te verdedigen  
op dinsdag 9 juni 1998  
des namiddags te vier uur in de Aula.

ISBN 954740

CIP-DATA KONINKLIJKE BIBLIOTHEEK, DEN HAAG

Veeken, A.H.M.

Removal of heavy metals from biowaste - Modelling of heavy metal behaviour and development of removal technologies / A.H.M. Veeken [S.I. : s.n.]

Thesis Wageningen Agricultural University, Wageningen, The Netherlands

- With ref. - With summary

ISBN 90-5485-884-2

Subject headings: biowaste recycling/heavy metals/removal technologies/modelling

BIBLIOTHEEK  
LANDBOUWUNIVERSITEIT  
WAGENINGEN

## Abstract

Veeken A.H.M. 1998. **Removal of heavy metals from biowaste - Modelling of heavy metal behaviour and development of removal technologies.** Doctoral Thesis, Wageningen Agricultural University, Wageningen, The Netherlands, 232 pages.

In the Netherlands, recycling of solid organic waste streams as compost only becomes possible if the compost complies with the heavy metals standards of the BOOM decree. This dissertation focuses on the removal of heavy metals from biowaste, i.e. the source separated organic fraction of municipal solid waste. Biowaste is referred to as an organic waste stream but surprisingly it was found that a large part of biowaste is composed of inorganic material, i.e. sand, silt and clay minerals. The inorganic part of biowaste originates from the collection of garden waste. Comparison of the natural background content of heavy metals in the original constituents of biowaste with the heavy metal content of biowaste showed that biowaste is not contaminated with heavy metals. Based on these results it can be stated that there is a conflict between two government policies of (1) preventing the accumulation of heavy metals in the soil (BOOM decree) and (2) promoting the recycling and reuse of organic waste streams (National Environmental Policy Plan). It is recommended that the different legislations concerning the dosage of various organic and artificial fertilisers have to be combined in a single legislative framework.

An analytical fractionation scheme was presented to determine the physico-chemical distribution of heavy metals in biowaste. The fractionation scheme was used to assess the application of physical separation and chemical extraction to reduce the heavy metal content of biowaste. On the basis of the results of the physical distribution of heavy metals in biowaste, a physical separation process was designed to valorise biowaste. A pilot plant study showed that physical separation of the biowaste is possible by a combination of physical wet separation units operated under wet conditions. The process results in (1) an organic fraction which can be converted to clean-compost, (2) a sand fraction which can be re-used in road and building construction and (3) a fraction high in humus and lutum which would make an excellent soil improver but which cannot be re-used because the heavy metal levels are too high. From a discussion of the advantages and disadvantages of the chemical extraction by inorganic acids and complexing agents it was concluded that these extracting reagents are not applicable on a practical scale due to the costs of the process and the negative environmental impacts of the discharged solid and liquid waste streams. Citric acid was proposed as an alternative extracting reagent which does not have these drawbacks.

Mechanistic models were developed in order to gain more insight into factors controlling the extraction efficiency and rate of extraction of heavy metals from biowaste. Chemical equilibrium modelling was used to calculate the speciation of heavy metals in biowaste. The NICA-Donnan model taking into account the complex binding characteristics of organic matter, i.e. polyfunctional and polyelectrolytic behaviour was applied to interpret the proton and Cu(II) binding to particle-sized organic particles of biowaste. The results indicate that the humic acid content of biowaste regulates the speciation of heavy metals in biowaste. Moreover, a mechanistic model was developed which describes the course of the acid extraction of heavy metals from solid organic particles of biowaste. The extent of the proton-metal exchange is determined by the competition between the heavy metal ion and the proton for the reactive sites of the organic particles. Diffusion of the ions in the film layer and inside the particles was described by the Nernst-Planck equations. This model is able to give a qualitative interpretation of the acid extraction of Cu(II) from the isolated particle-sized organic fractions in biowaste and the model can also explain the anomalies observed during the acid extraction of Cd, Cu and Zn from sewage sludge.

## Stellingen

- 1 Het NICA-Donnan model geeft aan dat het elektrostatische effect op de proton- en koperadsorptie aan humuszuren sterk verschilt. Het door Bartschat et al. ontwikkelde oligo-electrolytische model kan dit verschil alleen verklaren door de onwaarschijnlijke aanname te maken dat de humuszuurverbindingen zijn opgebouwd uit twee groepen met verschillende molecuulgrootte. Dit wijst er op dat humuszuren als een penetreerbare gelfase moeten worden gezien en niet als ondoordringbare bollen.

Dit proefschrift

**Bartschat B. M. et al.** 1992. Oligoelectrolyte Model for Cation Binding by Humic Substances. Environ. Sci. Technol. 26:284-294

- 2 Citroenzuurextractie is een veelbelovend extractiemiddel om zware metalen te verwijderen uit vaste organische afvalstromen en bodems.

Dit proefschrift

- 3 De mobiliteit van koper in stortplaatsen en in bodems, rijk aan organische stof, wordt bevorderd door het oplossen van de organische stof uit de vaste fase.

Dit proefschrift.

- 4 De sequentiële chemische extractie procedure kan niet de beoogde selectiviteit waarmaken die in de literatuur vaak aan deze procedure wordt toegeschreven.

Dit proefschrift

- 5 Voor de toediening van dierlijke mest aan de bodem als meststof moet net als voor het gebruik van compost uit GFT-afval een norm voor zware metalen worden opgelegd.

Dit proefschrift

- 6 In de beschrijving van de extractiekinetiek van zware metalen uit vaste deeltjes mag de diffusie van metaalionen niet worden berekend met de wet van Fick maar moet de Nernst-Planck vergelijking worden gehanteerd.

Dit proefschrift

- 7 Wershaw's membraan-micel concept, waarbij humuszuurverbindingen worden voorgesteld als agglomeraten van amfifiele moleculen, lijkt een beter beeld te geven van de conformatie van humuszuurverbindingen dan het concept van Stevenson, waarbij humuszuurverbindingen worden beschouwd als een mengsel van gecrosslinkte polymeren van verschillende molecuulgrootte.

Dit proefschrift

**Wershaw, R.L.** 1989. Application of a Membrane Model to the Sorptive Interactions of Humic Substances. *Environmental Health Perspectives* 83:191-203

**Stevenson, F. J.** 1994. *Humic Chemistry: Genesis, Composition, Reactions*. New York, John Wiley & Sons

- 8 Waarom zouden we nog werken?

In 1997 meer inkomen uit beursbeleggingen dan uit arbeid - *Volkskrant*, 12 januari 1998

- 9 De plaats van de universiteit binnen onze maatschappij kan op de lange termijn alleen verdiend worden met het geven van goed onderwijs en het verrichten van minder marktgericht wetenschappelijk onderzoek.

Wetenschap erodeert aan de oevers van de derde geldstroom - *Volkskrant*, 16 juli 1997

Ik ben 40 jaar nutteloos werkzaam geweest - *Chemisch Weekblad* 11, 15 maart 1997

- 10 De rappe toename in geheugencapaciteit en snelheid van de computer heeft er echter toe geleid dat het menselijke brein 'out of memory' is geraakt.

- 11 Door toepassing van het idee van hergebruik van bodems en sedimenten waarin de verontreinigingen geïmmobiliseerd zijn, kunnen verschillende nijpende maatschappelijke problemen in één klap worden opgelost. Allereerst kunnen de dijken zover opgehoogd worden dat Nederland zich geen zorgen hoeft te maken over de stijging van de zeespiegel in de komende eeuwen. Daarnaast kan Nederland worden uitgebouwd tot één grote snelweg.

- 12 Is een duurzaam produkt duurzaam?

*Stellingen behorende bij het proefschrift 'Removal of heavy metals from biowaste - Modelling of heavy metal behaviour and development of removal technologies'.*

*Adrie Veeken, 9 juni 1998*

## Voorwoord

De laatste Pb-tjes wegen het zwaarst maar wat als daar nog andere zware metalen zoals Cd, Cu en Zn moeten worden meegetorst. Komt er dan nooit eens een eind aan! Waarom al dat afzien om een S-je van je titel af te krijgen? Ondanks al deze gedachten toch maar doorgezet en vrije weekeinden en avonden opgeofferd om dit boekje af te krijgen. Uiteindelijk ligt het boekje er en daar ben ik best wel trots op! Vooral voor mijn vrienden en familieleden zal het een opluchting zijn omdat ze nooit meer die ene beladen vraag hoeven te stellen "hoe gaat het met het boekje?" en dan maar afwachten hoe Adrie zou reageren. Het voorwoord houdt meestal een dankwoord in dus wordt het maar eens tijd het hele rijtje af te gaan.

Allereerst dank ik Wim Rulkens dat hij de taak van promotor op zich wilde nemen. Natuurlijk had ook dit boekje niet geschreven kunnen worden zonder het werk dat vele studenten in het kader van afstudeervak of stage verricht hebben. Op deze plaats bedank ik jullie hiervoor allemaal hartelijk en ik hoop dat de meesten van jullie dit boekje op een of andere manier, vroeg of laat, in handen krijgen. In willekeurige volgorde: Ron Gerards, Marie-Ellen van Schendel, Paul Theeuwen, Erik-Jan Boots, Roger Schmid, Jack Braspenning, Coert Dijkhuizen, Servaes van der Meulen, Adrienne van der Padt, Rene Voorburg, Mark Eck, Wilbert Menkveld, Edwin de Buijzer, Jeroen Kemper, Jeroen de Vries, Joost Toebak, Geja Elving en Ard Jansen.

Sinds januari 1990 ben ik werkzaam bij de vakgroep en heb de naam zien veranderen van "Waterzuivering" in "Milieutechnologie". Nu gaat de groep door het leven onder de naam "sectie Milieutechnologie van het departement Agro-, Milieu- en Systeemtechnologie". Ondanks deze naamswijzigingen en het grote natuurlijke verloop op een vakgroep is er gelukkig een vaste basisploeg aanwezig waarop ik in de afgelopen jaren altijd een beroep kon doen: Jo Ackerman-Jacobs, Sjoerd Hobma, Johannes van der Laan, Ilse Gerrits-Bennehey, Heleen Vos en Liesbeth Kesaulya-Monster. In het speciaal bedank ik Vinnie de Wilde en Marieke Sloeserwij-Oostra die mij binnen verschillende projecten van het promotieonderzoek analytisch en praktisch ondersteund hebben. Dank aan alle collega-AIO's en TWP-ers die in de afgelopen jaren gekomen en gegaan zijn en hebben bijgedragen aan de gezellige sfeer op de werkvloer. Daarnaast dank aan de collega's waarmee ik de afgelopen jaren de dagelijkse frustraties en spanningen heb kunnen afreageren door middel van een partijtje zaalvoetbal, squash of tennis. Ook speciale dank aan de collega's die mij in de afgelopen jaren hebben moeten verdragen in de verschillende kamers op de 7de verdieping van het Biotechnion: Renze van Houten, Sjon Kortekaas, Miriam van Eckert en Luc Bonten.

Dank aan vrienden en familieleden die op de een of andere manier hebben gezorgd voor de broodnodige afleiding de afgelopen jaren. Daarbij denk ik speciaal aan Bathilde die de wisselvallige promotiestemmingen van dichtbij heeft moeten meemaken. Een andere speciale dank gaat uit naar Petra die de omslag heeft verzorgd.

Een klein gehucht is geen vanzelfsprekende basis voor de start van een academische opleiding. Daarom ben ik erg blij dat ik een vader en moeder heb getroffen die mij hebben gestimuleerd maar vooral ook de vrijheid en tijd gegund hebben om via allerlei omwegen te komen waar ik nu ben. Gelukkig bestonden in die tijd de Deetmans en Ritzens nog niet waardoor ook latente talenten zich langzaam konden ontwikkelen! Helaas kan mijn vader deze dag niet meer meemaken maar ik weet dat hij trots op me is.



Het onderzoek is mede mogelijk gemaakt door financiële bijdragen van nv VAM aan verschillende aspecten van het onderzoek waarbij ik Peter Bakkers, Tim Brethouwer en Hans Woelders hartelijk wil bedanken voor de prettige samenwerking gedurende de afgelopen jaren.

De allerlaatste dank gaat natuurlijk uit naar Bert Hamelers zonder wie dit proefschrift nooit zou zijn geworden wat het nu is. Samen met hem ben ik gekomen tot de wetenschappelijke verdieping van het onderwerp en heeft hij voor mij de noodzakelijke computermodellen geschreven. Bert nogmaals hartelijk dank voor alles en ik hoop dat we de komende jaren nog heel wat leuke modellen mogen ontwikkelen om de Milieutechnologie een eindje verder te helpen.

Adrie Veeken

*'Soms gaan de gedachten zo razendsnel  
dat ik ze bijna niet meer kan denken,  
ze spoelen door me heen en dan moet ik huilen.  
En opeens staat alles weer stil,  
verstard als op een toverlantarenplaatje  
en lijkt niets ooit meer van zijn plaats te kunnen komen  
en moet je weer gaan lopen om je omgeving op gang te krijgen.  
Zomaar lopen omdat je anders niet meer kunt voelen  
dat je ergens thuishoort, dat er tijd verstrijkt.'*

uit Hersenschimmen van J. Bernlef

Voor mijn vader en moeder

## Contents

Chapter 1	Introduction	1
Chapter 2	State of the art of technologies for the removal of heavy metals from solid wastes	11
Chapter 3	Materials and methods	23
Chapter 4	Sources of heavy metals in biowaste	51
Chapter 5	Physico-chemical fractionation of heavy metals in biowaste	69
Chapter 6	Development and validation of the NICA-Donnan model for describing proton and metal adsorption to natural organic complexants	91
Chapter 7	Role of humic acids in proton and Cu(II) adsorption to the organic fraction of biowaste	125
Chapter 8	Kinetics of heavy metal extraction from solid organic particles of biowaste	155
Chapter 9	Pilot plant study for the valorisation of biowaste	181
Chapter 10	General discussion	201
	Summary	209
	Samenvatting	221

# 1. Introduction

## 1.1. *Scope of the dissertation*

Solid organic wastes of biological origin can possibly be reused as soil improvers. This method of waste treatment reflects the Dutch governmental policy of prevention and recycling of waste, replacing such traditional disposal strategies as landfilling and incineration (RIVM, 1988). Solid organic wastes suitable for reuse are, for example, sewage sludge, the source-separated organic fraction of municipal solid waste, so-called biowaste<sup>1</sup>, and the top layer of moors. However, the recycling of solid organic wastes is hampered because the legal criteria for the heavy metal content of the compost prepared from this type of organic waste, as laid down in BOOM<sup>2</sup>, have been tightened (SDU, 1991).

In this thesis we will focus on the reduction of the heavy metal content of biowaste to levels at which it is possible to produce compost which complies with the legal standards for heavy metals in compost (BOOM). Feasible technologies for the removal of heavy metals from contaminated solid wastes are (1) solid-to-liquid extraction and (2) physical separation. The applicability of these technologies has to be evaluated and, if necessary, these technologies have to be adapted for biowaste. This research is primarily focused on the solid-to-liquid extraction process. To understand the physico-chemical behaviour of heavy metals in biowaste, mechanistic models were developed in order to gain an insight into the factors which determine the binding strength and extraction rate of heavy metals present in biowaste.

## 1.2. *Problems related to the recycling of biowaste*

Due to the growing volume of solid waste streams in the last decades, such management strategies as incineration and landfilling have become problematic in the Netherlands. In 1985, 5 million tons of municipal solid waste was produced in the Netherlands, and this amount is expected to increase to approximately 7.2 million tons in 2010 (RIVM, 1988; CBS, 1994). The main strategies for managing solid waste streams are landfilling,

---

<sup>1</sup> within the framework of this thesis, the *source separated organic fraction of municipal solid waste* will be referred to as *biowaste*; in the Netherlands, biowaste is referred to as *fruit, vegetable and yard waste*, the literal translation from Dutch of "groente-, fruit- en tuinafval"

<sup>2</sup> BOOM (Dutch abbreviation for Besluit Overige Organische Meststoffen): law which defines the quality and use of organic fertilisers other than organic manures

incineration and recycling. The problems related to landfilling are lack of space, the emission of greenhouse gases and the possibility of soil and groundwater contamination due to the leaching of components from landfill sites (Farquhar and Rovers, 1973; Hjelmar, 1995). Recent developments in waste management have led to a decree which forbids the landfilling of solid wastes with an organic matter content higher than 5% (Stax, 1995). Incineration can cause air pollution due to emissions (of e.g. heavy metals, chlorinated dioxins and dibenzofurans), and thus requires expensive after-treatment (White et al., 1995). Incineration also contributes to the greenhouse effect and leads to the production of highly contaminated and hazardous slags and fly ashes, which have to be landfilled (McBean et al., 1995). As a result of these problems, governmental policy has gradually shifted towards preventing and recycling solid waste streams (RIVM, 1988). In this way a significant reduction of the quantity of solid wastes that eventually have to be landfilled or incinerated can be achieved.

Table 1.1 presents the major constituents of municipal solid waste (Roosmalen and Langerijt, 1989). Although these data have changed slightly over the past years, they still give a fairly good impression of the current composition of municipal solid waste (CBS, 1994; Cornelissen et al., 1994; Nagelhout et al., 1989).

**Table 1.1 Average composition of municipal solid waste between 1970 and 1980 (Roosmalen and Langerijt, 1989)**

Component	Contribution (%)
organic part of biological origin	52
paper	22
glass	8
plastics	7
ferrous and non-ferrous	3
remainder	8

The separate collection of components of municipal solid waste and the development of methods of recycling have been intensified in the Netherlands during the last decade. In the National Environmental Policy Plan (NMP) of 1989 activities related to separate waste collection are formulated under article A67 following the NMP's philosophy concerning the durable use of the environment (SDU, 1991). These plans are further developed in the NMP-plus programme of 1990. The objective for the year 2010 is to recycle 50% of municipal solid waste and to incinerate the remaining 50%. By then, there should be no further landfilling of municipal solid waste.

Summarising, from the view of sustainable development, the recycling of solid organic wastes is preferred to incineration and landfilling because:

- incineration produces greenhouse gases, contaminated slags and fly ashes
- landfilling produces greenhouse gases in the long term and requires expensive measures to prevent emissions to soil and groundwater systems
- recycling of organic matter promotes closed cycles of carbon and nutrients; moreover, recycling reduces the emission of greenhouse gases when it can substitute peat as soil improver.

The organic fraction of biological origin in municipal solid waste (excluding paper and plastics) makes up 50% of the total amount of municipal solid waste. The organic part consists of indoor-collected organic material, such as food remainders and flowers, and outdoor-collected organic matter, such as grass and branches.

In the Netherlands, the Biowaste Action Programme has been developed to promote the recycling of the organic fraction of municipal solid waste (VROM, 1992). By June 1992, 312 municipalities in the Netherlands had an operational system for the separate collection of the organic fraction of municipal solid waste, representing 37% of Dutch households. The Biowaste Action Programme aimed at introducing the separate collection of biowaste in 78% of Dutch municipalities by the end of 1996.

Biowaste recycling can be achieved by biological conversion into compost. The compost thus produced can be reused as soil improver and natural fertiliser. The biological conversion of biowaste can be established by aerobic composting or anaerobic digestion (Vallini and Pera, 1989; Cecchi et al., 1988; Inbar et al., 1990). Advantages of the use of compost on arable land are:

- organic matter has a positive effect on the structure of the soil, thereby improving tilth, aeration, and retention of moisture; its capacity to bind soil particles into structural aggregates reduces soil erosion (Huang and Schnitzer, 1986; Stevenson, 1994)
- organic matter has a nutritive function: it is a source of nutrients and trace metals, and regulates the supply of nutrients from other sources in the soil (Vaughan and Malcolm, 1985)
- organic matter has a positive effect on the activity of microflora and microfaunal organisms (Burns et al., 1986; Len and Aviad, 1989).

On the other hand, the application of compost to soil systems is of great concern because the frequent supply of compost may lead to the accumulation of heavy metals in the soil. Increased levels of heavy metals in topsoils due to atmospheric deposition from industrial activities and input via fertilisers, pesticides and animal manure have already been observed (Ferdinandus, 1989).

The negative effects of increased heavy metal contents in soil systems are (Chaney and Ryan, 1993; De Haan and Van der Zee, 1993):

- the possibility of heavy metal leaching to groundwater
- heavy metal uptake by plants and animals which introduces more heavy metals into various, vital life-cycles
- inhibition of plant growth and of the activity of soil microorganisms.

The heavy metal content of composts should be limited to in order to guarantee the safe use of compost. The legal criteria for the quality and dosage of compost are laid down in the law concerning the quality and use of so-called other organic fertilisers: the BOOM decree (SDU, 1991; TCB, 1991). This law distinguishes two types of compost: compost and clean compost. The standards for heavy metals in compost and clean compost are listed in Table 1.2.

**Table 1.2 Legal demands for heavy metals and organic matter in compost and clean compost originating from so-called other organic fertilisers (SDU, 1991)**

Parameter	Compost	Clean compost
organic matter <sup>1</sup>	> 20	> 20
Cd <sup>2</sup>	< 1	< 0.7
Cr	< 50	< 50
Cu	< 60	< 25
Hg	< 0.3	< 0.2
Ni	< 20	< 10
Pb	< 100	< 65
Zn	< 200	< 75
As	< 15	< 5

<sup>1</sup> organic matter content in % of dry matter

<sup>2</sup> heavy metal content in mg.kg<sup>-1</sup> dry matter

The dosage of compost to arable land depends on the type of compost and the type of arable land. For compost the dosage is related to a fixed amount of compost, and for clean compost it is related the amount of dosed phosphate (P<sub>2</sub>O<sub>5</sub>). Table 1.3 gives the maximum dosages for compost and clean compost for different types of arable land.

Table 1.4 presents the heavy metal content of composts derived from municipal solid wastes (MSW) which were prepared in three different ways. The heavy metal content of compost is significantly reduced when the organic fraction is separated before composting. An even greater reduction is achieved when the organic fraction of MSW is source-separated before composting (Lustenhouwer, 1985; Richard et al., 1993; Roosmalen et al., 1988).

**Table 1.3 Dosage of compost and clean compost on arable land (SDU, 1991)**

Type of land	Compost (kg compost/ha/year)	Clean compost (kg P <sub>2</sub> O <sub>5</sub> /ha/year)
grassland	3,000	175
farm land	6,000	125
corn fields	6,000	125
nature areas	not allowed	not allowed
the rest <sup>1</sup>	12,000	70

<sup>1</sup> for example, sports fields, allotments and roadsides

A comparison of Tables 1.3 and 1.4 shows that MSW compost and OFMSW compost (see footnote of table 1.4) cannot meet the BOOM criteria for heavy metals. Biowaste-derived compost is critical in order to meet the legal standards for compost with respect to some heavy metals, and the heavy metal content is too high with respect to most heavy metals to meet the legal standards for clean compost.

**Table 1.4 Heavy metal and organic matter content of different types of MSW-derived composts**

Parameter	MSW compost <sup>3</sup>	OFMSW compost <sup>4</sup>	biowaste compost <sup>5</sup>
organic matter <sup>1</sup>	29	30	29 ± 7
Cd <sup>2</sup>	9	1.7 - 1.9	0.8 ± 0.2
Cr	140	20 - 59	16 ± 4
Cu	530	70 - 170	35 ± 8
Hg	3	1.0 - 1.6	-
Ni	80	20 - 45	9 ± 2
Pb	830	280 - 500	85 ± 18
Zn	1600	400 - 1000	134 ± 25
As	8	3 - 5	-

<sup>1</sup> organic matter content in % of dry matter; <sup>2</sup> heavy metal content in mg.kg<sup>-1</sup> of dry matter;

<sup>3</sup> MSW compost obtained from MSW which is integrally collected; the compost (organic fraction) is mechanically separated after composting; <sup>4</sup> OFMSW compost obtained from MSW which is integrally collected; the organic fraction (OFMSW) is mechanically separated before composting; <sup>5</sup> biowaste compost obtained from the organic fraction of municipal solid waste which is separated at the source before composting

Apart from meeting the legal standards for heavy metals as laid down in BOOM, the recycling of biowaste only makes sense if there is a market for the compost. Possible marketing areas for biowaste-derived compost are its application in horticulture, private gardens, public parks, and the agricultural sector. However, the level of acceptance of compost by the agricultural sector is low. This is mainly because of the quality of the compost, especially with respect to the content of heavy metals and low content of



organic matter. Besides that, the compost has to compete with other soil improvers, such as animal manure, inorganic fertilisers and potting compost. The recycling of biowaste can possibly be frustrated if biowaste-derived compost is not accepted by the market.

Existing aerobic and anaerobic treatment processes without any pretreatment steps cannot achieve these goals. There are two possible ways to guarantee the recycling of biowaste:

1. **Prevention.** By changing the collection criteria for biowaste, components which cause the low organic matter content and high heavy metal content of the waste can be avoided. However, the possibilities for changing the collection criteria for biowaste do not exist, due to economical and social obstacles.
2. **Technological approach.** Technological processes can be employed to valorise biowaste to biowaste-derived compost which can both meet the legal criteria as laid down in BOOM and compete with other fertilising and soil improving products.

This thesis will focus on technological solutions to reduce the heavy metal content of biowaste preceding the biological conversion to compost.

### **1.3. Outline of the dissertation**

Chapter 2 briefly reviews the state of the art of technologies for the removal of heavy metals from solid wastes. Two possible technological approaches are discussed: solid-to-liquid extraction and physical separation. Chapter 3 presents the materials and methods applied in the experimental part of the research, and discusses the physical and chemical characteristics of biowaste. Chapter 4 discusses the sources of heavy metals in biowaste. A physical classification scheme, based on differences in particle size and density of the constituents of biowaste, is applied in order to determine the heavy metal content of the various fractions of biowaste. The origin of the fractions is discussed and the heavy metal content of the fractions are compared to natural background concentrations of the original biowaste components. On the basis of these results it can be evaluated whether the biowaste is contaminated and which constituents of biowaste are the main contributors of the heavy metals present in biowaste. Chapter 5 presents an analytical approach for determining the physico-chemical forms of heavy metals in biowaste. A fractionation scheme based on physical separation followed by sequential chemical extraction is presented. The scheme can be applied for the assessment of physical separation and/or chemical extraction processes for the removal of heavy metals from biowaste. Chapter 6 presents a mechanistic model which describes the adsorption of protons and heavy metal ions to natural organic complexing compounds, such as humic substances and plant fibre, both of which are essential metal complexing components in biowaste. The mechanistic model is validated for proton and Cu(II) binding to the model compound Sephadex CM-25. Chapter 7 presents the proton and Cu(II) adsorption to particle-sized organic fractions

of biowaste. The adsorption is described and interpreted by the model developed in Chapter 6. Moreover, the role of humic acid in the binding strength and solubilisation of Cu(II) is evaluated. Chapter 8 presents a mechanistic model which describes the rate and efficiency of the acid extraction of heavy metals from solid organic particles. The model simulations are compared with the experimental results of the Cu(II) desorption from particle-sized organic fractions of biowaste and literature data on the extraction of Cd, Cu and Zn from sewage sludge. Chapter 9 presents an integral process (based on the results of Chapter 5) for the valorisation of biowaste. The valorisation is based on various physical separation processes coupled to aerobic and anaerobic treatment processes of the obtained organic process streams. Chapter 10 gives a general evaluation of the various topics presented in this thesis.

## References

- Burns, R. G.; Dell'Agnola, G.; Miele, S.; Nardi, S.; Savoini, G.; Schnitzer, M.; Sequi, P.; Vaughan, D.; and Visser, S. A. 1986. Humic substances: Effects on soil and plants. Italy, REDA
- CBS (Centraal Bureau voor de Statistiek) 1994. Environment Statistics of the Netherlands 1994. 's-Gravenhage: SDU (in Dutch)
- Chaney R.; and Ryan J. 1993. Heavy metals and toxic organic pollutants in MSW composts: Research results on phytoavailability, bioavailability, Fate, In: Science and Engineering of Composting: Design, Environmental, Microbiological and Utilization Aspects, Hoitink A.J. and Keener H.M. (eds.), Ohio:Renaissance Publications
- Cornelissen, A. A. J.; Oh, K. M. M.; and Otte P. P. 1994. Fysisch Onderzoek naar de Samenstelling van het Nederlandse Huishoudelijke Afval: Resultaten 1993. Bilthoven, RIVM rapportnummer 776201010 (in Dutch)
- Farquhar, G. J.; and Rovers, F. A. 1973. Gas production during refuse decomposition. Water, Soil and Air Pollution 2:483
- Ferdinandus, H. N. M. 1989. Berekening van zware-metaalbalansen voor de bodem. Leidschendam, Technische Commissie Bodembescherming, rapport A89/01-R (in Dutch)
- Haan, F. A. M. de; and Van der Zee, S. E. A. T. M. 1993. Composts Regulations in the Netherlands in View of Sustainable Soil Use, In: Science and Engineering of Composting: Design, Environmental, Microbiological and Utilization Aspects, Hoitink A.J. and Keener H.M. (eds.), Ohio:Renaissance Publications
- Hjelmar, O. 1995. Composition and Management of Leachate from Landfills within the EU. In: Proceedings Sardinia 1995, Fifth International Landfill Symposium, Cagliari:243
- Huang, O. M.; and Schnitzer, M. 1986. Interactions of Soil Minerals with Natural Organics and Microbes. Soil Science of America, Special Publication No. 17
- Inbar, Y.; Chen, Y.; and Hadar, Y. 1990. Humic substances formed during the composting of organic matter. Soil Sci. Soc. Am. J. 13: 137-148
- Joosten, J. M.; and Nagelhout, D. 1987. Scheiden aan de bron en gescheiden inzameling van delen van het huishoudelijk afval. Afvalstoffenreeks, VROM rapportnr. 841102001 (in Dutch)
- McBean, E. A.; Rovers, F. A.; and Farquhar, G.J. 1995. Solid Waste Engineering and Design. New Jersey:Prentice Hall PTR
- Naghelout, D. et al. 1989. Afval 2000, verkenning van de toekomstige afvalverwijderingsstructuur. RIVM rapportnr. 738605002 (in Dutch)
- Richard, T.; Woodbury, P; Breslin, V; and Crawford, S. 1993. MSW Composts: Impacts of Separation on Trace Metal Contamination, In: Science and Engineering of Composting: Design, Environmental, Microbiological and Utilization Aspects, Hoitink A.J. and Keener H.M. (eds.), Ohio:Renaissance Publications
- RIVM 1988. Zorgen voor Morgen - Nationale milieuverkenning 1985-2010 (National Environmental Survey 1985-2010). Alphen aan den Rijn, Samson H.D. Tjeenk Willink (in Dutch)
- RIVM/TAUW 1990. Analysis of Composition of Household Refuse in the Netherlands
- Roosmalen, G. R. E. M. van; Lusthouwer, J. W. A.; Oosthoek, J.; and Senden, M. M. G. 1988.

- Heavy Metal Sources and Contamination Mechanisms in Compost Production. *Resources and Conservation* 14: 321-334
- Roosmalen, G. R. E. M. van; and Langerijt, J.C. van de 1989. Green Waste Composting in the Netherlands. *Biocycle* 30: 32-35
- SDU 1991. Besluit Overige Organische Meststoffen (BOOM). *Staatblad* 613:1-45 (in Dutch)
- Stax, A. B. M. 1995. Landfill guidelines in the Netherlands. In: *Proceedings Sardinia 1995, Fifth International Landfill Symposium, Cagliari, Italy*
- Stevenson, F. J. 1994. *Humic Chemistry: Genesis, Composition, Reactions*. New York, John Wiley & Sons
- TCB (Technische Commissie Bodembescherming) 1991. Advies ontwerp-besluit gebruik en kwaliteit overige organische meststoffen. rapport A90/04, Leidschendam (in Dutch)
- Vallini, G.; and Pera, A. 1989. Green Composted Production from Vegetable Waste Separately Collected in Metropolitan Garden-Produce Markets. *Biological Wastes* 29:33 - 41
- Vaughan, D.; Malcolm, R.E. 1985. Soil organic matter and biological activity. *Developments in Plant and Soil Sciences* Vol. 16. Dordrecht, the Netherlands:Martinus Nijhoff/Dr W. Junk Publishers.
- VROM 1992. Biowaste Action Programme, Working Programme 1992. A publication of the Ministry of Housing, Planning and Environment, the Netherlands
- White, P. R.; Franke, W.; and Hindle, P. 1995. *Integrated Solid Waste Management - A Lifecycle Inventory*. London, Blackie Academic & Professional

## 2. State of the art of technologies for the removal of heavy metals from solid wastes

### 2.1. Introduction

The goal of this research was to develop technologies for the removal of heavy metals from biowaste. In this way, biowaste-derived compost can be made to comply with the legal standards as laid down in the law concerning the quality and dosage of compost: the BOOM decree (SDU, 1991). Up until now, no full-scale processes have been operational for the removal of heavy metals from biowaste or related solid organic wastes, such as sewage sludge. In the last decades, several studies have been published focusing on the development of technologies for the removal of heavy metals from contaminated soil and sewage sludge (Assink, 1986; Wong and Henry, 1988; Rulkens et al., 1989; Tuin, 1990). Most of these technologies can be grouped in one of the two following classes:

1. **Solid-to-liquid extraction.** This process is based on the extraction of metals from the solid-waste to an aqueous-liquid phase followed by separation of the solid and liquid phase. To promote solubilisation, an extracting agent (or extractant) is added directly (chemical extraction) or is produced by microorganisms (microbiological leaching).
2. **Physical separation.** This process is based on the physical separation of a specific fraction of the solid waste in which the heavy metals are concentrated. Physical separation processes are based on differences in the physical properties of the fractions of the solid waste stream.

This chapter discusses the principles and results of the chemical and physical removal processes.

### 2.2. Solid-to-liquid extraction processes

The extraction process for the removal of heavy metals from solids wastes usually consists of three steps (Figure 2.1):

1. the actual extraction process
2. separation of the solid and liquid phase
3. cleaning and recycling of the liquid phase.

The possibilities of the extraction process for solid organic waste streams are first of all determined by the extraction efficiency of the applied extracting reagent. The extraction efficiency is defined as the percentage of heavy metals extracted from the solid to the liquid phase. Other factors determining the applicability of the extraction process on a full-scale are of economical, technological and environmental concern. Some of the main aspects are:

1. costs of the process:
  - costs of the extracting reagent
  - number of process units
  - wastewater treatment
2. minimisation of the production of hazardous emissions:
  - air emissions
  - water emissions
  - final inert waste
3. possible negative effects of the leaching<sup>1</sup> process of the cleaned solid waste on:
  - the structure of the waste
  - the bioavailability of essential nutrients in subsequent biological processes
  - toxicity of heavy metals in subsequent biological processes.

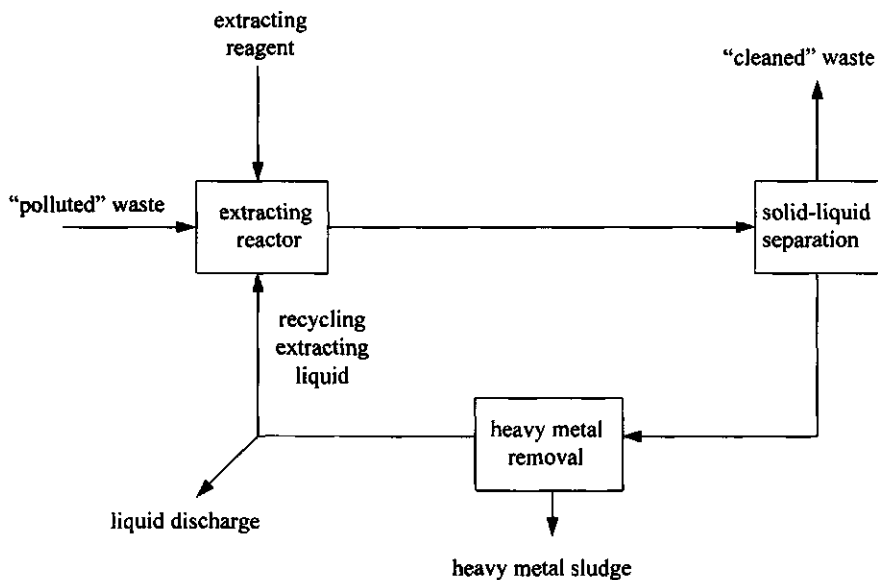


**Figure 2.1** Extraction scheme for the removal of heavy metals from solid wastes

<sup>1</sup> leaching equivalent to solubilization or solid-to-liquid extraction

The main mechanisms for the retention of heavy metals in the solid phase are:

1. adsorption to the organic and inorganic solid phases, e.g. Fe-(hydr)oxides, clay minerals, humic substances
2. presence as inorganic precipitates, e.g.  $\text{CdCO}_3$ ,  $\text{Cu}_3(\text{PO}_4)_2$ ,  $\text{PbS}$ .

For the chemical extraction of heavy metals from solid wastes, two types of reagents are generally used: acids and complexants. Acid extraction of heavy metals is brought about by the exchange of protons for heavy metals adsorbed to the solid phase and by the solubilisation of heavy metal precipitates. The protons can either be supplied directly by addition of a strong acid (e.g.  $\text{HCl}$ ,  $\text{HNO}_3$ ,  $\text{H}_2\text{SO}_4$ , citric acid) or be produced by microorganisms. Extraction through the production of acids by bacteria or fungi is referred to as microbiological leaching. For example,  $\text{H}_2\text{SO}_4$  can be produced by the oxidation of reduced sulphur compounds by *Thiobacilli* strains (Wong and Henry, 1988; Doddema et al., 1987), strong organic acids such as oxalic acid and citric acid can be produced by fungi (Burgstaller and Schinner, 1993), and weak organic acids such as lactic acid and acetic acid can be produced by anaerobic consortia (Schlegel, 1993).

Heavy metal extraction by complexants is based on the high affinity of the complexant for heavy metals. In this way, heavy metals adsorbed to the solid phase or present as heavy metal precipitates are dissolved. Complexants regularly applied for the extraction of heavy metals are ethylenediaminoacetic acid (EDTA) and nitrotriacetic acid (NTA).

Other processes, which are more or less based on these two types of reagents, are:

- extraction with lye (applicable to some solid organic wastes): at high pH values humic substances are solubilised, thus enhancing the solubilisation of heavy metals (Wong and Henry, 1988)
- ion exchange: the solid ion-exchanger is suspended in the liquid phase and the metal ions are transported from the contaminated solid waste to the complexing ion-exchanger. In the ion-exchange particles, the metal ions are covalently or electrostatically bound by the ion-exchanger sites (Wong and Henry, 1988). This process is very complex and rate-limited by mass transport of heavy metal ions from the bulk solution to the surface of the ion-exchange particles and by transport of the metal ions from the solid phase to the liquid phase
- electro-reclamation: in-situ removal of heavy metals from soil systems by electrically charging the system through the application of several electrode arrays; generally the process is promoted by acidification of the soil (Lageman et al., 1990).

There is no literature on the extraction of heavy metals from biowaste. However, sewage sludge (a solid waste stream comparable to biowaste) has been extensively studied. Table 2.1 present a compilation of literature data regarding the extraction efficiencies of Cd, Cu, Pb and Zn from sewage sludge. Table 2.1 shows a very broad range of extraction efficiencies for all heavy metals. The broad range in extraction efficiencies is due to differences in sludge composition, differences in pretreatment of the sludge and differ-

ences in extracting conditions. The variable extraction conditions, such as extracting time, reagent concentration, solids concentration and type of mixing, are important extracting parameters. Figure 2.2 shows the effect of pH and solids concentration on the extraction of Cd, Cu and Zn as a function of time. The data for Cu and Zn are taken from Wozniak and Huang (1982), and that for Cd are from Tyagi et al. (1988). Wozniak and Huang (1982) studied the extraction of heavy metals from activated sludge by HCl as a function of the extraction time, pH and solids content. The experiments were conducted in 600-ml reactors and stirring was provided by two six-unit stirrers. Tyagi et al. (1988) studied the acid extraction of digested sludge. The sludge samples were acidified with H<sub>2</sub>SO<sub>4</sub> in 500-ml Erlenmeyer flasks and stirring was provided by a Gallenkamp shaker at 25 rpm. The extraction data for Cd have been recalculated to extraction efficiencies (in %). The extraction data for Cu and Zn are given in mg.l<sup>-1</sup> because the total metal contents were not reported.

**Table 2.1** Extraction efficiency of heavy metals from sewage sludge

Extracting reagent	Extraction efficiency (%)			
	Cd	Cu	Pb	Zn
HCl, pH 1.5 <sup>1</sup>	10 - 90	0 - 70	5 - 100	50 - 90
0.5 M acetic acid <sup>2</sup>	40	0	5	25
HCl, pH 1.5 <sup>3</sup>	80 - 100	80 - 100	40 - 100	100
H <sub>2</sub> SO <sub>4</sub> <sup>4</sup>	10 - 70	<2	10 - 15	35 - 70
HCl, pH 1 <sup>5</sup>	90	50	-	90
HCl, pH 1 <sup>6</sup>	22 - 90	2 - 90	30 - 100	50 - 95
H <sub>2</sub> SO <sub>4</sub> , pH 1.5 <sup>7</sup>	-	50 - 75	50 - 60	80 - 95
H <sub>2</sub> SO <sub>4</sub> , pH 1.5 <sup>8</sup>	95 - 99	8 - 10	35 - 65	50 - 99

<sup>1</sup> Oliver and Carey, 1976; <sup>2</sup> Bloomfield and Pruden, 1975; <sup>3</sup> Wozniak and Huang, 1982;

<sup>4</sup> Jenkins, 1981; <sup>5</sup> Ried, 1988; <sup>6</sup> Rulkens et al., 1989; <sup>7</sup> Tyagi, 1988; <sup>8</sup> Lo, 1990.

As might be expected, both the extraction efficiency and the rate of extraction are higher at lower pH values. However, some peculiar behaviour is observed in the course of extraction. Firstly, the extraction of copper shows a lag phase, i.e. the extraction does not start immediately but is delayed for a certain period of time. The lag phase is longer for higher total solids concentrations although the final extraction efficiency is higher. Secondly, the extraction rate does not gradually decrease as equilibrium is reached, but shows two maxima during the course of extraction. Normally, it is expected that the extraction follows a pseudo-first-order equation or parabolic diffusion equation (Sparks and Suarez, 1991).

Theis and Hayes (1978) showed that the metal extractability depends on the redox conditions. The extraction efficiency decreases for most heavy metals when the sludge is



anaerobically digested. Especially the Cu extractability decreased drastically, from 61% to 1%. The lower solubility is caused by the reduction of sulphate to sulphide and the subsequent precipitation of heavy metal sulphides. Heavy metal sulphides, especially CuS and PbS, are very difficult to solubilise, even at low pH values (Fletcher and Beckett, 1987a,b).

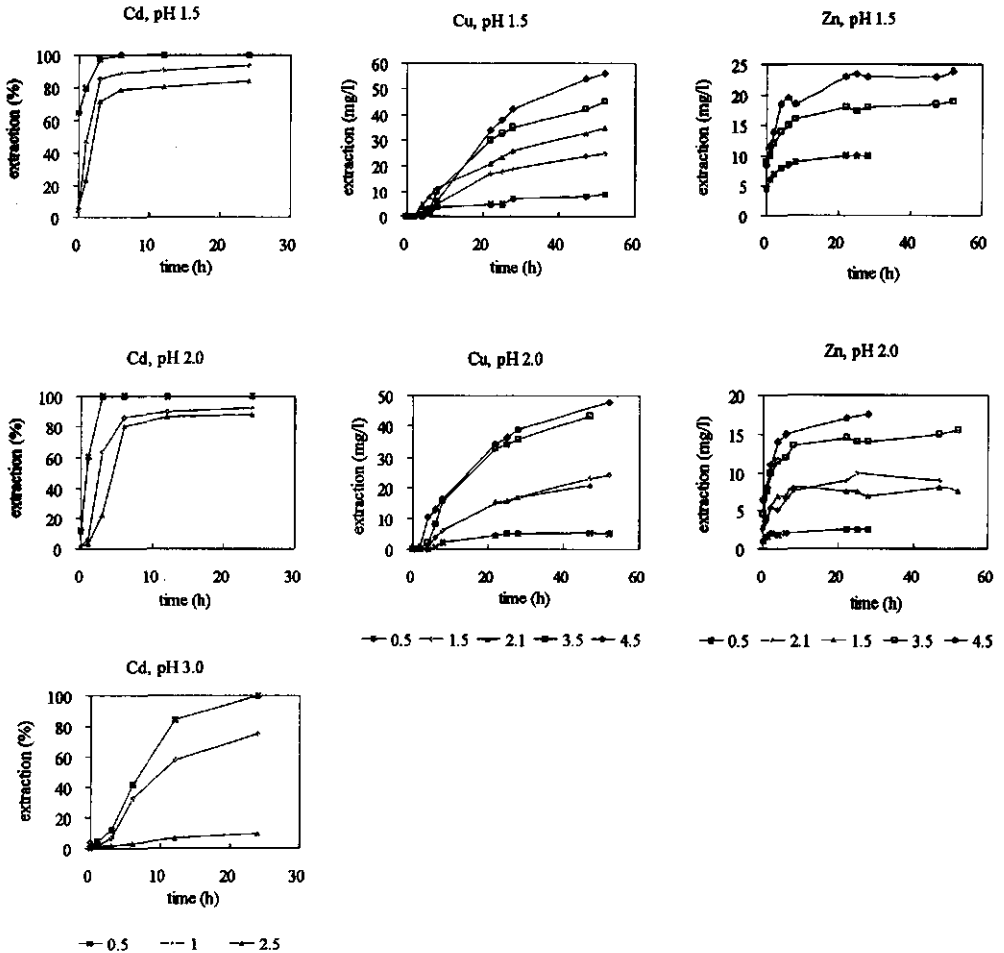


Figure 2.2 Heavy metal extraction from sewage sludge at variable total solids concentration (solids concentration in %)

### 2.3. Physical separation processes

If heavy metals are concentrated in specific solid fractions of a solid waste, the selective removal of these particles from the solid waste generally results in a small fraction that is highly contaminated and a large fraction that is relatively clean. The separation of a

specific fraction is achieved by means of physical separation processes. The term 'physical' is added to distinguish this process from molecular separation processes, such as distillation and dialysis. In this subchapter, a short review will be given of the available technologies. The processes are widely used in soil remediation, the mining industry and mineral processing (Svarovsky, 1985). Until now, adaptations of mining technologies in the field of environmental technology have been applied only in the cleaning of polluted soils and sediments, during which "non-polluted" sand is separated from "polluted" smaller size fractions (Van Dillen and Schotel, 1990; Kroenig, 1990; Werther and Willichowski, 1990). The separation of a specific fraction of the solid waste by a solid-solid separation process is established by differences in particles properties.

**Table 2.2 Wet solid-solid separation processes**

Process	Waste properties				
	Size	Density	Hydro-phobicity	Shape	Magnetic properties
screening or sieving	+			(+) <sup>1</sup>	
elutriation	+	+		(+)	
hydrocyclones	+	+		(+)	
air flotation			+		
magnetic separation					+

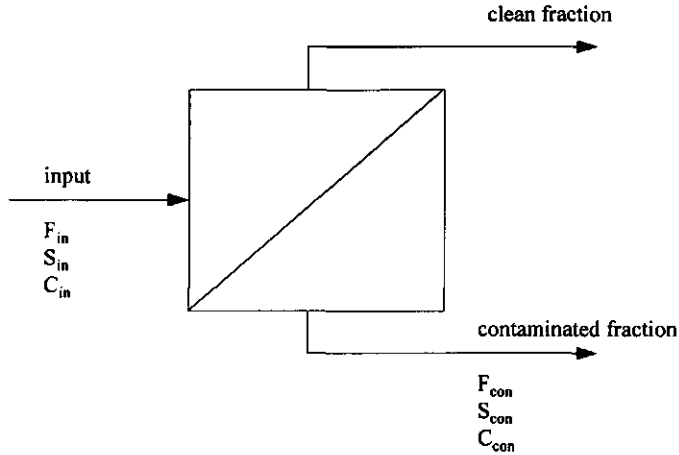
<sup>1</sup>brackets indicate secondary importance

Table 2.2 presents the wet solid-solid separation processes mostly widely used in waste treatment, together with the principal properties on which the separation is based. Descriptions and applications of these processes and adaptations of these processes can be found in various textbooks (Svarovsky, 1985; Metcalf and Eddy, 1991).

Physical wet-separation processes used in the field of environmental technology can be characterised by a clean solid stream and a contaminated solid stream. Figure 2.3 shows a schematic presentation of a physical wet-separation process where the contaminated waste (influent flow) is separated into a "clean" flow and a "contaminated" flow. The flows are characterised by the flow rate of the liquid ( $F$  in  $\text{m}^3 \cdot \text{s}^{-1}$ ), total solids concentration ( $S$  in  $\text{kg} \cdot \text{m}^{-3}$ ) and concentration of contaminant in the solids ( $C$  in  $\text{mg} \cdot \text{kg}^{-1} \text{DM}$ ). The separation efficiency ( $E_S$ ) with respect to the total contaminated flow is defined as the total solids mass flow of the contaminated fraction as a fraction of the total solids feed mass flow rate:

$$E_S = \frac{F_{\text{con}} S_{\text{con}}}{F_{\text{in}} S_{\text{in}}} \quad (2.1)$$

where the subscripts 'in' and 'con' refer to the incoming flow and contaminated flow, respectively.



**Figure 2.3** Schematic presentation of physical separation process for environmental applications

The efficiency of the solid-solid separation process is determined not only by the total separation efficiency but also by the distribution of the contaminant over the clean and contaminated flows. The separation efficiency with respect to the contaminants ( $E_C$ ) is defined as:

$$E_C = \frac{F_{con} S_{con} C_{con}}{F_{in} S_{in} C_{in}} = E_S \frac{C_{con}}{C_{in}} \quad (2.2)$$

Figure 2.4 shows a contour plot of the performance of the physical separation process as a function of  $E_S$  and  $E_C$ . The removal efficiency of a solid-solid wet-separation process is high when the  $E_S$  is low and the  $E_C$  is high (top left corner of Figure 2.4).

De Waaij and Van Veen (1988) studied the heavy metal decontamination by hydrocyclones of several types of sediment. Table 2.3 gives the total separation efficiency and contamination efficiencies, recalculated from their data. Hydrocyclone separation gives good results for sandy sediments; however, for muddy sediments, the performance of hydrocyclones is poor. This is caused by the poor separation efficiency and the high contaminant concentrations in the "clean" stream.

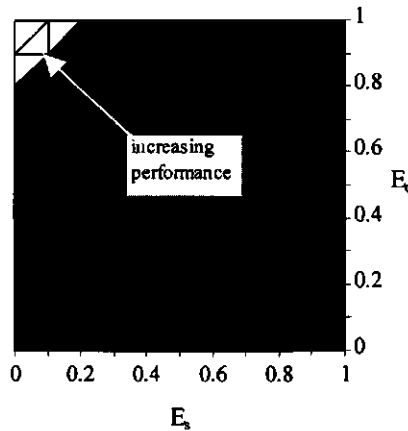


**Figure 2.4** Qualification of the performance of a solid-solid separation process on basis of the separation and contamination efficiencies

The separation efficiency as defined in equation 2.1 includes all the separated solids, irrespective of particle size. However, for most separation processes the separation efficiency varies with particle size. Therefore the grade efficiency is introduced, i.e. the separation efficiency as a function of particle size:

$$G(x) = E_c \frac{dF_{con}(x)}{dF(x)} = E_s \frac{C_{con}}{C_{in}} \frac{dF_{con}(x)}{dF(x)} \quad (2.3)$$

where  $G(x)$  is the grade efficiency,  $x$  is the particle size (m), and  $F(x)$  and  $F_{con}(x)$  are the cumulative particle size distributions of the feed and contaminated flow, respectively.

**Table 2.3** Performance of hydrocyclone separation for different types of sediments with respect to heavy metals (De Waaij and Van Veen, 1988)

Origin	Type	Metal	$E_s$	$E_c$
river	mud	Cd	0.50	0.90
river	sand	Cd	0.10	0.85
channel	sand	Cr	0.25	0.85
river	sand	Cd	0.10	0.70
channel	mud	Hg	0.50	0.80
harbour	mud	Cd	0.57	0.82
harbour	mud	Hg	0.40	0.75
channel	mud	Hg	0.46	0.86

Figure 2.5 shows the grade efficiency curves of several types of separators. Often a single number is used to replace the grade efficiency curve of a separation device. This number is called the "cut size" (or  $x_{50}$ ) and corresponds to the place on the curve where the grade efficiency is 50%.

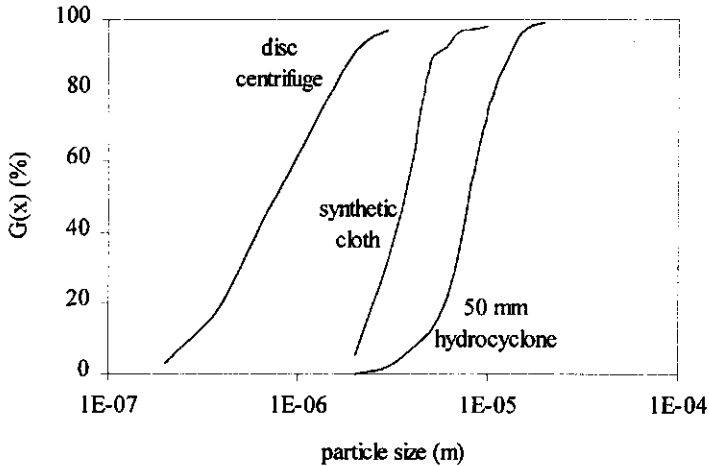


**Figure 2.5** Grade efficiency curves for several types of separators (adapted from Svarovsky (1985))

A second criterion for the performance of a separation process is the sharpness of the classification, as indicated by the steepness of the grade efficiency curve. An ideal separation would result in a step function, as might be obtained with an ideal screen. In most cases there is, however, some "misplaced" material. The less steep the grade efficiency curve, the greater the amount of misplaced material. The simplest measure of the classification sharpness ( $H$ ) is the ratio of two sizes corresponding to two different percentages (symmetrical around 50%) on the grade efficiency curve, such as for example the quartiles (Svarovksy, 1985):

$$H_{(25/75)} = \frac{x_{25}}{x_{75}} \quad (2.3)$$

where  $x_{25}$  and  $x_{75}$  are the particles sizes corresponding to grade efficiencies of 25 and 75%.

The solid waste has to be characterised with respect to particle size distribution and level of contamination before a separation technology is applied on a pilot-plant or practical scale. For this, the solid waste is physically separated by small, lab-scale devices which differentiate on one of the particle properties given in Table 2.2. After the classification, the heavy metal content of the separated fractions is determined. In this way it becomes

- McGraw-Hill, Inc.
- Oliver, B. G.; and Carey J. H. 1976. Acid Solubilization of Sewage Sludge and Ash Constituents for Possible Recovery. *Water Res.* 10: 1077
- Ried, M. 1988. Heavy Metal Removal from Sewage Sludge: Practical Experiences with Acid Treatment, Pretreatment in Chemical Water and Wastewater Treatment. Proceedings of the 3rd Gothenburg Symp. 1988
- Rulkens W. H.; Voorneburg, F. van; and Joziassse, J. 1989. Removal of Heavy Metals from Sewage Sludges. *Sewage sludge Treatment and Use*, Elsevier Applied Science
- Schegel H. G. 1993. *General Microbiology*. Cambridge, Cambridge University Press
- SDU 1991. Besluit Overige Organische Meststoffen (BOOM). *Staatblad* 613:1-45 (in Dutch)
- Sparks, D. L.; and Suarez D. L. (eds.) 1991. Rates of Soil Chemical Processes. *Soil American Society of America*, Special publication 27
- Svarovsky, L. 1985. *Solid-Liquid Separation Processes and Technology*. Amsterdam: Elsevier
- Theis, T.L.; and Hayes, T. D. 1978. *Chemistry of Heavy Metals in Anaerobic Digestion*, In: *Chemistry of Wastewater Technology*, Rubin, A.J. (ed.). Michigan: Ann Arbor Science Publ. Inc.
- Tuin, B. J. W.; and Tels, M. 1990. Extraction of Six Heavy Metals from Contaminated Clay Soils. *Environmental Technology* 11: 541-554
- Tyagi R. D.; Couillard D.; and Tran, F. 1988. Heavy Metals Removal from Anaerobically Digested Sludge by Chemical and Microbiological Methods. *Environ. Poll.* 50:295-316
- Waaij, A. C. de; and Van Veen, H. J. 1990. Processing of Contaminated Sediments in the Netherlands. In: *Contaminated Soil '90, Third International KfK/TNO Conference on Contaminated Soil*, Arendt, F.; Hinsenveld, M.; and Brink, W. J. (eds.). Dordrecht: Kluwer Academic Publishers
- Werther, J.; and Willichowski, M. 1990. Investigations of the Physical Mechanisms Involved in the Purification of Contaminated Soils by Washing Processes. In: *Contaminated Soil '90, Third International KfK/TNO Conference on Contaminated Soil*, Arendt, F.; Hinsenveld, M.; and Brink, W. J. (eds.). Dordrecht: Kluwer Academic Publishers
- Wong, L. T. K.; and Henry, J. G. 1988. Bacterial Leaching of Heavy Metals from Anaerobically Digested Sludge. In: *Biotreatment Systems, Vol. III*, Wise, D. L. (ed.), Boca Raton, CRC Press, Inc.
- Wozniak, D. J.; and Huang, J.Y.C. 1982. Variables Affecting Metal Removal from sludge. *Journal WPCF* 54:1574-1580

## **3. Materials and methods**

### **3.1. Introduction**

In this chapter the materials and methods used in the laboratory-scale experiments are described. Specific experimental conditions are discussed in the relevant chapters. The following subjects are dealt with in this chapter:

1. Flame and graphite furnace atomic absorption spectroscopy (FAAS and GFAAS) for measuring the total metal content of aqueous solution. Two aspects will be discussed:
  - the matrix effect of various extraction liquids on the FAAS and GFAAS signal
  - the variance and precision of aqua regia digestion of solid samples in combination with FAAS/GFAAS.
2. The use of the Cu(II)-ion-selective electrode for measuring the free  $\text{Cu}^{2+}$  activity in multicomponent solutions. The selectivity, linearity and kinetics of the electrode response are studied. Also the effect of the composition of the solution on the liquid-junction potential of the reference electrode is determined.
3. The laboratory set-up for the separation of physical entities of biowaste.
4. Extraction and characterisation methods of humic acids in biowaste.
5. The experimental set-up for measuring Cu(II) adsorption isotherms and Cu(II) desorption kinetics.
6. The physical and chemical composition of biowaste. Discussions on the chemical and physical properties of biowaste are addressed in the relevant chapters.

Cu(II) was chosen as the monitoring heavy-metal because there is an abundance of literature data with respect to Cu(II) binding to natural organic complexants and to Cu(II) extraction from sewage sludge and soils. Furthermore, the measurement of the free Cu(II) activity with ion-selective electrodes is well established.

### **3.2. Atomic Absorption Spectroscopy (AAS)**

#### **3.2.1. Introduction**

The total metal content in solution is measured by flame or graphite furnace atomic absorption spectroscopy. FAAS is a simple, rapid and accurate technique which is less

sensitive to interference. The detection limit is in the  $\text{mg.l}^{-1}$  region. GFAAS has a detection limit in the  $\mu\text{g.l}^{-1}$  region, but the determination is time-consuming and faces increasing problems with respect to interference. A comprehensive description of AAS can be found in Welz (1985).

Interference in AAS is divided into spectral and non-spectral interference. Genuine spectral interference caused by direct overlap of atomic lines is rare with both the graphite furnace and flame technique. Non-spectral interference affects the analytic signal immediately. Since AAS is a relative method (comparison with a reference solution) any behaviour of the sample that is different from the reference solution possibly brings about interference. Interference that cannot be specified because its cause is unknown or is of a complex nature is called a 'matrix effect'. Non-spectral interference can be eliminated by making the composition of the sample and that of the reference solution similar; thus the matrix effects will influence the signal in both the sample and the reference solution to equal degrees. However, this method is impracticable when a large number of samples of varying composition are to be analysed.

Background interference occurs relatively seldom with the flame technique, but is frequent in the graphite furnace technique. A background correction is usually necessary, but the sole use of a background corrector cannot guarantee accurate results, and may even introduce errors. The main cause for the failure of the background correction is a background signal that is too high. Since measurement of the background signal is time offset to the measurement of the total absorption, interference can arise in the graphite furnace technique if the background signal appears too quickly.

### **3.2.2. Apparatus and experimental conditions**

The analytical measurements were made on a Varian SpectrAA 300 Atomic Absorption Spectrometer coupled to a GTA-96 Graphite Tube Atomizer and a PSC-56 Programmable Sample Changer. The apparatus can be equipped with both a flame device and graphite furnace (GF). The spectrometer is equipped with a Deuterium background correction system. The conditions for selected metals are summarised in Table 3.1.

### **3.2.3. Matrix effect of extraction liquids**

The matrix effect of various extraction liquids is evaluated for Cd, Cu, Pb and Zn by adding a known amount of the metal nitrate salt to the extraction liquid. The concentrations are in the range expected in the extraction and digestion procedures (see Chapters 4, 5 and 8). The matrix effect is quantified by comparing the absorption of the metals in the



extraction liquids with their absorption in the calibration solution (0.3 M HNO<sub>3</sub> + 0.9 M HCl). The results are given in Table 3.2.

**Table 3.1 Experimental conditions for the AAS measurements (Welz, 1985)**

Metal	Technique	$\lambda^4$ (nm)	Concentration range <sup>2</sup> (mg.l <sup>-1</sup> )	Remarks
Na	flame <sup>3</sup> emission	589.0	0.0 - 2.0	addition of 1.0 g.l <sup>-1</sup> CsCl to suppress ionisation
K	flame emission	766.5	0.0 - 1.0	addition of 1.0 g.l <sup>-1</sup> CsCl to suppress ionisation
Ca	flame absorption	422.7	0.0 - 4.0	addition of 2 g.l <sup>-1</sup> La(NO <sub>3</sub> ) <sub>2</sub> to suppress interference
Mg	flame absorption	202.6	0.0 - 10.0	addition of 2 g.l <sup>-1</sup> La(NO <sub>3</sub> ) <sub>2</sub> to suppress interference
Fe	flame absorption	248.3	0.0 - 10.0	
Al	flame absorption	309.3	0.0 - 40.0	nitrous oxide-acetyl flame
Cr	flame absorption	357.9	0.0 - 8.0	
Mn	flame absorption	279.5	0.0 - 5.0	
Cd	GF absorption	228.8	0.0 - 4.0 <sup>1</sup>	platform, matrix modifier (NH <sub>4</sub> ) <sub>2</sub> HPO <sub>4</sub> + Mg(NO <sub>3</sub> ) <sub>2</sub> , T <sub>as</sub> <sup>5</sup> 800 °C, T <sub>atom</sub> <sup>6</sup> 1500 °C
Cu	flame absorption	324.8	0.0 - 8.0	
Cu	GF absorption	324.8	0.0 - 20.0 <sup>1</sup>	T <sub>as</sub> 800 °C, T <sub>atom</sub> 2000 °C
Pb	flame absorption	217.0	0.0 - 8.0	
Pb	GF absorption	217.0	0.0 - 50.0 <sup>1</sup>	platform, matrix modifier (NH <sub>4</sub> ) <sub>2</sub> HPO <sub>4</sub> + Mg(NO <sub>3</sub> ) <sub>2</sub> , T <sub>as</sub> 800 °C, T <sub>atom</sub> 1800 °C
Zn	flame absorption	213.9	0.0 - 0.8	

<sup>1</sup> graphite furnace in  $\mu\text{g.l}^{-1}$ ; <sup>2</sup> all calibration curves are made with 0.9 M HCl + 0.3M HNO<sub>3</sub> as background electrolyte; <sup>3</sup> flame measurements normally made in an oxidised air-acetylene flame; <sup>4</sup> wavelength; <sup>5</sup> ashing temperature; <sup>6</sup> atomisation temperature

In the low concentration regions, the matrix effect is significant for Cd and Cu in some extraction liquids. This is due to the fact that the composition of the extraction liquid differs significantly from that of the calibration solution because the samples were not diluted. For higher metal concentrations where the samples were diluted with the calibration solution, the matrix effect for most extraction liquids is negligible. The matrix effect for Zn is in all cases negligible, which is expected for the flame technique (Welz, 1985). For the determinations with the graphite furnace the matrix effect increases in the order Cu < Pb < Cd. Most probably the interference is caused by light scattering in the graphite furnace tube. Salts of extraction liquids remaining in the graphite furnace after the drying and ashing stages are evaporated in the atomisation phase leading to light scattering (Welz, 1985).

**Table 3.2 Matrix effects of GFAAS for Cd, Cu and Pb and FAAS for Zn**

extraction liquid	Cd		Cu		Pb		Zn	
	level <sup>1</sup> (mg.l <sup>-1</sup> )	error (%)	level <sup>1</sup> (mg.l <sup>-1</sup> )	error (%)	level <sup>1</sup> (mg.l <sup>-1</sup> )	error (%)	level <sup>1</sup> (mg.l <sup>-1</sup> )	error (%)
0.5 M NH <sub>4</sub> Ac <sup>3</sup>	2	-10 to 10	12.5	0	100	0	1	0
	20	0	125	0	1000	0	2	0
0.1 M NaAc/HAc	2	b <sup>2</sup>	12.5	0	100	0	1	0
	20	0	125	0	1000	0	2	0
1 M NH <sub>2</sub> OH·HCl	2	-40 to 40	12.5	-10	100	0	1	0
	20	-20 to 20	125	0	1000	0	2	0
0.1 M EDTA	2	b <sup>2</sup>	12.5	-50	100	10	1	0
	20	b <sup>2</sup>	125	0	1000	0	2	0
H <sub>2</sub> O <sub>2</sub> +3.2 M NH <sub>4</sub> Ac	2	50	12.5	-40	100	0	1	0
	20	0	125	0	1000	0	2	0

<sup>1</sup> concentration level; <sup>2</sup> background level too high; <sup>3</sup> Ac = acetate

### 3.3. Aqua regia digestion of biowaste

#### 3.3.1. Introduction

The standard procedure for determining the total metal content of biowaste consists of a digestion step with aqua regia followed by measurement of the metals in solution by AAS. The procedure is derived from the determination of the total metal content of soils and plants (Lustenhower, 1991). Lustenhower et al. (1990a, 1990b, 1990c) studied the total procedure for the determination of heavy metals in biowaste-derived compost: (1) sampling, (2) digestion with aqua regia, and (3) metal analysis. They showed that the performance of the digestion procedure by conventional and by microwave heating is satisfactory with respect to variance and precision. The precision of the digestion with aqua regia is appropriate, although it is known that some metals (especially Cr) can evaporate during digestion as chromium chlorides.

The variance and precision of the aqua regia digestion in combination with heavy metal analysis by AAS is tested for the reference material BCR No. 144, a sewage sludge of domestic origin (CBR, 1985). The total analytical procedure is tested for four biowaste samples of different origin.

### 3.3.2. Material and methods

Samples of approx. 20 to 30 kg of biowaste, collected at VAM Wijster, were cut and homogenised in a 10-litre stainless-steel kitchen blender. 1-2 kg of the sample was dried at 70 °C and 100-200 g of the sample was crushed with an agate planet ball mill (Retsch) to produce particles smaller than <0.1 mm. Of the ball-milled sample, 0.5-2 g was digested with 10 ml of aqua regia by conventional heating under reflux at 250 °C for 4 hr (Gehhardt Kjeldatherm). The solution was filtered through a paper filter (Schleicher & Schuell 589<sup>1</sup> Schwarzband) and made up to 100 ml with bidistilled water.

Heavy metal concentrations in solution were determined by FAAS and GFAAS, as described in subchapter 3.2. The certified total heavy metal content and the aqua-regia-soluble heavy metal content of the reference materials BCR No. 144 are given in Table 3.3.

**Table 3.3 Heavy metal content of reference material BCR 144 (in mg.kg<sup>-1</sup> DM<sup>1</sup>)**

Element	Total	Aqua regia
Cd	3.4 ± 0.3	3.6 ± 0.3
Cu	713 ± 26	694 ± 44
Pb	495 ± 19	479 ± 51
Zn	3143 ± 103	3055 ± 273

<sup>1</sup>DM = dry matter

The differences between the certified value of the total content and aqua regia contents are small for samples with a high organic matter content. Silicates are not digested by aqua regia, but the contribution of heavy metals incorporated in the sand is very low compared to the total content of the other components in biowaste. Therefore, the aqua regia content of heavy metals in biowaste provides a reliable estimate of the total content.

### 3.3.3. Results and discussion

Table 3.4 presents the content of Cd, Cu, Pb and Zn in BCR 144 and the four biowaste samples. The determinations were carried out in duplicate.

The standard deviation of the procedure shows that the repeatability of the procedure for the reference sample BCR 144 is very good. The values are within the 95% confidence interval of the aqua regia content of Table 3.3, demonstrating that the precision of the procedure is satisfactory.

**Table 3.4 Heavy metal content (in mg.kg<sup>-1</sup> DM) after digestion with aqua regia and FAAS or GFAAS**

Sample	Cd		Cu		Pb		Zn
	GFAAS	FAAS	GFAAS	FAAS	GFAAS	FAAS	FAAS
BCR 144	3.5 ± 0.2	688 ± 8	687 ± 5	466 ± 2	495 ± 4	3153 ± 5	
<b>biowaste:</b>							
sample 1	0.50 ± 0.02	18.0 ± 0.5	17.5 ± 0.3	21 ± 1	26 ± 2	103 ± 1	
sample 2	0.33 ± 0.02	20 ± 2	20.1 ± 0.6	67 ± 1	73 ± 2	131 ± 3	
sample 3	0.26 ± 0.01	16.3 ± 0.1	17.9 ± 0.2	26 ± 2	30 ± 2	89 ± 4	
sample 4	0.36 ± 0.01	15.9 ± 0.1	16.9 ± 0.2	53 ± 1	62 ± 2	136 ± 5	

The results for the four biowaste samples shows that the repeatability of the procedure is very good. Particle size reduction of the biowaste sample to particles smaller than 0.1 mm by the planet ball mill results in a homogeneous sample which gives a good reproducibility of the digestion procedure when 1-2 g of material is used (Lustenhouer, 1991). Moreover, the small particle size results in the complete solubilisation of the heavy metals from the solid sample. The difference between FAAS and GFAAS for Cu are small, but the values measured by GFAAS for Pb are significantly higher than for FAAS. The values are 20% higher for biowaste samples with low Pb contents, but only 6% higher for the reference sample and 9% higher for the biowaste with a relatively high Pb content. The discrepancy between FAAS and GFAAS for the samples with low Pb contents results from the fact that the FAAS signal is below the first standard of the calibration curve, thus giving rise to large errors.

For the metals Na, K, Ca, Mg, Fe, Al, PO<sub>4</sub> and Mn, total concentrations were determined after aqua regia digestion with FAAS for the reference sample BCR 144. The results of the aqua-regia-soluble content (results not shown here) were in good agreement with the certified total values (CBR, 1985).

### 3.4. Cupric ion-selective electrode

#### 3.4.1. Introduction

In this research the cupric ion-selective electrode, Cu(II)-ISE, was applied in two types of studies:

- measurement of Cu(II) adsorption isotherms (see Chapters 6 and 7)
- measurement of the kinetics of the Cu(II) desorption from organic particles of biowaste at low pH (see Chapter 8).

The Cu(II)-ISE is a solid state electrode, for which the electrode response is regulated by the precipitation reaction of  $\text{Cu}^{2+}$  in the  $\text{CuS}_{(s)}$  membrane. This chemical reaction induces the  $\text{Cu}^{2+}$  transfer from the sample solution to the membrane. The behaviour of ion-selective electrodes is extensively reviewed by Buffle (1988) and Ammann (1986). In this subchapter we will focus on the behaviour of the Cu-ISE coupled to an Ag/AgCl reference electrode.

### 3.4.2. Nernstian behaviour of the electrode

By the selective transfer of ion  $i$  from the sample solution to the membrane phase of the electrode, an electromotive force (EMF) is generated. The EMF should be a linear function of the logarithm of the activity of the ion in the bulk solution if all other potential differences are assumed to be constant. In that case, the EMF of the electrode is described by the Nernst equation:

$$\text{EMF} = E_0 + S \log a_i \quad (3.1)$$

where EMF is the electromotive force or cell potential (mV),  $E_0$  the reference potential (mV),  $a_i$  the activity of ion  $i$  ( $\text{mol.l}^{-1}$  or M) and  $S$  the Nernstian slope. The Nernstian slope is defined as:

$$S = 2.303 \frac{RT}{Z_i F} = \frac{59.16}{Z_i} \quad (3.2)$$

where  $Z_i$  is the charge of ion  $i$ ,  $T$  is the absolute temperature (K),  $R$  is the gas constant ( $8.314 \text{ J.K}^{-1}.\text{mol}^{-1}$ ) and  $F$  is the Faraday equivalent ( $9.6487 \cdot 10^4 \text{ C.mol}^{-1}$ ).  $E_0$  has no thermodynamic significance and it includes all the measurement-circuit constants. In practice, the ideal electrode behaviour is not observed and deviations from the Nernst equation become significant at low activities. For most neutral carrier-based membrane electrodes, the response curve follows Nernstian behaviour up to  $10^{-7}$ - $10^{-6}$  M but flattens out at lower concentrations (Ammann, 1986).

The response of the electrode system (Cu-ISE and Ag/AgCl reference electrode) was measured in the total  $\text{Cu}(\text{NO}_3)_2$  concentrations range of  $10^{-9}$  to  $10^{-2}$  M. Figure 3.1 shows the electrode response (in mV) as a function of the total Cu(II) concentration. The slope of 29.5 mV per decade is in good agreement with the theoretical slope of 29.6 mV. Deviation from Nernstian behaviour starts off at a concentration of approx.  $10^{-8}$  M Cu(II) which is due to both the slow response of the electrode and the presence of interfering ions (Buffle, 1988). The slow response of the electrode at low total Cu(II) concentrations is due to the slow mass transport of ions from the bulk to the surface of the electrode

(aqueous diffusion layer) and diffusion of the ions in the membrane. Interfering ions, mostly cations, are present in low concentrations in the salts and bidistilled water (demineralised and subsequently distilled) used.

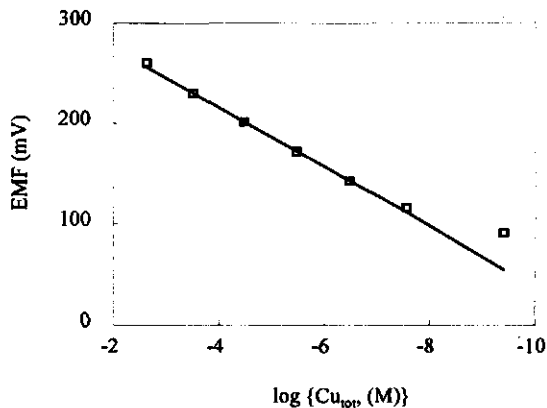


**Figure 3.1** Response of the Cu(II)-ion-selective electrode as a function of the total Cu(II) activity

### 3.4.3. Linear response of the electrode

The limit of Nernstian behaviour as observed in Figure 3.1 does not reflect the true detection limit of the electrode. Lower free metal activities can be measured for metal-buffered solutions. Metal-buffered solutions are made up of metal ions in the presence of a metal-complexing agent. Metal-buffered calibration solutions eliminate the effects of the slow response of the electrode system and rule out the interference of other metal ions (Avdeef et al., 1983).

The linear response of the Cu(II)-ISE was determined for a solution containing  $10^{-5}$  M  $\text{Cu}(\text{NO}_3)_2$  and  $10^{-3}$  M salicylic acid in 0.1 M  $\text{NaNO}_3$ . Salicylic acid forms metal complexes with Cu(II) and protons. The free Cu(II) concentration ( $\text{Cu}^{2+}$ ) depends on the pH of the solution. At low pH salicylic acid is protonated and  $\text{Cu}^{2+}$  is equal to the total Cu(II) concentration in solution. At higher pH values Cu(II) complexes to the salicylate and  $\text{Cu}^{2+}$  therefore decreases with increasing pH. All reactions and equilibrium constants for this system are known and tabulated (Martell and Smith, 1977). The chemical equilibrium for this system at variable pH was calculated by the thermodynamic equilibrium model EQUILIB (see Appendix 6A of Chapter 6). The calculations,  $-\log(\text{Cu}^{2+})$  as a function of pH are plotted in Figure 3.2. The results are in excellent agreement with the

equilibrium models ECCLESS and GEOCHEM (McGrath, 1986; Sanders and McGrath, 1988).

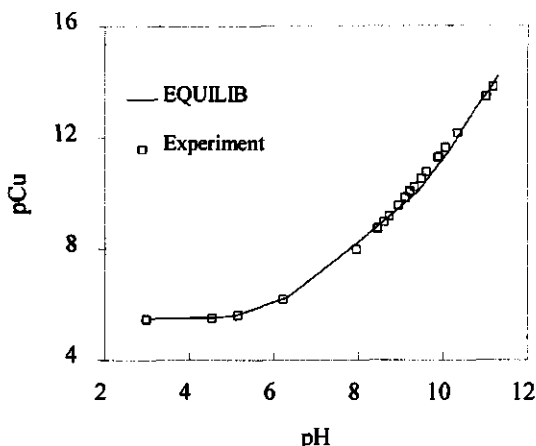


**Figure 3.2** Comparison of the measured Cu(II) activity with the results of EQUILIB for the system  $10^{-5}$  M  $\text{Cu}(\text{NO}_3)_2$  and  $10^{-3}$  M salicylic acid in 0.1 M  $\text{NaNO}_3$

The Cu(II)-ISE was calibrated at Cu(II) concentrations of  $10^{-5}$  and  $10^{-2}$  M. Figure 3.2 shows the results of the experiment for the system of  $10^{-5}$  M  $\text{Cu}(\text{NO}_3)_2$  and  $10^{-3}$  M salicylic acid in 0.1 M  $\text{NaNO}_3$  for pH 3 to 11. As expected, the free Cu(II) concentrations decreases with increasing pH. The free Cu(II) concentration is calculated on the basis of linear response of the electrode; i.e. the calibration results at  $10^{-5}$  and  $10^{-2}$  M is linearly extrapolated to lower electrode responses. The excellent agreement between model calculations and measurements shows that the electrode gives a linear response up to at least  $10^{-14}$  M. According to Avdeef et al. (1983) the response of the Cu(II)-ISE in a metal buffering system of  $\text{Cu}(\text{NO}_3)_2$  and ethylenediamine behaves in a linear fashion from  $10^{-3}$  to  $10^{-19}$  M. In general, the electrode response is linear when the total metal concentration is higher than  $10^{-6}$  M and the dissociation kinetics of metal complexes is rapid on the time scale of the measurement (Buffle, 1988).

#### 3.4.4. Magnitude of the liquid-junction potential

The difference in electrode potential can only be assigned to a change in activity of ion  $i$  when  $E_0$  is constant (see equation 3.1). The reference potential ( $E_0$ ) of the electrode system is determined by, among other things, the liquid-junction potential ( $E_j$ ) at the reference electrode. A liquid-junction potential is always generated when electrolytic solutions of different ionic composition are in contact with each other. It is often assumed that the liquid-junction potential is independent of the sample composition, but in some

cases it may vary considerably. In this subchapter, the liquid-junction potential at the junction of the reference electrode and the sample solution is examined on the basis of the Henderson Formalism (Ammann, 1986).

The total flux of ions at the junction of the reference electrode is given by (Ammann, 1986):

$$J_i = u_i C_i RT \frac{d \ln a_i}{dx} - Z_i u_i C_i F \frac{d \phi}{dx} + C_i v_x \quad (3.3)$$

where  $J_i$  is the flux of ion  $i$  ( $\text{mol} \cdot \text{m}^{-2} \cdot \text{s}^{-1}$ ),  $u_i$  is the absolute mobility of the ion ( $u_i = D_i / RT$ ,  $\text{m}^2 \cdot \text{s}^{-1} \cdot \text{J}^{-1} \cdot \text{mol}^{-1}$ ;  $D_i$  is the diffusivity of ion  $i$ ,  $\text{m}^2 \cdot \text{s}^{-1}$ ),  $\phi$  is the electrical potential across the liquid junction (V), and  $v_x$  is the convectional transport of the liquid phase across the liquid junction ( $\text{m}^2 \cdot \text{s}^{-1}$ ). Henderson derived an approximated equation, based on Planck's theory, to calculate the liquid-junction potential (Ammann, 1986):

$$E_j = \frac{\sum_i Z_i u_i (a_i - a_i^*)}{\sum_i Z_i^2 u_i (a_i - a_i^*)} \frac{RT}{F} \ln \frac{\sum_i Z_i^2 u_i a_i^*}{\sum_i Z_i^2 u_i a_i} \quad (3.4)$$

where  $a_i$  and  $a_i^*$  refer to the concentration of ion  $i$  in the sample and the reference solution (M), respectively.

In general, 3 M KCl is used as reference solution to minimise  $E_j$ . However,  $\text{Cl}^-$  diffusion from the reference solution to the sample solution gives rise to complexation with  $\text{Cu(II)}$  to form  $\text{Cu(Cl)}_n^{(2-n)}$  ( $n=1,2,3$ ) complexes. Therefore  $\text{NaNO}_3$  is used as reference electrolyte. For a system of  $10^{-5}$  M  $\text{Cu(NO}_3)_2$  and a variable  $\text{NaNO}_3$  concentration, the junction potential is calculated by equation 3.4 as a function of pH (see Figure 3.3). The reference solution is composed of 2 M  $\text{NaNO}_3$ . The values of the mobilities for the ions of the system are taken from Newman (1973). Figure 3.3 shows the following features:

- changes in the ionic strengths of the sample solutions give rise to changes in the liquid-junction potential
- at low pH values, the junction potential changes significantly; this is due to both the high proton concentration and the high proton mobility.



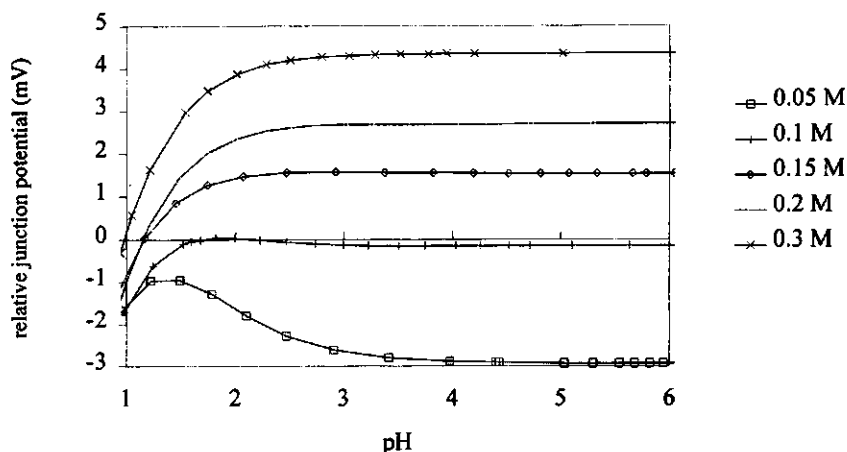


**Figure 3.3** Relative liquid-junction potential as a function of pH at variable ionic strengths of the sample solution as calculated by the Henderson equation (reference solution: 2 M  $\text{NaNO}_3$ )

#### 3.4.5. Kinetics of the electrode response

One of the limiting factors for the application of ion-selective electrodes is the response time of the electrode. The factors contributing to slow response times are numerous. The main factors are (Ammann, 1986):

- response time of the electronic measurement circuit
- diffusion rate of the ion in the unstirred layer of the sample solution near the electrode surface
- exchange rate of the ion at the membrane-solution interface
- diffusion rate within the membrane
- rate of stabilisation of the liquid-junction potential when the composition of the sample solution is modified.

Extensive studies were carried out to determine the dynamic behaviour of membrane electrodes (for a more comprehensive discussion, see Buffle (1988) and Ammann (1986)). Often the response depends on the transport processes in the aqueous diffusion layer. The transport is influenced by the shape and condition of the membrane surface and the composition of the sample. The response time can be reduced by minimising the diffusion layer (fast stirring, flowing sample) or by using samples of higher activities. Low total ion concentrations always lead to very long response times of the electrode.

However, so far no studies have been made of the electrode response with very fast changes in sample composition. Here, the response of the electrode system is studied for a metal-buffered solution containing  $10^{-5}$  M  $\text{Cu}(\text{NO}_3)_2$  and  $10^{-3}$  M salicylic acid. The response of the Cu(II)-ISE is registered at an instant lowering of the pH of the solution from pH 10 to 2. Figure 3.4 shows the pH and Cu(II)-ISE response for this system as a function of time.

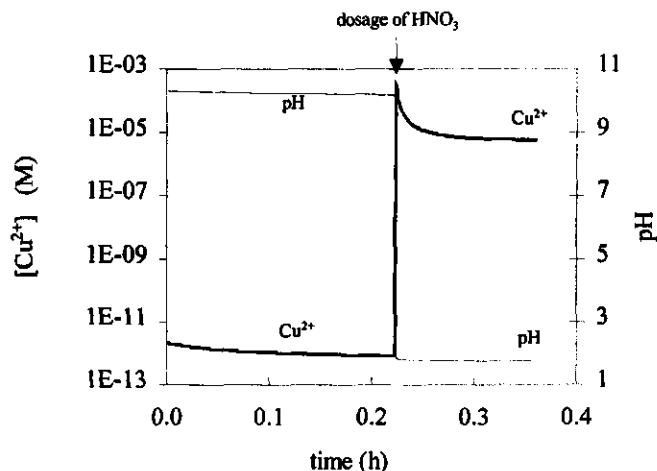


**Figure 3.4** Response of the Cu(II)-ISE at an instant pH lowering for a metal-buffered solution of  $10^{-5}$  M Cu(II) and  $10^{-3}$  M salicylic acid

At high pH values, Cu(II) is complexed to salicylate and  $\text{Cu}^{2+}$  is much lower than the total Cu(II) concentration. As the pH is lowered to 2, Cu(II) is completely exchanged for protons from the salicylate complex and  $\text{Cu}^{2+}$  should be equal to the total Cu(II) concentration. The Cu(II)-ISE however does not increase from  $10^{-12}$  M to  $10^{-5}$  M but gives an overshoot during the pH drop and slowly returns to the level of  $10^{-5}$  M. Additional experiments (not shown here) show that the overshoot is smaller at higher  $\text{Cu}^{2+}$  concentrations and at slower rates of pH lowering. The overshoot followed by a slow response is not due to changes in the liquid-junction potential of the reference electrode. Fast pH changes for a system of two coupled reference electrodes as a function of time only showed changes in EMF of 1-2 mV and the EMF returned to its original value within a few seconds.

The overshoot of the Cu(II)-ISE is most probably due to the mass transport of  $\text{Cu}^{2+}$  over the film layer at the electrode surface against a concentration gradient (Wesselingh and Krishna, 1990). The diffusion of charged species is not regulated only by the concentration gradient but also by an electrical potential gradient made up of the total ionic composition of the solution. Mass transport of charged species is described by the Nernst-Planck diffusion equation. The electrical potential gradient during the pH drop

causes an accumulation of  $\text{Cu}^{2+}$  ions near the membrane surface, giving rise to an overshoot during a certain time period, after which the gradients will level out. In Chapter 8 the diffusion of charged species will be treated more quantitatively.

### 3.4.6. Selectivity factor of the Cu(II)-ISE for interfering ions

Ideally, the potential difference of the ion-selective electrode should be a linear function of the logarithm of the activity of ion  $i$  (equation 3.1). In practice, however, such ideal electrode behaviour is not observed, as was shown in subchapter 3.4.2. In addition to ion  $i$  also interfering ions  $j$  contribute to the measured EMF. Therefore, the effect of interfering ions  $j$  on the electrode potential have to be accounted for. A semi-empirical approach to correct for the interference of other ions is given by the extended Nicolsky-Eisenheim equation (Ammann, 1986):

$$\text{EMF} = E_0 + S \log \left( a_i + \sum_j K_{ij}^{\text{pot}} \left( a_j \right)^{\frac{z_i}{z_j}} \right) \quad (3.5)$$

where  $K_{ij}^{\text{pot}}$  is the selectivity factor and  $a_j$  the activity of the interfering ion  $j$  (M). The selectivity factor is a measure of a preference by the electrode for the interfering ion  $j$  relative to the ion  $i$ . For selective membranes without any interfering effects, the selectivity factor  $K_{ij}^{\text{pot}}$  is zero.

In this chapter, the selectivity factors of interfering cations as a function of pH are determined by the so-called fixed primary ion method, where the concentration of the interfering ion  $j$  is varied at a constant concentration of the primary ion  $i$ . The selectivity factor is then given by (Ammann, 1986):

$$K_{ij}^{\text{pot}} = \frac{a_{i0} * 10^{\frac{\Delta \text{EMF}}{S}} - a_{i0}}{\left( a_j \right)^{\frac{z_i}{z_j}}} \quad (3.6)$$

where  $a_{i0}$  is the activity of the primary ion in absence of the interfering ion,  $a_i$  and  $a_j$  the activity of the primary and interfering ion, and  $\Delta \text{EMF}$  is the difference in EMF with and without the interfering ion. In Table 3.5 the measured  $K_{ij}^{\text{pot}}$  values for several ions are given at variable pH for the Cu(II)-ISE.

**Table 3.5** Selectivity factor of the Cu(II)-ISE for various interfering ions at variable pH

Interfering ion j	pH	$K_{Cu,j}^{pot}$	Interfering ion j	pH	$K_{Cu,j}^{pot}$
Cr <sup>3+</sup>	1	3	Pb <sup>2+</sup>	1	<0.0001
	3	0.002		4.8	0.04
	5	0.001	Zn <sup>2+</sup>	1	0.0004
Fe <sup>3+</sup>	1	0.3		5.5	0.004
	2.3	0.2		Mg <sup>2+</sup>	1
	3	0.02	5.4		0.0009
Al <sup>3+</sup>	1	0.0003	Ca <sup>2+</sup>		1
	3.6	0.0005		4.3	0.0007
	4.7	0.0002		5.5	0.009
Cd <sup>2+</sup>	1	0.0005			
	5.5	0.005			

As stated before, the precipitation reaction of Cu<sup>2+</sup> and S<sup>2-</sup> to CuS<sub>(s)</sub> in the membrane induces the Cu<sup>2+</sup> transfer from the sample solution to the membrane. All ions that precipitate with S<sup>2-</sup> can potentially be interfering ions. The selectivity factor is determined by the free ion activity and not by the total concentrations. Therefore, the selectivity factor for strongly interfering ions (Cr<sup>3+</sup> and Fe<sup>3+</sup>) is lower at higher pH values because the free metal activity of these interfering ions is lower at higher pH due to the formation of soluble metal hydroxide complexes (Table 3.5). Cu(II) forms less strong soluble hydroxide complexes and becomes relevant at higher pH values. For the same reason some interfering ions (Cd<sup>2+</sup>, Pb<sup>2+</sup> and Zn<sup>2+</sup>) have higher selectivity factors at higher pH values because they form less strong complexes with hydroxide as compared to Cu<sup>2+</sup> (Smith and Martell, 1976).

### 3.4.7. Suspension effect

The suspension effect is caused by the different conductivities of solutions with and without suspended/colloidal particles. The difference in conductivity effects the  $E_j$  of the electrode circuit. Quantitative interpretations of this effect are not described in the literature (Ammann, 1996). It particularly occurs in natural systems where colloids are present. To quantify the suspension effect, suspensions of the clay mineral illite and particle-sized organic fractions of biowaste were investigated. The EMF of suspensions was measured during stirring (when the suspension effect should be effective) and after the solution was allowed to settle. No differences in EMF were measured, showing that the suspension effect is negligible for this type of samples.

### 3.4.8. Conclusions

The following general conclusions can be made with respect to the application of the cupric ion-selective electrode for measuring free  $\text{Cu}^{2+}$  activities in natural samples:

1. the response of the electrode is linear up to a total Cu(II) concentration of approx.  $10^{-7}$  M
2. free Cu(II) concentration can be measured to at least  $10^{-14}$  M if the total Cu(II) concentration is higher than  $10^{-6}$  M
3. the response of the electrode shows peculiar behaviour with sudden pH changes, most probably due to Nernst-Planck diffusion in the film layer at the electrode surface
4. changes in the liquid-junction potential have to be considered at low pH and when calibration and sample solutions have different ionic strengths
5. Fe(III) and Cr(III) have a high selectivity factor and thus interfere with the Cu(II) measurement, especially at a low pH; other heavy metals such as Cd(II), Pb(II) and Zn(II) only interfere when the concentration is much higher than the Cu(II) concentration.

The Cu(II)-ISE can be used quantitatively for systems where the composition of the solution is known and no interfering ions are present. These systems are presented in Chapters 6 and 7. The Cu(II)-ISE can only be used qualitatively for less well-defined systems where the composition is not exactly known and interfering ions are present. This application of the ISE will be employed in Chapter 8.

## 3.5. Lab-scale physical separation processes

### 3.5.1. Introduction

The physical separation of components of biowaste by sieving and water elutriation are employed for two purposes:

1. physical characterisation of biowaste: determining the particle size distribution of the organic and inorganic components
2. distribution of heavy metals over the physical entities of the waste.

For the particle size distribution of biowaste, a three-step physical separation process is applied to determine the organic and inorganic fractions of the waste:

1. wet-sieving process; To fractionate biowaste with respect to particle size, a wet-sieving process is used with the following sieve dimensions: 5, 2, 1, 0.5, 0.2, 0.1 and 0.05 mm. The smallest sieve diameter used is 0.05 mm because of practical limitations and because this diameter is commonly used in soil science to distin-

guish between sand and silt. The fraction  $<0.05$  mm consists of silt, clay and organic matter. The fraction  $>0.05$  mm consists of sand, gravel, organic material and other inorganic contaminants, such as glass.

2. water elutriation; The fractions between 0.05 and 2 mm are further separated by a water-elutriation column into an organic fraction and an inorganic fraction. The separation is based on difference in density between the organic fraction (density between 1,100 and 1,400  $\text{kg.m}^{-3}$ ) and the sand fraction (density approx. 2,600  $\text{kg.m}^{-3}$ ). The separation is brought about increasing the upflow velocity of water until the organic fraction is elutriated and the sand remains at the bottom of the elutriation column.
3. sedimentation set-up; The silt and lutum and silt fraction of the fraction  $<0.05$  mm are determined according to Houba et al. (1988).

### 3.5.2. Materials and methods

To obtain a representative sample, approximately 50 litres of biowaste was collected. Very large components and impurities, such as plastics and tins, were removed. To minimise aerobic or anaerobic conversion of the waste, the samples were stored at 4 °C when not directly used. Before fractionation the waste was homogenised in a plastic container and 4 to 5 kg was used for the physical fractionation.

The separation process comprised a wet-sieving process, a water-elutriation process and a sedimentation unit. A presentation of the wet-sieving set-up is given in Figure 3.5. A vibrating sieving apparatus (Retsch Labor-Siebmaschine Type VIBRO) was equipped with stainless-steel sieves of sizes 5.0, 2.0, 1.0, 0.50, 0.20, 0.10 and 0.05 mm (Retsch Analysensiebe). The top sieve of 5 mm was filled with a sample of biowaste, and bidistilled water was sprayed over the sample using a showering device. The top layer was turned over several times until the water running through the 0.05 mm sieve was clear. The material and the top sieve were removed and the procedure was repeated several times. Periodically the material was removed from the other sieves to prevent blocking of the sieves. The total sieving procedure was repeated until 4-5 kg of biowaste had been fractionated. The water and the particles  $<0.05$  mm were collected in an 80-litre container.

The fractions 0.05-0.1, 0.1-0.2, 0.2-0.5 and 0.5-1 mm were exposed to the water elutriation process (Figure 3.5). First, a small part of the column was filled with a particle-sized fraction. Then, bidistilled water was pumped through the bottom of the column and the organic particles were visually separated from the sand fraction by varying the pump water flow. The organic matter coming out at the top of the column (upflow) was collected in a 0.05 mm sieve. The mineral fraction at the bottom (underflow) was

removed periodically by dismantling the column.

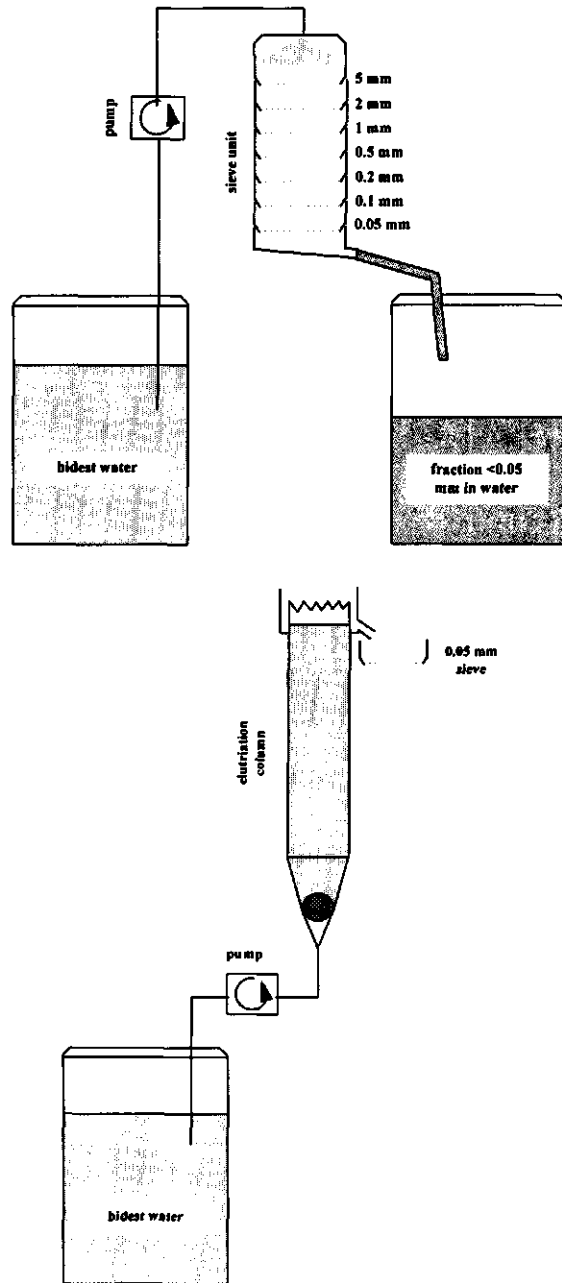


Figure 3.5 Presentation of the wet-sieving set-up (top) and water elutriation set-up (bottom)

The suspended solids <0.05 mm were concentrated by separation in a semi-continuous tubular centrifuge (Sharples) at 50,000 rpm. The solids were resuspended in bidistilled water at a concentration of approx. 2 g.l<sup>-1</sup>. The organic matter of the fraction <0.05 mm was digested by peroxide and the silt and lutum fractions were determined by sedimentation as described by Houba et al. (1988).

### **3.6. Extraction and characterisation of humic acids in biowaste**

#### **3.6.1. Introduction**

Biowaste consists of organic matter of different origin, e.g. vegetables and flowers from kitchens, and grass, leaves, and soil organic matter from gardens. Plant material and soil organic matter contains a large range of organic molecules, ranging from low molecular weight molecules to macromolecular substances.

Plant material is primarily comprised of cellulose, hemicellulose and lignin. The extractives of plant fibres are soluble in organic solvents or water. The extractive part of plant material is made up of a large number of individual compounds of both lipophilic and hydrophilic types and can be regarded as non-structural plant components, almost exclusively composed of extracellular and low molecular weight compounds. The most important organic extractives are terpenoids, steroids, fats, waxes and phenolic constituents such as stilbenes, lignins, hydrolyzable- and condensed tannins, and flavonoids (Fengel and Wegener, 1984).

The nature and content of soil organic matter (SOM) depends on various soil formation factors such as climate, soil type and agricultural practice (Aiken et al., 1985). The major part of SOM is made up of humic substances which are end products of the biological decay of biota residues. They consist of organic acids of low and high molecular weights, i.e. mono-, oligo-, and polysaccharides, proteins, peptides, amino acids, lipids, waxes, polycyclic hydrocarbons and lignin fragments (Saiz-Jimenez, 1992). The resistant organic matter plays a role in the formation of humic acids by bacteria and fungi. Humic acids are the most stable compounds in soil and are slowly degraded. They play an important role in the physico-chemical behaviour of heavy metals in natural systems (Buffle, 1988; Stevenson, 1994).

The amount of humic acids in biowaste and the particle-sized organic fractions of biowaste is determined. In the next subchapters the extraction procedure and some characterisation methods for humic acids are described.



### 3.6.2. Extraction procedure for humic acids

The extraction scheme proposed by the International Humic Substances Society (IHSS) is applied to extract and purify humic substances present in biowaste and its fractions (Aiken et al., 1985). The extraction of fulvic and humic acids is based on their solubility in acid and basic solutions. Fulvic acids are defined as the organic fraction soluble at pH 1; humic acids are soluble between pH 1-13; and the insoluble fraction is called humine. During the last decade, the IHSS has stimulated the standardisation of extraction procedures (Aiken et al., 1985; Hayes et al., 1989). The extraction techniques are in general non-specific and this means that in practice a distinction between non-humic and humic substances cannot always be made (Adani et al., 1997). The scheme for the extraction and purification of humic acids from natural waters is presented in Table 3.6.

**Table 3.6 Extraction procedure for isolation of humic acids from biowaste (Aiken et al., 1985)**

Step	Procedure
1	The sample is dried at 40 °C and homogenised and milled in an agate planet ball mill
2	5 to 10 g of the sample is weighed in a 250 ml polypropylene centrifuge tube, diluted with 0.1 M HCl to a solid-liquid ratio of 1:25. The pH of the solution is adjusted to 1 with 6 M HCl. The mixture is shaken for 1 hour and the suspension allowed to settle. The mixture is centrifuged at 4500 rpm for 20 minutes and the supernatant is separated from the sediment.
3	The sediment is diluted with bidistilled water to a solid-liquid ratio (S/L) of 1:10 and the solution is neutralised with 6 M NaOH. The solution is further diluted to 1:25 with 0.2 M NaOH under nitrogen. The mixture is shaken for 4 hours and allowed to settle overnight. The supernatant is separated from the sediment by centrifugation.
4	The pH of the supernatant is adjusted to 1 with 6 M HCl and allowed to settle for 12-16 hours. The mixture is separated by centrifugation.
5	The sediment is redissolved in 0.1 M KOH to a S/L of 1:25 under nitrogen and the K <sup>+</sup> concentration adjusted to 0.3 M with 2 M KCl. The solution is shaken for 4 hours and allowed to stand overnight. The solution is centrifuged and the sediment is discarded.
6	The supernatant is acidified with 6 M HCl to pH 1 and the solution is allowed to settle overnight and then centrifugated.
7	The sediment is suspended in a solution of 0.1 M HCl and 0.3 M HF and shaken overnight to remove mineral matter.
8	The mixture is centrifuged. The precipitated humic acid is transferred to a dialysis casing and dialysed against bidistilled water until the conductivity has dropped below 5 mS.
9	The humic acid is freeze-dried.

The solid-liquid ratio (S/L) is decreased to 1:25 in order to completely solubilise the humic acids from biowaste.

### 3.6.3. Characterisation of humic acids

The structure, composition and properties of humic substances have been extensively discussed by Stevenson (1994), Buffle (1988) and Schnitzer (1978). Analytical tools to characterise humic acids are, among others, chromatographic separation, functional group analysis, spectroscopic methods, thermal analysis, chemical degradation and mass spectroscopy. In this study the following analytical methods were applied:

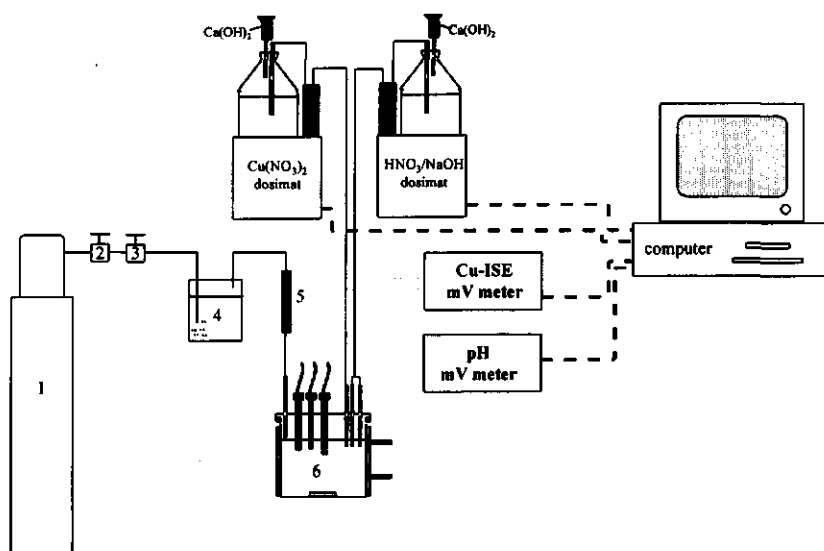
- **UV/VIS spectroscopy:** determines the light absorption in the ultraviolet range (285 nm) and in the visible range (465 and 665 nm) (Stevenson, 1994).
- **elemental composition:** determines the C, H, O and N content of the humic acids (Aiken et al., 1985).
- **gel permeation chromatography:** determines the molecular weight distribution of the humic acids (Buffle, 1988).

### 3.7. Computer-controlled batch titration apparatus

Cu(II) adsorption and desorption experiments were made with a computer-controlled batch titration apparatus as shown in Figure 3.6. The system consisted of a computer (Estate XT), two high-precision burettes (665 Dosimat, Metrohm Ltd.) and two mV meters (691 pH meter, Metrohm Ltd.). The burettes and mV meters were connected to the computer via an RS232 interface and the devices were controlled and registered by software programs written in QuickBasic 4.5. The experiments were conducted in a closed batch system and nitrogen gas was led over the solution to prevent CO<sub>2</sub> absorption from the atmosphere into the solution. With this experimental set-up various types of measurements were made: acid-base titrations, Cu(II) adsorption experiments at constant pH, and kinetic studies of Cu(II) adsorption-desorption. The significant advantages of the computer-controlled titrations over manually-controlled titrations are, amongst others:

- proton and Cu(II) adsorption isotherms at "equilibrium" are controlled by a drift criterion (see Chapter 6); the drift criterion is automatically controlled and registered by the computer
- pH for Cu(II) adsorption isotherms is kept constant at a pre-fixed pH by computer control
- for studying adsorption and desorption kinetics the response as a function of time is relevant; this is automatically controlled and registered by the computer
- computer-controlled handling provides excellent reproducibility of experiments.

## OVERVIEW OF THE SET-UP



## DETAIL OF REACTION VESSEL

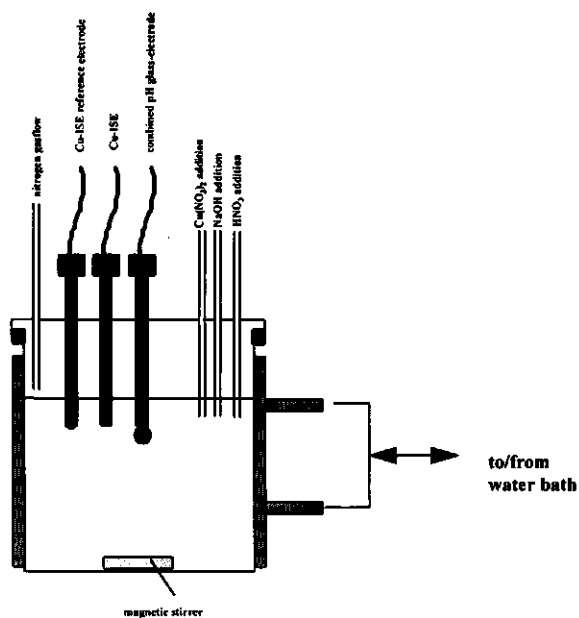


**Figure 3.6** Schematic presentation of the computer-controlled batch system: 1 gas cylinder (99.995%  $N_2$ ); 2 pressure regulator; 3 flow regulator; 4 washing bottle (water); 5  $CO_2$  absorber; 6 titration vessel

### 3.8. Chemicals

All reagents were of analytical grade or better. Water was demineralised and subsequently distilled (bidistilled water) to reduce the background level of heavy metals. When heavy metals were measured, all plastics and glassware were cleaned before use by immersion in 4 M HNO<sub>3</sub> for at least 24 hours.

### 3.9. Results of the characterisation of biowaste

The composition of biowaste varies largely with time of year and place of collection. This subchapter gives a general impression of the physico-chemical composition of biowaste as encountered in this study.

#### 3.9.1. Physical characterisation

Several samples of biowaste of different origin were physically separated as described in subchapter 3.5. The samples of different origin were collected at VAM Wijster, the Netherlands. The fraction <0.05 mm was digested by peroxide and the silt and clay content were determined by sedimentation as described in subchapter 3.5. Table 3.8 gives the results of the physical characterisation.

**Table 3.8** Physical characterisation of biowaste<sup>1</sup>

Component	Content (% of total DM)
<b>organic:</b>	
>5 mm	25-35
1-5 mm	5-10
0.05-1 mm	4-9
<0.05 mm	15-20
soluble	1-5
<b>inorganic:</b>	
>0.5 mm	3-5
sand: 0.05-0.5 mm	20-30
silt: 2-50 µm	4-7
lutum (<2 µm)	2-5

<sup>1</sup> it is assumed that metallic forms of metals are not present in biowaste

The organic fractions >5 mm and 0.5-5 mm were made up of recognisable plant materials such as leaves, grass, branches, grains, grass and vegetables. Microscopic observations showed a distinct cell wall structure. For the organic fractions from 0.05-0.5 mm no identifiable organic material was present and no distinct cell wall structure could be observed. The particles possessed a spongelike structure of partially degraded and humified organic material. The inorganic fraction larger than 0.5 mm comprised small stones, gravel and impurities (such as glass). The inorganic particles of 0.05-0.5 mm consisted of sand and the fraction < 0.05 mm represented a brown-coloured fraction for which it was impossible to segregate the organic from the inorganic material. The soluble fraction consisted of salts and soluble organic material, extracted during the sieving process.

### 3.9.2. Chemical characterisation

Sampling, handling and determination of the total element content were performed as described in subchapter 3.3.2. The water-soluble fraction of the elements was determined after shaking with bidistilled water for 12 hours at a solid-liquid ratio of 1:10. Table 3.9 gives the composition of three biowaste samples of different origin and the composition of a sample made up of biowaste of 9 different origins.

The content of the major cations and some heavy metals in the particle-sized organic fractions, obtained after wet-sieving and water elutriation, are given in Table 3.10.

The IHSS scheme was used to extract humic acid from the total biowaste sample and its organic fractions. The humic acid fraction was purified and dialysed. The humic acid content was determined after freeze-drying. Table 3.11 shows the humic acid content of total biowaste and the particle-sized organic fractions, and the UV/VIS characteristics.

**Table 3.9 Elemental composition of biowaste (in g.kg<sup>-1</sup> DM)**

Element	Purmerend		Lemmer		Zoetermeer		Mixture	
	total	soluble	total	soluble	total	soluble	total	soluble
Na	2.91	2.74	2.20	2.02	1.92	1.68	1.92	1.85
K	7.96	5.91	11.9	9.89	11.4	8.60	9.98	8.26
Mg	20.6	1.81	2.33	1.06	2.66	0.30	5.11	1.04
Ca	37.0	8.51	10.5	4.15	16.3	4.43	16.5	3.31
Fe	8.07	0.01	3.16	0.02	3.43	0.02	4.76	0.01
NH <sub>4</sub>	3.65	0.12	2.23	-	1.53	-	3.18	-
Al	9.19	0.01	2.40	0.02	6.28	0.02	4.27	0.00
Mn	0.13	0.01	0.12	0.04	0.11	0.01	0.12	0.02
Cd <sup>1</sup>	0.50	-	0.26	-	0.26	-	0.36	-
Cu <sup>1</sup>	17.9	-	20.0	-	17.9	-	16.8	-
Pb <sup>1</sup>	26.2	-	73.3	-	30.3	-	61.7	-
Zn <sup>1</sup>	108	-	167	-	88.8	-	136	-
PO <sub>4</sub>	8.11	0.83	5.47	2.13	5.42	1.45	6.03	1.65
Cl	NA	4.50	NA	4.37	NA	4.10	NA	4.17
SO <sub>4</sub>	NA	1.84	NA	1.79	NA	0.90	NA	1.51
CO <sub>3</sub>	37.5		<2		-		10.2	
S total	6.16	2.75	5.66	2.39	5.63	1.51	5.71	2.08
NO <sub>3</sub>	NA	0.0	NA	0.1	NA	0.0	NA	0.01
N-tot	13.4		-		14.9		-	

<sup>1</sup> in mg.kg<sup>-1</sup> DM; NA cannot be determined after aqua regia digestion

**Table 3.10 Cation composition of particle-sized organic fractions**

Fraction (mm)	Na	K	Ca	Mg	Fe	Al	Cu	Pb	Zn	CEC <sup>1</sup> (meq.g <sup>-1</sup> )
	(g.kg <sup>-1</sup> OM <sup>2</sup> )						(mg.kg <sup>-1</sup> OM)			
1-2	0.05	0.19	5.12	0.37	1.24	1.32	20	38	138	0.51
0.5-1	0.03	0.14	4.48	0.37	1.41	1.04	20	32	122	0.45
0.2-0.5	0.08	0.40	6.11	0.79	2.70	2.80	28	94	527	0.86
0.1-0.2	0.07	0.76	8.48	1.29	4.03	6.02	42	232	748	1.46
0.05-1	0.17	1.48	14.9	2.51	4.83	10.6	52	311	982	2.47

<sup>1</sup> CEC (cation exchange capacity) was calculated on basis of the total cation content; <sup>2</sup> OM organic matter

**Table 3.11 Humic acid content and UV/VIS characteristics of total biowaste and the particle-sized organic fractions**

Size (mm)	Content (g.g <sup>-1</sup> OM)	UV/VIS		
		$\epsilon_{285}^1$ (l.g <sup>-1</sup> .cm <sup>-1</sup> )	285/465 <sup>2</sup>	465/665 <sup>2</sup>
total	0.13	4.9	5.4	6.3
2-5	0.12	4.9	6.4	6.5
1-2	0.11	6.7	6.0	6.2
0.5-1	0.10	7.4	5.9	6.7
0.2-0.5	0.11	8.7	5.7	6.7
0.1-0.2	0.13	-	5.3	6.6
0.05-1	0.21	6.3	6.1	6.8
<0.05	0.23	6.4	5.9	5.9

<sup>1</sup> extinction coefficient at 285 nm; <sup>2</sup> ratio of extinction at two wavelengths

## References

- Adani, F.; Genevini, P. L.; Gasperi, F.; and Zorzi, G. 1997. Organic Matter Evolution Index (OMEI) as a Measure of Composting Efficiency. *Compost Science & Utilization* 5:53-62
- Aiken, G. R.; McKnight, D. M.; Wershaw, R.L.; and MacCarthy, P. (eds.) 1985. Humic substances in soil, sediment, and water: geochemistry, isolation and characterization. New York, USA; John Wiley & Sons
- Ammann, D. 1986. Ion-Selective Microelectrodes, Principles, Design and Application. Berlin, Springer-Verlag
- Avdeef, A.; Zabronsky, J.; and Stuting, H. H. 1983. Calibration of Copper Ion Selective Electrode Response to pCu 19. *Anal. Chem.* 55: 298-304
- Buffle, J. 1988. Complexation reactions in Aquatic Systems - An Analytical Approach. Chichester, Ellis Horwood Limited
- CBR (Community Bureau of Reference, Commission of the European Communities) 1985. The Certification of the Contents of Compounds in a Sewage Sludge of Domestic Origin. BCR Report No.144., EUR 8836 EN
- Fengel, D. and Wegener, G. 1984. Wood: chemistry, ultrastructure, reactions. Berlin: De Gruyter
- Hayes, M.H. B.; MacCarthy, P.; Malcolm, R.L.; Swift, R.S. (eds.) 1989. Humic substances II. In search of structure. Chichester, John Wiley & Sons Ltd.
- Houba, V. J. G.; Lee, J. J. van der; Novozamsky, I.; and Walinga, I. 1988. Soil and Plant Analysis. Part 5: Soil Analysis Procedures. Wageningen, The Netherlands: Department of Soil Science and Plant Nutrition, Wageningen Agricultural University
- Lustenhouwer, J. W. A. 1991. Characterisation of Compost with Respect to its Content of Heavy Metals, PhD thesis. Amsterdam, University of Amsterdam.
- Lustenhouwer, J. W. A.; Hin, J. A.; Maessen F.; and Den Boef G. 1991a Characterization of Compost with Respect to its Content of Heavy Metals. Part I: Sample Digestion and ICP-AES Analysis. *Intern. J. Environ. Anal. Chem.* 39: 209-222
- Lustenhouwer, J. W. A.; Hin, J. A.; Maessen F.; and Den Boef G. 1991b. Characterization of Compost with Respect to its Content of Heavy Metals. Part II: Sample Preparation, *Intern. J. Environ. Anal. Chem.* 39:391-400
- Lustenhouwer, J. W. A.; Hin, J. A.; Maessen F.; Den Boef G.; and Kateman G. 1991c. Characterization of Compost with Respect to its Content of Heavy Metals. Part III: Precision of the Total Analytical Procedure. *Intern. J. Environ. Anal. Chem.* 44:103-115
- Martell, A. E.; and Smith, R. M. 1977. Critical Stability Constants, Vol. 3: Other organic Ligands. New York, Plenum Press
- McGrath, S.P. 1986, Experimental Determinations and Computer Predictions of Trace Metal Ion Concentrations in Dilute Complex Solutions. *Analyst* 111: 459-465
- Newman, J. 1973. Electrochemical Systems. Englewood Cliffs, N.J., Prentice-Hall, Inc.
- Saiz-Jimenez, C. 1992. Applications of pyrolysis-gas chromatography/mass spectrometry to the study of soils, plant materials and humic substances. A critical appraisal. In: Humus, its structure and role in agriculture and environment, Kubat, J. (ed.). Amsterdam, Elsevier Science Publishers
- Sanders, J. R.; and McGrath, S.P. 1988. Experimental measurements and computer predictions of copper complex formation by soluble soil organic matter, *Environ. Poll.* 49:63-76



- Schnitzer, M. 1978. In: Soil Organic Matter, Schnitzer M.; and Khan S.U. (eds.). Amsterdam, Elsevier
- Smith, R. M.; and Martell, A. E. 1976. Critical Stability Constants, Vol. 4: Inorganic Ligands. New York:Plenum Press
- Stevenson, F. J. 1994. Humic Chemistry: Genesis, Composition, Reactions. New York, John Wiley & Sons
- Welz, B. 1985. Atomic Absorption Spectroscopy. Weinheim: VCH
- Wesselingh, J. A.; and Krishna, R. 1990. Mass Transfer. Chichester: Ellis Horwood Limited

## 4. Sources of heavy metals in biowaste

### 4.1. Introduction

In the Netherlands, biowaste (the organic fraction in municipal solid waste of biological origin) is separately collected at the source and composted (Lustenhouwer, 1987; Roosmalen & Langerijt, 1989; VROM, 1992). As discussed in subchapter 1.2, the recycling of biowaste can possibly be frustrated because the heavy metal content of the compost does not always meet the legal criteria for compost as laid down in the BOOM decree on the quality and use of other organic fertilisers (SDU, 1991). In this chapter, the heavy metal content of biowaste is compared with the natural background content of heavy metals in the different constituents of biowaste. On the basis of this comparison it can be established whether biowaste is contaminated with heavy metals. The comparison can also assess whether the collection of various biowaste components with an elevated heavy metal content should be prevented in future in order to reduce the heavy metal content of biowaste.

Biowaste is composed of the organic waste products from indoors and outdoors. The indoor fraction is composed of organic matter collected in the kitchen (e.g. food remainders and coffee filters) and indoor plant material, such as flowers and houseplants. The outdoor fraction is mostly collected in gardens and mainly consists of leaves, grass and branches, but also of garden topsoil. In this way soil components can contribute to biowaste.

In this study the heavy metal content (Cd, Cu, Pb and Zn) of the particle-sized fractions of biowaste is determined. For this, an experimental set-up was developed on a lab-scale to separate the physical entities of biowaste. The fractionation is based on differences in the size and density of the particles. The set-up comprises a wet-sieving process followed by a water-elutriation step. In this way organic and inorganic fractions of various particle sizes are obtained. The heavy metal content and organic matter content of these fractions are determined. On the basis of particle size and visual appearance, the particle-sized fractions are assigned to various indoor and outdoor origins of the waste.

The heavy metal content of the various fractions in biowaste is compared with natural background contents of heavy metals in the constituents of biowaste, i.e. food products, plant material, soil organic matter and soil minerals. The background contents are obtained by collecting literature data on the natural background content of heavy metals in fruit, vegetables, flowers, house plants, leaf tissue, needles, grass and surface soils.

## **4.2. Materials and methods**

Four samples of biowaste were collected at VAM Wijster. The samples originated from Zaandam, Purmerend, Wolvega and an unknown location. One sample of biowaste was collected at the central collection containers baskets for biowaste at an apartment building in Wageningen.

The fractionation of biowaste was performed by a two-step separation process, wet-sieving followed by water elutriation, as described in subchapter 3.5. The wet-sieving process separated biowaste into size fractions of >5, 1-5, 0.5-1, 0.2-0.5, 0.1-0.2, 0.05-0.1 and <0.05 mm. The fractions of 0.5-1, 0.2-0.5, 0.1-0.2 and 0.05-0.1 mm were subsequently fractionated by water elutriation into upflow and underflow fractions. The upflow largely consisted of organic matter, and the underflow was mainly comprised inorganic matter. The fractions within a particular range of particle size are specified as particle-sized organic and inorganic fractions.

The obtained particle-sized organic and inorganic fractions were dried at 105 °C. The organic matter content of fractions was determined by ashing the dried samples at 550 °C. The heavy metal content of the fractions was determined by AAS after aqua regia digestion of the dried samples as described in subchapter 3.3.

## **4.3. Results**

The raw data of the results of the two-step separation process for the five biowaste samples are given in Appendix 4A. It was assumed that the sample from the rural village of Wolvega is representative of outdoor biowaste. The sample collected at the central collection containers for biowaste at an apartment building in Wageningen was assumed to be characteristic of indoor biowaste. The discrepancy between total mass balances of dry matter, organic matter and heavy metals before and after the separation process was 10-20%. This is acceptable, considering the methods used and the heterogeneity of biowaste and the particle-sized fractions. It was assumed that the particle-sized fractions of the biowaste were not disrupted during the separation processes and that heavy metals were not significantly redistributed among the particle-sized fractions. From the obtained fractions, the mass distribution as a function of particle size was calculated for the organic and inorganic part of the waste. For this an average ash content of 5% for organic matter (Houba et al., 1991) and of 100% for inorganic matter was assumed. The results of the calculations are presented in Table 4.1. Integral biowaste is defined as the average composition of total biowaste, i.e. the average results for all studied samples. The organic matter content of the upflow and underflow fractions from 0.05 to 1 mm (see Appendix 4A) shows that the separation by water elutriation in an organic upflow and an inorganic

underflow is not complete. This is due to the overlap in sedimentation velocity of large organic particles and smaller inorganic particles within one specific particle-sized fraction.

**Table 4.1 Average distribution of organic and inorganic fractions in biowaste (% of total dry matter)<sup>A</sup>**

Fraction (mm)	Integral		Indoor		Outdoor	
	organic	inorganic	organic	inorganic	organic	inorganic
integral	47 ± 15	52 ± 19	83	17	39	61
>5	25 ± 5	7 ± 4	48.9	7.6	19	6
1-5	3 ± 1	4 ± 3			2.0	2.0
0.5-1	4 ± 3	5 ± 2	21.4 <sup>1</sup>	2.6 <sup>1</sup>	0.8	2.2
0.2-0.5	3 ± 1	23 ± 9			5.4	35.6
0.1-0.2	<1	3 ± 3	6.6 <sup>2</sup>	1.4 <sup>2</sup>	0.4	4.6
0.05-0.1	1 ± 1	3 ± 2			0.5	2.5
<0.05	11 ± 6	6 ± 3			6.9	7.1
liquid <sup>3</sup>	5 ± 2	1 ± 1	14	1	4	2

<sup>A</sup> due to the heterogeneity of biowaste and the fractions of biowaste and the experimental method of fractionation, the sum of the organic and inorganic fractions does not add up to exactly 100% ; <sup>1</sup> fraction 0.2-2 mm ; <sup>2</sup> fraction <0.2 mm ; <sup>3</sup> fraction found in the water after centrifugating the fraction <0.05 mm (see subchapter 3.5)

If it is assumed that the heavy metal content of organic and inorganic particles is constant within a single particle-size range, the heavy metal content of the organic and inorganic particle-sized fraction can be calculated with the following relations:

$$HVM_{up} = x_{org}HVM_{org} + x_{in}HVM_{in} \quad (4.1)$$

$$HVM_{un} = x_{org}HVM_{org} + x_{in}HVM_{in}$$

where  $HVM_{up}$  and  $HVM_{un}$  are the heavy metal content (in  $mg.kg^{-1}$  DM) of the upflow and underflow fraction,  $x_{org}$  and  $x_{in}$  are the weight fractions of the organic and inorganic parts, and  $HVM_{org}$  and  $HVM_{in}$  are the heavy metal content (in  $mg.kg^{-1}$  DM) of the organic and inorganic particles. Table 4.2 presents the results of the calculations based on equation 4.1 for the data of Table 4.1. The fractions >5 and 1-5 mm could not be separated into an organic and an inorganic part by the lab-scale elutriation set-up due to the limited capacity of the elutriation column. The fraction <0.05 mm could not be separated into an organic and an inorganic fraction because the inorganic and organic part were present in aggregates. For the fractions which could not be separated, the total content is given.

**Table 4.2 Heavy metal content of the particle-sized organic and inorganic fractions of biowaste (in mg.kg<sup>-1</sup> DM)**

Fraction (mm)	Total				Organic				Inorganic			
	Cd	Cu	Pb	Zn	Cd	Cu	Pb	Zn	Cd	Cu	Pb	Zn
integral	0.36	17	62	136								
>5	0.25	17	39	117								
1-5	0.29	15	57	103								
0.5-1					0.3	20	54	137	0.07	6	52	40
0.2-0.5					0.8	32	109	235	0.02	2	22	19
0.1-0.2					0.9	43	181	323	0.04	3	12	18
0.05-0.1					1.2	41	170	280	0.21	5	27	43
<0.05	0.9	73	133	338								

Table 4.3 compares the mean heavy metal content of the fractions in integral biowaste to the heavy metal content of fractions of indoor biowaste. For the experiment with biowaste from indoors, fewer screens were used and no water-elutriation step was carried out. The results for integral biowaste for this type of size classification were recalculated from Tables 4.1 and 4.2.

**Table 4.3 Comparison of the heavy metal content of the particle-sized organic fractions of integral and indoor biowaste (in mg.kg<sup>-1</sup> DM)**

Fraction (mm)	Integral				Indoor			
	Cd	Cu	Pb	Zn	Cd	Cu	Pb	Zn
>5	0.25	17	39	117	0.05	7	10	31
2-5	0.29	15	57	103	0.19	10	13	37
0.2-2	0.85	32	110	230	0.20	16	18	42
<0.2	1.0	60	150	330	0.24	44	52	55

## 4.4. Discussion

### 4.4.1. Contribution of indoor and outdoor biowaste to integral biowaste

The results for biowaste collected at an apartment building in Wageningen (Table 4A.5) show that the organic matter content of biowaste from such buildings is high. Taking into account the inorganic content of organic matter, almost 90% of biowaste from apartment buildings is of organic origin (see Table 4.1). Biowaste from villages (Wolvega, Table

4A.2) is much lower in organic matter content, indicating that a large part of the waste is made up of inorganic matter. This is due to the presence of soil minerals in the top layer of gardens, which are collected together with the organic matter in the gardens.

The composition of biowaste strongly depends on the type of household. In cities there are relatively more apartment buildings than in rural villages, which consist of low-rise houses (Beek et al. 1989; Cornelissen, 1989). Biowaste collected at apartment buildings mainly contains food remainders while a large part of biowaste collected at low-rise houses originates from gardens. Indoor organic waste consists of kitchen waste, flowers and house plants. The amount and composition of this waste is virtually independent of the time of year and the place of collection. Outdoor waste comprises, among other things, leaves, branches, grass and the topsoil of gardens, and its amount and composition varies greatly with time and place.

A study by TAUW (1990) in which components in biowaste were separated by hand showed that the biowaste comprised 10% indoor waste, 50% garden waste and a fraction of 40% which was composed of unrecognisable small particles. This fraction probably originates from the topsoil of gardens. A study in Germany (Mühl und Abfall, 1992) showed that on the average 200-250 kg of biowaste per inhabitant per year is collected in villages as opposed to 50 kg of biowaste per inhabitant per year at apartment buildings. Both studies indicate that approx. 20% of biowaste originates from indoor collection and 80% is collected outdoors.

When biowaste is subjected to a wet-sieving process, the different fractions of indoor and outdoor waste are separated and distributed over the screens. For indoor waste (Table 4.1) 70% of the organic part is larger than 1 mm, while for villages only 40-50% is larger than 1 mm. A large part of the organic fraction from villages shows up in the smaller organic fractions and the fraction <0.05 mm. The difference is caused by the different composition of the organic waste. Indoor organic waste mainly consists of food remainders and plants, while a large part of the organic matter from gardens contains soil organic matter from the topsoil of gardens. The amount of soluble organic matter is high for apartment buildings (Table 4.1) because a significant fraction of food remainders are readily dissolved in water. The soluble fraction is much lower for garden waste because grass, leaves, branches, and soil organic matter contain low contents of water-soluble components.

The suggestion that a large part of garden waste originates from the topsoil is confirmed by the large amount of sand found in it. Approximately 40% of biowaste from villages consists of sand, compared to only 3% for apartment buildings (Table 4.1). The fact that a large amount of soil is collected in gardens is also apparent from the large fraction <0.05 mm which is made up of silt, clays and humus. The fraction <0.05 mm is small for biowaste collected indoors (Table 4.1).

The large inorganic content of the fraction >5 mm for integral biowaste (see Table 4.1 and the tables in Appendix 4A) indicates that the separation by wet-sieving is incomplete because inorganic components >5 mm are supposed to be absent from indoor and outdoor organic waste. The high inorganic content of the fraction >5 mm is caused by small organic and inorganic particles being enclosed within the matrix of large organic particles which are not fully separated by the wet-sieving process. Despite the incomplete separation by the 5 mm screen, the results give a good indication of the contribution of the various components to biowaste.

#### 4.4.2. Natural background-content of heavy metals in the original components of biowaste

The components of biowaste collected indoors and outdoors can be roughly divided into four groups:

1. organic matter comprising the food remainders collected indoors, such as fruit and vegetable waste and prepared food products
2. organic matter in biowaste consisting of plant material not intended for consumption, such as flowers, house plants, grass, leaves, branches, etc.
3. organic matter made up of more or less degraded and humified organic matter present in the humus layer of the topsoil of gardens
4. soil minerals and humus present in the topsoil of gardens.

Various literature sources were consulted to obtain an idea of the natural background concentration of heavy metals in the above-mentioned classes of components. The results are summarised in Table 4.4.

**Table 4.4** Range of heavy metal content (in mg.kg<sup>-1</sup> DM) of four classes of components collected in biowaste (mean value between brackets)

metal	Indoor organic	Outdoor organic	Humus layer <sup>3</sup>	Soil <sup>6</sup>		
	waste <sup>1,2,3</sup>	waste <sup>4</sup>		sand	loess	clay
Cd	0.01-2 (0.3)	0.03-3 (0.4)	0.1-7 (2)	0.01-1 (0.2)	0.2	0.4
Cu	1-73 (7)	3-29 (8)	2-75 (20)	1-70 (12)	7-100 (25)	7-70 (30)
Pb	0.1-10 (1)	1-100 (5)	1-350 (100)	2-70 (15)	10-30 (20)	10-70 (30)
Zn	7-100 (45)	10-300 (60)	10-1000 (150)	5-160 (35)	20-10 (55)	20-220 (70)

<sup>1</sup> data of fruits, vegetables and some data on flowers and houseplants (Houba, 1991; Nriagu, 1978; Nriagu, 1979; Nriagu, 1980); <sup>2</sup> data of food products (CCRX, 1985; CCRX, 1990); <sup>3</sup> separately collected food remainders from households (Boxtel, 1982); <sup>4</sup> data of grass, leaf tissues, needles, and clover (Crump and Barlow, 1982; Fiedler, 1988; Guha and Mitchell, 1966; Kabata-Pendias and Pendias, 1985; Smith, 1973); <sup>5</sup> humus layer of leaves and needles (Coughtrey et al., 1979; Nilsson, 1972; Van Hook et al., 1977); <sup>6</sup> natural background levels of heavy metals in surface soils (Kabata-Pendias and Pendias, 1985; Lexmond and Edelman, 1987)

The heavy metal content of food products is low especially for those heavy metals which are not essential nutrients, such as Cd and Pb. The heavy metal content of plant material from gardens is slightly higher in comparison to indoor waste, because outdoor plant material is more susceptible to anthropogenic contamination. An increased heavy metal content of plants can take place by foliar uptake and by root uptake from contaminated soil (Kabata-Pendias and Pendias, 1985). Besides that, deposited heavy metals can be adsorbed to the plant exterior and be attached to the outside of plant tissue as particulates (Garber, 1970). Various studies show that plants grown in the vicinity of industrial activities (Dueck et al., 1984; Little and Martin, 1972) and those grown in urban gardens can have increased heavy metal contents, especially Pb near roadsides (Rodriguez-Florez and Rodriguez-Castellon, 1982; Selmer-Olson and Myhre, 1970; Sommer et al., 1971). Also plants grown on sludge-irrigated farmland have increased levels of heavy metals (Kabata-Pendias and Pendias, 1985).

The topsoil of gardens is built up of a humus layer and soil components. The heavy metal content of the humus layer is much higher than that of fresh plant material. The degradation of organic matter in the top layer of soil leads to a concentration of heavy metals. Moreover, heavy metals from atmospheric deposition accumulate in the humified organic matter (Nilsson, 1972).

The natural background concentration of heavy metals in soil depends on the mineral composition of the parent material and on the natural soil-formation processes (Kabata-Pendias and Pendias, 1985). The natural background content of heavy metals in soil increases with increasing lutum and organic matter content (Lexmond and Edelman, 1987). This is the result of the higher content of heavy metals in secondary minerals and the higher specific surface and higher binding strength of surface-specific groups of secondary minerals and organic matter. The main routes for soil contamination by heavy metals are atmospheric deposition and the application of fertilisers, pesticides, and sewage-derived materials (Kabata-Pendias and Pendias, 1985).

On the basis of the physical and chemical characterisation of biowaste and the visual and microscopic inspection of the fractions in biowaste (described in subchapter 3.9), the particle-sized fractions of biowaste can be divided into:

1. organic fraction >1 mm: fresh plant material, food remainders
2. organic fraction 0.05-1 mm: more or less humified organic matter
3. inorganic fraction 0.05-0.5 mm: sand
4. organo-mineral fraction <0.05 mm: silt, clay, humus.

The soluble fraction is made up of soluble organic matter and minerals. The Cd, Cu, Pb and Zn content of the fraction >5 mm originating from apartment buildings is in good agreement with the content of heavy metals in indoors and outdoors organic matter (compare Tables 4.3 and 4.4). The organic fractions >1 mm of integral biowaste show



increased levels of all metals; especially the content of Pb and Zn is higher. This is mainly caused by the incomplete physical separation of the larger fractions, as discussed in subchapter 4.4.1. Smaller particles with higher heavy metal content are trapped in the larger fractions, leading to an increased heavy metal concentration. It is also possible, but very unlikely, that the fractions are contaminated by contact with other components of biowaste which have higher heavy metal levels.

For biowaste from apartment buildings, the heavy metal content of the organic fractions 0.05-1 mm slightly increases as the particle size decreases (Table 4.3). However, the increase is not as drastic as observed with the organic fractions 0.05-1 mm of integral biowaste (Tables 4.2 and 4.3). The values measured in the organic fraction 0.05-1 mm cannot be attributed to fresh plant material from indoors and outdoors. The organic fractions within the size range 0.05-1 mm in integral biowaste most probably originate from the humus layer and the topsoil in gardens. This is confirmed by the literature values for heavy metals in the humus layer, which are in good agreement with the values found in these organic fractions.

On the basis of visual appearance, the inorganic fraction from 0.05-0.5 mm is completely made up of sand. The Cd, Cu, Pb and Zn content of these fractions is lower than measured for sandy soils (compare Tables 4.3 and 4.4). This is due to the wash-out of small amounts of silt, clays and organic matter which are generally present in sandy soils.

The particle-sized fraction <0.05 mm is made up of the humus layer and soil components, i.e. lutum, silt and soil organic matter (or humus). The levels in these fractions are in good agreement with the heavy metal contents in soil with high contents of lutum and humus (Kabata-Pendias and Pendias, 1985; Lexmond and Edelman, 1987).

A comparison of the heavy metal content of the biowaste fractions obtained after physical fractionation (Tables 4.2 and 4.3) and literature data on the natural background content of the original components of biowaste (Table 4.4) shows that the heavy metal content of the physically separated fractions in biowaste corresponds very well with the natural background concentrations of heavy metals in the original biowaste components. Therefore, it can be concluded that the heavy metal content of biowaste is not additionally increased due to contamination from various sources.

#### **4.4.3. Calculation of the heavy metal content of biowaste-derived-compost**

The good agreement between heavy metal content of biowaste fractions and the original components of biowaste validates the calculation of the heavy metal content of biowaste-derived compost on the basis of the heavy metal content of the original components of biowaste. For this, we have to take into account the concentration of heavy metals due to

the degradation of organic matter during composting. The concentration factor (CF) for heavy metals during composting is a function of the initial organic matter content and organic matter degradation:

$$CF = \frac{100}{100 - OM_{ini} - \frac{OM_{deg}}{100}} \quad (4.2)$$

where  $OM_{ini}$  is the initial organic matter content (in % of DM) and  $OM_{deg}$  is the organic matter degradation during composting (in % of  $OM_{ini}$ ). It is assumed that heavy metals do not leach from the biowaste during composting. In Figure 4.1 the concentration factor is shown as a function of organic matter degradation for several initial organic matter contents.

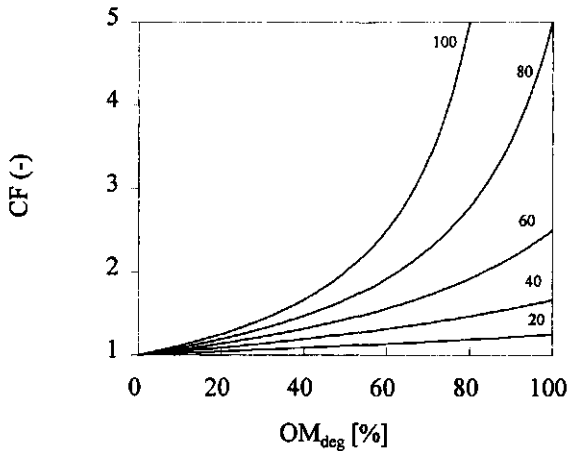


**Figure 4.1** Concentration of heavy metals during composting of biowaste for various initial organic matter contents (20, 40, 60, 80 and 100%)

The degradation rate of organic matter during composting depends on the composition and structure of the organic matter. Compounds such as carbohydrates, hemicellulose and lipids are easily biodegradable (Schlegel, 1993). Cellulose is also easily biodegradable, but the degradation of cellulose is partially inhibited when it is incorporated in the lignocellulosic complex (Tong et al., 1990). Lignin is considered to be recalcitrant under aerobic and anaerobic conditions in the short term (Schlegel, 1993).

Composting or digestion results in a high concentration factor for food remainders (e.g. lettuce, cabbage, potatoes) because they are largely made up of biodegradable organic matter. Plant material from gardens (e.g. branches, leaves, grass and flowers) on the other hand will have a low concentration factor due to its high lignocellulosic content (Tong et

al., 1990; Chinoweth et al., 1992). Organic matter originating from the humus layer of soil is already degraded and humified to a large extent and will have a concentration factor close to 1. Assuming an average concentration factor of 2 for fresh indoor waste and of 1.2 for outdoor waste results in the following heavy metal contents in compost derived from:

- fresh plant material: Cd: 0.75, Cu: 5, Pb: 6 and Zn: 100 mg.kg<sup>-1</sup>
- the humus layer: Cd: 2.4, Cu: 24, Pb: 120 and Zn: 180 mg.kg<sup>-1</sup>

For these calculations the natural background contents from Table 4.4 were used. This shows that the production of clean compost (see Table 1.2) from fresh plant material is critical with respect to Cd and Zn. It is not possible to produce compost from organic matter originating from the humus layer. Fortunately, the presence of sand significantly reduces the heavy metal content of biowaste-derived composts because the natural background concentration is low and sand is not degraded during composting. Without the presence of sand in biowaste, compost would not meet the legal standards of BOOM.

An example can show the discrepancy between the BOOM decree and the natural background content of heavy metals in fresh indoor waste: the fate of lettuce during composting. Lettuce with an initial organic matter content of 90% and Cd levels of 0.7-1.0 mg.kg<sup>-1</sup> DM (Houba et al., 1991) is easily degraded during composting. A degradation of 80% of the organic matter results in a heavy metal concentration factor of 4. This means that lettuce will have a final Cd content of 3-4 mg.kg<sup>-1</sup> DM in compost. With respect to the legal standards of Cd (compare with Table 1.2, BOOM), lettuce should be regarded as a major contaminant in biowaste.

The examples show that there is a conflict between two government policies:

1. preventing the accumulation of heavy metals in the soil (BOOM decree)
2. promoting the recycling and reuse of organic waste streams (National Environmental Policy Plan).

The legal standards for heavy metals in compost as laid down in the BOOM decree are based on the recommendations made by the Technische Commissie Bodembescherming concerning the quality of soil (Ferdinandus, 1989). The reference point of these recommendations is the demand that the delivery of heavy metals (through precipitation, deposition, artificial fertilisers and animal manure) and the discharge of heavy metals (through uptake by plants and leaching to the groundwater system) in the soil system should be in balance. However, the legal demands for heavy metals apply only to composts derived from so-called other organic manure, as laid down in the BOOM decree. It is also known that animal manure and artificial fertilisers contribute significantly to the heavy metal content of the soil (Kabata-Pendias and Pendias, 1985).

However, the dosage of animal manure is limited only with respect to the total phosphate content as laid down in the BGDМ decree (Besluit Gebruik Dierlijke Meststoffen (SDU, 1987)).

To preserve optimal soil conditions for agricultural use, the organic carbon content of the topsoil should be kept at a constant level by dosing with organic matter. The degradation rate of organic matter in the soil depends on the type of organic matter which is dosed. The addition of a soil improver is more effective when it contains more stable organic matter. The stable organic matter is expressed by the effective organic carbon content: the higher the effective organic carbon content, the less organic matter degraded in the soil (Janssen, 1984). The effective organic matter content is substantially higher for biowaste-derived compost than animal manure (Oogst, 1997).

To guarantee an optimal quality of the soil, all types of fertilisers and soil improvers have to be treated equally with respect to the supply of macronutrients (P, K), organic carbon and heavy metals. Van Erp and Evers (1995) showed that for the amount of effective organic carbon dosed (in kg per ha), the heavy metal and phosphate dosage to the soil is much lower for biowaste-derived composts than for various types of animal manure.

#### **4.5. Conclusions**

The physical fractionation of biowaste by wet-sieving and water elutriation on a lab-scale gives a clear separation of the biowaste into its physical entities. The size fractions obtained after classification can roughly be assigned to the following components:

- |                                     |  |
|-------------------------------------|--|
| 1. fraction >1 mm:                  | fresh plant material and food remainders   |
| 2. organic fractions 0.05-1 mm:     | partly decayed and humified organic matter |
| 3. inorganic fractions 0.05-0.5 mm: | sand                                       |
| 4. fraction <0.05 mm:               | silt, clay and humus                       |

Surprisingly, a large amount of biowaste is not organic but is made up of soil minerals; this is because approx. 80% of biowaste is collected outdoors, i.e. in gardens. The collection of biowaste from gardens introduces a substantial amount of soil components into biowaste. For biowaste collected in villages, soil minerals make up more than 50% of the total. The amount of soil minerals is very low when the biowaste comes from indoor-collected organic waste.

The heavy metal content in the fractionated physical entities of biowaste corresponds with the natural background concentration of the components of which they are composed. The heavy metal content of fresh plant material and food remainders is very low. The heavy metal content of partly decayed and humified organic matter originating from

the humus layer of soils is significantly higher. The measured concentrations are, however, the normal background concentrations found in humus layers. The soil minerals originating from gardens contribute to the sand fraction and to the fraction  $<0.05$  mm in biowaste. The levels found in sand of biowaste are natural background values found for sandy soils, and the metal content levels found in the fraction  $<0.05$  mm are natural background concentrations found in soils with high humus and lutum contents.

The literature survey shows that heavy metal contamination could be introduced by the collection of outdoor waste originating from industrial and urban regions. However, the results do not indicate that biowaste is contaminated by anthropogenic sources.

A comparison of the BOOM standards and the theoretical calculations of heavy metal contents in biowaste-derived compost shows that there is a conflict between the two government policies of (1) protecting soil systems and (2) promoting the recycling and reuse of solid organic waste streams. It is postulated that the protection of soil systems could be better guaranteed if the input of stable organic matter, phosphate and heavy metals were to be evaluated for all fertiliser inputs, i.e. animal manure, various types of compost and artificial fertilisers.

There are some restrictions with respect to the laboratory procedure on such a small scale. The question is whether one or two samples are representative of biowaste, because the composition of biowaste varies strongly depending on time and place. A complementary study in which sampling of the indoor and outdoor waste at the source is performed would be preferable. In this way, the effect of the type of household, place of collection and time of year on the composition and heavy metal content of biowaste could be studied in more detail. Studies of the heavy metal content of gardens located in different areas could reveal possible effects of atmospheric deposition near industrial regions or roadsides. Collection throughout the year and from different types of households would give an indication of the variation of composition of biowaste. This type of approach, however, would have been too extensive and too expensive to be executed within the framework of this dissertation.

**Appendix 4A Results of the physical fractionation of biowaste****Table 4A.1 Mass distribution and heavy metal content for biowaste sample from unknown source**

Fraction (mm)	Contribution (on DM basis)	OM (% DM)	Heavy metal content (mg.kg <sup>-1</sup> DM)			
			Cd	Cu	Pb	Zn
total		47	0.31	20	54	154
>5	22	85	0.1	15	30	130
2-5 organic	0.5	93				
2-5 inorganic	1	10				
1-2 organic	1	91	0.24	20	5	111
1-2 inorganic	2	24				
0.5-1 organic	8	95	0.14	10	39	67
0.5-1 inorganic	4	5	0.09	9	67	48
0.2-0.5 organic	3	83	0.45	30	63	169
0.2-0.5 inorganic	22	1	0.03	2	14	21
0.1-0.2 organic	1	70	0.6	34	127	194
0.1-0.2 inorganic	7	0	0.04	2	12	18
0.05-0.1 organic	2	54	0.53	26	117	168
0.05-0.1 inorganic	2	2	0.22	6	30	48
<0.05	24	59	0.87	53	194	388

**Table 4A.2 Mass distribution and heavy metal content for biowaste sample from Zaandam**

Fraction (mm)	Contribution (on DM basis)	OM (% DM)	Heavy metal content (mg.kg <sup>-1</sup> DM)			
			Cd	Cu	Pb	Zn
total	-	51	0.34	18	42	180
>5	60	77	0.25	13	39	114
1-5 organic	3	91	0.37	16	51	136
1-5 inorganic	2	15				
0.5-1 organic	3	87	0.39	20	62	154
0.5-1 inorganic	5	5	0.09	7	34	62
0.2-0.5 organic	2	78	0.79	23	96	198
0.2-0.5 inorganic	20	1	0.04	2	24	25
0.1-0.2 total	0.5	9				
0.05-0.1 organic	2	68	1.62	29	117	236
0.05-0.1 inorganic	1	2				
<0.05	17	70	1.68	66	152	391

**Table 4A.3 Mass distribution and heavy metal content for biowaste sample from Purmerend**

Fraction (mm)	Content (on DM basis)	OM (% DM)	Heavy metal content (mg.kg <sup>-1</sup> DM)			
			Cd	Cu	Pb	Zn
total	-	62	0.41	15	50	154
>5	32	70	0.34	16	43	148
1-5 organic	4	79	0.29	16	66	139
1-5 inorganic	8	8	0.4	6	35	
0.5-1 organic	4	85	0.31	20	54	145
0.5-1 inorganic	8	4	0.06	3	28	33
0.2-0.5 organic	4	61	0.71	20	91	153
0.2-0.5 inorganic	11	1	0.02	5	41	19
0.1-0.2 total	0	0				
0.05-0.1 organic	3	69	0.56	23	107	184
0.05-0.1 inorganic	5	8				
<0.05	20	69	1.02	34	121	295

**Table 4A.4 Mass distribution and heavy metal content for biowaste sample from Wolvega**

Fraction (mm)	Content (on DM basis)	OM (% DM)	Heavy metal content (mg.kg <sup>-1</sup> DM)			
			Cd	Cu	Pb	Zn
total	-	39	0.28	17	58	136
>5	25	76	0.2	13	43	89
1-5 organic	2	79	0.14	18	79	129
1-5 inorganic	2	22				
0.5-1 organic	1	76	0.26	23	61	133
0.5-1 inorganic	2	4	0.07	7	81	33
0.2-0.5 organic	9	40	0.28	17	64	130
0.2-0.5 inorganic	32	0	0.02	1	13	17
0.1-0.2 organic	1	37	0.43	18	82	162
0.1-0.2 inorganic	4	0	0.03	4	11	17
0.05-0.1 organic	1	43				
0.05-0.1 inorganic	2	2	0.05	5	23	30
<0.05	16	-	0.45	97	162	431

**Table 4A.5** Mass distribution and heavy metal content for biowaste sample from Wageningen

Fraction (mm)	Content (on DM basis)	OM (% DM)	Heavy metal content (mg.kg <sup>-1</sup> DM)			
			Cd	Cu	Pb	Zn
total	-	83	-	11	16	57
>5	54	86	-	7	10	31
2-5	4	87	-	10	13	37
0.2-2	24	89	-	16	18	42
<0.2	8	82	-	44	52	55
liquid <sup>1</sup>	16	82	-	-	-	-

<sup>1</sup> fraction found in the water after centrifugating the fraction <0.05 mm (see subchapter 3.5)



## References

- Beek, A. I. M. van de; Cornelissen, A. A. J.; and Aalbers, T. G. 1989. Fysisch en Chemisch Onderzoek aan Huishoudelijk Afval van 1987. RIVM 738505007, Bilthoven (in Dutch)
- SDU 1987. Besluit Gebruik dierlijke meststoffen, besluit van 25 maart 1987. 's Gravenhage: Staatblad van het Koninkrijk der Nederlanden no. 114
- Boxtel, L. 1982. Samenstelling en Contaminatie van Voedselresten Afkomstig van Particuliere Huishoudingen, CIVO Instituten TNO, Zeist (in Dutch)
- CCRX (Coördinatie-commissie voor de meting van radioactiviteit en xenobiotische stoffen) 1985. Cadmium, de belasting van het Nederlandse Milieu. VROM (in Dutch)
- CCRX (Coördinatie-commissie voor de meting van radioactiviteit en xenobiotische stoffen) 1990. Lood in milieu en voeding Nederland. VROM (in Dutch)
- Chynoweth, D. P.; Owens, J.; O'Keefe, D.; Earle, J. F. K.; Bosch, G.; and Legrand, R. 1992. Sequential Batch Anaerobic Composting of the Organic Fraction of Municipal Solid Waste. *Wat. Sci. Technol.* 25:327-339
- Cornelissen, A. A. J. 1989. Fysisch Onderzoek naar de Samenstelling van het Nederlands Huishoudelijk Afval, resultaten 1988. RIVM 738505009, Bilthoven (in Dutch)
- Coughtrey, P. J. 1979 Litter Accumulation in Woodlands Contaminated by Pb, Zn, Cd and Cu. *Oecologia* 39:51-60
- Crump, D. R.; and Barlow, P. J. 1982. Factors Controlling the Lead Content of a Pasture Grass. *Environmental Pollution B* 3:181-192
- Dueck, T. A.; Ernst, W. H. O.; Faber, J.; and Pasman, F. 1984. Heavy Metal Immission and Genetic Constitution of Plant Populations in the Vicinity of Two Metal Emission Sources. *Vereinigung für Angewandte Botanik* 58:47-59
- Erp, P. van; and Evers M. 1995. GFT-compost, Aanvoer zware metalen binnen de wettelijke norm. *Bloembollencultuur* 14:34-35 (in Dutch)
- Ferdinandus, H. N. M. 1989. Berekening van Zware-Metaalbalansen voor de Bodem. Leidschendam, Technische commissie Bodembescherming, rapport A89/01-R (in Dutch)
- Fiedler, H. J. 1988. Spurenelemente in Waldpflanzen, In: Spurenelemente in der Umwelt, Fiedler, H. J.; and Rösler H. J. (eds.). Stuttgart: Ferdinand Enke Verlag (in German)
- Garber, K. 1970. Atmospheric Pollution by Heavy Metal Containing Dust: Effects on Plants. *Sonderh. Landw. Forsch* 225:59-68
- Guha, M. M.; and Mitchell, R. L. 1966. The Trace and Major Element Composition of the Leaves of Some Deciduous Trees. II. Seasonal Changes. *Plant and Soil* 24:90-112
- Hook, R. I. van; Harris, W. F.; and Henderson, G. S. 1977. Cadmium, Lead, Zinc Distributions and Cycling in a Mixed Deciduous Forest. *Ambio* 6:281-286.
- Houba, V. J. G.; Uitenbogaard, J.; and Lange-Harmse, A. M. de 1991. Chemical Composition of Various Plant Species. International Plant-Analytical Exchange. Wageningen, Agricultural University
- Janssen, B. H. 1984. A Simple Model for Calculating Decomposition and Accumulation of Young Soil Organic Matter. *Plant and Soil* 76: 297-304
- Kabata-Pendias, A.; and Pendias, H. 1985. Trace Elements in Soils and Plants. Boca Raton: CRC Press, Inc.

- Lexmond, T. M.; and Edelman, T. 1987. Huidige Achtergrondwaarden van het Gehalte aan een Aantal Zware Metalen en Arseen in grond. In: Handboek voor Milieubeheer, deel IV Bodembescherming. Alphen aan de Rijn: Samson Uitgeverij bv (in Dutch)
- Little, P.; and Martin, M. H. 1972. Survey of Zinc, Lead and Cadmium in Soil and Natural Vegetation Around a Smelting Complex, Environ. Poll. series B 3:241-254
- Lustenhouwer, J. W. A.; Reijenga, F. A.; and Weenen H. C. van 1987. Source Separation and Collection of Household Compostables. Biocycle 28: 33
- Mühl und Abfall 1992. Bioabfall kompostierung, Vermeidung und Verwertung von Bioabfällen im Rhein-Sieg-Kreis. Mühl und Abfall 8 (in German)
- Nilsson, I. 1972. Accumulation of Metals in Spruce Needles and Litter. Oikos 23:132-136
- Nriagu, J. O. 1979. Copper in the Environment, Part I: Ecological Cycling, New York, John Wiley and Sons Inc.
- Nriagu, J. O. 1978. The Biogeochemistry of Lead in the Environment, New York, John Wiley and Sons
- Nriagu, J. O. 1979. Zinc in the Environment, New York, John Wiley and Sons
- Oogst 1997. Andere Meststoffen Noodzakelijk om Organische Stof te Handhaven. Oogst 14 (in Dutch)
- Parker, G. R.; McFee, W. W.; Kelly, J. M. 1978. Metal Distribution in Forested Ecosystems in Urban and Rural Northwestern Indiana. Journal of Environmental Quality 7:337-342
- Rodriguez-Flores, M.; and Rodriguez-Castillon, E. 1982. Lead and Cadmium Levels in Soil and Plants near Highways and Their Correlation with Traffic Density. Environmental Pollution Series B 4:281-290
- Roosmalen, G. R.; and Langerijt, J.C. van de 1989. Green Waste Composting in the Netherlands. Biocycle 30: 32-35
- Schlegel H.G. 1993. General Microbiology. Cambridge, University Press
- SDU 1991. Besluit Overige Organische Meststoffen (BOOM). Staatblad 613: 1-45 (in Dutch)
- Selmer-Olsen, A. R.; and Myhre, A. 1970. Determination of Lead in Plant Material along a Main road in Norway. Meldinger fra Norges Landbrukshogeskole 49
- Smith, W. H. 1973. Metal Contamination of Urban Woody Plants. Environmental Science and Technology 7:631-636
- Sommer, G.; Rosopulo, A.; and Klee, J. 1971. The Contamination of Plants and Soils by Lead from Vehicle Exhaust Fumes. Zeitschrift für Pflanzenernährung und Bodenkunde 130:193-205
- TAUW 1990. Resultaten Sorteeraanlyse Groente-, Fruit-, en Tuinafval Gemeente Arnhem. Deventer, rapportnummer 3141888 (in Dutch)
- Tong, X.; Smith L. H.; and McCarty, P.L. 1990. Methane Formation of Selected Lignocellulosic Materials. Biomass 21: 239-255
- VROM 1992. Biowaste Action Programme, Working programme 1992. A publication of the Ministry of Housing, Planning and Environment, the Netherlands

## 5. Physico-chemical fractionation of heavy metals in biowaste

### 5.1. Introduction

In Chapter 4 it was shown that the heavy metal content of the various components in biowaste are within the same range as the natural background concentrations of the original biowaste constituents. No indications were found that biowaste is contaminated to any extent. It was shown that for some heavy metals the legal demands laid down in BOOM for compost can hardly be met for the starting material. Moreover, heavy metals are concentrated in the compost because organic matter is partly degraded during composting. Changes in collection criteria for biowaste (prevention) will not have beneficial results, and adaptations of the BOOM decree are not expected in the near future. Therefore, other solutions must be found to neutralise the conflict between the recycling of biowaste as soil improver and preventing the accumulation of heavy metals in soil systems by the application of biowaste-derived compost. This can only be achieved through a technological solution, i.e. by reducing the heavy metal content of biowaste before composting.

Chapter 2 described two feasible approaches to remove heavy metals from solid organic wastes: physical separation and chemical extraction. The application of these technologies can be assessed through determination of the physico-chemical fractionation of heavy metals in biowaste. In this study, physico-chemical fractionation is performed in two steps. Firstly, the distribution of heavy metals (Cd, Cu, Pb and Zn) over the various size fractions of biowaste is determined through a fractionation scheme based on differences in particle size and particle density of the biowaste constituents. Secondly, the chemical forms of heavy metals in the various size fractions are determined by chemical extraction with selective chemical reagents; this is so-called sequential chemical extraction (Martin et al., 1987).

The physical fractionation of heavy metals in biowaste reveals whether heavy metals are concentrated in a specific fraction of the biowaste. If this is the case, the fractions with elevated heavy metal levels can selectively be removed from the biowaste by physical wet-separation processes (see subchapter 2.3). Sequential chemical extraction provides insight into the binding strength of heavy metals to the various size fractions of the biowaste. From these results it can be assessed whether heavy metals can be extracted from the biowaste under mild or rigorous extraction conditions. For the assessment of both physical wet-separation and chemical extraction processes, the removal efficiencies

have to be compared with the standards of heavy metals in compost and clean compost as laid down in the BOOM decree (SDU, 1991).

## **5.2. Development of a physico-chemical fractionation scheme**

### **5.2.1. Introduction**

The physico-chemical forms of heavy metals in solid matrices can experimentally be determined by a distribution scheme. The scheme comprises a series of analytical operations, based on a series of classical physical separation steps or on a detection method which is directly applied to the unfractionated sample (Buffle, 1988).

Biowaste is composed of various types of organic material and soil components. Organic material ranges from fresh organic matter originating from kitchens and gardens to dead, partly degraded organic matter from the top layer of soils in gardens. The soil components which can be distinguished in biowaste are sand, silt, lutum and humus. It is assumed that no distinct (pure) metal particles are present in biowaste. The following chemical forms of heavy metals can be present in biowaste:

- soluble metal forms, e.g. free metal ions and metal ions bound to dissolved organic compounds
- exchangeably bound to organic and inorganic matter
- covalently bound to organic matter
- incorporated in organic matter
- metal precipitates: e.g. carbonates, (hydr)oxides, sulphides
- covalently bound to inorganic matter, e.g. Fe- and Mn-hydroxides, clay minerals
- incorporated in inorganic matter
- adsorbed to organo-mineral complexes
- incorporated in mineral-organic matter aggregates.

For the determination of physico-chemical forms of heavy metals in biowaste, a two-step approach is used. First, biowaste is physically separated into different particle-sized fractions by a wet-sieving process, after which the organic and mineral particles in one size class are separated by a water-elutriation process. Secondly, the obtained organic and mineral particle-sized fractions are subjected to a sequential chemical extraction (SCE) procedure. SCE is the only quantitative approach for the fractionating of heavy metals fixed to solid particles, e.g. organisms, soil particles, sediment particles or water-suspended matter (Buffle, 1988). SCE is widely applied in studies of heavy metal association with solid phases in environmental samples, such as soils and sediments (Rudd et al., 1988).

### 5.2.2. Physical fractionation

The distribution of heavy metals in biowaste over its physical entities is performed according to the methods described in Chapter 4. The physical fractionation with respect to particle size and density results in the following fractions:

- >5 mm
- 1-5 mm
- 0.5-1 mm organic, 0.5-1 mm inorganic
- 0.2-0.5 mm organic, 0.2-0.5 mm inorganic
- 0.1-0.2 mm organic, 0.1-0.2 mm inorganic
- 0.05-0.1 mm organic, 0.05-0.1 mm inorganic
- <0.05 mm organo-mineral.

The fractions 1-5 mm and >5 mm could not be separated further into an organic and mineral fraction due to the limitations of the lab-scale water-elutriation set-up.

As discussed in Chapter 4, the different size fractions can be assigned to different components in biowaste. The fractions >1 mm consists of fresh plant material and food remainders; the organic fractions between 0.05-1 mm are made up of more or less humified organic matter; the inorganic fractions between 0.05-0.5 mm are made up of sand; and the fraction <0.05 mm is made up of silt, clay and humus. On basis of their contribution to the total mass of biowaste (see Table 4.1) and the similarity of various size fractions, the following size fractions are subsequently subjected to the SCE procedure:

- >5 mm
- 0.5-1 mm organic
- 0.5-1 mm inorganic
- 0.2-0.5 mm organic
- 0.2-0.5 mm inorganic
- <0.05 mm organo-mineral.

These six fractions make up 92% of the total dry mass of biowaste and contain approx. 95% of the total content of Cd, Cu, Pb and Zn. Therefore, these fractions are considered to be representative of the total biowaste sample.

### 5.2.3. Sequential chemical extraction

The sequential extraction procedure comprises the use of a series of chemical extractants in a sequential order. In each extraction step, a specific chemical form of the metal is expected to dissolve. Usually, a SCE scheme comprises five or six extraction steps (Stover et al., 1976; Tessier et al., 1979; Martin et al., 1987):

1. water-soluble metal ions
2. exchangeable metal ions

3. carbonate or easily reducible forms of metal ions
4. metal ions adsorbed to Fe- and Mn-hydroxides
5. metal ions adsorbed to organic matter and metal ions present as sulphide precipitates
6. residual metal ions.

One of the first applications of SCE has been the prediction of the bioavailability and mobility of trace elements in natural systems (Pickering, 1981). Martin et al. (1987) critically examined the prediction of SCE and came to the conclusion that the original idea of the estimation of trace elements' bioavailability generally fails, although some useful information has been obtained in the fields of engineering and geoscience. Some authors, on the other hand, claim considerable success in obtaining information on bioavailability (Luoma and Jenne, 1976) and geochemistry (Lion et al, 1982; Tessier et al., 1983). The ability of extraction techniques to simulate the results of natural processes is questionable, because the physico-chemical conditions for SCE differ drastically from natural ones: strong reagents and fast reactions for SCE versus weak reagents and slow reactions for natural processes (Martin et al., 1987). Prediction of the efficiency of a chemical extraction process based on SCE seems more promising because the conditions of the extraction process are similar to the SCE procedure: a relatively fast process applying strong reagents.

Several problems with the sequential chemical extraction are intrinsic to the experimental procedure (Martin et al., 1987; Belzille et al., 1989; Ajayi and VanLoon, 1989):

1. lack of specificity: extraction reagents are not able to destroy one phase<sup>1</sup> without solubilising the other phases
2. lack of selectivity: extraction reagents are not able to extract metals bound to one specific phase and not to other phases
3. readsorption: heavy metals released during solubilisation by an extraction liquid can be readsorbed to the remaining solid phases
4. extraction rate and efficiency depend on the experimental conditions: e.g. contact time, particle size, temperature, and solid-to-liquid ratio.

The specific and selective extraction of heavy metals from a phase requires the existence of discrete phases that may be dissolved independently. However, natural systems do not contain chemically or physically distinct phases (Kheboian and Bauer, 1987). Natural systems such as soils and sediments are physico-chemically very complex (Buffle, 1988). These systems are made up of aggregates which have to be considered as a complex assemblage of different inorganic and organic components, i.e. clay minerals, oxides, natural organic matter (NOM), and microorganisms. It is therefore hardly possible for a reagent to selectively destroy one phase without solubilising the others.

---

<sup>1</sup> a phase is defined as a distinct physical or chemical identity to which the heavy metals are adsorbed

Besides that, the phase to which heavy metals are adsorbed are both heterogeneous and polyfunctional in nature (see subchapter 6.2.2 for the definition of heterogeneous and polyfunctional; Buffle, 1988). This implies that one phase is made up of components of heterogenic composition and that they contain various functional groups. As a consequence of the heterogeneity and polyfunctionality, the binding of metals shows a broad affinity distribution which cannot be covered by a single extractant. Problems are likely to arise when trying to find a reagent which will selectively extract one chemical form of metals.

Several SCE schemes are proposed in the literature, all of which promise high selectivity and high specificity. The SCE scheme of Tessier et al. (1979) is the best studied scheme and the one most often used for the determination of the metal distribution in soil systems and sediments. The application of the extraction scheme of Stover et al. (1976) is limited to sewage sludge. There are many more SCE schemes (e.g. Bradley and Cox, 1987; Petruzelli et al., 1989; Gupta et al., 1990) but all are more or less identical, with only small differences in types of reagent and extraction conditions used. After critical evaluation of SCE schemes with respect to the selectivity of reagents, the Tessier scheme was chosen as the basis for determining the chemical distribution of heavy metals in biowaste. Because biowaste is largely made up of organic matter, an additional step was introduced to differentiate between metals adsorbed to organic matter and metals incorporated in organic matter. On top of that, several extraction steps were modified to increase their selectivity. The modified sequential extraction scheme used in this study is given in Table 5.1. The mineral fractions 0.5-1 mm and 0.2-0.5 mm are subjected only to extraction steps 1, 4 and 6 because they do not contain carbonates, metal oxides or organic matter. The organic fractions 0.5-1 mm and 0.2-0.5 mm are subjected to steps 1, 4, 5 and 6 because they do not contain carbonates or metal oxides. Total biowaste and the organo-mineral fraction <0.05 mm are subjected to the complete SCE scheme.

**Table 5.1** Modification of the Tessier SCE scheme for application to biowaste

Step	Extraction step	Modifications with respect to the Tessier scheme
1	soluble and exchangeable	0.5 M ammonium acetate is used because the GF-AAS matrix effect of 1 M MgCl <sub>2</sub> is too large to measure Cd and Cu in the extraction liquid (see subchapter 3.2)
2	carbonates	pH of the extraction solution is adjusted to 5.5 to prevent the solubilisation of metals adsorbed to organic and inorganic phases
3	Fe- and Mn-oxides	the reagents are the same as in the Tessier scheme but the pH was raised to 4 to prevent the solubilisation of metals adsorbed to organic and inorganic phases; the temperature was lowered to room temperature to prevent digestion of organic matter and organo-mineral aggregates
4	adsorbed to organic matter and inorganic particles	metals adsorbed to organic matter and available for extraction are solubilised by EDTA
5	incorporated in the organic matrix and sulphides	metals which are incorporated in organic matter and not available for extraction are dissolved by digestion of the organic matter with peroxide
6	residual	aqua regia does not solubilise metals incorporated in silicate lattices. The contribution of the heavy metals incorporated in this fraction is however very small (see subchapter 3.3)

### 5.3. Materials and methods

#### 5.3.1. Physical fractionation

Approx. 25 kg of biowaste (origin Zaandam) was collected at VAM Wijster. Very large components and impurities (e.g. plastics and tins) were removed. The biowaste was homogenised in a plastic container, and 4 to 5 kg was used for the physical separation process as described in subchapter 3.5. The fractions 1-5 mm and >5 mm were dried at 40 °C and reduced in a stainless-steel kitchen blender to particles <0.5 mm. The inorganic and organic fractions from 0.05 to 5 mm were dried at 40 °C. The fraction <0.05 mm was dried at 40 °C and pulverised in a planet ball mill. The total biowaste was dried at 40 °C and reduced in a stainless-steel kitchen blender to particles <0.5 mm.



### 5.3.2. Sequential chemical extraction

The reagents and conditions of the SCE procedure are listed in Table 5.2. The sequential chemical extraction procedure was carried out in triplicate. Ten grams of sample was weighed in a 250 ml polypropylene centrifuge tube. After each extraction step the suspension was centrifuged at 4,000 rpm for 20 minutes. The extraction liquid was decanted and the residue washed with distilled water (10 ml per g dry sample) for 1 hour, centrifuged and decanted. From the extraction liquid and wash water, 20 ml samples were taken and stored at 4 °C for heavy metal determination.

**Table 5.2** Experimental conditions of the sequential chemical extraction procedure

Step	Extraction liquid	Reagent	Experimental conditions		
			L/S <sup>1</sup> (v/w)	Time (h)	T (°C)
1	soluble and exchangeable	0.5 M NH <sub>4</sub> Ac <sup>2</sup>	10	3	20
2	carbonates	0.1 M NaAc/HAc, pH 5	10	5	20
3	Fe- and Mn-oxides	1 M NH <sub>2</sub> OH·HCl, pH 4	20	6	20
4	adsorbed to organic and inorganic matter	0.1 M EDTA, pH 4.5	20	16	20
5	incorporated in organic matter and organic-mineral aggregates	H <sub>2</sub> O <sub>2</sub> , HNO <sub>3</sub> and	10	20	85
		3.2 M NH <sub>4</sub> Ac	20	0.5	20
6	residual	aqua regia	10	4	250

<sup>1</sup> liquid-to-solid ratio (volume-weight ratio); <sup>2</sup> Ac: acetate

### 5.3.3. Determination of heavy metals

The total heavy metal content of the samples was determined in duplicate by aqua regia digestion as described in subchapter 3.3. Cd, Cu and Pb were determined by GFAAS, and Zn by FAAS. The experimental conditions for AAS are listed in Table 3.1 (subchapter 3.2.2). Because the composition of the extraction liquids differed from that of the calibration solutions, matrix effects arose. The AAS results were corrected for the matrix effect of the extractants (see Table 3.2).

## 5.4. Results

### 5.4.1. Physical fractionation

Biowaste was subjected to the physical separation process by wet-sieving and water elutriation. Table 5.3 shows the mass distribution of the various size fractions and their organic matter and heavy metal content.

**Table 5.3 Physical distribution of heavy metals in biowaste**

Fraction	Contribution (on DM basis)	OM (% DM)	Heavy metal content (mg.kg <sup>-1</sup> DM)			
			Cd	Cu	Pb	Zn
Total	-	51	0.34 ± 0.01	18 ± 1	42 ± 1	181 ± 2
>5	40	78	0.24 ± 0.02	13 ± 1	40 ± 10	113 ± 3
1-5 organic	2.9	91	0.37 ± 0.02	16 ± 1	51 ± 4	136
1-5 inorganic	2	15	-	-	-	-
0.5-1 organic	3	87	0.39 ± 0.01	20 ± 1	62 ± 1	154 ± 5
0.5-1 inorganic	5	5	0.09 ± 0.01	7 ± 4	34 ± 1	62 ± 1
0.2-0.5 organic	2	78	0.79 ± 0.02	23 ± 1	96 ± 6	198 ± 2
0.2-0.5 inorganic	20	99	0.04 ± 0.01	2 ± 1	24 ± 13	25 ± 1
0.1-0.2 total	0.4	8	-	-	-	-
0.05-0.1 organic	1.7	68	1.6 ± 0.1	28 ± 2	116 ± 3	235 ± 5
0.05-0.1 inorganic	1.2	2	-	-	-	-
<0.05	17	70	1.7 ± 0.1	67 ± 7	152 ± 2	391 ± 4

#### 5.4.2. Sequential chemical extraction

Figure 5.1 presents the results of the sequential chemical extraction experiments in stacked bars for the various fractions and for total biowaste. The extraction efficiency of every extraction step was corrected for the extraction liquid remaining in the solid pellet after centrifugation and subsequent washing of the pellet with distilled water. Unresolved GFAAS matrix effects for Cu and Pb were met only at low heavy metal levels (see Table 3.2). Because these low heavy metal levels do not significantly contribute to the total extraction, the matrix effect was ignored. The sum of the extraction steps for Cu, Pb and Zn made up 90 and 110% of the total heavy metal content as determined by aqua regia digestion. To make the comparison of the SCE schemes more surveyable, the extraction results of all experiments were recalculated to 100%. Unresolved matrix effects of EDTA were present for high Cd levels (see Table 3.2). Therefore, the contribution of the EDTA extraction step was calculated by subtracting the total sum of the other extraction steps from the total aqua regia digestion.

On the basis of the sequential chemical extraction results of the six studied fractions and the mass contribution of the corresponding fractions, also a "theoretical" SCE was calculated for total biowaste (see Figure 5.1). The calculated SCE for total biowaste is made up from the SCE results of the fractions >5 mm, 0.5-1 mm organic, 0.5-1 mm inorganic, 0.2-0.5 mm organic, 0.2-0.5 mm inorganic and <0.05 mm organo-mineral.

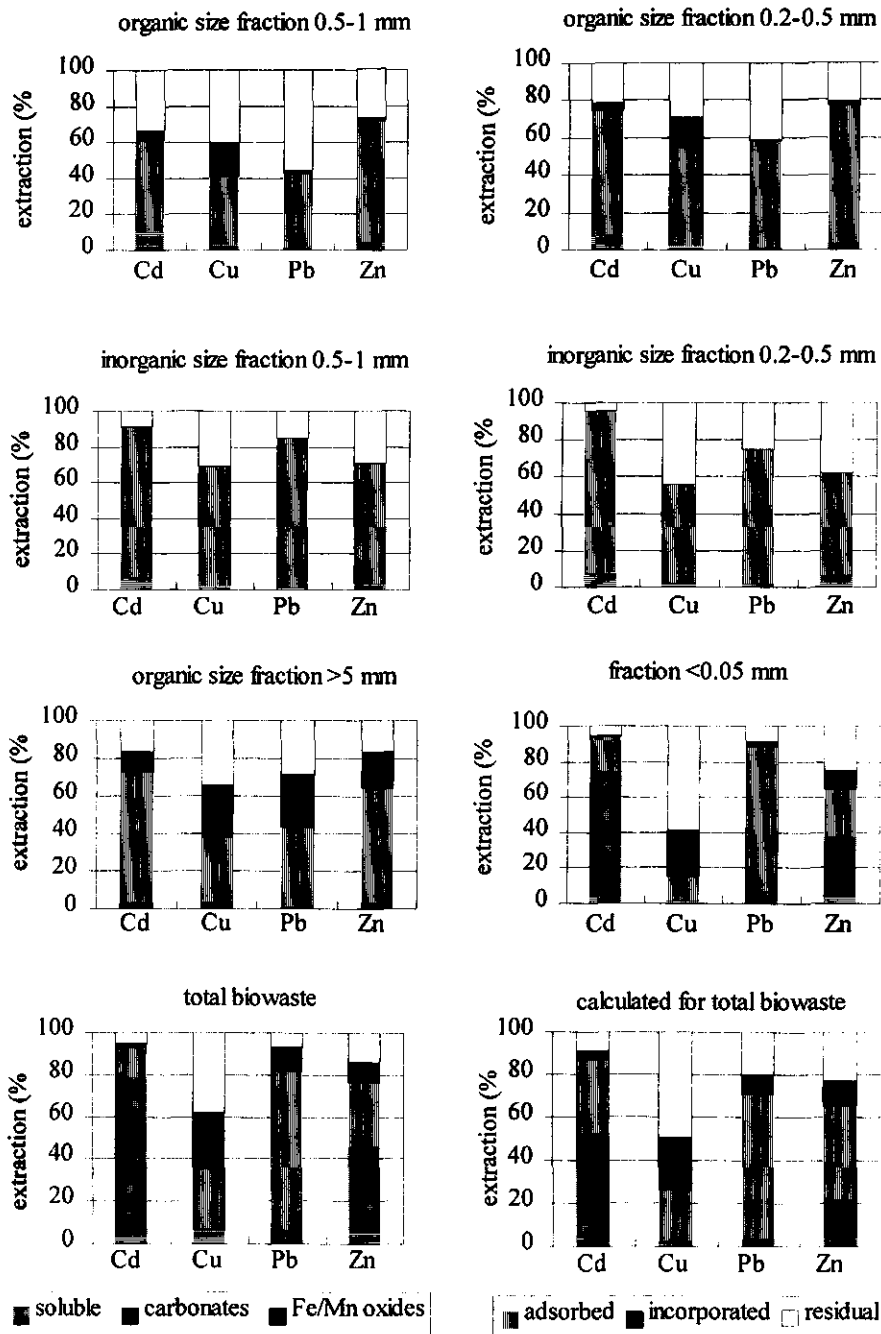


Figure 5.1 Sequential chemical extraction of heavy metals for various fractions of biowaste and total biowaste

## 5.5. Discussion

### 5.5.1. Physical fractionation

As discussed in Chapter 4, biowaste can be fractionated into 4 major fractions:

1. fraction >1 mm largely made up fresh organic matter
2. organic fraction from 0.05-1 mm made up of partly decayed and humified organic matter
3. inorganic fraction from 0.05 to 1 mm made up of sand
4. fraction <0.05 mm made up of humus, silt and clay.

Table 5.4 gives the contribution of these fractions to the total heavy metal content of the total sample (recalculated from Table 5.3).

**Table 5.4 Mass and heavy metal contribution of the 4 major fractions in biowaste**

Fraction (mm)	Contribution (on DM basis)	Heavy metal contribution (% of total)			
		Cd	Cu	Pb	Zn
>1	47.0	24.6	29.8	32.3	36.6
0.05 - 1 organic	7.1	11.7	10.2	13.1	11.8
0.05 - 1 inorganic	28.2	2.3	4.1	9.5	3.9
<0.05	17.7	61.3	55.9	45.1	47.7

Table 5.4 shows that heavy metals are largely concentrated in the fraction <0.05 mm; this fraction comprises only 17% of the total mass, but contributes 45-61% of the heavy metals present in biowaste. The mineral fraction from 0.05 to 1 mm, made up of sand, comprises 28% of the mass of biowaste but contributes only 3-10% of the heavy metals present in it. The heavy metal levels in the organic fraction >1 mm are somewhat lower than those in total biowaste.

The sources of the four major fractions in biowaste and the corresponding heavy metal contents were discussed in Chapter 4. Subchapter 5.5.3.1 will discuss the results of the physical fractionation of heavy metals in biowaste for the assessment of a physical wet-separation process preceding the composting process.

### 5.5.2. Sequential chemical extraction

The results of the SCE scheme are separately discussed for the organic fractions, the inorganic fractions and the organo-mineral fraction. These results are compared to the sequential extraction scheme for total biowaste.

### 5.5.2.1. Inorganic fractions

The inorganic fractions 0.5-1 mm and 0.2-0.5 mm, made up of sand, both show the same trend for the studied metals (Figure 5.1). A small percentage of Cd and Zn is weakly bound to the inorganic fractions and a large part of Cd, Cu, Pb and Zn are extracted by EDTA. A small part of Cd and Pb and a substantial part of Cu and Zn are incorporated in the inorganic fractions. On average, the extractability is in the order Cd>>Pb>Cu>>Zn. Gibson and Farmer (1986) found the order Cd>>Pb>Zn>Cu when applying a modified Tessier to 90 soil samples. Bradley and Cox (1987) found the order Cd>Pb>Zn>Cu for soils and sediments from flood plains.

The binding of heavy metals with the inorganic fractions (sand) is due to the presence of surface hydroxyl sites. In principle EDTA should be able to desorb Cd, Cu, Pb and Zn adsorbed to SiO<sub>2</sub> (Farrah and Pickering, 1978). However, a small amount of heavy metals is incorporated in the matrix and adsorbed to the interior sites of the solid phase. Therefore a small portion of the heavy metal ions are not accessible to EDTA or the heavy metals are not extracted within the time span of the experiment. Generally, Pb is more strongly bound to the inorganic fractions than Zn. In this case, Zn is less accessible for EDTA because Pb is mainly adsorbed to the surface of the particles, while Zn is partly adsorbed in the interior of the solid particles.

### 5.5.2.2. Organic fractions

All the organic fractions (>5 mm, 0.5-1 mm and 0.2-0.5 mm) show the same trends in extraction behaviour for the studied heavy metals. A small part of Cd and Zn is weakly bound to the organic matter, while Cu and Pb are more strongly bound to the organic matter. The trend is observed that with increasing particle size, heavy metals are less extracted by EDTA and more incorporated in organic matter. This is probably due to the fact that complete extraction by EDTA was limited in time for larger particle sizes. A large part of the heavy metals is present in the residual extraction step. The extractability of heavy metals from the organic fractions is in the order Cd>>Zn>Cu>>Pb. The heavy metal affinity follows the Irving-Williams order of complex stability of metals with organic ligands, i.e. Cd<Zn<Pb<Cu (Stumm and Morgan, 1996).

Petruzelli et al. (1989) found the order Cd>Pb>Zn>Cu for compost of municipal solid waste. Jones (1987) found the order Zn>Pb>Cu for peat. The results for the organic fractions are difficult to interpret because the fractions are ill defined. The general trend is that Cd is easily extracted and Cu is bound the strongest. Differences found in the order of extractability for sludges and municipal solid waste, especially for Pb and Zn, are again caused by the fact that Zn is incorporated in organic or inorganic matter while Pb, originating from anthropogenic sources, is present on the surface.

### 5.5.2.3. *Organo-mineral fraction*

The extraction from the fraction <0.05 mm shows the same trends as determined for the organic and inorganic fractions: Cd and Zn are more easily extracted than Pb and Cu. The only exception is the EDTA extraction step for Pb. Pb largely originates from anthropogenic sources and thus a larger part is adsorbed to the surface of the particles instead of incorporated into the organo-mineral fractions. Cd and Zn are adsorbed for 72% and 40% to Fe- and Mn-oxides, respectively. Most probably these metals are not adsorbed to metal oxides but are also extracted from weakly or moderately bound metals from the organic and organo-mineral phases. Cu is mainly present in the peroxide digested and residual fractions, indicating the strong association of Cu with organic and organo-mineral fractions.

### 5.5.2.4. *Total biowaste*

Evaluation of the Cd, Cu, Pb and Zn extractability from the inorganic, organic and organo-mineral fractions shows the order  $Cd \gg Zn > Pb > Cu$ . This is in agreement with the Irving-Williams order for stability of metals with organic ligands (Stumm and Morgan, 1996). The order of extractability for Pb and that for Zn are sometimes reversed because the extraction is not only determined by the adsorption strength but also by the accessibility of adsorbed metals. Zn is mainly incorporated in the solid matrix and not accessible for extraction or not extracted within the available extraction time. Pb on the other hand is mainly present at the surface of the solid and accessible for extraction, and is rapidly extracted. Pb is largely adsorbed to the surface of the solids because it originates from anthropogenic sources.

Despite the fact that heavy metals are more strongly bound to humus and clay minerals, the contribution of the residual extraction step is highest for the inorganic and organic fractions. This is most probably due to the fact that the fraction <0.05 mm was pulverised by a planet ball mill, while the organic and inorganic fractions were kept intact. Metals present in the organo-mineral fraction are therefore more readily accessible to the extraction reagent in the subjected extraction time.

Based on the SCE results of the physically-separated size fractions and taking into account the mass contribution of every size fraction to total biowaste, the SCE of total biowaste can be theoretically assembled. Figure 5.1 shows the theoretically calculated SCE for Cd, Cu, Pb and Zn together with the experimental SCE for total biowaste. The two SCE schemes agree well, except for extraction step 3. This fraction is larger for total biowaste, especially for the metals Cd and Zn. This is due to the aselectivity of the third extraction step (Fe/Mn-oxides) not being taken into account for the inorganic and organic fractions. Cd and Zn weakly bound to the organic and inorganic size fractions are extracted at pH 4-5 in the total biowaste sample but are not taken into account in the theoretically calculated SCE scheme. The effect is less pronounced for Cu and Pb

because these metals are more strongly bound to organic fractions and not extracted at pH 4-5. The good agreement between the theoretical and the experimental SCE scheme indicates that the physical fractionation step gives additional insight into the heavy metal binding in biowaste which could not be elucidated by merely applying the SCE scheme to total biowaste.

#### *5.5.2.5. Evaluation of the SCE scheme*

A SCE scheme cannot quantitatively elucidate the chemical forms of heavy metals in biowaste because this system is physico-chemically too complex. Biowaste is made up of a complex assemblage of different inorganic and organic components, i.e. clay minerals, oxides, and natural organic matter. It is therefore impossible for a reagent to selectively destroy one phase without solubilising the others. Besides that, the metal binding properties of the components themselves are both heterogeneous and polyfunctional. As a result the binding of metals shows a broad affinity distribution which cannot be covered by a single extraction liquid. The extraction steps should therefore be considered 'operationally-defined', reflecting the chemical properties of the metals rather than the actual association with particulate components (Martin et al., 1987). With respect to these considerations, the sequential chemical extraction scheme applied to biowaste should be regarded as follows:

- fraction 1: very weakly adsorbed and exchangeably bound to organic and inorganic phases
- fraction 2: weakly adsorbed to organic matter or minerals
- fraction 3: moderately adsorbed to organic matter or minerals
- fraction 4: strongly adsorbed to organic matter or minerals
- fraction 5: very strongly bound to or incorporated into organic matter or other oxidizable species, e.g. sulphides
- fraction 6: extremely strongly bound to non-digested organic matter or minerals and incorporated within resistant minerals.

Besides the lack of specificity and selectivity, the SCE scheme meets problems related to the readsorption and redistribution of heavy metals during the extraction. In the literature this topic is not properly addressed and studies on readsorption and redistribution have resulted in contradictory statements. Kim and Fergusson (1991), Belzille et al. (1989), and Ajayi and Van Loon (1989) observed minimal redistribution for several trace elements, while Kheboian and Bauer (1987), Tipping et al. (1985) and Rendell et al. (1980) measured substantial redistribution of metals between phases.

In our opinion, possible readsorption and redistribution of heavy metals during the extraction depends on the physico-chemical state of the studied sample. For a system in thermodynamic chemical equilibrium the distribution of the metal ions among the

different solid phases and the liquid phase is determined by the number and affinity of the metal-binding sites for each phase. To reach thermodynamic equilibrium the metals must have had the time and opportunity to redistribute among the phases, i.e. all phases must be in good contact and the system must have had time to reach equilibrium when it is subjected to chemical changes. When a system which is not in equilibrium is mixed with an extraction liquid, redistribution will evidently occur. The extent of redistribution depends not only on the affinity of the remaining undissolved phases but also on the ability of the extractant to inhibit the readsorption of metal by those phases and to keep the dissolved metals in solution (Kheboian and Bauer, 1987). The experimental approaches used to study redistribution do not always fulfil these demands. Mixing different phases (e.g. clay minerals, humic substances, metal (hydr)oxides) spiked with heavy metals and subjecting them to a chemical extraction scheme will evidently lead to redistribution because the metals initially adsorbed to the separate phases do not reflect the equilibrium status of the mixed system. The distribution depends on the amount of metals extracted and the strength of the extractant. The addition of metal-spiked phases to real, natural systems meets the same problems.

The best experimental approach to study redistribution is the standard addition technique (Belzille et al., 1989). However, the amount of metals added to the system should be in the same order as the metals already extracted. In some studies large metal spikes are added, resulting in overestimation of readsorption (Ajayi and Van Loon, 1989).

### **5.5.3. Assessment of chemical extraction and physical separation technologies**

Chapter 2 presented two possible approaches for the reduction of heavy metal contents in solid waste streams: physical separation and chemical extraction. The results of this chapter can be employed to evaluate both removal technologies for biowaste. The prospects for these removal technologies will be discussed here.

#### ***5.5.3.1. Physical separation process***

Specific fractions of solid organic wastes can selectively be removed by physical separation processes (see subchapter 2.3). Most processes are based on differences in size, density or surface properties of the particles. By the selective removal of fractions with higher heavy metal contents, a relatively clean fraction is obtained which can be composted. The particle-size classification on lab-scale (see subchapter 4.4.1 and Table 5.3) shows that biowaste can be divided into three major fractions on particle scale:

1. fraction >1 mm: mainly composed of fresh plant material which is low in heavy metals and high in organic matter
2. inorganic fraction 0.05-1 mm: very low in heavy metals and predominantly comprised of sand



3. organic fraction 0.05-0.5 mm and organo-mineral fraction <0.05 mm: relatively high heavy metal level and high organic matter content.

Table 5.5 shows the mean heavy metal content of total biowaste, the size fraction >1 mm, and the organic fraction <1 mm (made up of the organic fraction 0.05-1 mm and the organo-mineral fraction <0.05 mm) along with the BOOM standards for compost and clean compost. The heavy metal content of the organic fractions cannot directly be compared to the BOOM standards because heavy metals are concentrated during composting (see subchapter 4.4.1). It is assumed that the heavy metals in the fraction >1 mm are concentrated by a factor of 1.3 (an initial organic matter content of 75% and 40% degradation of organic matter, see Figure 4.1). The heavy metal level of the organic fraction >1 mm is low enough to produce compost of high quality (Table 5.5). However, the levels for Pb and Zn are too high with respect to the standards for clean compost. For the organic fraction <1 mm, the heavy metal levels are too high to produce compost, even when a concentration factor of 1 is assumed. This fraction of biowaste originates from the topsoil and humus layer in gardens (see subchapter 4.4.3) and contains a large amount of lutum and silt (see Table 3.8) and a high content of stabilised and humified organic matter (see Table 3.11). This fraction would make a good-quality soil improver because of its high humic acid content (see Table 3.11) and should be regarded as a valuable fraction of biowaste. Therefore chemical extraction can be an option to reduce the heavy metal content of the organic fraction <1 mm. This option will be discussed in the next subchapter.

**Table 5.5 Heavy metal (mg.kg<sup>-1</sup> DM) content of biowaste and several size fractions compared with the BOOM standards**

Metal	Total biowaste	Organic part		BOOM standards	
		>1 mm	<1 mm	Compost	Clean compost
Cd	0.6	0.25	1.0	1	0.7
Cu	20	23	60	60	25
Pb	65	40	150	100	65
Zn	140	110	300	200	75

The feasibility of a physical separation process on a practical scale will be further addressed in Chapter 9, where the results of a process on a pilot-plant scale are evaluated.

### 5.5.3.2. Chemical extraction process

#### Evaluation of extraction reagents

Figure 2.1 (Chapter 2) presents a possible process scheme for the chemical extraction of heavy metals from solid organic wastes. In the first step, the heavy metals are solubilised from the solid to the aqueous phase. In the second step, the solid and liquid phases are separated. Low pH values or the presence of toxic compounds in the cleaned solid waste after extraction and solid-liquid separation can disturb subsequent microbiological processes during composting and is unfavourable for the quality of the compost. Therefore, the cleaned solid waste has to be conditioned (e.g. washed with water) to make possible the production of compost by anaerobic or aerobic conversion.

The extraction liquid has to be recycled to reduce the costs of the extractant and the amount of wastewater. To prevent accumulation of heavy metals in the recycled extraction liquid, heavy metals have to be removed from the liquid. Removal of heavy metals from water is possible by e.g. chemical precipitation, ion exchange, electrolysis, adsorption to immobilised biomass, or membrane processes (Peters and Ku, 1988; Patterson and Passino, 1989). Excess extracting liquid contains extractant and possibly other hazardous compounds which must be treated before it can be disposed of to surface water or a wastewater treatment plant. Finally, the ideal situation would be for the produced metal sludge to be reused.

The choice of extracting reagent will depend on the following criteria:

- extraction efficiency and rate of extraction: high efficiency and fast rate
- the total costs of the process: the process has to compete with other treatment processes, such as incineration and biomass gasification
- toxic effects of extracting reagent for subsequent biological processes (e.g. composting of cleaned waste stream, wastewater treatment) should be prevented
- the discharge of wastewater and metal sludge should be minimised.

In the literature, various acids and complexing agents are proposed for the extraction of heavy metals from solid wastes (see Chapter 2). Here, the utilisation of various extraction liquids is evaluated.

*Extraction with inorganic acids* The major advantages of inorganic acids are their high extraction efficiency at low pH and the relatively low costs of the extractant. On the other hand, a lot of disadvantages are associated with the use of inorganic acids. The extraction is indifferent to the type of metal ion, thus also other metal ions such as Ca, Mg, Fe and Al are extracted. The cleaned solid waste also has to be washed to remove inorganic acid before composting, thus producing an additional amount of wastewater.

*Extraction with complexing agents* Ethylenedinitrilotetraacetic acid (EDTA) is a strong, inorganic, water-soluble complexing agent capable of extracting heavy metals from solid wastes to a large extent. However, EDTA is expensive and the removal of heavy metals from the recycling stream is problematic due to the strong binding strength of EDTA. Besides that, the wastewater cannot be disposed of because of the environmental problems associated with the discharge of EDTA to surface waters or wastewater treatment plants (Siegrist, 1988). EDTA also has to be removed from the cleaned solid waste by washing with water, producing an additional amount of wastewater.

*Extraction with organic acids* Extraction with inorganic acids and strong complexing agents both have severe drawbacks. Organic acids such as citric and oxalic acid could be promising for the extraction of solid organic wastes for the following reasons:

- oxalic and citric acid are strong acids, and oxalate and citrate anions are strong metal complexing agents
- the organic acids are microbiologically degradable and non-toxic
- heavy metals can more easily be removed from oxalic or citric acid solutions.

The properties of oxalic and citric acid have the following advantages for the extraction process:

- the required extraction efficiency can be reached at higher pH values
- the cleaned solid waste does not need to be washed, because organic acids are microbiologically degraded during composting
- organic acids in the wastewater can be treated by conventional aerobic and anaerobic treatment
- organic acids can be recycled and thus significantly reduce the costs of the extracting reagent.

Oxalic and citric acid can be added directly or they can be produced by fungi. The solubilisation of heavy metals from sewage sludge and coal waste by fungi has been demonstrated (Strasser and Schinner, 1991).

#### **Assessment of chemical extraction for biowaste**

There are several approaches to reduce the heavy metal content of compost by chemical extraction:

- extraction of heavy metals from total biowaste before composting
- extraction of heavy metals from compost-derived biowaste
- physical wet-separation of contaminated components from biowaste, followed by chemical extraction of the contaminated fraction.

Humic acids bind heavy metals more strongly than fresh plant material (Ciavatta, 1987; Garcia et al. 1990). Various studies show that the humic acid content increases during

composting (Deiana et al., 1990; Garcia et al. 1992; Iglesias-Jimenez and Perez-Garcia, 1992; N'dayegamiye and Isfan, 1991; Govi et al., 1995). Therefore extraction of heavy metals is preferred before composting because more rigorous extraction conditions have to be applied to extract metals from compost. Moreover, part of the drying of compost after the extraction step is achieved naturally through the heat produced during the composting process. Extracting heavy metals from compost will result in a wet compost which has to be dried with hot air.

From the results of the sequential chemical extraction, predictions can be made regarding to what extent heavy metals can be solubilised from biowaste and its particle-sized fractions. It is assumed that heavy metals extracted in sequential extraction steps 1 to 4 (see Table 5.2) are available for solid-to-liquid extraction. Heavy metals present in extraction steps 5 and 6 are incorporated in organic matter and minerals and are therefore not readily available for extraction.

The organic fraction >1 mm of biowaste can be composted directly and complies with the BOOM standards for compost. The organic/organo-mineral fraction <1 mm can comply with BOOM only when the levels for Cd, Cu, Pb and Zn have been significantly reduced (see Table 5.5). The results of the SCE scheme and the contribution of the various size fractions (Figure 5.1 and Table 5.4) show that approx. 80% of Cd, 45% of Cu, 70% of Pb and 70% of Zn are available for extraction (sum of extraction steps 1-4). These extraction efficiencies should be sufficient to reduce the heavy metal content of compost derived from the organic fraction <1 mm to values below the BOOM standards for compost.

## 5.6 Conclusions

A physico-chemical fractionation scheme was developed in order to gain insight into (i) the distribution of heavy metals over the physical entities of biowaste and (ii) to get an indication of the binding strength of heavy metals to biowaste and the particle-sized fractions. The results of the fractionation scheme can be used to assess physical wet-separation and chemical extraction technologies for biowaste.

The physical fractionation shows that the heavy metals are accumulated in the organo-mineral fraction <0.05 mm. This fraction contains 45-60% of the heavy metals while making up only 17% of the total mass of biowaste. This fraction is composed of humic substances, metal oxides and clay minerals which all bind heavy metals very strongly. This is confirmed by the sequential chemical extraction of this fraction. Low pH and extraction by EDTA are needed to extract the heavy metals Cd, Pb and Zn. Cu can be extracted only after digestion of the organic matter by peroxide and further digestion of the matrix by aqua regia. Pb can largely be extracted by EDTA because Pb most probably originates from anthropogenic sources and is thus adsorbed to the surface of the particles.

A large part of biowaste is made up of sand (28% comprising the inorganic fraction 0.05-1 mm), of which the heavy metal content is very low. This fraction contributes only approx. 2-10% to the heavy metal content of biowaste. The main part of the heavy metal content can be extracted by EDTA, but a small portion is incorporated in the matrix not accessible to extracting liquids. The extraction of heavy metals, however, does not have to be considered because the levels of heavy metals are already extremely low.

The organic fraction >1 mm contributes 40% of the mass of biowaste and the heavy metal content is somewhat lower than for total biowaste. This fraction meets the BOOM standards for compost and can be directly composted.

Based on the physico-chemical fractionation of the heavy metals Cd, Cu, Pb and Zn in biowaste, the best approach for processing of biowaste on practical scale to produce (clean) compost is physical separation of biowaste in three fractions:

1. organic fraction >1 mm
2. inorganic fraction 0.05-1 mm (sand)
3. organic/organo-mineral fraction <1 mm.

The organic fraction >1 mm can be directly composted and complies with the BOOM standard for compost. The sand fraction is very low in heavy metals and can be reused in road and building construction. The heavy metal content of the organic fraction <1 mm (a good quality compost, comprising the organic fraction 0.05-1 mm and the organo-mineral fraction <0.05 mm) have to be reduced in order to reach the BOOM standards for compost. The SCE scheme shows that the amount of heavy metals available for extraction is sufficient. Citric and oxalic acid turn out to be the best options for the removal of heavy metals from solid organic waste streams.

Several comments can be made with respect to the physico-chemical fractionation scheme. Due to the physical fractionation under wet conditions some redistribution of heavy metals can occur. This redistribution is probably negligible for the strongly adsorbing organic fractions, but heavy metals can be partly washed off from the less strongly binding inorganic fractions. This probably results in the very low heavy metal content measured for the sand fractions. The metals that are washed off most probably end up in the fraction <0.05 mm. For the assessment of a physical separation process, the redistribution is not an artifact because also in full-scale processes wet conditions are encountered and thus the process of redistribution will also take place.

The sequential chemical extraction cannot elucidate the chemical forms of heavy metals in natural systems because these systems are too complex. The extraction steps should therefore be considered 'operationally-defined', reflecting the chemical properties of the metals rather than the actual association with particulate components.

## References

- Ajayi, S. O.; and VanLoon, G. W. 1989. Studies on Redistribution During the Analytical Fractionation of Metals in Sediments. *Sci. Tot. Environ.* 87/88:171-187
- Belzille, N.; Lecomte, P.; and Tessier, A. 1989. Testing Readsorption of Trace Elements During Partial Chemical Extractions of Bottom Sediments. *Environ. Sci. Technol.* 23:1015-1020
- Bradley, S. B.; and Cox, J. J. 1987. Heavy Metals in the Hamps and Manifold Valleys, North Staffordshire, UK: Partitioning of Metals in Floodplain Soils. *Sci. Tot. Environ.* 65:135-153
- Buffle, J. 1988. Complexation reactions in Aquatic Systems: An Analytical Approach. Chichester, Ellis Horwood Limited
- Ciavatta, C. 1987. Evaluation of Heavy Metals During Stabilization of Organic Matter in Compost Produced with Municipal Solid Wastes. *Biores. Technol.* 43:147-153
- Deiana, S.; Gessa, C.; Manunza, B.; Rausa, R.; and Seeber, R. 1990. Analytical and Spectroscopic Characterization of Humic acids Extracted from Sewage Sludge, Manure, and Worm Compost. *Soil-Science* 150:419-424
- Farrah, H.; and Pickering, W. F. 1978. Extraction of Heavy Metal ions Sorbed on Clays. *Water, Air and Soil Pollution* 9:491-498
- Garcia, C.; Hernandez, T.; and Costa, F. 1990. The Influence of Composting and Maturation Processes on the Heavy Metal Extractability from some Organic Wastes Biological Wastes 31:291-301
- Garcia, C.; Hernandez, T.; and Costa, F. 1992. Comparison of Humic Acids derived from City Refuse With More Developed Humic Acids. *Soil Science and Plant Nutrition* 38:339-346
- Gibson, M. J.; and Farmer, J.G. 1986. Multi-step Sequential Chemical Extraction of Heavy Metals from Urban Soils. *Environ. Poll.series B* 11:117-135
- Govi, M.; Ciavatta, C.; Sitti, L.; and Gessa, C. 1995. Evaluation of the Stabilization Level of Pig Organic Waste: Influence of Humic-like Compounds. *Communications in Soil Science and Plant Analysis* 26:425-439
- Gupta, S.; Mehrota, I; and Vir Singh, O. 1990. Simultaneous Extraction Scheme: a Method to Characterise Metal Forms in Sewage Sludge. *Environ. Technol.* 11:229-238
- Iglesias-Jimenez, E.; and Perez-Garcia, V. 1992. Determination of Maturity Indices for City Refuse Composts. *Agriculture, Ecosystems and Environment.* 38:331-343
- Jones, J. M. 1987. Chemical Fractionation of Copper, Lead and Zinc in Ombrothrophic Peat. *Environ. Poll.* 48:131-144
- Kheboian C.; and Bauer, C. F. 1987. Accuracy of Selective Extraction Procedures for Metal Speciation in Model Aquatic Sediments. *Analytical Chemistry* 59:1417-1423
- Kim, N. D.; and Fergusson, J. E. 1991. Effectiveness of a Commonly Used Sequential Extraction Technique in Determining the Speciation of Cadmium in Soils. *Sci. Tot. Environ.* 105:191-209
- Lion, L. W.; Altmann, R. S.; and Leckie J. O. 1982. Trace Metal Adsorption Characteristics of Estuarine Particulate Matter: Evaluation of Contributions of Fe/Mn oxides and Organic Surface Coatings. *Environ. Sci. Technol.* 16:960-971
- Luoma, S. N.; and Jenne, E. A. 1976. Estimating Bioavailability of Sediment-Bound Trace Metals with Chemical Extractants. In: *Trace Substances in Environmental Health*, Hemphill, D. D. (ed.). Columbia, Univ. Missouri Press

- Martin, J. M.; Nirel, P.; and Thomas, A. J. 1987. Sequential Extraction Techniques: Promises and Problems. *Marine Chemistry* 22:313-341
- Mehrotra, A.; Mehrotra, I.; and Tandon, S. N. 1989. Speciation of Copper and Zinc in Sewage Sludge. *Environmental Technology Letters* 10:195-200
- N'dayegamiye, A. ; and Isfan, D. 1991. Chemical and Biological Changes in Compost of Wood Shavings, Sawdust and Peat Moss. *Canadian Journal of Soil Science* 71:475-484
- Patterson, J. W.; and Passino R. (eds.) 1989. Metals separation, speciation and recovery: proceedings of the second international symposium on metals separation, speciation and recovery Rome, Italy, 1989. Chelsea: Lewis
- Peters, R. W.; and Ku, Y. 1988. Evaluation of Recent Treatment Techniques for Removal of Heavy Metals from Industrial Wastewaters, Separation of Heavy Metals, AIChE Symposium Series 81
- Petruzzelli, G.; Szymura, I.; Lubrano, L.; and Pezzarossa, B. 1989. Chemical Speciation of Heavy Metals in Different Size Fractions of Compost from Solid Urban Wastes. *Environmental Technology Letters* 10:521-526
- Pickering, W. F. 1981. Selective Chemical Extraction of Soil Components and Bound Metal Species. *Crit. Rev. Anal. Chem.* 2:233-266
- Rendell, P. S.; Batley G. E.; and Cameron A. J. 1980. Adsorption as Control of Metal Concentration in Sediments Extracts. *Environ. Sci. Technol.* 14:314-318
- Rudd T.; Lake, D.L.; Mehrotra, I.; Sterrit, R. M.; Kirk, P. W. W.; Campbell, J. A.; and Lester, J. N. 1988. Characterisation of Metal Forms in Sewage Sludge by Chemical Extraction and Progressive Acidification. *Sci. Tot. Environ.* 74:149-175
- SDU 1991. Besluit Overige Organische Meststoffen (BOOM). *Staatblad* 613: 1-45 (in Dutch)
- Stover, R. C.; Sommers, L. E.; and Silviera, D. J. 1976. Evaluation of Metals in Wastewater Sludge. *Journal WPCF* 48:2165-2172
- Strasser, H.; and Schinner, F. 1991. Copper and Zinc Removal from Sewage Sludge and Refuse Compost with Heterotrophic Microorganisms. In: International Symposium Environmental Biotechnology Oostend, Belgium
- Stumm, W.; and Morgan, J.J. 1996. *Aquatic Chemistry, Chemical Equilibria and Rates in Natural Waters*. New York, John Wiley & Sons, Inc.
- Tessier, A.; Campbell, P. G. C.; and Bisson M. 1979. Sequential Extraction Procedure for the Specification of Particulate Trace Metals. *Analytical Chemistry* 51:844-851
- Tessier, A.; Campbell P. G. C.; and Auclair, J. C. 1983. Relationship between Trace Metal Partitioning in Sediments and their Bioaccumulation in Freshwater Pelecypods. *Proc. Int. Conf. on Heavy Metals in the Environment, Heidelberg, Edinburgh*
- Tipping, E.; Hetherington, N. B.; Hilton, J.; Thompson, D. W.; Bowles E.; Hamilton-Taylor, J. 1985. Artifacts in Use of Selective Chemical Extraction to Determine Distributions of Metals between Oxides of Manganese and Iron. *Anal. Chem.* 57:1944-1946
- Tuin, B. J. W.; and Tels, M. 1990. Extraction of Six Heavy Metals from Contaminated Clay Soils. *Environmental Technology* 11 541-554
- Wong, L. T. K.; and Henry, J. G. 1988. Bacterial Leaching of Heavy Metals from Anaerobically Digested Sludge. In: *Biotreatment Systems, Vol. III*, Wise, D. L. (ed.), Boca Raton, CRC Press, Inc.

## 6. Development and validation of the NICA-Donnan model for describing proton and metal adsorption to natural organic complexing compounds

### 6.1. Introduction

The bioavailability, toxicity, and transport of heavy metals in natural systems depend on the speciation of heavy metals (Buffle, 1988; Stumm and Morgan, 1996). The possible chemical forms of heavy metals in a natural system are hydrated metal ions, soluble metal complexes, metal precipitates, metal ions adsorbed to organic matter and bacterial residues, and metal ions adsorbed to the surface and interstices of minerals. Various analytical and modelling approaches can be used to determine the speciation of heavy metals in a natural system. The analytical approaches include physico-chemical fractionation, potentiometric methods, electrode kinetics, and direct detection of atomic structures (Buffle, 1988). As discussed in Chapter 5, sequential chemical extraction is the only quantitative experimental approach for the speciation of heavy metals fixed on solid particles. However, it was shown that the sequential chemical extraction method merely gives an 'operationally-defined' binding strength and cannot differentiate between distinct chemical forms of heavy metals in natural systems. Along with analytical methods, modelling approaches can provide an additional understanding of the environmental factors controlling metal distribution in natural systems. For the same reasons, the extractability of heavy metals from biowaste can be better interpreted and predicted if more insight is available with respect to the metal binding properties of the biowaste particles.

Chemical equilibrium modelling is a common approach to gain more insight into the speciation of heavy metals in natural systems (Jenne, 1978; Kramer and Duinker, 1984; Buffle, 1988; Melchior and Basset, 1990). Equilibrium models have been applied to calculate the speciation of heavy metals in soils (Behel, 1983; Sposito, 1985), sewage sludge (Fristoe, 1983; Fletcher, 1987a; Fletcher, 1987b) and natural waters (Vuceta, 1978; Sposito, 1981). To obtain valuable information from chemical modelling, it is important to acquire as much information as possible on the reactive components (in relation to the heavy metal speciation) present in the natural system, the type of reactions taking place and the corresponding reaction constants. Distribution of chemical species at equilibrium is calculated using known values for the total metal and ligand<sup>1</sup> concentra-

---

<sup>1</sup> a ligand is defined as an anion or molecule which forms a coordination compound with a metal cation; the term complexant is assigned to a ligand of higher molecular weight with a more complex structure



tions and published values of the relevant metal-ligand stability constants (Florence and Batley, 1980; Sposito, 1981). A general description of the application of chemical equilibrium models is presented in Appendix 6A. Chemical equilibrium modelling requires accurate values for the stability constants for reactions involved, such as precipitation, complexation, adsorption and redox reactions (see Appendix 6A). Critical stability constants are available for reactions between protons and metal ions with well-defined small molecules like EDTA,  $\text{Cl}^-$ , histidine and acetate (Martell and Smith, 1977; Smith and Martell, 1976; Stumm and Morgan, 1996). However, biowaste is largely composed of ill-defined natural organic complexants such as plant fibres and humic substances. Humic substances are known to bind heavy metals strongly and to generally determine the behaviour and fate of heavy metals in natural systems (Sposito, 1986; Livens, 1991; Stevenson, 1994). Humic substances control the mobility of metals in natural waters and play an important role in the bioavailability and toxicity of trace metals to plants and living organisms in soil systems (Kramer and Duinker, 1984; Buffle, 1988). In contrast to well-defined ligands, the affinity constants for proton and metal ion adsorption to natural organic complexants are often not known or are too empirical to be suitable for model calculations (Buffle, 1988). Therefore, adsorption models have to be developed in order to obtain a better quantitative description of proton and metal ion binding to natural organic complexants.

Various approaches to model proton<sup>2</sup> and metal ion binding to natural organic complexants have been proposed in the literature. These models range from simple mixture models (Sposito, 1981; Fristoe, 1983) to models incorporating electrostatics (Marinsky et al., 1982; Tipping et al., 1988; Bartschatt et al., 1992) and continuous affinity distributions for proton and metal ion binding (Nederlof, 1992; De Wit, 1992). A comprehensive review of the applicability of these models is given by Buffle (1988).

In this study, a general binding model has been developed which incorporates the binding site heterogeneity, non-ideality of local binding and the electrostatic effect of proton and metal ion adsorption to natural organic complexants. The binding site heterogeneity and non-ideality of local proton and metal ion binding are described by the NICA model (Koopal et al., 1994; Benedetti et al., 1995). The electrostatic effect is handled by the Donnan formalism (Marinsky and Ephraim, 1986; Miyajima, 1992). The NICA-Donnan model should be able to describe the proton and metal binding to natural organic complexants under variable environmental conditions and metal-ligand ratios.

The model has been validated by comparing model calculations with experimental adsorption isotherms of proton and Cu(II) binding to Sephadex CM-25 for variable pH and ionic strength. Sephadex CM-25, a synthetic polymeric gel, is used as a well-defined model compound with properties which resemble those of natural organic complexants, such as plant fibres and humic acids.

---

<sup>2</sup> in this thesis, protons are treated separately from metal ions

## 6.2. Description of adsorption model

This subchapter describes the theoretical basis of the adsorption model used to describe proton and metal ion binding to natural organic complexants present in biowaste. The description of proton and metal ion adsorption is transformed into a computer algorithm that can be integrated in standard chemical equilibrium algorithms (see Appendix 6A).

### 6.2.1. Introduction

The distribution of the chemical forms of heavy metals in natural systems is determined by the chemical reactions of heavy metals with available ligands. Competition with protons and other metals ions for the same binding sites influences the heavy metal speciation. Natural systems are composed of organic macromolecules (e.g. humic substances, plant fibres), minerals (e.g. Fe/Al/Mn-oxides, clay minerals) and a large number of cations and low-molecular-weight anions. The number of chemical forms and reactions are therefore numerous. The major chemical reactions in natural ecosystems are acid-base reactions, gas-liquid equilibria, precipitation, simple complexation reactions in solution (ion association and covalent bonding), redox reactions and adsorption<sup>3</sup> processes at solid particles and colloids. Figure 6.1 shows a simplified schematic presentation of the possible chemical forms and reactions of metal ions ( $M^{n+}$ ) in natural systems.

For reactions of metal ions with well-characterised (or simple) ligands like  $Cl^-$ , acetate and EDTA, the nature of reaction is known and the equilibrium constants can be found in various tables (Martell and Smith, 1977; Smith and Martell, 1976; Stumm and Morgan, 1996). For reactions with natural organic complexants the nature of the reactions are complex and equilibrium constants are not well established. A study of Buffle et al. (1984) showed a large variation in affinity constants for collected data of published values of equilibrium quotients for the complexation of  $Cu^{2+}$  to fulvic acids at 25 °C and an ionic strength of 0.1 M. The collected affinity constants vary from  $10^4$  to  $10^9$   $l.mol^{-1}$  at pH 6 and from  $10^7$  to  $10^{13}$   $l.mol^{-1}$  at pH 8. The large variation in stability constants found for humic substances can be accounted for by the complex character of the complexants, i.e. the stability constants change as a function of pH, ionic strength, and metal-ligand ratio.

---

<sup>3</sup> the term adsorption is used when the exact nature of the reactions and location of adsorption of metal ions to the complexant is not known

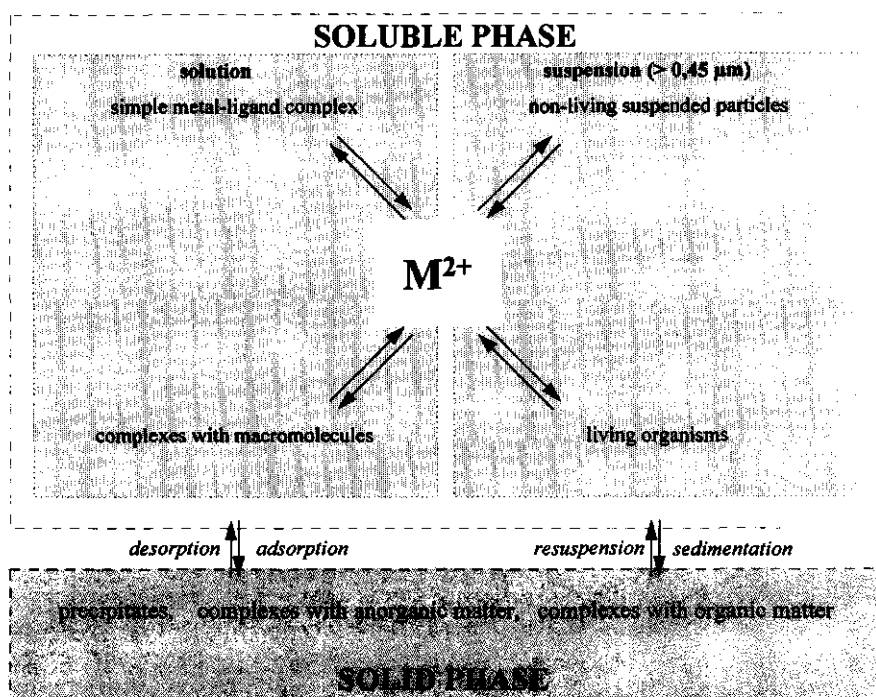


**Figure 6.1** Speciation of a heavy metal ion ( $M^{2+}$ ) in a natural system (after Buffle, 1988)

Natural organic complexants such as humic substances are poorly characterised, heterogeneous compounds. Table 6.1 gives the main differences in characteristics between simple ligands and several natural organic complexants (Buffle, 1988).

**Table 6.1** Characteristics of complexants found in natural systems (adapted from Buffle (1988))

Type of complexant	Example(s)	Character		
		Polyfunctional <sup>1</sup> character	Change in conformation	Polyelectrolytic <sup>1</sup> character
simple ligands	Cl <sup>-</sup> , acetate, amino-acids	weak or none	weak or none	weak or none
dissolved polyfunctional compounds	fulvic compounds	strong	aggregation	strong
monofunctional polyelectrolyte (permeable gel)	humic acids, cell walls, polysaccharides	intermediate	swelling or coiling	strong
monofunctional polyelectrolyte (surface reaction)	clays, metal oxides	intermediate	coagulation	strong

<sup>1</sup> the terms polyfunctional and polyelectrolytic will be explained in subchapter 6.2.2

## 6.2.2. Properties of natural organic complexants

### 6.2.2.1. Introduction

Natural organic complexants (i.e. macromolecules generally present as organic polymers and colloids) often contain a large number and variety of hydrophilic sites (e.g. COOH, OH, NH<sub>2</sub>, SH), which gives these compounds a high degree of hydration. In comparison to small dissolved molecules, the hydrated macromolecules possess a tertiary structure due to the formation of inter- and intramolecular bonds (Buffle, 1988). When the hydrated macromolecule formed is sufficiently rigid it should be considered a gel-like phase, distinct from the bulk solution as found by Marinsky et al. (1982) for biological and synthetic macromolecules and humic acids. Many hydrophilic sites of macromolecules are easily dissociable acidic and basic sites. Accordingly, the macromolecules possess a pH-dependent charge, which is generally negative under natural pH conditions (6 < pH < 9). Whether complexation takes place in the interior (gel phase) of the macromolecule or at the surface of the macromolecule, in both cases the complexation occurs in an electric field that strongly influences the stability of the complex because of electrostatic forces between the metal ion and the binding site (or functional group). The properties of the natural organic complexants can be divided into two categories:

1. polyfunctional character: large number and types of functional groups
2. polyelectrolytic character: negative charge of the complexant induces an electric field which depends on the charge density and conformation.

The proton and metal ion binding properties of humic substances, cell walls, and cell wall components have been studied extensively (Marinsky et al., 1980, 1982; Huang and Schnitzer, 1986; Herrington and Petzold, 1992a,b; Sentenac and Grignon, 1981; Laszlo, 1987; Buffle, 1988). Numerous modelling approaches are presented to describe proton and metal complexation to humic substances (Tipping et al., 1991; Marinsky et al., 1980; Nederlof et al., 1990; De Wit, 1992; De Wit et al. 1993a,b; Bartschatt et al., 1992; Vermeer, 1996) and for cell walls of plant material (Sentenac and Grignon, 1981; Kinraide et al., 1992). A mechanistic model for the adsorption of heavy metals to natural organic complexants should at least incorporate the interactions of cations with functional groups, competitive binding between protons and metal ions, and the polyfunctional and electrolytic character of the complexant. The conformation of the complexant depends on pH, ionic strength of the solution, metal loading and concentration of the complexant (Brannon-Peppas and Peppas, 1991). In this study, the following assumptions are made for the description of proton and metal ion binding to the natural organic complexants present in biowaste:

1. protons and free metal ions react with reactive sites and form an unidentate<sup>4</sup> complex;

<sup>4</sup> ligands occupying 1, 2, 3, etc. coordination positions in the complex are referred to as unidentate, bidentate, tridentate, etc.

the reaction is represented by the mass law of action and a corresponding thermodynamic affinity constant

2. the effect of the electric field on the binding is taken into account
3. the complexant is considered to be a gel phase distinct from the bulk solution with a fixed conformation in which the reactive sites are distributed homogeneously.

### 6.2.2.2. Polyfunctional character

For the binding of protons and metal ions to functional groups of the natural organic complexant, two different types of polyfunctionality can be distinguished. Firstly, a natural organic complexant can possess different types of coordinating sites, such as carboxyl, phenolic and amino groups. The binding strength (or affinity constant) of protons and metal ions with these functional groups differs significantly. Secondly, one type of functional group experiences a different steric and electric environment within the same macromolecule because of the different residues attached to the functional groups. The variable steric and electric environment influences the affinity of protons and metal ions for the functional group to a certain extent.

Natural organic complexants such as humic substances and components of cell walls contain various functional groups. The major functional groups of humic substances are carboxylic phenolic in nature. Minor functional groups identified on humic substances are alcoholic OH, quinones and ketones (C=O) and N- and S-containing sites (Buffle, 1988; Livens, 1991; Stevenson, 1994). Cell walls of plants are predominantly made up of cellulose, hemicellulose and lignin (Fengel and Wegener, 1984). The major groups of cells walls are carboxyl, aliphatic OH and phenolic OH groups (Schonherr, 1973, 1977; Kinraide et al., 1992). Minor groups such as C=O originate from plant extractives such as terpenoids, steroids, fats, waxes and phenolic compounds (Fengel and Wegener, 1984).

Because the description of proton and metal ion adsorption to natural organic complexants at a molecular level is very complicated, Sposito (1981, 1985) introduced the concept of quasi-particle models. A quasi-particle model is a mathematical description in which the complexant is replaced by a set of hypothetical, non-interacting functional groups. The differences in electric and steric environment for each functional group gives rise to a different affinity for protons and metal ions. This variable affinity can be described by a continuous probability density function, the Sips distribution (Sips, 1948):

$$f(\log K) = \frac{\ln(10) \sin(p\pi)}{\pi \left( \left( \frac{K}{\bar{K}} \right)^p + 2\cos(p\pi) + \left( \frac{\bar{K}}{K} \right)^p \right)} \quad (6.1)$$

where  $f(\log K)$  is the probability density function,  $K$  the affinity constant,  $\bar{K}$  the median value of the affinity distribution and  $p$  ( $0 < p < 1$ ) determines the width of the distribution.

In Figure 6.2 the Sips distribution is given for several values of  $p$ . For  $p=1$  a Dirac delta function is obtained and the distribution becomes broader for smaller values of  $p$ .

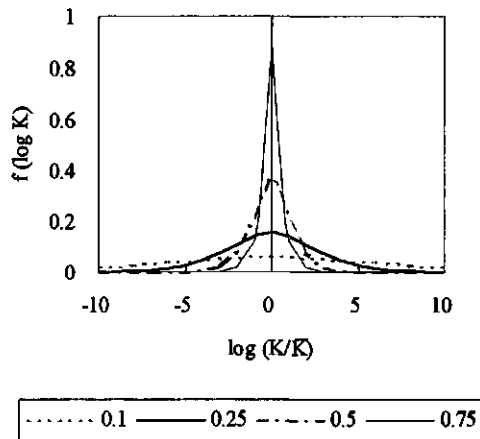


**Figure 6.2** Sips distribution for several values of Sips distribution parameter  $p$

The overall adsorption isotherm of metal ion Me with affinity distribution  $f(\log K_i)$  is given by (Nederlof et al., 1990):

$$\theta_{i,t} = \int_{\Delta \log K_i} \theta_{i,l} f(\log K_i) d \log(K_i) \quad (6.2)$$

where  $\theta_{i,t}$  is the total adsorption of metal ion  $i$ ,  $\theta_{i,l}$  the local adsorption isotherm (i.e. the binding to a group of identical sites),  $f(\log K_i)$  the distribution function of the affinity constant and  $\Delta \log K_i$  the range of  $\log K_i$  to be considered. For a complexant carrying one site and 1:1 stoichiometry of the reaction of site S and metal ion Me (unidentate complex,  $S + Me \leftrightarrow SMe$ ) multicomponent adsorption is given by the Langmuir-Freundlich isotherm (Buffle, 1988; Koopal, 1994):

$$\theta_{i,t} = \frac{Q_{i,t}}{Q_{max}} = \frac{\bar{K}_i c_i}{\sum_i \bar{K}_i c_i} \times \frac{\left( \sum_i \bar{K}_i c_i \right)^p}{1 + \left( \sum_i \bar{K}_i c_i \right)^p} \quad (6.3)$$

where  $Q_{i,t}$  is the total amount of metal ion  $i$  bound,  $Q_{max}$  is the total site density,  $\bar{K}_i$  is the median affinity constant for metal ion  $i$  and  $c_i$  is the activity of metal ion  $i$ . Koopal et al. (1994) showed that competitive adsorption for humic substances cannot be described by

the classical multicomponent model of equation 6.3. As a result of the non-ideality of local adsorption of metals ions, an ion-specific non-ideality has to be considered explicitly from the binding site heterogeneity. Incorporating the non-ideality of local adsorption in the Langmuir-Freundlich equation gives (Koopal et al., 1994; Benedetti et al., 1995):

$$Q_{i,f} = Q_{\max} \frac{(\bar{K}_i c_i)^n}{\sum_i (\bar{K}_i c_i)^n} \times \frac{\left( \sum_i (\bar{K}_i c_i)^n \right)^p}{1 + \left( \sum_i (\bar{K}_i c_i)^n \right)^p} \quad (6.4)$$

where  $n$  ( $0 < n < 1$ ) is the non-ideality parameter for metal ion  $i$ . Equation 6.4, developed by Koopal et al. (1994) is known as the Non-Ideal Competitive Adsorption model (NICA) model. The non-ideality is most probably due to the high ionic strength in the gel phase and different structure of hydration water in the gel phase compared to bulk water (Buffle, 1988). The changed structure and dielectric constant of water affects the electrostatic interaction between charged groups (Nishio, 1991). Because of these effects, the stability of the complexes between metal ions and the sites in this micro-environment can differ significantly from those in bulk water.

### 6.2.2.3. Polyelectrolytic character

A natural organic complexant carrying carboxyl and hydroxyl groups is negatively charged at neutral pH values. The negative charge on the molecule creates an electric field which affects the stability of metal complexes. The strength of the electric field depends on the type, density and distribution of the sites. The energy contribution of the electric field corresponds to the electrostatic work ( $ZF\phi$ ) necessary to bring the ion  $Me^{z+}$ , with charge  $Z$ , from the bulk solution ( $\phi=0$ ) to the complexing site:

$$\Delta G^0 - \Delta G_{\text{int}}^0 = ZF\phi \quad (6.5)$$

where  $\Delta G^0$  is the energy contribution at the complexing site,  $\Delta G_{\text{int}}^0$  the energy in the bulk solution,  $\phi$  the strength of the electrical field (V),  $Z$  the charge of ion  $Me$  and  $F$  the Faraday constant. The strength of the electrical field  $\phi$  depends on the charge carried by the complexant and thus on the total degree of site occupation. The affinity constant  $K$  is changed by the electrical field, according to:

$$K = K_{\text{int}} \exp\left(\frac{ZF\phi}{RT}\right) \quad (6.6)$$

where  $K_{\text{int}}$  is the intrinsic affinity constant in the absence of the electrical field. The electrical field does not depend on the nature of the complexant but is a result of the spatial distribution of charges on the complexant. Theoretical relationships between the spatial charge distribution and the electrical field  $\phi$  have been derived for organic macromolecules and inorganic solid surfaces. Bartschat et al. (1992) reviewed the advantages and disadvantages of various electrostatic models. The key variable for the electrostatic effect on the complexation reaction is the electrical field  $\psi$  usually obtained from the Poisson-Boltzmann equation:

$$\nabla\phi^2 = -\frac{1000F}{\epsilon} \left( \sum_i Z_i C_i \exp\left(-\frac{Z_i e \phi}{kT}\right) + \rho_0 \right) \quad (6.7)$$

where  $\epsilon$  is the dielectric constant,  $e$  the elementary charge ( $1.602 \cdot 10^{-19}$  C),  $k$  the Boltzmann constant ( $1.381 \cdot 10^{-23}$  J.K<sup>-1</sup>),  $T$  the temperature (in K).  $\rho_0$  represents the charge in the region in the absence of mobile ions (in mol.l<sup>-1</sup>) and the summation term represents the charge density produced by the distribution of co- and counterions (of charge  $Z_i$  and bulk-phase concentration  $c_i$ ) in the electrical field. This equation assumes that  $\phi$  is created by a central charged region and that the small, mobile ions arrange themselves according to this potential. As discussed by Bartschat et al. (1992) equation 6.7 has some theoretical flaws but for now it is the most practical and flexible method of studying electrostatics in aqueous solution.

Various researchers have used or modified the general Poisson-Boltzmann equation for specific applications. Tanford (1961) solved the linearised Poisson-Boltzmann equation for a penetrable sphere but this approximation is inappropriate when  $\psi$  becomes large. Bartschat et al. (1992) and De Wit (1992) studied the electrostatic effect by using the Poisson-Boltzmann theory and assuming the organic molecules to be impenetrable spheres. However, for humic acids the calculated molecular weights based on the assumption of impenetrable spheres did not correspond to the molecular weight determined by gel chromatography (Benedetti, 1996).

Here, the Donnan formalism is adopted. The Donnan concept for permeable spheres, developed by Marinsky et al. (1982), assumes that two states of bound counterions are present (see Figure 6.3):

1. 'site-bound': the cations are covalently bound to one or several functional groups
2. 'territorially-bound': the cations are spatially trapped in a polymer domain due to electrostatic binding, i.e. the Donnan gel-phase with gel-phase volume  $V_D$

The negative charge in the Donnan gel-phase leads to an electrostatic Donnan potential ( $\phi_b$ ) at the gel phase-bulk interface which is assumed to be independent of the position in the gel phase. Cations are accumulated in the gel phase whereas anions are excluded from



the gel phase. For these conditions the concentration of ion  $i$  in the gel phase can be related to the concentration in the bulk by the equation:

$$\lambda^{z_i} = \frac{(c_{i,D})^{z_i}}{(c_i)^{z_i}} = \exp\left(-\frac{Z_i \phi_D}{RT}\right) \quad (6.8)$$

where  $\lambda$  is the Donnan potential term, and  $c_{i,D}$  and  $c_i$  are the concentration of ion  $i$  in the Donnan phase and bulk, respectively. The Donnan potential  $\phi$  is determined by the charge density in the Donnan gel-phase (i.e. the number of undissociated sites and the Donnan gel-phase volume,  $V_D$ ) and the ionic strength in the bulk solution. Bartschatt et al. (1992) showed that the Donnan model approaches the Poisson-Boltzmann solution for penetrable spheres with a radius larger than 20-30 Å in combination with a charge density of 3.7 M. Benedetti et al. (1996) showed that the Donnan model can describe the electrostatic effect for proton binding to humic acids. The calculated Donnan gel-phase volumes are physically realistic and in correspondence with experimental data. Mineral interaction of K, Mg, Ca and Zn with the insoluble dietary fibre of Soy Hull (Sentenac and Grignon, 1981) and the adsorption of Ca, Mg and K to purified cell walls of Horse bean roots (Laslo, 1987) were also satisfactorily described by the Donnan model. Kinraid et al. (1992) found that the Gouy-Chapman theory and Donnan model are both able to predict the toxic effect of  $Al^{3+}$ ,  $La^{3+}$ ,  $H^+$  and other cations at the cell surface of wheat roots.

#### 6.2.2.4. Parameters of NICA-Donnan model

Proton and metal ion adsorption to natural organic complexants is described by the following parameters in the NICA-Donnan model:

1. concentration of functional groups (in  $mmol.g^{-1}$ )
2. affinity constant of unidentate complexes of protons and metal ions for each functional group (in  $l.mol^{-1}$ )
3. affinity distribution parameter  $p$  for each functional group
4. ion specific non-ideality parameter  $n_i$  for each functional group
5. Donnan gel-phase volume,  $V_D$  (in  $ml.g^{-1}$ ).

The NICA-Donnan model can readily be incorporated into standard chemical equilibrium algorithms such as EQUILIB (the thermodynamic equilibrium concept and the computer program EQUILIB are described in Appendix 6A).

### 6.2.3. Validation of the NICA-Donnan model with Sephadex CM-25

Sephadex CM-25, a synthetic weak-acid cation-exchanger carrying methoxycarboxyl groups coupled to a cross-linked dextran matrix of Sephadex G-25, was chosen as model compound. The physico-chemical properties of Sephadex are well characterised:

- beads are spherical with a diameter of 40-125  $\mu\text{m}$  in dry form
- functional group: methoxycarboxyl ( $-\text{CH}_2\text{-O-COO}^-$ ) with total capacity of 4.5  $\text{mmol.g}^{-1}$  dry gel
- gel-phase volume of 6.5  $\text{ml.g}^{-1}$  dry gel.

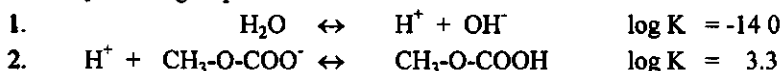
Other features of Sephadex CM-25 which make it suitable as a model compound:

- functional groups are homogeneously distributed over the beads
- the dextran matrix is strongly hydrophilic, displaying minimal non-specific metal adsorption
- due to a high degree of cross-linking, conformational changes are negligible during acid-base titration and at variable ionic strength (from pH 3 to 9 and ionic strength 0.05-0.5 M)
- stoichiometry and stability constants are known for the reaction of methoxyacetic acid with protons and Cu(II) ions (Smith and Martell, 1976).

The acid-base properties at variable ionic strength and Cu(II) adsorption at variable pH and ionic strength of Sephadex CM-25 are modelled for the same conditions as the experiments.

#### 6.2.3.1. Acid-base titration

The following reactions have to be considered for the description of proton binding to the methoxyacetate group:



Dissociation of water (reaction 1) takes place in both the gel phase and the bulk solution, and reaction 2 takes place only in the gel phase of Sephadex CM-25. The intrinsic equilibrium constants at 293 K for reactions 1 and 2 were taken from Smith and Martell (1976). It is assumed that the functional groups experience the same chemical environment and therefore the Sips distribution parameter  $p$  is one. For proton binding no distinction can be made between the Sips distribution parameter  $p$  and the non-ideality parameter  $n$ . For the model calculations, the non-ideality parameter  $n$  is also set to unity.

From the data points generated by EQUILIB the  $\text{OH}^-$  adsorption isotherms were calculated by equation 6.9 (see subchapter 6.3.1.1). The calculated hydroxyl adsorption isotherms are shown in Figure 6.3.

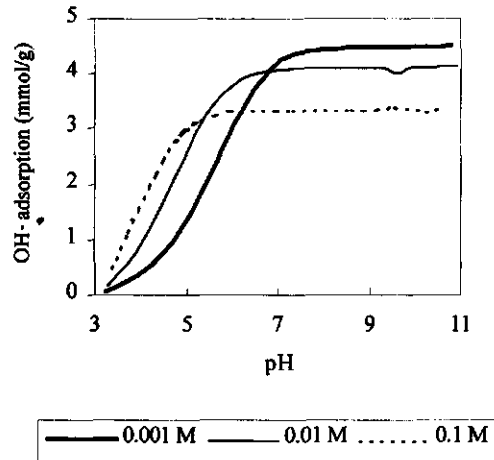


**Figure 6.3**  $\text{OH}^-$  adsorption isotherms of Sephadex CM-25 as function of pH at variable ionic strength as calculated by the NICA-Donnan model

Due to the electrostatic effect, which is caused by the negatively-charged carboxyl groups, the apparent proton affinity constant felt in the bulk solution is higher. Therefore the  $\text{OH}^-$  adsorption curve shifts to higher pH values at lower ionic strengths. Figure 6.4 shows the Donnan potential term  $\lambda$  as a function of pH at variable ionic strengths.

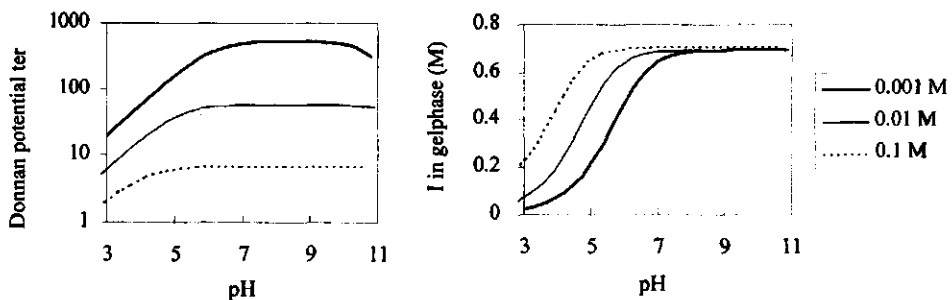
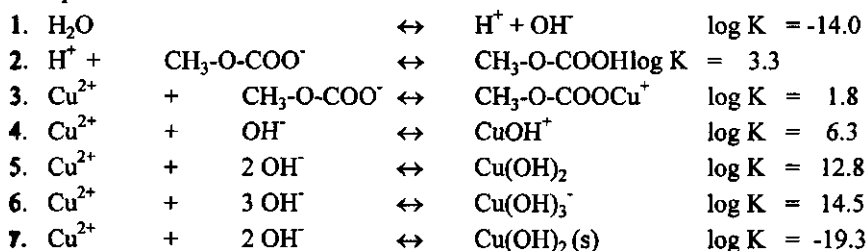


**Figure 6.4** Donnan potential term ( $\lambda$ ) and ionic strength ( $I$ ) in the gel phase of Sephadex as function of pH at variable ionic strength as calculated by the NICA-Donnan model

The lower Donnan potential term at higher ionic strength is due to the shielding of the negative charge density by the monovalent inert<sup>5</sup> cations. The potential term increases at higher pH values because the negative charge density increases due to the proton dissociation of the carboxylic sites. At even higher pH values (pH>10) the potential term again drops due to the increasing ionic strength of the bulk solution which again shields the negative charge density of the complexant. Figure 6.4 shows that the ionic strength in the gel phase at higher pH values is far beyond the validity of the Davies equation (see Appendix 6A). Several semi-empirical approaches are available for calculating the activity coefficients of ions at high ionic strength, e.g. Pitzer and Chen equations (Zemaitis et al., 1988). Application of the Pitzer equations or the Chen equations, however, is only useful for well-defined systems such as sea-water desalination, ion-exchange processes and hydrometallurgical processes. In the NICA-Donnan model, the non-ideality in the gel phase can be incorporated in the non-ideality parameter *n*, i.e. ion-specific non-ideality of local adsorption in the gel phase.

#### 6.2.3.2. Cu(II) adsorption

The following reactions have to be considered for the description of Cu(II) ion adsorption to Sephadex CM-25<sup>6</sup>:



Reactions 1, 4, 5, and 6 take place in both the gel- and the bulk phase; reactions 2 and 3 take place only in the gel phase. The intrinsic equilibrium constants for reactions 1-7 at 293 K were taken from Smith and Martell (1976). In the model calculations, the Sips distribution parameter *p* and the ion-specific non-ideality parameter *n* were both set to one.

The Cu(II) adsorption isotherms were calculated by equation 6.10 (see subchapter 6.3.1.2). The model calculations show that the contribution of soluble free Cu(II) and Cu(II)-hydroxide complexes accumulated in the gel phase to the total Cu(II) adsorption are negligible (results not shown here). In Figure 6.5, the Cu(II) adsorption isotherms (Cu(II) adsorbed as a function of the free Cu(II) activity) at variable pH and ionic

<sup>5</sup> the term inert (or indifferent) is used for ionic species not showing any significant complexation reactions

<sup>6</sup> reactions 4, 5 and 6 describe reactions for soluble Cu-hydroxide complexes and reaction 7 represents the precipitation reaction where (s) stands for solids (or precipitate)

strength are presented. A lower free Cu(II) activity corresponds to a stronger binding of Cu(II). The model shows that the binding strength decreases at lower pH values and with higher ionic strengths.

Two effects play a role in decreasing binding strength at lower pH values. First, Cu(II) adsorption decreases at lower pH values because Cu(II) ions are exchanged for protons at the methoxycarboxyl site. Secondly, the electrostatic effect decreases because the charge density of Sephadex CM-25 decreases due to the protonation of the carboxylic sites.

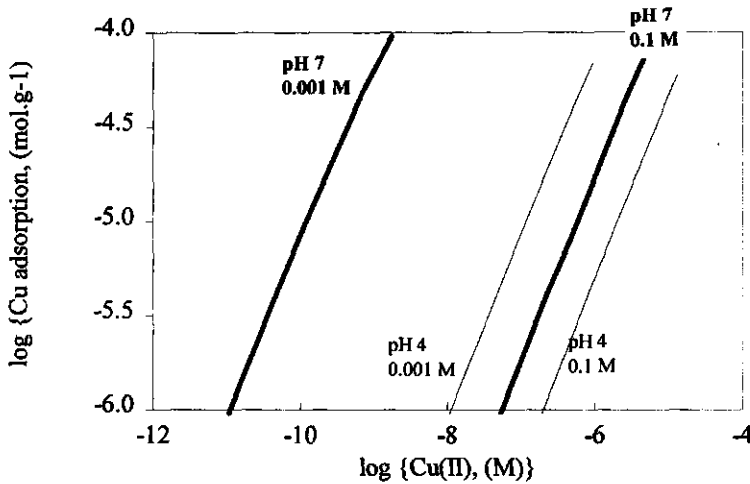


**Figure 6.5** Cu(II) adsorption to Sephadex CM-25 model at variable pH (4 and 7) and ionic strength (0.001 and 0.1 M) as calculated by the NICA-Donnan model

The sole effect of electrostatics can be seen from the Cu(II) adsorption at constant pH and variable ionic strength. Figure 6.5 shows that at higher ionic strength the Cu(II) binding strength decreases due to the decreased electrostatic effect caused by the shielding of the charge density by inert cations (it is assumed that  $\text{Na}^+$  ions are inert and do not react with the carboxylic sites). Cu(II) ions are more strongly attracted by the negative charge in the gel phase because the charge of Cu(II) ions is twice the charge of protons. The ionic strength effect is more pronounced at pH 7 because the dissociation degree of the carboxylic sites is higher, leading to a higher negative charge density and accordingly to a stronger electric field. It is remarkable to see that, due to the electric field, the adsorption at pH 4 and I of 0.001 M is almost equal to the adsorption at pH 7 and I of 0.1 M. Generally it is assumed that the pH effect on the metal ion adsorption is much larger than the effect of the ionic strength. However, the model calculations presented here for Sephadex CM-25 show that proton competition can be exceeded by ionic strength effects.

### 6.3. Materials and methods

#### 6.3.1. Titration experiments

The acid-base and Cu(II) titration measurements were made with a home-made, computer-controlled titration apparatus coupled to a batch titration set-up as described in subchapter 3.7. The acid-base titrations and Cu(II) adsorption experiments for Sephadex CM-25 were made at a solids concentrations of  $1 \text{ g.l}^{-1}$ . The  $\text{H}^+$  and  $\text{Cu}^{2+}$  activities were measured potentiometrically using a glass-electrode (Schott, type N32A) and a solid-state cupric ion-selective electrode (ORION, model 94-29), respectively. The use of both ion-selective electrodes was described in subchapter 3.5. The combined glass electrode was calibrated with solutions of pH 4.0 and 7.0 (Merck) and the Cu(II)-ISE with solutions of  $10^{-3} \text{ M}$  and  $10^{-5} \text{ M}$   $\text{Cu}(\text{NO}_3)_2$  in  $0.01 \text{ M}$   $\text{NaNO}_3$ . The electrodes were calibrated before and after the measurement to reveal changes in electrode response. Calibrations of the glass electrode and the Cu(II)-ISE before and after the measurement should not differ more than  $1 \text{ mV}$ . Titrations were made in  $\text{CO}_2$ -free solutions under a nitrogen atmosphere to prevent  $\text{CO}_2$  interfering with the measurements.

##### 6.3.1.1. Acid-base titrations

The acid-base titration experiments were conducted from low to high pH values. The results, pH measured as a function of the added NaOH, were imported into a spreadsheet. Correcting for the buffercapacity of water, the  $\text{OH}^-$  adsorption (in  $\text{mmol.g}^{-1}$ ) of the sample was calculated by:

$$\text{OH}^- \text{ adsorption} = \frac{[\text{Na}^+]_{\text{added}} - [\text{NO}_3^-]_0 - \frac{(10^{-(14-\text{pH})} - 10^{-\text{pH}})}{\gamma^+} V_{\text{sol}}}{W_{\text{ads}}} \quad (6.9)$$

where  $[\text{Na}^+]_{\text{added}}$  is the amount of NaOH added (in mmol),  $[\text{NO}_3^-]_0$  is the amount of nitrate present at the beginning of the titration (in mmol),  $V_{\text{sol}}$  is the volume of the solution (in ml),  $\gamma^+$  is the activity coefficient for monovalent ions (protons), and  $W_{\text{ads}}$  is the weight of the sample (in g). In principle, when no hysteresis effects take place, the hydroxyl adsorption should be identical to the proton adsorption isotherms, i.e. titrations from high to low pH values.

##### Calibration of acid-base titrations

Acid-base titrations of  $0.01 \text{ M}$   $\text{NaNO}_3$  made without a  $\text{N}_2$  atmosphere showed that  $\text{CO}_2$  is absorbed from the air, especially at high pH values. This will lead to unwanted  $\text{OH}^-$  adsorption especially at high pH values. Moreover, variations of  $\pm 5\%$  in the ISE calibra-

tion and in the molarity of the titrant have large effects on the  $\text{OH}^-$  adsorption at high pH values. Large deviations at high pH are due to the logarithmic scale of the measurement which is inherent to the experimental procedure. A deviation of 1 mV at pH 11 will result in a deviation in adsorption of  $4 \cdot 10^{-5} \text{ mol.l}^{-1}$  compared to a deviation of  $4 \cdot 10^{-8} \text{ mol.l}^{-1}$  at pH 8.

A set of data points for a blank experiment (0.01 M  $\text{NaNO}_3$ ) was generated with the model EQUILIB. These calculations showed that small variation in the water dissociation constant or small deviations in constant A of the Davies equation (see Appendix 6A) also resulted in unwanted  $\text{OH}^-$  adsorption at high pH values.

Histidine, an amino acid carrying three functional groups with proton affinity constants of  $10^{1.7}$ ,  $10^{6.02}$  and  $10^{9.08}$ , was titrated at 25 °C and 0.1 M ionic strength. The  $\text{OH}^-$  adsorption isotherm was employed to calculate the site affinity distribution function (SADF) which represents the number of sites with a corresponding affinity or equilibrium constant. Nederlof (1992) developed a method to calculate the SADF based on the LOGA approximation for the local isotherm. To obtain reliable results a smoothing spline routine was used to reduce the scattering of data points of the experimental adsorption isotherm. The features of the LOGA procedure are discussed by Nederlof (1990). The computer programs of Nederlof were used to calculate the SADF. The maxima of the SADF at log K values of 6.1 and 9.1 and the number of sites were in excellent agreement with the tabulated affinity constants and the number of sites for histidine (Martell and Smith, 1977).

The experimental set-up and spreadsheet calculations are appropriate for the determination of the acid-base properties of simple ligands. The detection limit is approx.  $0.05 \text{ mmol.l}^{-1}$  and the 'titration window' is limited from pH 4 to 10 due to the logarithmic nature of the measurement (Nernstian behaviour). Careful calibration and  $\text{CO}_2$  elimination can extend the window to pH 3-11. For titrations at high pH values and for longer titrations times,  $\text{CO}_2$  absorption from the air is possible, giving rise to unwanted  $\text{OH}^-$  adsorption.

### 6.3.1.2. *Cu(II) titrations*

For the  $\text{Cu(II)}$  adsorption experiments at constant pH, the solution was titrated with  $\text{Cu(NO}_3)_2$  and maintained at a fixed pH by the addition of  $\text{NaOH}$  (so-called pH-stat experiments). For every data point, pH, pCu, and added volume of  $\text{NaOH}$  and  $\text{Cu(NO}_3)_2$  were registered and imported into a spreadsheet program. For the calculation of the  $\text{Cu(II)}$  adsorption (in  $\text{mmol.g}^{-1}$ ) a correction was made for the complexation of  $\text{Cu}^{2+}$  with  $\text{NO}_3^-$  and  $\text{OH}^-$  (soluble complexes) in the bulk solution:

$$\text{Cu(II) adsorption} = \frac{[\text{Cu}^{2+}]_{\text{added}} - \sum_{n=1}^2 [\text{Cu}(\text{NO}_3)_n^{(2-n)+}] - \sum_{n=1}^4 [\text{Cu}(\text{OH})_n^{(2-n)+}] - \frac{10^{-\text{pCu}}}{\gamma^{2+}} V_{\text{sol}}}{W_{\text{ads}}} \quad (6.10)$$

where  $[\text{Cu}^{2+}]_{\text{added}}$  is the amount of  $\text{Cu}(\text{NO}_3)_2$  added (in mmol), pCu the measured copper activity by the Cu(II)-ISE (in M) and  $\gamma^{2+}$  is the activity coefficient for Cu(II) ions. The amount of  $\text{Cu}(\text{NO}_3)_n$  complexes and  $\text{Cu}(\text{OH})_n$  complexes (in mmol) were calculated from the tabulated equilibrium constants (Smith and Martell, 1976), the  $\text{NO}_3^-$  concentration and the measured pH and pCu.

### 6.3.2. Drift criterion for titration of solid and colloidal complexants

Sequenced titration experiments were conducted by the computer-controlled titration apparatus to generate titration curves with a large number of data points. For colloidal and solid complexants, the reactions of protons and metal ions with reactive sites are not instantaneous because the ions have to reach the reactive sites by diffusion through the film layer and inside the particles. For reliable comparison of model calculations with experimental results, it is necessary for chemical equilibrium to be reached at every data point of the adsorption isotherm. It is difficult to evaluate the equilibrium status of the solution, i.e. when all reactive sites are equally occupied. The concept of a drift criterion is introduced to judge when equilibrium is reached after the addition of a dosage of titrant (drift is defined as the change in the electrode reading per unit of time, in  $\text{mV}\cdot\text{min}^{-1}$ ). The next dose of titrant is added when the drift of the electrode is less than the drift criterion. Expression of the drift criterion is somewhat awkward due to the fact that pH measurements are carried out on a logarithmic scale while diffusion processes are expressed in  $\text{mol}\cdot\text{m}^{-2}\cdot\text{s}^{-1}$ . This means that the drift criterion is more strict at higher pH values due to the logarithmic scale of the measurement. At pH 3 a drift criterion of  $0.1 \text{ mV}\cdot\text{min}^{-1}$  corresponds with a drift of  $2 \times 10^{-5} \text{ mol}\cdot\text{l}^{-1}\cdot\text{min}^{-1}$  and at pH 10 to  $2 \times 10^{-12} \text{ mol}\cdot\text{l}^{-1}\cdot\text{min}^{-1}$ . Another option is to express the drift criterion in  $(\text{mol}\cdot\text{l}^{-1} \text{ H}^+\cdot\text{min}^{-1})$  but this will lead to unrealistically long experiment times, because a drift criterion of  $0.1 \text{ mV}\cdot\text{min}^{-1}$  at pH 10 would correspond to a drift criterion of  $1 \times 10^{-8} \text{ mV}\cdot\text{min}^{-1}$  at pH 3 (1 mV drift in 3 years!). The titration experiment should therefore be considered a 'quasi-equilibrium' experiment.

## 6.4. Results

The acid-base properties at variable ionic strength and Cu(II) adsorption isotherms at variable pH and ionic strength were measured for Sephadex CM-25.



### 6.4.1. Acid-base titrations

Acid-base titrations at variable drift criteria were made to get an impression of the time required to reach equilibrium. In Figure 6.6 the  $\text{OH}^-$  adsorption and cumulative titration time are shown for drift criteria of 1, 0.2 and 0.02  $\text{mV}\cdot\text{min}^{-1}$  at an ionic strength of 0.01 M. The adsorption isotherms are compared to the model calculation made with EQUILIB. The adsorption depends on the drift criteria; for longer titration times the adsorption increases. This shows that  $\text{OH}^-$  ions need time to reach the reactive sites in the solid phase of Sephadex beads.

The electrostatic effect was studied by varying the ionic strength of the bulk solution. The 'equilibrium'  $\text{OH}^-$  adsorption isotherms at a drift criterion of 0.02  $\text{mV}\cdot\text{min}^{-1}$  for ionic strengths of 0.001, 0.01, and 0.1 M are shown in Figure 6.7. Figure 6.7 shows that the  $\text{OH}^-$  adsorption decreases with increasing ionic strength.

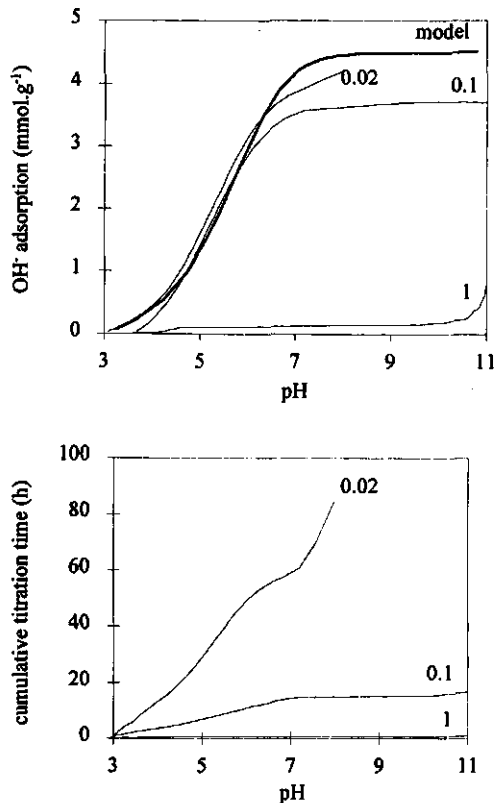


**Figure 6.6**  $\text{OH}^-$  adsorption isotherm (top) and cumulative titration time (bottom) as function of pH for Sephadex CM-25 at variable drift criteria (in  $\text{mV}/\text{min}$ )

### 6.4.2. Cu(II) adsorption isotherms

Cu(II) adsorption isotherms were made at pH 4 and 7 at 0.1 and 0.001 M ionic strength. Cu(II) adsorption isotherms are affected by both the charge density of the complexant and the competition of protons with Cu(II) ions for the same binding sites. Only experiments at variable ionic strength give distinct information on the electrostatic effect on the Cu(II) adsorption. The adsorption experiments were carried out in the same concentration range in which Cu(II) is present in biowaste. The Cu(II) titration experiments were started at  $10^{-6}$  mol Cu.  $g^{-1}$  to avoid slow and non-linear response of the Cu(II)-ISE. The Cu(II) adsorption isotherms were made at a drift criterion of  $0.2 \text{ mV} \cdot \text{min}^{-1}$ , for which it was assumed that equilibrium was reached for every data point on the adsorption isotherm. This assumption will be addressed in subchapter 6.5.3.

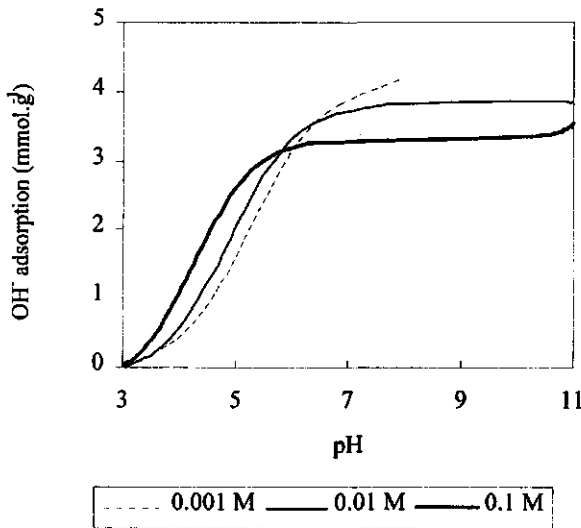


**Figure 6.7** OH<sup>-</sup> adsorption for Sephadex CM-25 as function of pH ‘at equilibrium’ at variable ionic strength

Figure 6.8 shows the Cu(II) adsorption isotherms at variable pH (4 and 7) and ionic strength (0.001 and 0.1 M NaNO<sub>3</sub>). The results show that Cu(II) adsorption is stronger at higher pH values and lower ionic strength.

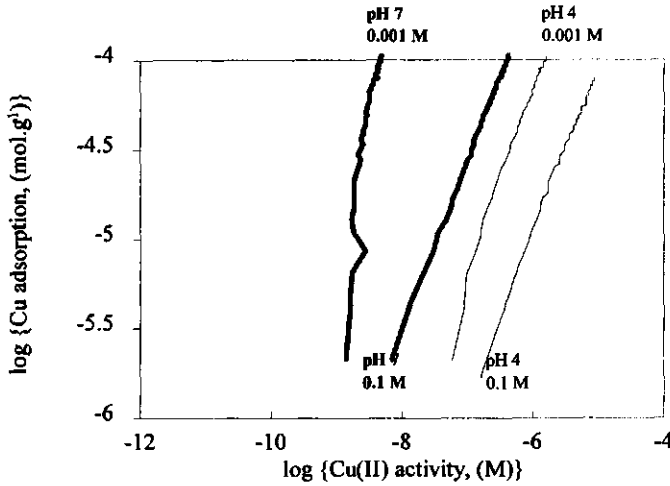


**Figure 6.8** Cu(II) adsorption of Sephadex CM-25 at pH 4 and 7 and 0.001 and 0.1 M ionic strength

## 6.5. Discussion

### 6.5.1. Acid-base titration

The experimental  $\text{OH}^-$  adsorption isotherms for Sephadex CM-25 at variable ionic strength are qualitatively described by the NICA-Donnan model without parameter fitting (compare Figures 6.3 and 6.7). The model gives the best fit of the experimental adsorption isotherms when the gel volume is raised from 6.5 to 10  $\text{ml.g}^{-1}$ . The gel volume of 6.5  $\text{ml.g}^{-1}$  was based on dry weight and can change in water. However, the small discrepancy between model and experiment could also be due to the relatively high ionic strength in the gel phase. Activity coefficients are calculated by the Davies equation which can be applied only up to an ionic strengths of 0.3 M. Here, the non-ideality was taken into account by an increase of the Donnan gel volume, but the model can also adequately describe the experiments by fitting the non-ideality parameter  $n$ .

The model and experiment both show that the affinity constant observed in the solution is higher than in the intrinsic affinity of the methoxycarboxyl group in the gel phase. As discussed in subchapter 6.2.3.1, this is due to the electrostatic effect of the negatively charged Sephadex CM-25. The electrostatic effect becomes smaller at higher ionic strength because the negative charge of the Sephadex is shielded by  $\text{Na}^+$  ions.

### 6.5.2. Cu(II) adsorption

Both the model and the experiment show a stronger Cu(II) binding at higher pH and lower ionic strength. As explained in subchapter 6.2.3.1 this is caused by a stronger electrostatic effect and less competition with protons for the methoxycarboxyl site. Both model and experiment are in good agreement at pH 4 and 0.1 M NaNO<sub>3</sub> but the model predicts stronger Cu(II) binding at decreasing ionic strength and higher pH values. This indicates that the electrostatic effect is smaller than predicted by the model. The electrostatic effect can be reduced by increasing the Donnan gel-phase volume. However, increasing the gel-phase volume has no physico-chemical meaning because the gel volume is constant over a large range of pH and ionic strength (see subchapter 6.2.3). As discussed in subchapter 6.2.2.1 the discrepancy must be due to the non-ideality of local adsorption of protons and metal ions to the methoxycarboxyl sites in the gel phase. At high ionic strength, as met in the gel phase of Sephadex CM-25 (see Figure 6.3), calculation of the activity coefficient ( $\gamma$ ) by the Davies equation is not valid above ionic strengths of 0.3 M (Stumm and Morgan, 1996). Cu(II) is a divalent ion for which the deviation from the Davies equation is even more pronounced at increasing ionic strength compared to monovalent protons. As discussed in subchapter 6.2.2.1, the non-ideality of local adsorption can elegantly be handled by introducing the ion-specific non-ideality parameter  $n$  (see equation 6.4). This approach will be treated more extensively in Chapter 7.

Closer comparison of the experimental and model Cu(II) adsorption isotherms shows further discrepancies. The model results for the Cu(II) adsorption isotherms show a linear behaviour on log-log scale from Cu(II) loadings of  $10^{-6}$  to  $10^{-4}$  mol.g<sup>-1</sup>. On the other hand, the experimental Cu(II) adsorption isotherms show non-linear behaviour, especially at low Cu(II) loadings, higher pH values and lower ionic strength. These phenomena will be discussed in the next subchapter.

#### 6.5.2.1. Kinetic aspects of the titrations

The OH<sup>-</sup> adsorption isotherms of Sephadex CM-25 at 0.01 M NaNO<sub>3</sub> at variable drift criterion (Figure 6.4) show that adsorption increases with lower drift criteria and that the increase is more pronounced at low pH values. As mentioned in subchapter 6.3.2, a drift for ions should be expressed in mol.l<sup>-1</sup>.s<sup>-1</sup>. Expressing the drift criterion in mV.min<sup>-1</sup> results in a pH-dependent drift criterion, i.e. for an equal drift criterion the drift is less at low pH values. The experimental OH<sup>-</sup> adsorption isotherms show that a drift criterion of 1 mV.min<sup>-1</sup> is too high to allow the OH<sup>-</sup> ions to diffuse in the Sephadex gel-phase and reach the methoxycarboxyl sites, especially at low pH (Figure 6.6). Lower drift criteria result in it taking more time for the hydroxyl ions to reach the methoxycarboxyl sites, i.e. to reach equilibrium. With lower drift criteria, both the cumulative titration time and the

OH<sup>-</sup> adsorption increase (Figure 6.6). A comparison of experiment and model calculations (Figure 6.6) shows that a drift criterion of  $0.02 \text{ mV}\cdot\text{min}^{-1}$  is sufficient to reach equilibrium over the complete adsorption isotherm. However, this leads to undesirably long titration times and the possibility of unwanted  $\text{CO}_2$ -stripping from the air. Long titration times can be reduced by introducing a pH-dependent drift criterion, small at low pH values and larger at high pH values.

The time dependence of the acid-base titrations is due to the location of the reactive sites of Sephadex inside the beads. These sites can only be reached by diffusion inside the particles through the gel phase. When OH<sup>-</sup> ions react with undissociated carboxylic groups, a concentration profile will be established in the Sephadex beads and it will be a long time before all sites have the same degree of dissociation. The time required to reach equilibrium depends on various factors, such as particle size, diffusivity ( $D$ ) of ions in the gel phase, proton affinity constant for the reactive sites, degree of site occupation, pH of the gel phase and the total charge density inside the particles.

A comparison of experiments and model calculations for the Cu(II) adsorption isotherms (Figure 6.5 and 6.8) shows that at low Cu(II) loadings the model results show linear Cu(II) adsorption isotherms (on log-log scale) whereas the experimental adsorption isotherms show a non-linear behaviour, especially at low Cu(II) loadings and higher binding strengths. This difference can also be accounted for by diffusion phenomena. As only soluble Cu(II) ions (i.e. Cu(II) ions not adsorbed to the methoxycarboxyl sites) can diffuse through the Sephadex gel-phase, it takes a long time before the Cu(II) ions are uniformly distributed over the entire gel phase. A drift criterion of  $0.2 \text{ mV}\cdot\text{min}^{-1}$  is not small enough to reach thermodynamic equilibrium when  $\text{Cu}^{2+}$  is low; this is at low Cu(II) loadings, lower ionic strengths and higher pH values. Therefore, the Cu(II) adsorption is limited to the outer shell of the beads, experiencing only part of the total amount of carboxyl groups. This explains the less strong binding at low Cu(II) loadings in comparison to model calculations for which all sites are available.

The time required to approach equilibrium depends on the radius ( $R$ ) of the particles and the effective diffusion ( $D_e$ ) of Cu(II) ions through the gel phase. In analogy to heat transport, the dimensionless time as expressed by the Fourier number  $Fo = \frac{D_e \cdot t}{R^2}$  should be approx. 0.5 in order to achieve equilibrium (Carslaw and Jaeger, 1959). Therefore, as a rule of thumb the experimental time should be approx.  $t = \frac{R^2}{D_e}$  in order to reach equilibrium. The effective diffusion of Cu(II) is restricted by the pore structure of the particles and the adsorption of Cu(II) to carboxyl groups, as only free ions can diffuse through the gel phase. The higher the binding strength, the more Cu(II) ions are bound and the lower the effective diffusion (Buffle, 1988). For an affinity constant  $K$  of  $10^3 \text{ M}$  for Cu(II) ions, a diffusivity  $D$  of  $10^{-11} \text{ m}^2\cdot\text{s}^{-1}$  and a particle radius of 0.1 mm, this results in a period of

115 days to reach equilibrium! Based on this simplified approach it becomes clear that the deviation is greater for a higher binding strength (i.e. a lower Cu(II) loading, higher affinity constant, lower ionic strength and higher pH) and for larger particles. The experiments confirm this concept and show that titration experiments should be regarded with care when interpreted by a chemical equilibrium model. For the correct interpretation of the experiments, the adsorption isotherms must be at equilibrium at every titration point. This results in very long titration times for Cu(II) adsorption experiments at low Cu(II) loadings and high pH values and could be a practical problem.

## 6.6. Conclusions

The presented NICA-Donnan model can describe the proton and metal ion adsorption to natural organic complexants. The model accounts for the polyfunctional and polyelectrolytic character of the complexant. The binding site heterogeneity and non-ideality of local metal ion binding are described by the NICA model. The electrostatic effect is handled by the Donnan formalism.

The model is easily incorporated in EQUILIB, an algorithm used to calculate thermodynamic chemical equilibrium. The NICA-Donnan model can be extended for metal adsorption to complexants with more types of functional groups and can handle e.g. metal competition. The model will be used in Chapter 7 to describe the acid-base properties and Cu(II) adsorption of the particle-sized organic fractions isolated from biowaste.

The acid-base behaviour of Sephadex CM-25 at different ionic strengths is quantitatively described by the model. Adsorption of protons is described by unidentate complexes of protons with the monomeric methoxyacetic acid unit. Experiments clearly show the polyelectrolytic properties of the gel phase, which is handled excellently by the Donnan formalism. This works out well because the reactive sites are homogeneously distributed over the gel phase and the conformation of the Sephadex gel-phase does not change with ionic strength and pH.

Cu(II) adsorption isotherms at variable ionic strength and pH are also adequately described by the model. Cu(II) binding is described by an unidentate complex with the monomeric methoxyacetic acid group and no evidence is found for the presence of mixed complexes. The discrepancy between model and experiments becomes larger at lower ionic strengths and higher pH. These effects can be assigned to the high ionic strength inside the gel phase of Sephadex CM-25. This phenomena can be accounted for by the ion-specific non-ideality parameter  $n$  for the local adsorption of metal ions to reactive sites in the gel phase.

The acid-base titration and Cu(II) adsorption experiments showed that the titration time is an important parameter for the titrations. This is because the diffusion of ions inside the particles is the rate-limiting step of the adsorption process. A certain period of time is needed for the ions to diffuse inside the solid particles and reach the reactive sites. At true thermodynamic equilibrium, all protons and metal ions are equally distributed over the available sites. The time required to reach equilibrium depends on the free proton or metal ion concentration, which are again related to the particle properties and chemical conditions of the solution. As demonstrated for Sephadex CM-25, the rate of adsorption is limited by the slow diffusion of ions in the gel phase, leading to long titration times before true equilibrium is reached.

The computer-controlled batch titration apparatus is well suited for measuring reproducible proton and metal ion adsorption isotherms for solid complexants. "Quasi-equilibrium" is weighed by a computer-controlled drift criterion and the elapsed time for every titration step is automatically recorded. The pH of the solution is recorded and automatically corrected. Quasi-equilibrium is weighed by a drift criterion: the next aliquot of titrant is added when the change in Cu(II) electrode reading is less than a preset value, i.e. the drift criterion (in  $\text{mV}\cdot\text{min}^{-1}$ ). The results show that the titrations can be improved by defining a pH- and pCu-dependent drift criterion, i.e. small drift criteria at high proton and Cu(II) ion activities and larger drift criteria for lower activities.

## **Appendix 6A      Thermodynamic equilibrium model EQUILIB**

### **6A.1 Introduction**

There are two classes of modelling approaches to describe the behaviour of heavy metals in natural systems (Sposito, 1985):

1. empirical models
2. mechanistic models.

Empirical models treat the system as a black box and in this approach only conservation principles and parametric statistics are employed. An empirical model can have some predictive value but only on a limited scale. Moreover, the empirical approach provides no insight into the chemistry of the system. The effect of variations in pH, ionic strength or competing cations cannot be predicted by empirical models and must be measured for every new situation.

Mechanistic models, on the other hand, describe the underlying chemical and physical or biological processes (Jenne, 1978). Therefore, a mechanistic model provides insight into the underlying processes which control the system and can have a more predictive value. In this appendix we will briefly discuss the numerical method for calculating the equilibrium concentration of species in a multicomponent system.

### **6A.2 Thermodynamic equilibrium concept**

The speciation of heavy metals in their equilibrium state can be described by chemical thermodynamics (Buffle, 1988). As defined by Stumm and Morgan: "Equilibrium is the time-invariant state of a closed system and a stationary-state thermodynamic model requires that the system is closed and no matter is exchanged with the surrounding". Additionally, the thermodynamic equilibrium approach requires that the temperature and pressure be fixed and all components homogeneously distributed (Stumm and Morgan, 1996). Information is needed on the total concentration of the components and the equilibrium constant of the reactions. The key thermodynamic functions for describing reaction equilibrium and phase equilibria at constant temperature and pressure are the Gibbs free-energy ( $G$ ) and the chemical potential ( $\mu$ ). Excellent descriptions of chemical reactions in natural aquatic systems and the treatment of chemical thermodynamics are given by Stumm and Morgan (1996) and Buffle (1988).

The results of the thermodynamic calculations are no proof of the formation of a given species. The existence of species can only be demonstrated by experiments. The results of the model depend on the choices and assumptions made with respect to the chosen description of the chemical processes of the system. These considerations must be kept in mind when assessing the quality of chemical models. The main limitations of chemical



equilibrium models are (Buffle, 1988):

1. the hypothesis that thermodynamic equilibrium is reached is not always justified; chemical reactions kinetics and diffusion processes can play a significant role
2. ignorance of the nature and even the existence of certain complexes
3. ignorance of nature and properties of many natural complexants, e.g. clay minerals and humic substances
4. difficulty of calculating activity coefficients at high ionic strengths.

To illustrate the equilibrium constant concept, the formation of a 1:1 complex of the cation  $\text{Me}^{n+}$  with a simple ligand  $\text{L}^-$  is taken as an example:



The corresponding intrinsic affinity constant is defined by the law of mass action:

$$K_{\text{int}} = \frac{(\text{MeL}^{(n-1)+})}{(\text{Me}^{n+})(\text{L}^-)} \quad (6A.2)$$

The subscript 'int' denotes the intrinsic thermodynamic constant, expressed as a function of activities indicated by round brackets ( ). The thermodynamic equilibrium constant is linked to the corresponding free-energy,  $\Delta G^0$ , by the expression:

$$K_{\text{int}} = \exp\left(-\frac{\Delta G^0}{RT}\right) \quad (6A.3)$$

and

$$\Delta G^0 = \Delta H^0 - T\Delta S^0 \quad (6A.4)$$

Generally, only concentrations are analytically measurable and it is therefore useful to define:

$$K_c = \frac{[\text{MeL}^{(n-1)+}]}{[\text{Me}^{n+}][\text{L}^-]} = K_{\text{int}} \frac{\gamma_M \gamma_L}{\gamma_{ML}} \quad (6A.5)$$

where  $K_c$  is the conditional equilibrium constant and the square brackets [ ] denote concentrations.  $\gamma$  is the activity coefficient, which relates activity to concentration as:

$$(C) = \gamma_c [C] \quad (6A.6)$$

The concentration of each species of Me is obtained by combining the corresponding

equilibrium constant with the mass-balance equation of cation Me for all species:

$$[Me]_{tot} = [M^{n+}] + \sum [ML] \quad (6A.7)$$

In order to combine the thermodynamic equilibrium constant with the mass-balance equation, it is necessary to know the activity coefficient. Table 6A.1 gives some expressions for calculating the activity coefficient in solutions for individual ions. The theoretical expression of Debye-Hückel has been established for simple electrolytes in dilute solutions, and the semi-empirical approaches by Güntelberg and Davies are useful for mixtures of electrolytes in moderately concentrated solutions. For the calculation of activity coefficients in highly concentrated solutions (e.g. brines, sea water, the gel phase of an organic macromolecule) a suitable thermodynamic framework is lacking (Buffle, 1988). Discussed in the Handbook of Aqueous Electrolyte Thermodynamics (Zemaitis et al., 1988) are several semi-empirical approaches for calculating activities at high ionic strengths, among others the Pitzer equations and the Chen equation. These equations can describe the activity for well-defined ionic systems up to 10 M. These semi-empirical equations, however, are composed of many parameters which have to be determined experimentally. Implication of the Pitzer equations or the Chen equation is useful only for well-defined systems, e.g. sea-water desalination, ion-exchange processes and hydrometallurgical processes. This approach, however, seems overdone for a natural system where even the reactive components, types of reactions and equilibrium constants are unknown or ill-defined. For now the Davies equation is used to calculate the activity coefficient of ions. The activities of water and inorganic precipitates are both set to 1 (Stumm and Morgan, 1996).

**Table 6A.1 Expressions for calculation of the individual ion activity coefficient (adapted from Stumm and Morgan, 1996)**

Approximation	Equation	Applicability in ionic strength (M)
Debye-Hückel	$\log \gamma = -AZ^2 \sqrt{I}$	$< 10^{-2.3}$
extended Debye-Hückel	$\log \gamma = -AZ^2 \frac{\sqrt{I}}{1 + Ba\sqrt{I}}$	$< 10^{-1}$
Güntelberg	$\log \gamma = -AZ^2 \frac{\sqrt{I}}{1 + \sqrt{I}}$	$< 10^{-1}$
Davies	$\log \gamma = -AZ^2 \left( \frac{\sqrt{I}}{1 + \sqrt{I}} - 0.2I \right)$	$< 0.2-0.3$

The ionic strength  $I$  is defined as  $\frac{1}{2} \sum C_i Z_i^2$ ;  $\epsilon$  is the dielectric constant;  $A = 1.82 \times 10^6 (\epsilon T)^{-3/2} \cong 0.5$  for water at 25 °C;  $Z$  is the charge of ion,  $B = 50.3 (\epsilon T)^{-1/2} \cong 0.5$  in water at 25 °C;  $a$  = adjustable parameter (in Å) corresponding to the size of the ion

For a system with more components and numerous reactions, the equilibrium composition cannot be calculated analytically and we have to resort to numerical methods. Finding the equilibrium composition of a multicomponent system can be reduced to a mathematical problem which can be solved in two ways (Buffle, 1988):

1. minimise the Gibbs free-energy of the system subject to the constraints of the mass balance
2. the so-called equilibrium constant approach: a set of non-linear equilibrium constant expressions for basic components and derived species are incorporated in the set of linear stoichiometric mass conservation equations for the basic components.

These approaches have been reviewed by Zeggeren and Storey (1970). The free-energy minimisation method always converges towards the solution, no matter how poor the starting estimates are. The efficiency of the equilibrium constant method critically depends on the initial estimate of the equilibrium concentration of the species (Zeggeren and Storey, 1970). Free-energy data are less available than equilibrium constants. Additionally, equilibrium constants can always be derived from free-energy data while the opposite is not necessarily true (Buffle, 1988). Moreover, for natural complexants the concept of equilibrium constants is generally used to describe metal ion binding. Therefore, the equilibrium constant method is adapted because it seems more suitable for natural systems. Brinkley (1948) introduced the equilibrium constant approach and improvements in the computer algorithms were made by Ting Po and Nancollas (1972) and Crerar (1975). Shear (1968) proved that for a chemical reaction system only one equilibrium point exists. Numerous computer programs have been developed for calculating chemical equilibrium in order to optimise the calculation time and the convergence (Jenne, 1978). Leggett (1977) tested three algorithms for solving the non-linear equations and found the Newton-Raphson the most efficient.

The values of equilibrium constants for well-defined complexation, solubility, redox reactions as well as the corresponding values of  $\Delta G^\circ$ ,  $\Delta H^\circ$ , and  $\Delta S^\circ$  necessary for these theoretical calculations have been compiled in numerous tables (see Buffle (1988) and Stumm and Morgan (1996)). Two difficulties should be borne in mind when searching for the equilibrium constants:

1. published values sometimes vary over a wide range, although the more recent tables tend to present critically evaluated results
2. the equilibrium constants for numerous complexes (especially mixed complexes) are still unknown.

### 6A.3 Description of EQUILIB

It was decided to develop our own computer program, called EQUILIB. This computer algorithm can easily be incorporated in other computer programs taking into account transport processes or biological and chemical conversion processes. These options are

not possible when applying commercially-available computer programs. The method is based on the approach of Crerar (1975) combining the mass balances for the components, the electro-neutrality balance and the mass action expressions for the chemical reactions. The electro-neutrality condition states that the total charge of the cations and anions of a chemical system is zero. The thermodynamic equilibrium model EQUILIB can handle the following types of reactions:

1. acid-base reactions
2. gas-solution equilibria for closed and open systems
3. redox reactions
4. precipitation reactions
5. complexation by soluble simple ligands:
6. outer-sphere complexes or ion-association
7. inner-sphere complexes or covalent bonds
8. adsorption to soluble and insoluble organic and inorganic macromolecules, which is described by the NICA-Donnan model (see Chapters 6 and 7).

The following phases can be distinguished for this concept:

1. bulk solution
2. gas phase
3. solid phase (or precipitates)
4. gel phase of natural organic complexant.

The activity coefficient for solutes is calculated by the Davies equation and the activities of water and precipitates are set to 1.

For the speciation of heavy metals in natural systems, the distribution of metal species over the solid and liquid phases is very important. The distribution is largely affected by the distribution of humic substances over the solid and liquid phases because these compounds strongly bind metals. It is very difficult to quantitatively describe the distribution of the humic substances (Tipping et al., 1991). For now no algorithm is included in the computer program to describe the distribution of the organic macromolecules over the solid and liquid phases.

Figure 6A.1 presents the flow chart of the EQUILIB computer program. The system is defined in an ASCII file, together with the initial guess values for the Newton-Raphson iteration method. The computer program goes through the following routine procedures:

1. Newton-Raphson iteration: solves a set of non-linear equations numerically (Van Zeggeren and Storey, 1970)
2. SipsOK: calculates the adsorption to natural organic complexants by the NICA model (see Chapter 6)
3. PrecipOK: adds or removes precipitates from the system by checking if the solubility product is exceeded

4. IonStrOK: checks that the ionic strength (and thus activity coefficients) has not changed.

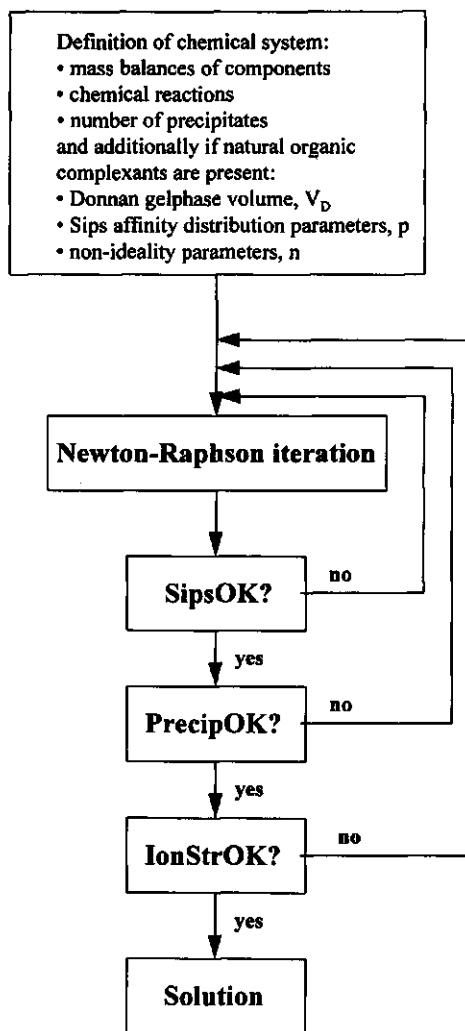


Figure 6A.1 Flow chart of the EQUILIB computer program for calculating chemical equilibrium of a multicomponent system

## References

- Bartschat, B. M.; Cabaniss, S. E.; and Morel, F. M. M. 1992. Oligoelectrolyte Model for Cation Binding by Humic Substances. *Environ. Sci. Technol.* 26:284-294
- Behel, D.; Nelson, J., Darrell, W.; and Sommers, L. E., 1983. Assessment of Heavy Metal Equilibriums in Sewage Sludge-Treated Soil. *J. Environ. Qual.* 12:181-186
- Benedetti, M. F.; Milne, C. J.; Kinniburgh, D. G.; Riemsdijk, W. H. van; and Koopal, L. K. 1995. Metal Ion Binding to Humic Substances: Application of the Non-Ideal Competitive Adsorption Model. *Environmental Science and Technology* 29:446-457
- Benedetti, M. F.; Riemsdijk, W. H. van; and Koopal, L. K. 1996. Humic Acids Considered as a Heterogeneous Donnan Gel Phase. *Environmental Science and Technology* 30:1805-1813
- Brannon-Peppas, L.; and Peppas N. A. 1991. Equilibrium Swelling Behavior of pH-sensitive Hydrogels. *Chemical Engineering Science* 46:715-722
- Brinkley, S. R. 1948. Calculation of the Equilibrium Composition of Systems of Many Constituents. *J. Chem. Phys.* 15:107
- Buffle, J.; Tessier, A.; and Haerdi W. 1984. In: *Complexation of Trace Metals in Natural Waters*, Kramer, C. J. M.; and Duinker, J. C. (eds.), The Hague, Nijhoff/Junk
- Buffle, J. 1988. *Complexation Reactions in Aquatic Systems: An Analytical Approach*. Chichester, Ellis Horwood Limited
- Carslaw, H. S.; and Jaeger, J. C. 1959. *Conduction of Heat in Solids*. Pxford: Clarendon Press
- Crerar, D. A. 1975. A Method for Computing Multicomponent Chemical Equilibria Based on Equilibrium Constants. *Geochim. Cosmochim. Acta* 39:1375-1384
- Fengel, D. and Wegener, G. 1984. *Wood: chemistry, ultrastructure, reactions*. Berlin: De Gruyter
- Fletcher, P.; and Beckett, P. H. T. 1987a. The Chemistry of Heavy Metals in Digested Sewage Sludge - I. Copper(II) Complexation with Soluble Organic Matter. *Wat. Res.* 21:1153-1161
- Fletcher, P.; and Beckett, P. H. T. 1987b. The Chemistry of Heavy Metals in Digested Sewage Sludge - II. Heavy Metal Complexation with Soluble Organic Matter. *Wat. Res.* 21:1163-1172
- Florence, T. M.; Batley, G. E. 1980. Chemical Speciation in Natural Waters, *CRC Critical Reviews in Analytical Chemistry* 9:219-296
- Fristoe, B. R.; and Nelson, P. O. 1983. Equilibrium Chemical Modelling of Heavy Metals in Activated Sludge. *Water Res.* 17:771-778
- Herrington, T. M.; and Petzold, J. C. 1992a. An Investigation into the Nature of Charge on Surface of Papermaking Woodpulp 1. Charge/pH Isotherms. *Colloids and Surfaces* 64:97-108
- Herrington, T. M.; and Petzold, J. C. 1992b. An Investigation into the Nature of Charge on Surface of Papermaking Woodpulp 2. Analysis of potentiometric titration data. *Colloids and Surfaces* 64:109-118
- Huang, O. M.; and Schnitzer, M. 1986. Interactions of Soil Minerals with Natural Organics and Microbes. *Soil science of America , Special Publication No 17*
- Jenne, E. A. (ed.) 1978. *Chemical Modeling in Aqueous Systems*. New York, American Chemical Society

- Kinraide, T. B.; Ryan, P. R.; and Kochian, V. 1992. Interactive Effects of  $Al^{3+}$ ,  $H^{+}$  and other Cations on Root Elongation Considered in Terms of Cell-Surface Electrical Potential. *Plant Physiol.* 99:1461-1468
- Koopal, L. K.; Riemsdijk, W. H. van; Wit, J. C. M. de; and Benedetti M.F. 1994. Analytical Isotherm Equations for Multicomponent Adsorption to Heterogeneous Surfaces. *L. Colloid Interface Sci* 166:51-60
- Kramer, C. J. M.; and Duinker C. (eds.) 1984. *Complexation of Trace Metals in Natural Waters*, Martinus Nijhoff
- Laszlo, J. A. 1987. Mineral Binding Properties of Soy hull. Modelling Mineral Interactions with an Insoluble Dietary Fiber Source. *J. Agric.Food Chem.* 35:593-600
- Legget, D. J. 1977. Machine Computation of Equilibrium Concentrations- Some Practical Considerations. *Talanta* 24:535-542
- Livens, F. R. 1991. Chemical Reactions of Metals with Humic Material. *Environ. Poll.* 70:183-208
- Marinsky, J. A.; Wolf, A.; and Bunzl, K. 1980. The Binding of Trace Amounts of Lead, Copper, Cadmium, Zinc and Calcium to Soil Organic Matter. *Talanta* 27:461-468
- Marinsky, J. A.; Gupta, S.; and Schindler, P. 1982. A Unified Physicochemical Description of the Equilibria Encountered in Humic Acid Gels. *J. Colloid Interface Sci.* 89:412-426
- Marinsky, J. A.; Ephraim, J.; 1986. A unified physicochemical description of the protonation and metal ion complexation equilibria of natural organic acids (humic and fulvic acids). 1. Analysis of the influence of polyelectrolyte properties on protonation equilibria in ionic media: fundamental concepts. *Environmental Science and Technology* 20:349-354
- Martell, A. E.; and Smith, R. M. 1977. *Critical Stability Constants, Vol. 3: Other organic Ligands*. New York, Plenum Press
- Melchior, D. C.; and Basset, R. L. (eds.) 1990. *Chemical Modeling of Aqueous Systems II*. Washington, American Chemical Society
- Miyajima, T. 1992. A Donnan model for the analysis of metal complexation of weak-acidic polyelectrolytes. An approach to the quantitative analytical treatment of the metal complexation equilibria of humic substances. *Sci. Tot. Environm.* 117/118:129-137
- Nederlof, M. M.; Riemsdijk, W. H. Van; and Koopal, L. K. 1990. Determination of Adsorption Affinity Distributions: A General Framework for Methods Related to Local Isotherm Approximations. *J. Colloid and Interface Sci.* 135:410 - 426
- Nederlof, M. 1992. *Analysis of Binding Heterogeneity*. PhD thesis. Wageningen, The Netherlands: Wageningen Agricultural University
- Nishio, T. 1991. Development of an Equation for Potentiometric Titration of Polyelectrolytes Using a Periodic Lattice Model. *Biophysical Chemistry* 40:19-31
- Schönherr, J.; and Bukovac, M. 1973. Ion Exchange Properties of Isolated Tomato Fruit Cuticular Membrane: Exchange Capacity, Nature of Fixed Charges and Cation Selectivity. *Planta* 109: 73
- Schönherr, J.; and Huber, R. 1977. Plant Cuticles are Polyelectrolytes with Isoelectric Points around Three. *Plant Physiol.* 59:145-150
- Sentenac, H.; and Grignon, C. 1981. A Model for Predicting Ionic Equilibrium Concentrations in Cell Walls. *Plant Physiol.* 68:415-419

- Shear, D. B. 1968. Stability and Uniqueness of the Equilibrium Point in Chemical Reaction Systems. *J. Chem. Phys.* 48:4144-4147
- Sips, R. 1948. *J. Chem. Phys.* 16:490
- Smith, R.M.; and Martell A.E. 1976. Critical Stability Constants, Vol. 4: Inorganic Ligands. New York, Plenum Press
- Sposito, G. 1981. Trace Metals in Contaminated Waters. *Environ. Sci. Technol.* 15:396-403
- Sposito, G. 1985. Chemical Models of Inorganic Pollutants in Soils. *CRC Critical Reviews in Environmental Control* 15:1-24
- Sposito, G. 1986. Sorption of Trace Metals by Humic Materials in Soils and Natural Waters. *CRC Critical Reviews in Environmental Control* 15:193-229
- Stevenson, F. J. 1994. *Humic Chemistry: Genesis, Composition, Reactions.* New York, John Wiley & Sons
- Stumm, W.; and Morgan, J.J. 1996. *Aquatic Chemistry, Chemical Equilibria and Rates in Natural Waters.* New York, John Wiley & Sons, Inc.
- Tanford, C. 1961. *Physical Chemistry of Macromolecules.* New York, Wiley
- Ting-Po, I.; and Nancollas, G. H. 1972. EQUIL - A General Computational Method for the Calculation of Solution Equilibria. *Anal. Chem.* 44:1940-1950
- Tippling, E.; Backes, C. A.; and Hurley, M. A. 1988. The Complexation of Protons, Aluminium and Calcium by Aquatic Humic Substances: A Model Incorporating Binding-Site Heterogeneity and Macroionic Effects. *Water Research* 22:597-611
- Tippling, E.; Woof, C.; and Hurley, M. A. 1991. Humic Substances in Acid Surface Waters; Modelling Aluminium Binding, Contribution to Ionic Charge-Balance and Control of pH. *Wat. Res.* 25:425-435
- Vermeer, A. W. P. 1996. Interactions Between Humic Acid and Hematite and Their Effects on Metal Speciation. Ph.D. Thesis. Wageningen, The Netherlands: Agricultural University Wageningen
- Vuceta, J.; and Morgan, J.J. 1978. Chemical Modeling of Trace Metals in Fresh Waters: Role of Complexation and Adsorption. *Environm. Sci. Technol.* 12:1302-1308
- Wit, J. C. M de; Riemsdijk, W. H. van; Nederlof, M. M.; Kinniburgh, D. G.; and Koopal, L. K. 1990. Analysis of Ion Binding on Humic Substances and the Determination of Intrinsic Affinity Distributions. *Analytica Chimica Acta* 232:189-207
- Wit, J. C. M. de 1992. Proton and Metal Ion Binding to Humic Substances. PhD thesis, Agricultural University Wageningen
- Wit, J. C. M de; Riemsdijk, W. H-van; and Koopal, L. K. 1993b. Proton Binding to Humic Substances. 2. Chemical heterogeneity and adsorption models. *Environmental Science and Technology* 27:2015-2022
- Zeggeren, F. Van; and Storey S. H. 1970. *The Computation of Chemical Equilibria.* Cambridge, Cambridge University Press
- Zemaitis, J. F.; Clark, D. M.; Rafal, M.; and Scrivner, N. C. 1988. *Handbook of Aqueous Electrolyte Thermodynamics, Theory and Applications.* A Publication of the Design Institute for Physical Property Data. New York, American Institute of Chemical Engineers



## **7. Role of humic acids in proton and Cu(II) adsorption to the organic fraction of biowaste**

### **7.1. Introduction**

**T**he application of organic wastes and composts to soil systems alters the soil fertility through the addition of nutrients, heavy metals and natural organic matter. Although the regular addition of organic waste and compost to arable land can be beneficial, the application is of great concern because an accumulation of heavy metals in the soil can lead to toxicity of heavy metals for plants and microorganisms, heavy metal leaching to the ground-water system and the inhibition of plant growth (Vaughan and Malcolm, 1985; Burns et al., 1986; Chaney and Ryan, 1993; Stevenson, 1994). Therefore, the heavy metal content of compost should be limited in order to guarantee the safe use of that compost. The legal criteria for the quality and dosage of compost are laid down in the law concerning the quality and use of so-called other organic fertilisers, the BOOM decree (see Chapter 1). If biowaste-derived compost does not meet the legal criteria with respect to the heavy metal content, the recycling of biowaste can be prevented (see Chapter 4). In that case, extraction of heavy metals from organic wastes preceding composting can be considered in order to reduce the heavy metal content of the derived composts (see Chapter 5).

The impact of heavy metals on the ecosystem by the application of organic wastes and the extractability of heavy metals from organic waste can be better predicted if the physico-chemical behaviour of heavy metals is better understood. Natural organic matter, especially humic substances, are known to bind heavy metals strongly and they often determine the behaviour and fate of heavy metals in natural systems (Stevenson, 1994). Humic substances control the mobility of metals in natural waters and play an important role in the bioavailability of trace metals and toxicity of heavy metals to plants and living organisms in soil systems (Buffle, 1988). Although natural organic matter is present in much lower concentrations than mineral constituents in soils and sediments, many important physical and chemical properties are strongly influenced by the presence of humic substances in soil organic matter (Schnitzer, 1991). As discussed in Chapter 4, organic matter in biowaste can roughly be divided into two groups, i.e. humic substances and fresh plant material. The distribution of fresh plant material and humic substances in the organic fraction of biowaste is a function of the particle size. The organic fraction >1 mm is largely made up of fresh plant material. The organic fraction from 0.05 to 1 mm originates from the litter layer of garden soils and is mainly composed of humified plant material. The content of humic acids in the organic fractions increases with decreasing

particle size. The organo-mineral fraction <0.05 mm is made up of silt, clay minerals and organic matter which are structured in soil aggregates. The structure and composition of these soil aggregates is very complex and metal adsorption is predominantly regulated by the organic matter coated on the mineral surfaces (Chassin et al., 1978; Greenland and Hayes, 1981; Buffle, 1988). In this chapter, it is postulated that the humic acid fraction in biowaste determines the binding strength of heavy metals in biowaste and promotes the solubilisation and transport of heavy metals by the solubility of humic acids.

The role of humic acids in the binding and solubility of Cu(II) in biowaste is studied for the various particle-sized organic fractions in biowaste. For this, acid-base titrations are made to determine the functional group content of the isolated organic particles, and Cu(II) titrations at fixed pH are made to determine the Cu(II) binding strength to the isolated organic particles between 0.05 and 2 mm (as described in subchapter 6.3.1). The proton and Cu(II) adsorption isotherms at variable ionic strength and pH are interpreted by the NICA-Donnan model developed in Chapter 6.

As humic acids are important for the regulation of metal ions in natural environments, the fate and transport of heavy metals is largely influenced by the solubility of humic substances. For biowaste in contact with water, the distribution of heavy metals over the solid and liquid phase will be significantly influenced by the solubilisation of the humic acid fraction in biowaste. Therefore, the effect of the humic acid solubilisation on the promotion of soluble Cu(II) is studied by determining the solubility of Cu(II) and humic acid from the particle-sized organic fractions between 0.05 and 2 mm at variable pH values.

## ***7.2. Theoretical description of proton and Cu(II) binding to the organic fraction of biowaste***

### **7.2.1. Introduction**

A general adsorption model to describe proton and metal ion binding to humic substances (the NICA-Donnan model) was developed in Chapter 6. The binding site heterogeneity and polyelectrolytic behaviour of proton and metal binding to natural organic complexants were taken into account by the model. The model presumes monodentate complexes of protons and metal ions with carboxylic and phenolic sites. The binding site heterogeneity and non-ideality of local metal binding were described by the Non-Ideal Competitive Adsorption (NICA) model (Benedetti et al., 1995). The electrostatic effect was handled explicitly by the Donnan formalism (Marinsky, 1982). The model should be able to describe acid-base properties, metal complexation and competition reactions

between metals to natural organic complexants. In this study the model is applied to describe acid-base titrations and Cu(II) adsorption isotherms to particle-sized organic fractions of biowaste. The NICA-Donnan model has also been applied by Vermeer (1996) to describe proton and Cd(II) binding to purified Aldrich humic acid.

First, a survey is made of the binding site heterogeneity, polyelectrolytic behaviour and non-ideality of local binding for natural organic complexants. This survey produces parameters to model the acid-base properties and Cu(II) adsorption isotherms of the particle-sized organic fractions of biowaste. For this it is assumed that the binding properties of the organic particles are determined by the humic acid fraction of the particles.

#### 7.2.1.1. Binding site heterogeneity

It is generally accepted that heavy metal ions and protons form complexes with the functional groups of natural organic matter (Stevenson, 1994; Buffle, 1988). A major disadvantage of titration experiments is the fact that these do not give information on the type of binding on molecular scale. Spectroscopic studies show that carboxylic ( $\text{COO}^-$ ) and phenolic ( $\text{PhO}^-$ ) groups are involved in complexation (electrostatic and covalent binding) with metal ions (Buffle, 1988). Complexes of metals ions with minor sites (e.g.  $\text{NH}_2$  and  $\text{SH}$  groups) have not been demonstrated (Livens, 1991). Most probably, these minor sites are not necessary to explain the strong binding of Cu(II) to natural organic complexants.

The affinity constants of protons with  $\text{COO}^-$  and  $\text{PhO}^-$  groups are strongly influenced by the steric and electric environment. To demonstrate these effects, the affinity constants for various monomers carrying carboxylic or phenolic acids are first discussed. Proton affinity constants ( $K_{\text{HL}}$ ) for  $\text{COO}^-$  groups range from  $10^{4.9}$  for isobutyric acid to  $10^{1.3}$  for oxalic acid. Proton affinity constants for  $\text{PhO}^-$  groups range from 14.6 in salicylic acid to 8.4 in catechol. Figure 7.1 shows the metal affinity constants ( $K_{\text{ML}}$ ) for  $\text{Ca}^{2+}$ ,  $\text{Fe}^{3+}$ ,  $\text{Cu}^{2+}$  and  $\text{Zn}^{2+}$  as a function of  $K_{\text{HL}}$  for monomeric carboxylic and phenolic acids (data compiled from Martell and Smith, 1977). Figure 7.1 shows a strong correlation between  $\log K_{\text{HL}}$  and  $\log K_{\text{ML}}$  as was also found for simple inorganic ligands by Martell et al. (1988). The steeper slope of the plot expresses the higher covalent character of the metal-ligand complex. The observed trend of metal binding strength  $\text{Fe}^{3+} > \text{Cu}^{2+} > \text{Zn}^{2+} > \text{Ca}^{2+}$  is in accordance with theory (Stumm and Morgan, 1996). It is surprising to see that the character of the binding (i.e. the slope of the linear plot) does not change from carboxylic to phenolic groups. The same trends for the effect of pH (from pH 3 to 10) on the affinity constant of  $\text{Cu}^{2+}$ ,  $\text{Pb}^{2+}$  and  $\text{Zn}^{2+}$  with humic substances (Buffle, 1988) have been observed. This indicates that carboxylic and phenolic sites are the major reactive sites of humic substances.

The polyfunctionality of each type of functional group in humic substances can be described by a Sips distribution (see Chapter 6). Nederlof et al. (1992) obtained a proton affinity distribution for fulvic acid which could be modelled by two sites with mean  $\log K_{HL}$  values of 2.8 (carboxylic) and 9.8 (phenolic) and corresponding Sips distribution parameters  $p$  of 0.4 and 0.48. De Wit et al. (1990) described acid-base titrations for 14 humic substances with an average mean  $\log K_{HL}$  value of 3.1 for the carboxylic site and an average heterogeneity parameter of 0.48. For the phenolic site only one data series was available with a mean  $\log K_{HL}$  of 8.5 and a heterogeneity parameter of 0.6.

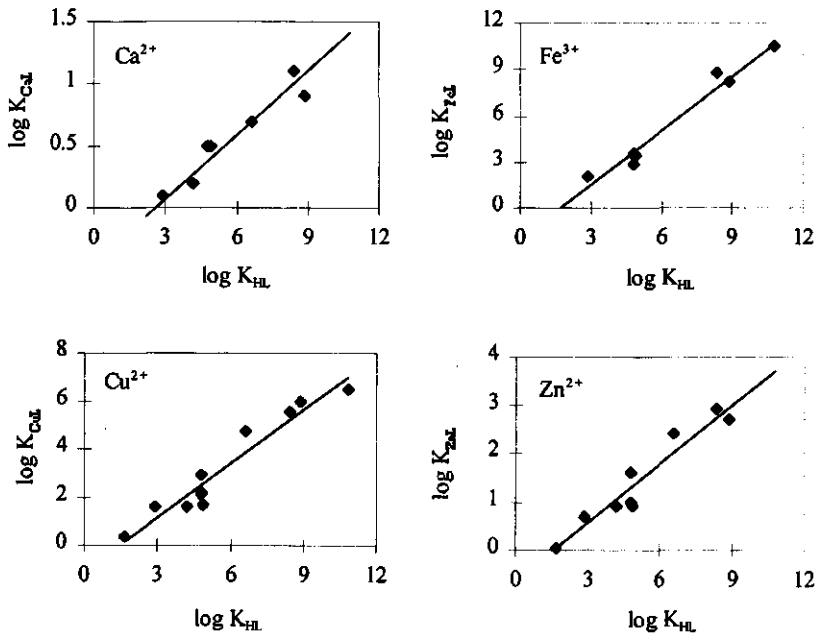


Figure 7.1 Correlation between  $\log K_{HL}$  and  $\log K_{ML}$  ( $M$  is  $Ca^{2+}$ ,  $Fe^{3+}$ ,  $Cu^{2+}$  and  $Zn^{2+}$ ) for monomers carrying carboxylic and phenolic groups (data extracted from Martell and Smith, 1977)

### 7.2.1.2. Polyelectrolytic character

The importance of the polyelectrolytic character of natural organic complexants on proton and metal ion binding has indirectly been shown by acid-base titrations and metal adsorption isotherms at variable ionic strengths for various types of natural organic material, e.g. plant cuticles (Schonherr and Huber, 1977), humic substances (De Wit, 1993a,b), cell walls (Sentenac and Grignon, 1981), and papermaking woodpulp (Herrington, 1992a,b). Direct evidence of the electrostatic binding of metal ions has been shown for humic substances and cell walls by fluorescence quenching (Green et al., 1992).

The heterogeneity of natural organic complexants makes it difficult to make an exact description of the electrostatic effect. The functional groups are not uniformly distributed, and the organic components are very heterogeneous with respect to size and geometry. The Donnan formalism assumes a permeable gel-phase in which the functional groups are homogeneously distributed (see Figure 6.3). Benedetti et al. (1996) derived a charge density of 0.5 to 2 mol.l<sup>-1</sup> for humic substances from acid-base titrations by applying the Donnan theory. The calculated gel-phase volumes of Benedetti et al. (1996) are in good agreement with experimental measurements of the size of humic colloids (Buffle, 1988). For plant tissues, charge densities in the Donnan gel phase ranging from 0.5 to 5 mol.l<sup>-1</sup> have been reported (Schonherr and Huber, 1977; Laszlo, 1987).

### 7.2.1.3. Non-ideality of local adsorption

As discussed in Chapter 6, the metal ion adsorption cannot be described by an ideal multicomponent Langmuir-Freundlich adsorption isotherm. Benedetti et al. (1995) applied the NICA model to describe the binding of H<sup>+</sup>, Ca<sup>2+</sup>, Cd<sup>2+</sup>, Cu<sup>2+</sup> and Pb<sup>2+</sup> to a purified peat humic acid. Unfortunately, the electrostatic effect was not accounted for explicitly but was incorporated in the non-ideality parameter *n*. Vermeer (1996) applied the NICA-Donnan model to interpret the metal ion binding to humic acids and distinguish between the electrostatic effect and the non-ideal local adsorption. The non-ideality parameter *n* has a thermodynamic basis (see Chapter 6) but can better be regarded as a fitting parameter to describe proton and metal ion adsorption isotherms.

## 7.2.2. Model calculations

As mentioned in the introduction, it is postulated that the proton and metal binding properties of the particle-sized organic fractions can be attributed to the humic acid fraction of the particles. The humic acid content of the organic fractions is given in Table 3.11. Model calculations are made for organic particles with a humic acid content of 20%, resembling the particle-sized organic fraction 0.05-0.1 mm. The functional group content of humic acid ranges from 5-10 mmol.g<sup>-1</sup>. As will be seen later, humic acid extracted from integral biowaste contains 8-9 mmol.g<sup>-1</sup> of functional groups, approx. 4 mmol carboxylic groups.g<sup>-1</sup> and 4 mmol phenol groups.g<sup>-1</sup> (see subchapter 7.5.1).

The polyfunctionality of natural organic matter was modelled by a carboxylic (COO<sup>-</sup>) and a phenolic (PhO<sup>-</sup>) group, on each of which a Sips distribution parameter *p* was superimposed. Local metal adsorption was described by a monodentate affinity constant ( $\bar{K}$ ) and non-ideality was considered explicitly from the binding site heterogeneity by the non-ideality parameter *n*. For proton binding no distinction can be made between the Sips

distribution parameter  $p$  and the non-ideality parameter  $n$ . The proton binding is expressed by (see subchapter 6.2.2.1):

$$\theta_{H, \text{tot}} = Q_{\text{max,COO}} \frac{(\bar{K}_{\text{COOH}} H)^{p_{\text{COO}}}}{1 + (\bar{K}_{\text{COOH}} H)^{p_{\text{COO}}}} + Q_{\text{max,PhO}} \frac{(\bar{K}_{\text{PhOH}} H)^{p_{\text{PhO}}}}{1 + (\bar{K}_{\text{PhOH}} H)^{p_{\text{PhO}}}} \quad (7.1)$$

where  $\theta_{H, \text{tot}}$  is the total proton adsorption,  $Q_{\text{max,COO}}$  and  $Q_{\text{max,PhO}}$  are the total number of carboxylic and phenolic sites,  $\bar{K}_{\text{COOH}}$  and  $\bar{K}_{\text{PhOH}}$  are the median proton affinity constants for carboxylic and phenolic sites,  $H$  is the proton activity, and  $p_{\text{COO}}$  and  $p_{\text{PhO}}$  are the Sips distribution parameters for the carboxylic and phenolic sites.

The Cu(II) binding is given by (see subchapter 6.2.2.1):

$$\begin{aligned} \theta_{\text{Cu, tot}} = & Q_{\text{max,COO}} \frac{(\bar{K}_{\text{COOCu}} \text{Cu})^{n_{\text{COOCu}}}}{\sum_i (\bar{K}_{\text{COOM}_i} M_i)^{n_{\text{COOM}_i}}} \frac{\left( \sum_i (\bar{K}_{\text{COOM}_i} M_i)^{n_{\text{COOM}_i}} \right)^{p_{\text{COO}}}}{1 + \left( \sum_i (\bar{K}_{\text{COOM}_i} M_i)^{n_{\text{COOM}_i}} \right)^{p_{\text{COO}}}} \\ & + Q_{\text{max,PhO}} \frac{(\bar{K}_{\text{PhOCu}} \text{Cu})^{n_{\text{PhOCu}}}}{\sum_i (\bar{K}_{\text{PhOM}_i} M_i)^{n_{\text{PhOM}_i}}} \frac{\left( \sum_i (\bar{K}_{\text{PhOM}_i} M_i)^{n_{\text{PhOM}_i}} \right)^{p_{\text{PhO}}}}{1 + \left( \sum_i (\bar{K}_{\text{PhOM}_i} M_i)^{n_{\text{PhOM}_i}} \right)^{p_{\text{PhO}}}} \end{aligned} \quad (7.2)$$

where  $\theta_{\text{Cu, tot}}$  is the total Cu(II) adsorption,  $Q_{\text{max,COO}}$  and  $Q_{\text{max,PhO}}$  are the total number of carboxylic and phenolic sites,  $\bar{K}_{\text{COOCu}}$  and  $\bar{K}_{\text{PhOCu}}$  are the median Cu(II) affinity constants for carboxylic and phenolic sites,  $\bar{K}_{\text{COOM}}$  and  $\bar{K}_{\text{PhOM}}$  are the median affinity constants of competing metal ions  $M$  (including protons) with carboxylic and phenolic sites,  $\text{Cu}$  is the Cu(II) activity,  $M$  is the activity of competing ions (including protons),  $n_{\text{COOM}}$ ,  $n_{\text{COOCu}}$ ,  $n_{\text{PhOCu}}$ ,  $n_{\text{PhOM}}$  are the non-ideality parameters, and  $p_{\text{COO}}$  and  $p_{\text{PhO}}$  are the Sips distribution parameters.

The Donnan formalism is formulated for a permeable gel-phase in which the functional groups are homogeneously distributed (see Chapter 6). The Donnan potential is determined by the total charge density and the Donnan gel-phase volume,  $V_D$ . The NICA-Donnan model requires the following parameters to describe proton and Cu(II) ion adsorption to natural organic complexants (in the absence of other competing metal ions):

- Donnan volume:  $V_D$  (in  $\text{ml.g}^{-1}$ )
- type and concentration of reactive sites:  $Q_{\text{max, COO}}$  and  $Q_{\text{max, PhO}}$  (in  $\text{mmol.g}^{-1}$ )

- mean affinity constants for protons with each site:  $\bar{K}_{\text{COOH}}$  and  $\bar{K}_{\text{PhOH}}$  (in  $\text{mol.l}^{-1}$ )
- mean affinity constant for Cu(II) with each site:  $\bar{K}_{\text{COOCu}}$  and  $\bar{K}_{\text{PhOCu}}$  (in  $\text{mol.l}^{-1}$ )
- Sips distribution parameter  $p$  for each site:  $p_{\text{COO}}$  and  $p_{\text{PhO}}$
- non-ideality parameter for protons and Cu(II) with each site:  $n_{\text{COOH}}$ ,  $n_{\text{COOCu}}$ ,  $n_{\text{PhOH}}$ ,  $n_{\text{PhOCu}}$

The acid-base titrations are described by 7 parameters and the Cu(II) adsorption is described by 13 parameters. Table 1 summarises the parameters which were extracted from literature data (see subchapter 7.2.1). Model calculations were made to show the effect of ionic strength on the acid-base titrations and the Cu(II) adsorption isotherms at pH 4, 6 and 8. The Cu(II) adsorption was modelled for a Cu(II) loading range of  $1 \times 10^{-7}$  to  $5 \times 10^{-6} \text{ mol.g}^{-1}$ . Moreover, calculations are made to show the effect of variation of the heterogeneity parameter  $p$  and non-ideality parameter  $n$  on the Cu(II) binding.

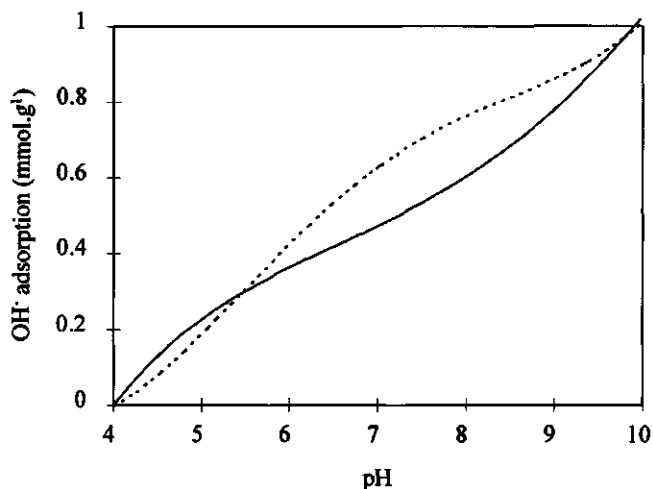
**Table 7.1. Parameters for describing proton and Cu(II) adsorption to humic acid**

Parameter	Unit	Value	Parameter	Unit	Value
Donnan volume	$\text{ml.g}^{-1}$	1 <sup>1</sup>	$p_{\text{COO}}$	-	0.5 <sup>1</sup>
$[\text{COO}^-]$	$\text{mmol.g}^{-1}$	5 <sup>2</sup>	$p_{\text{PhO}}$	-	0.5-0.7 <sup>1</sup>
$[\text{PhO}^-]$	$\text{mmol.g}^{-1}$	5 <sup>2</sup>	$n_{\text{COOH}}$	-	0.9 <sup>1</sup>
$\bar{K}_{\text{COOH}}$	$\text{M}^{-1}$	3.5 <sup>3</sup>	$n_{\text{PhOH}}$	-	0.6-0.9 <sup>1</sup>
$\bar{K}_{\text{PhOH}}$	$\text{M}^{-1}$	9 <sup>3</sup>	$n_{\text{COOCu}}$	-	0.5 <sup>1</sup>
$\bar{K}_{\text{COOCu}^+}$	$\text{M}^{-1}$	2 <sup>3</sup>	$n_{\text{PhOCu}}$	-	0.3 <sup>1</sup>
$\bar{K}_{\text{PhOCu}^+}$	$\text{M}^{-1}$	7 <sup>3</sup>			

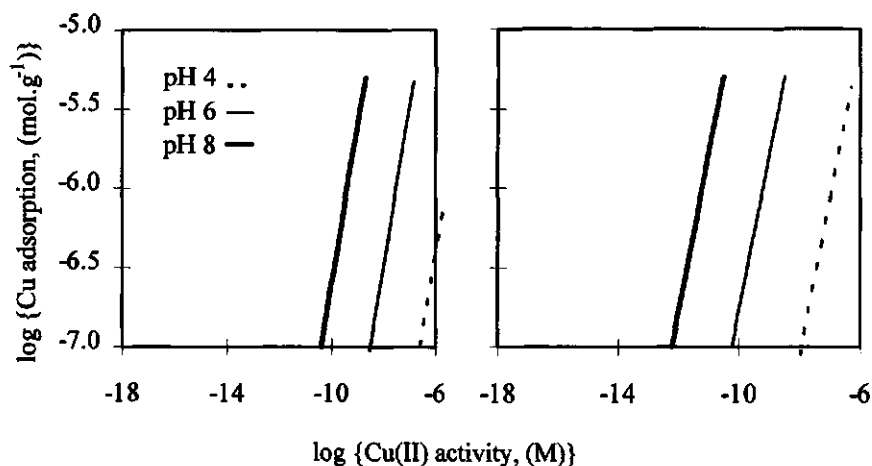
<sup>1</sup> Benedetti et al., 1995; <sup>2</sup> Vermeer et al. 1996; <sup>3</sup> De Wit, 1993a,b; <sup>3</sup> Martell and Smith, 1977

Figure 7.2 shows OH<sup>-</sup> adsorption isotherms (acid-base titrations from pH 4 to 10) for electrolyte concentration of 0.001 and 0.1 M NaNO<sub>3</sub> ( $p=n=1$ ). As discussed in Chapter 6, the electrostatic effect shifts the apparent  $pK_a$  in the bulk phase to higher values. This effect is larger for higher negative charge densities, i.e. for smaller gel-phase volumes, higher negative functional groups and at higher pH values. The model calculations show that the effect of ionic strength on acid-base properties is very small. This is due to the low charge density (a combination of functional group content and gel-phase volume) of the model particles. It is also shown that only part of total functional groups ( $1 \text{ mmol.g}^{-1}$  of the total content of  $2 \text{ mmol.g}^{-1}$ ) can be observed because the titration window is limited from pH 4 to 10.

Figure 7.3 shows the Cu(II) adsorption isotherms for an ionic strength of 0.001 and 0.1 M ( $p=n=1$ ). The Cu(II) binding strength (equivalent to lower Cu(II) activity) increases with higher pH values and lower ionic strength, as discussed in subchapter 6.3.2.2. The complexation at low pH values is accounted for by both carboxylic and phenolic sites. At higher pH values, binding to phenolic sites becomes dominant (results not shown here).



**Figure 7.2**  $\text{OH}^-$  adsorption of the model particles as function of pH as calculated by the NICA-Donnan model at variable ionic strength (0.001 M  $\text{NaNO}_3$ : dotted line and 0.1 M  $\text{NaNO}_3$ : solid line)



**Figure 7.3** Effect of ionic strength on the Cu(II) adsorption of the model particles at pH 4, 6 and 8 as calculated by the NICA-Donnan model ( $p=n=1$ ): 0.1 M  $\text{NaNO}_3$  (left) and 0.001 M  $\text{NaNO}_3$  (right)

A comparison of Figures 7.2 and 7.3 shows that the effect of ionic strength on the acid-base titrations is very small, but that the effect on the Cu(II) binding is very pronounced. The same effect was observed for fulvic acid where the ionic strength effect was small for



acid-base titrations while at the same time a strong electrostatic effect was exhibited for Cu(II) titrations (Bartschat et al., 1992). However, no size heterogeneity of humic substances has to be taken into account to explain these differences as proposed by Bartschat et al. (1992).

The effect of the non-ideality of local adsorption on the Cu(II) adsorption isotherms are shown in Figure 7.4. Realistic values for  $p$  and  $n$  were taken from Table 7.1. Distribution of binding sites for both groups and variations in the Donnan gel-phase volume showed no effect on the Cu(II) binding strength (results not shown here). However, non-ideality of local binding has a pronounced effect on Cu(II) binding, the Cu(II) binding increases with decreasing values of  $n_{Cu}$ . The thermodynamic basis for higher non-ideality of Cu(II) can be related to the high ionic strength in the gel phase which has a stronger effect on the non-ideality for divalent over monovalent cations.

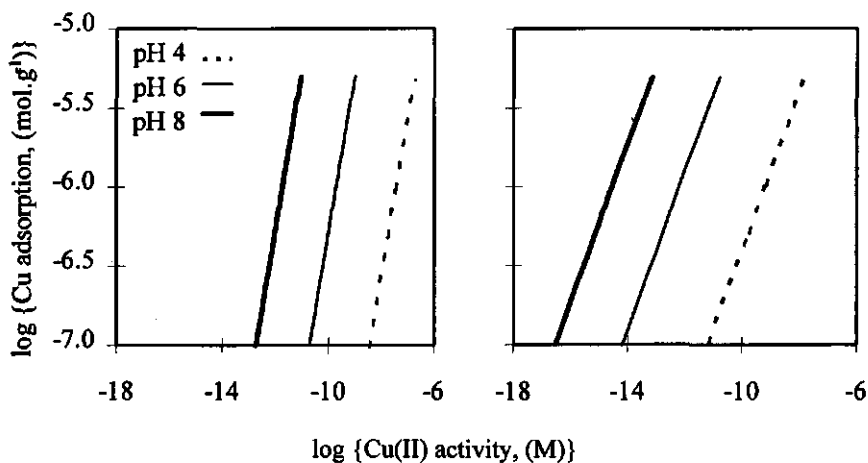


**Figure 7.4** Effect of non-ideality parameter  $n_{Cu}$  on the Cu(II) adsorption for the model particles at pH 4, 6 and 8 at 0.01 M NaNO<sub>3</sub> as calculated by the NICA-Donnan model (left:  $p=0.5$ ,  $n_H=n_{Cu}=1$ ; right:  $p=0.5$ ,  $n_H=0.9$ ,  $n_{Cu}=0.4$ )

### 7.3. Materials and methods

#### 7.3.1. Isolation and preparation of solid organic particles

Biowaste was sampled at VAM, Wijster and physically separated by wet sieving and water elutriation as described in subchapter 3.5. The particle-sized organic fractions were twice mildly washed for 16 h with 0.1 M nitric acid to remove the fulvic acid fraction and metals to a large extent. The samples were dried at 40 °C and stored in a desiccator. Five particle-sized organic fractions in the range of 0.05 to 1 mm were studied: 1-2, 0.5-1, 0.2-0.5, 0.1-0.2, and 0.05-0.1 mm.

#### 7.3.2. Characterisation of humic acid

Humic acid (HA) in integral biowaste and in the particle-sized organic fractions was extracted by a standard extraction scheme of the International Humic Substances Society (IHSS) as described in subchapter 3.6. The HA was purified and dialysed according to the IHSS scheme (Aiken et al., 1985). The humic acid content of the particle-sized organic fractions is given in Table 7.2 (taken from Table 3.11).

**Table 7.2 Humic acid content of the particle-sized organic fractions of biowaste**

Organic fraction (mm)	HA (g.g <sup>-1</sup> OM)
1 - 2	0.11
0.5 - 1	0.10
0.2 - 0.5	0.11
0.1 - 0.2	0.13
0.05 - 0.1	0.21

The humic acid extracted from integral biowaste had an ash content of 0.5% after isolation and purification. The elemental composition of this humic acid amounts to 57.3% C, 8.1% H, 2.1% N and 32.5% O (S and P were not determined). A stock solution of 0.80 g.l<sup>-1</sup> HA was prepared by dissolving freeze-dried HA in 0.1 M NaNO<sub>3</sub> at pH 8. The HA solution was stored at 4 °C before use.

The molecular weight distribution of HA was determined by gel permeation chromatography (GPC) on Sephacryl S-100 (Kipton et al., 1992). Figure 7.5 shows the GPC chromatogram for HA, where UV-285 is a measure of the concentration and the elutriation time is a measure of the molecular weight. HA shows a broad distribution pattern, indicating a large heterogeneity in size and therefore most probably also in composition.

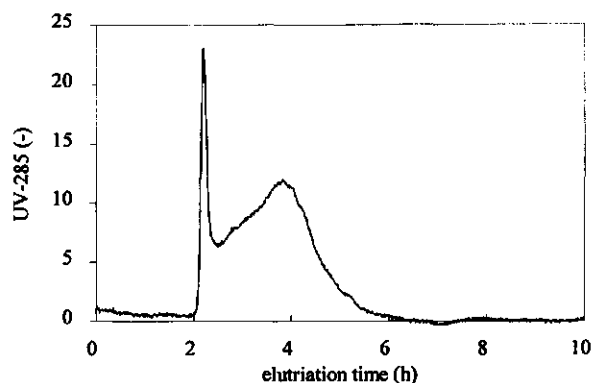


**Figure 7.5** Gel permeation chromatogram of humic acid extracted from integral biowaste

### 7.3.3. Titration experiments

The titrations experiments were carried out with the computer-controlled titration device equipped as described in subchapter 3.7. The pH activity and the  $\text{Cu}^{2+}$  activity were produced with a glass electrode (Schott, type N32A) and Cu(II)-ISE (ORION, model 94-29), respectively. The electrodes were calibrated before and after the measurement in order to reveal changes in electrode response. The calibration before and after the measurement should not differ by more than 1 mV. OH adsorption and Cu(II) adsorption isotherms were calculated by equations 6.9 and 6.10, respectively. Acid-base titrations were made for the solid organic particles and the extracted humic acid from pH 4 to 10. Cu(II) adsorption isotherms at fixed pH were made in the same concentration range in which Cu(II) is present in biowaste, i.e. from  $10^{-7}$ - $10^{-5.5}$  mol  $\text{Cu.g}^{-1}$ , at pH 4, 6 and 8.

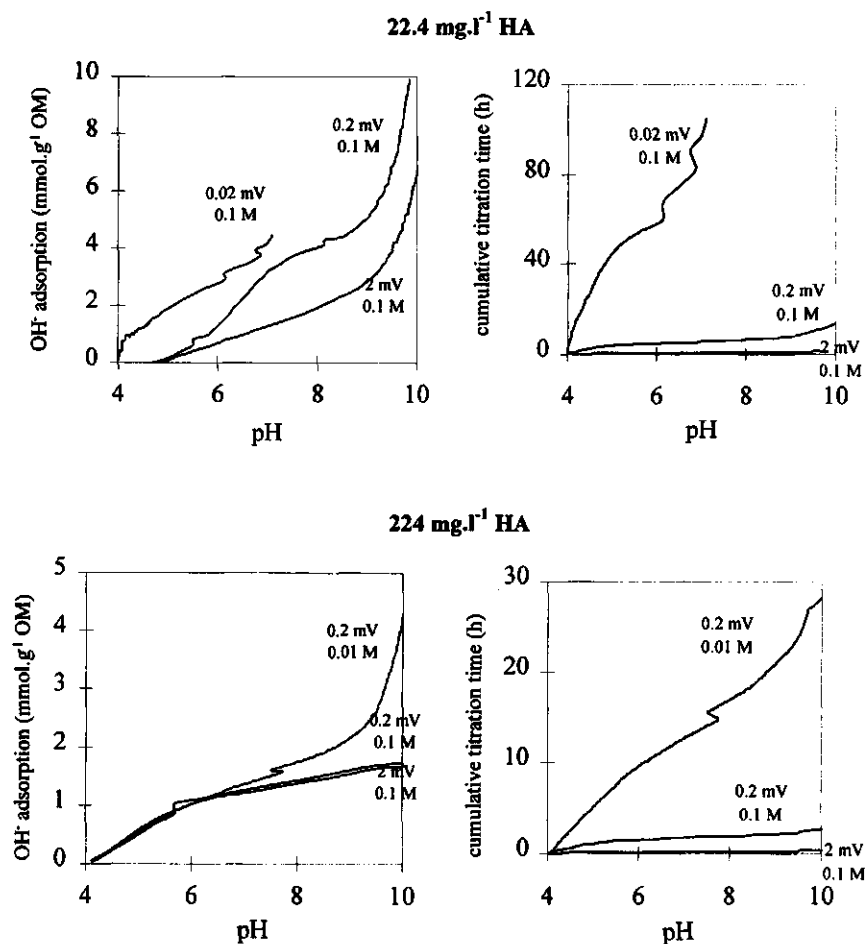
At the end of each Cu(II) titration experiment, a sample was taken and centrifuged at 10,000 rpm for 5 minutes. For the sample, total Cu(II) in solution ( $\text{Cu}_{\text{sol}}$ ) was measured by GFAAS as described in subchapter 3.2. Dissolved organic matter (DOM) was quantified by UV-285 as described in subchapter 3.6.

## 7.4. Results

Acid-base titrations of the extracted humic acid from biowaste and [of] the five particle-sized organic fractions were made. Cu(II) adsorption isotherms were determined for the five particle-sized organic fractions at pH 6 and for the organic fractions 0.2-0.5 mm and 0.05-0.1 mm at pH 4, 6, 8 and 10. At the end of the Cu(II) adsorption experiment, total Cu(II) in solution and dissolved organic matter were determined.

### 7.4.1. Acid-base properties of humic acid

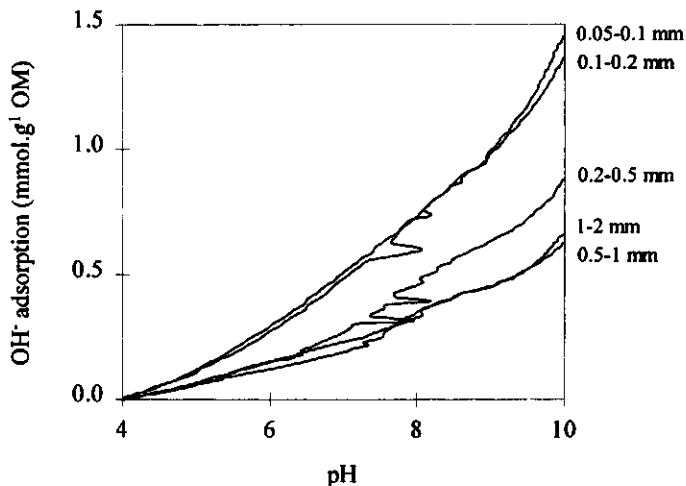
Figure 7.6 shows the experimental acid-base titrations for humic acid extracted from total biowaste at variable concentration ( $22.4$  and  $224 \text{ mg.l}^{-1}$ ), variable drift criterion ( $0.02$ ,  $0.2$  and  $2 \text{ mV.min}^{-1}$ ) and variable ionic strength ( $0.01$  and  $0.1 \text{ M}$ ). It is clearly seen that for the same HA sample, the  $\text{OH}^-$  adsorption strongly depends on HA concentration, drift criterion and ionic strength.



**Figure 7.6**  $\text{OH}^-$  adsorption isotherms as function of pH for humic acid isolated from biowaste at variable HA concentration ( $22.4$  and  $224 \text{ mg.l}^{-1}$ ), drift criterion ( $0.02$ ,  $0.2$  and  $2 \text{ mV.min}^{-1}$ ) and ionic strength ( $0.01 \text{ M}$  and  $0.1 \text{ M}$ )

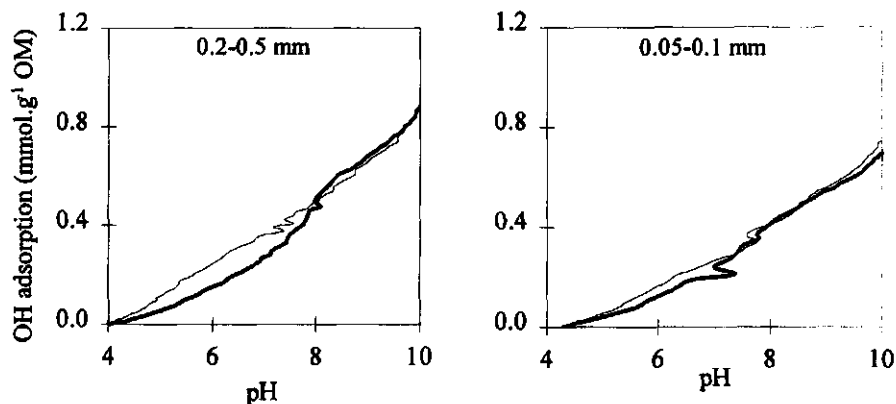
#### 7.4.2. Proton and Cu(II) adsorption to particle-sized organic fractions of biowaste

Figure 7.7 presents the  $\text{OH}^-$  adsorption isotherms for the five particle-sized organic fractions at 0.01 M  $\text{NaNO}_3$  and a drift criterion of  $0.2 \text{ mV}\cdot\text{min}^{-1}$ . Smaller drift criteria are not considered because they would lead to extremely long titration times and possible  $\text{CO}_2$  stripping from the air at higher pH values (see subchapter 6.3.1.1). The  $\text{OH}^-$  adsorption increases with decreasing particle size.



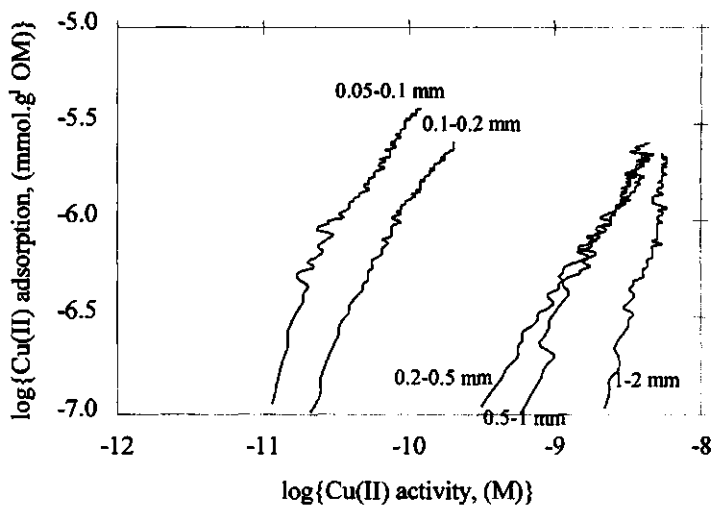
**Figure 7.7**  $\text{OH}^-$  adsorption isotherms of particle-sized organic fractions as function of pH at 0.01 M  $\text{NaNO}_3$  and  $0.2 \text{ mV}\cdot\text{min}^{-1}$

Figure 7.8 shows the  $\text{OH}^-$  adsorption isotherms for the organic fractions 0.2-0.5 mm and 0.05-0.1 mm at variable ionic strength. The experiments were conducted at a drift criterion of  $0.2 \text{ mV}\cdot\text{min}^{-1}$ . No clear differences are seen with variable ionic strength.



**Figure 7.8** OH adsorption isotherms at variable ionic strength (0.001 M NaNO<sub>3</sub> (light line) and 0.1 M NaNO<sub>3</sub> (solid line) for the particle-sized organic fractions 0.2-0.5 mm and 0.05-0.1 mm

Figure 7.9 shows Cu(II) adsorption isotherms of the five particle-sized organic fractions at pH 6 and 0.01 M NaNO<sub>3</sub>. The experiments were conducted at a drift criterion of 0.2 mv.min<sup>-1</sup>. The Cu(II) binding strength increases (decreasing Cu(II) activity) with decreasing particles sizes.



**Figure 7.9** Cu(II) adsorption isotherms of the particle-sized organic fractions at pH 6 and an ionic strength of 0.01 M NaNO<sub>3</sub>

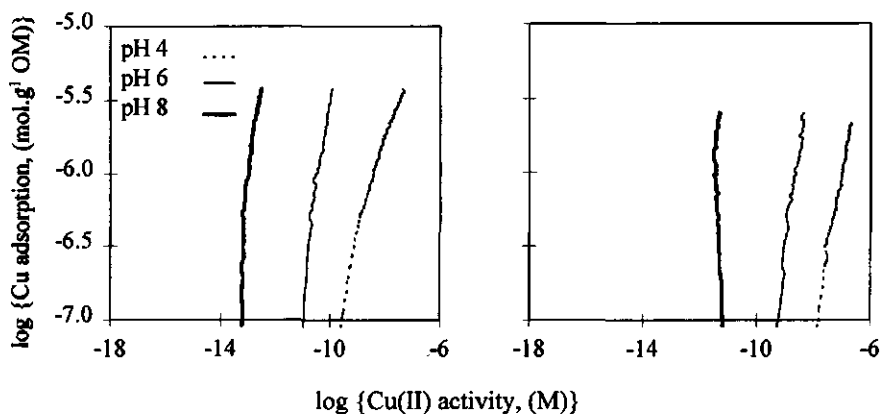


**Figure 7.10** Cu(II) adsorption isotherms of the particle-sized organic fractions of 0.05-0.1 mm (left) and 0.2-0.5 mm (right) at pH 4, 6 and 8 and 0.01 M NaNO<sub>3</sub>

Cu(II) adsorption isotherms at pH 4, 6 and 8 and 0.01 M NaNO<sub>3</sub> for the organic fractions 0.2-0.5 mm and 0.05-0.1 mm are presented in Figure 7.10. Cu(II) adsorption experiments were conducted at a drift criterion of 0.2 mv.min<sup>-1</sup>. Adsorption isotherms at pH 10 are not shown due to the very slow kinetics of the electrode response.

#### 7.4.3. Solubilisation of Cu(II) and humic acid from biowaste particles

The Cu(II)-ISE measures only the free Cu<sup>2+</sup> activity and does not distinguish between Cu(II) adsorbed to soluble humic acids and Cu(II) adsorbed to solid humic acids. To distinguish between these two Cu(II) species, samples were withdrawn from the solution at the end of each Cu(II) titration experiment. Total Cu(II) in solution ( $Cu_{sol}$ ) was determined by GFAAS, and dissolved organic matter (DOM) was quantified by UV-285. Figure 7.11 shows  $Cu_{sol}$  and DOM as a function of particle size for the five particle-sized at pH 6 and  $Cu_{sol}$  as a function of pH (pH 4 to 10) for the organic fractions of 0.2-0.5 and 0.05-0.1 mm.  $Cu_{sol}$  and DOM both increase with decreasing particle size and increasing pH.

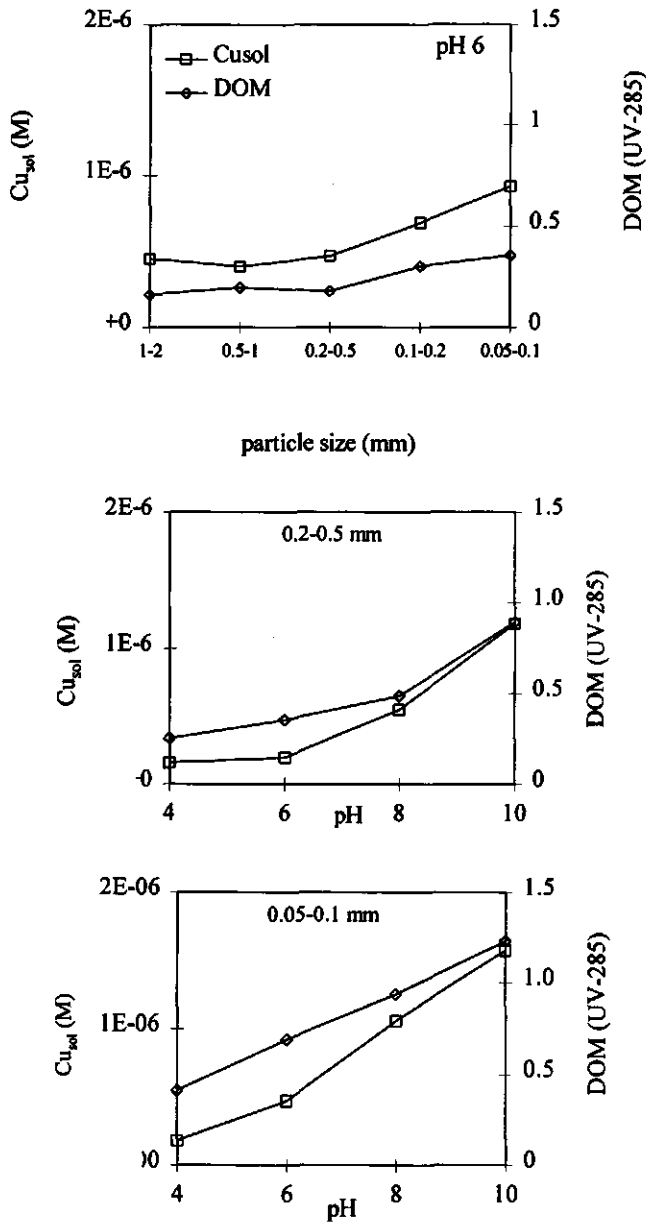


Figure 7.11  $Cu_{sol}$  and UV-285 for the different fractions at pH 6 (top), and for the fractions 0.2-0.5 mm and 0.05-0.1 at pH 4, 6, 8 and 10



## 7.5. Discussion

### 7.5.1. Acid-base properties of humic acid extracted from biowaste

$\text{OH}^-$  adsorption isotherms of humic acid (HA) at  $22.4 \text{ mg.l}^{-1}$  for variable drift criteria (Figure 7.6) show an increase in adsorption with lower drift criteria, especially at low pH values. The increasing adsorption capacity is accompanied by increasing titration times. This behaviour was also seen with Sephadex CM-25 and can be attributed to restricted diffusion of hydroxyl ( $\text{OH}^-$ ) ions in the gel phase of the humic acid macromolecules. When equilibrium is not reached in the available time, the adsorption isotherm does not give a true picture of the acid-base properties of the complexant. For example, when equilibrium is not reached at a particular pH value, the  $\text{OH}^-$  adsorption is postponed to higher pH values. This means that enough time should be taken to reach equilibrium at every point of the adsorption isotherms. We must therefore be very careful to assign the adsorption to a specific functional group. The  $\text{OH}^-$  adsorption can be shifted to higher pH values when the adsorption process is diffusion limited. If equilibrium is not reached,  $\text{OH}^-$  adsorption at pH 8-10 normally assigned to phenolic sites can also be caused by adsorption of carboxylic sites normally exposed at pH 3-6.

The acid-base titrations at a HA concentration of  $224 \text{ mg.l}^{-1}$  (Figure 7.6) show a significant lower total  $\text{OH}^-$  adsorption compared to the adsorption isotherms for  $22.4 \text{ mg.l}^{-1}$  HA. This is accompanied by low cumulative titration times. Also decreasing the drift criterion from 2 to  $0.2 \text{ mV.min}^{-1}$  has no effect on the acid-base properties for  $224 \text{ mg.l}^{-1}$  HA. This indicates that the reactive sites of the humic acid macromolecules are not accessible for the hydroxyl ions when the HA concentration is higher. However, when the ionic strength of the solution is decreased to  $0.01 \text{ M}$ , the  $\text{OH}^-$  adsorption increases. This indicates that the reactive sites again become accessible at lower ionic strength for the  $\text{OH}^-$  ions.

Both phenomena described above can be explained by the properties of the humic acid macromolecules. Schnitzer and co-workers showed that the colloidal structure becomes more condensed at lower pH, higher ionic strength and higher humic acid concentration (Huang and Schnitzer, 1986). Marinsky et al. (1986) showed that humic acid molecules can become impermeable for ions if the conformation becomes more condensed. This concept can explain the time dependence of the acid-base titrations: hydroxyl ions have to diffuse through the micelle-like structure to reach the reactive sites. The diffusivity of  $\text{OH}^-$  ions in the gel phase of the HA aggregates is very slow and it takes a long time to reach the reactive sites. The diffusion of ions inside the gel phase is smaller in more condensed micelle-like structure as the diffusivity of ions decreases (Brannon-Peppas and Peppas, 1991). The aggregates are more condensed at higher HA concentrations, higher ionic strengths and lower pH values. In some cases the aggregates are extremely

condensed, even preventing the penetration of OH<sup>-</sup> ions in the gel phase. In this case only the reactive sites at the exterior of the aggregates are reached, resulting in apparently lower adsorption capacities. When the ionic strength is lowered, the aggregates become less condensed, giving hydroxyl ions the opportunity to diffuse in the gel phase. Due to the fact that the pH is measured in the bulk solution, we cannot distinguish between binding and diffusion. Therefore, phenolic groups at the exterior of the gel phase can overlap with carboxylic groups which are situated in the interior of the gel phase.

The large spreading in acid capacities found in literature is often attributed to differences in origin of humic substances and differences in isolation and purification techniques (Buffle, 1988). This study shows that experimental conditions are very important, because the sample concentration, ionic strength and titration time (drift criterion) have significant effects on the adsorption isotherms.

We use the adsorption isotherms at  $22.4 \text{ mg.l}^{-1}$  to estimate the functional group content of the extracted HA. The exact concentration of different types of sites cannot be determined accurately because of the effects described above. We assume that for the titration at a drift criterion of  $0.02 \text{ mV.min}^{-1}$  all sites are reached in the low pH range and at a drift criterion of  $0.2 \text{ mV.min}^{-1}$  the total adsorption is reached up to pH 10. Making these assumptions,  $4\text{-}5 \text{ mmol.g}^{-1}$  can be attributed to carboxylic groups and  $4\text{-}5 \text{ mmol.g}^{-1}$  phenolic groups. These results are in the same range as humic acids extracted from soils for which a broad range of values between  $2\text{-}6 \text{ mmol.g}^{-1}$  carboxylic and  $2\text{-}6 \text{ mmol.g}^{-1}$  phenolic groups are reported (Banerjee and Rao, 1981; Choudhry, 1984; Perdue, 1985; Schnitzer, 1978; Buffle, 1988; Stevenson, 1994).

## **7.5.2. Complexation properties of particle-sized organic fractions of biowaste**

### **7.5.2.1. OH<sup>-</sup> adsorption isotherms**

The OH<sup>-</sup> adsorption isotherms of the particle-sized organic fractions (Figure 7.7) show an increase in adsorption capacity with decreasing particle size. Figure 7.12 shows the functional group content as a function of humic acid content for the organic particles at pH 6 (HA contents taken from Table 7.2).

Figure 7.12 shows that the functional group content is proportional to the humic acid fraction of the particles. From the slope of the plot, a functional group content of  $7.7 \text{ mol.g}^{-1}$  HA can be derived which corresponds well with the functional group content of  $8\text{-}9 \text{ mol.g}^{-1}$  found for humic acid isolated from integral biowaste. This indicates that the functional group content of the organic particles in biowaste is largely due to the humic acid fraction of the organic particles.

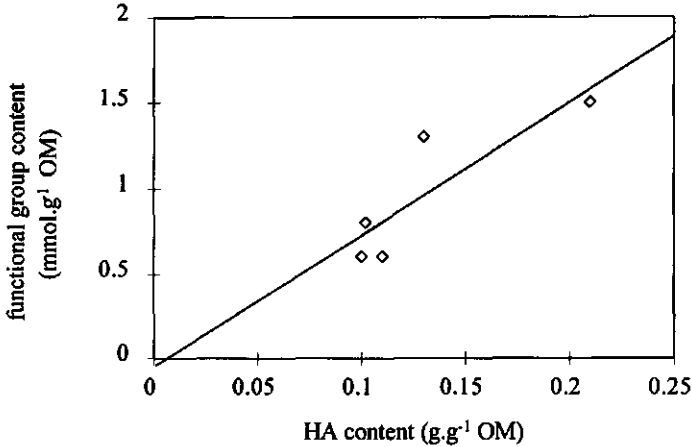


**Figure 7.12** Functional group content of particle-sized organic fractions as a function of the humic acid content

Adsorption capacities found for the organic fractions are in good agreement with values found for plant roots ( $0.1\text{--}0.9\text{ mmol.g}^{-1}$ ) and plant cuticles ( $1.05\text{--}1.2\text{ mmol.g}^{-1}$ ) (Schonherr and Huber, 1977; Buffle, 1988). The adsorption from pH 4-7 can be assigned to carboxyl groups and from pH 7-10 to weak-acid phenolic groups. Carboxyl groups are present in both plant material and humic substances. Phenolic groups are mainly present in humic substances. Therefore, the COOH content increases only slightly with decreasing particle size, and the phenolic OH adsorption increases significantly with decreasing particle size.

Acid-base titrations at variable ionic strength for the organic fractions of 0.2-0.5 mm and 0.05-0.1 mm (Figure 7.8) show no clear difference in OH<sup>-</sup> adsorption isotherms for 0.001 and 0.1 M NaNO<sub>3</sub>. This indicates that the electrostatic effect is small for the studied organic fractions. This will be further discussed in subchapter 7.5.3.

#### 7.5.2.2. Cu(II) adsorption isotherms

Cu(II) adsorption isotherms at pH 6 for variable particle-size (Figure 7.9) show an increasing Cu(II) binding strength with decreasing particle-size. Both the OH<sup>-</sup> adsorption and the Cu(II) binding strength are significantly higher for fractions <0.2 mm compared to the fractions >0.5 mm. Figure 7.13 shows the Cu(II) binding strength (equivalent to free Cu(II) activity) as a function of functional group content at pH 6 and Cu(II) loading of  $10^{-5.5}\text{ mol.g}^{-1}\text{ OM}$  (compiled from Figures 7.7 and 7.9).

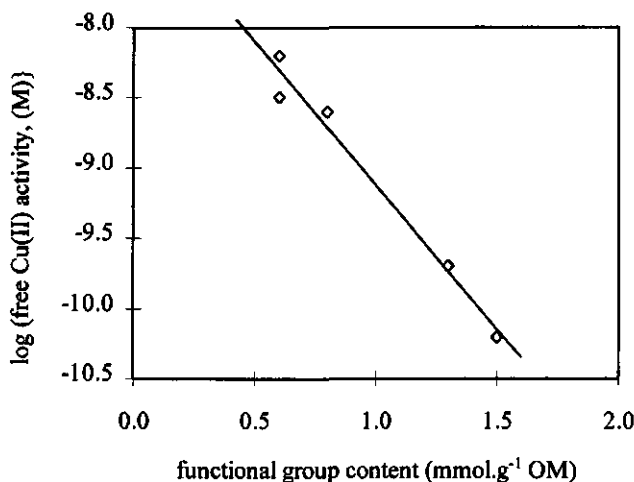


**Figure 7.13** Cu(II) binding strength as a function of the functional group content for the particle-sized organic fractions at pH 6 and Cu(II) loading of  $10^{-5.5}$  mol.g<sup>-1</sup>

The Cu(II) binding strength increases with increasing functional group content. The stronger Cu(II) binding strength for the smaller particles cannot be explained merely by the lower degree of occupation of Cu(II). For this, an increase in functional group content by a factor 2 should give an increase in binding strength by a factor of 2. However Figure 7.13 shows that with an increase in functional group content by a factor of 2 the binding strength increases by a factor 30. This indicates that the stronger binding has to be due to the presence of stronger binding sites or a higher charge density for the smaller particles. The stronger binding for the smaller particles with higher functional content is most probably caused by the higher degree of humification of organic matter. The humic acid fraction extracted from the larger organic particles (0.5-2 mm) is comprised not only of humified organic matter (see subchapter 3.9.1). Adani et al. (1995) showed that the extraction with 0.1 M NaOH is non-selective and that lipids, carbohydrates and proteins are likely to be present in the humic acid fractions. The larger organic fractions (>0.5 mm) originate from fresh waste with low contents of humic acid but high levels of carbohydrates, lipids and proteins. The smaller fractions (<0.2 mm) originate from the topsoil of gardens and contain a high content of humified organic matter. Humified organic matter contains binding sites with a stronger affinity for metal ions, most probably phenolic sites.

Figure 7.10 shows that the Cu(II) binding increases at higher pH values. As discussed for Sephadex CM-25, stronger binding is due to two phenomena. Firstly, at lower pH values Cu(II) has to compete with protons for the available reactive sites. Secondly, at higher pH values more sites are dissociated resulting in an increased electric field. The electrostatic

attraction is stronger for divalent Cu(II) ions than monovalent protons (see subchapter 7.5.3).

### 7.5.3. Model validation

The course of the calculated  $\text{OH}^-$  adsorption isotherms is in good agreement with experimental results. The absence of the electrostatic effect from the experimental  $\text{OH}^-$  adsorption isotherms is confirmed by model calculations. This is due to the small charge density of the complexants compared to the charge density of Sephadex CM-25 (see Chapter 6) and fulvic acid (De Wit, 1990). Marinsky (1986) showed that the polyelectrolytic effect for high molecular weight humic acids on acid-base titrations is very small compared to fulvic acids due to the small charge density. The small charge density of HA is also confirmed by conductimetric titrations of HA for which the overall charge density on humic acid was too low to bind the monovalent counter ions (Van den Hoop and Van Leeuwen, 1990). Moreover, for the organic particles the small electrostatic effect is obscured by several other phenomena, such as kinetic aspects (non-equilibrium due to diffusion limitations in the gel phase), conformational changes during the titration and the inhomogeneous distribution of charge density and polydispersity of the complexants.

Model calculations (Figure 7.2) show that the titration window from pH 4 to 10 is insufficiently broad to determine the total adsorption of carboxylic and phenolic groups with mean affinity constants of 3.5 and 9.0. The narrow titration window makes it impossible to reveal strong acidic carboxyl sites and sulfonic acid sites and weak phenolic sites which are probably present.

Stronger binding of Cu(II) at higher pH is a result of a higher charge density and less competition with protons for the carboxylic and phenolic sites. Model calculations with  $p=n=1$  show that, in contrast to acid-base titrations, the electrostatic effect is much more pronounced for the Cu(II) binding (Figure 7.3). Model calculations also show that the heterogeneity parameter and Donnan gel-phase volume do not have a significant effect on the Cu(II) binding strength. On the other hand, the Cu(II) binding strength increases when the non-ideality parameter for Cu(II) is smaller than the non-ideality parameter for protons (Figure 7.4). The thermodynamic basis for higher non-ideality (smaller  $n$  values) of Cu(II) can be related to the high ionic strength in the gel phase of the complexant. The ionic strength has a larger effect on non-ideality for divalent over monovalent cations (Stumm and Morgan, 1996).

Experimental Cu(II) adsorption isotherms do not show a linear behaviour as observed with the model (compare Figures 7.10 to 7.4). In Chapter 6, this phenomenon was also

observed with the Cu(II) adsorption to Sephadex CM-25. Deviations from linear behaviour are more pronounced at lower  $\text{Cu}^{2+}$  activities, i.e. high pH values, lower Cu(II) loadings and for smaller particle size. A reason for this deviation can be found in the dynamics of the system. As discussed in Chapter 6 (subchapter 6.5.3) only free metal ions can diffuse through the gel phase to the reactive sites. True thermodynamic equilibrium at every location of the adsorption isotherm is reached when Cu(II) ions are uniformly distributed over all reactive sites. In that case, Cu(II) adsorption isotherms are linear as observed for the model calculations. The time needed to approach equilibrium depends on the radius (R) of the particles and the effective diffusion coefficient. As a rule of thumb (see subchapter 6.5.3), the experimental time should be of the magnitude  $t = \frac{R^2}{D}$  in order to achieve equilibrium. The diffusion of Cu(II) in the organic particles is restricted by the adsorption of Cu(II) to the reactive sites. The higher the binding strength, the lower the effective diffusion coefficient (see subchapter 6.5.2.1). For an affinity constant of  $10^6$  M for Cu(II) ions with the reactive sites, a diffusion coefficient of  $10^{-11} \text{ m}^2 \cdot \text{s}^{-1}$  and a radius of 0.1 mm, it will take 11,500 days to reach equilibrium! Based on this simplified approach it becomes clear that Cu(II) adsorption isotherms are less linear at a higher binding strength (i.e. at a lower Cu(II) loading or higher pH) and for larger particles.

As has become clear from the discussion, modelling the adsorption of protons and metal ions to solid organic particles and humic acids is very complex, because:

- solid organic particles are an assemblage of different natural organic compounds, e.g. humic substances and cell wall components
- the isolated solid organic particles are not well characterised with respect to composition, structure and conformation
- the nature and stoichiometry of reactions of metal ions and functional groups are not exactly known; e.g. mixed complexes are possible
- the spatial distribution of charge densities is not homogeneous, making calculation of the polyelectrolyte effect difficult
- the conformation and solubilisation of humic acids depends on pH, ionic strength and metal loading
- it is very hard to measure proton or metal ion adsorption isotherms which are at true chemical equilibrium; evaluation of the Fourier number showed that it takes years to reach equilibrium.

Despite these problems the NICA-Donnan model can adequately describe proton and Cu(II) binding to the particle-sized organic fractions of biowaste. Metal-ligand binding is described by monodentate complexes. The Donnan formalism can simultaneously account for covalent and electrostatic binding of different types of metal ions. Ion-specific non-ideality of the local binding is handled by introducing a non-ideality parameter in the Langmuir-Freundlich adsorption isotherms. The model can be seen as a

semi-empirical model for which the model parameters are partially fitted on proton and metal ion adsorption isotherms. However, the parameters have a thermodynamic basis. The mean affinity constants are in good agreement with affinity constants for carboxylic and phenolic groups. The Sips distribution parameter  $p$  can be explained by the variation of affinity constant in different steric and electric environments. The non-ideality parameter  $n$  can be accounted for by the high ionic strength in the Donnan gel phase which increases for ions with a higher valency.

Only carboxylic and phenolic sites have to be considered in order to explain the strong binding at low Cu(II) loadings. No bidentate complexes (e.g. dicarboxylic, phthalic, salicylic and catechol) and N- or S-type of sites have to be considered in order to explain strong adsorption of Cu(II) at low metal loadings to natural organic complexants as suggested by other authors (Livens, 1991).

#### 7.5.4. Solubility and Cu(II) reactivity of humic acids in biowaste

The proton and Cu(II) adsorption studies showed that the Cu(II) binding of organic particles of biowaste can be assigned to the humic acid fraction of these particles. However, the Cu(II)-ISE can not distinguish between Cu(II) adsorbed to soluble or Cu(II) adsorbed to solid humic acid. Figure 7.11 shows that total Cu(II) in solution ( $Cu_{sol}$ ) and dissolved organic matter (DOM) both increase with increasing pH and decreasing particle size. It is assumed that DOM is completely made up of solubilised humic acid. DOM increases with decreasing particle size because the smaller fractions have a higher humic acid content (Table 7.2). The increase in DOM with increasing pH can be explained by Wershaw's model for humic substances (Wershaw et al., 1986; Wershaw, 1989). According to Wershaw's model, humic substances are amphiphilic molecules which form ordered aggregated structures by hydrogen bonds, electrostatic interactions and hydrophobic forces. As pH increases, more functional groups are ionised which brings about the release of molecules of the humus aggregates into solution because of the increase in electrostatic repulsion and disruption of hydrogen bonds. Figure 7.14 (compiled from the data of Figure 7.11) shows  $Cu_{sol}$  as a function of DOM. The linear relationship between  $Cu_{sol}$  and DOM ( $r^2=0.98$ ) clearly demonstrates that the solubility of Cu(II) is enhanced by the dissolution of humic acids.

Additional information on the reactivity of soluble and solid humic acids can be obtained when the amount of solubilised humic acids is quantified. For this, DOM (UV-285) has to be converted to the amount of solubilised humic acid (in  $g.l^{-1}$ ). This is possible when the extinction coefficient of humic acid at 285 nm (in  $l.g^{-1} HA.cm^{-1}$ ) is known. For this we have to determine the extinction coefficient at 285 nm ( $g carbon.l^{-1}$ ) of the soluble humic acid fraction and the molecular weight of the HA unit. An extinction coefficient of  $33 l.g^{-1} carbon.cm^{-1}$  was extracted from a plot of UV-285 as a function of dissolved

organic carbon ( $\text{g carbon.l}^{-1}$ ) for the solubilisation of the organic fraction 0.2-0.5 mm at variable pH (results not shown here). It was assumed that this extinction coefficient was valid for humic acid of all the organic fractions of biowaste. The elemental composition of humic acid isolated from integral biowaste was  $\text{CH}_{1.3}\text{O}_{0.67}\text{N}_{0.09}$ . This results in an average extinction coefficient of  $15 \text{ l.g}^{-1} \text{ HA.cm}^{-1}$  for humic acid in biowaste. Figure 7.15 shows the fraction of solubilised Cu(II) as a function of the fraction of solubilised humic acid using this extinction coefficient.

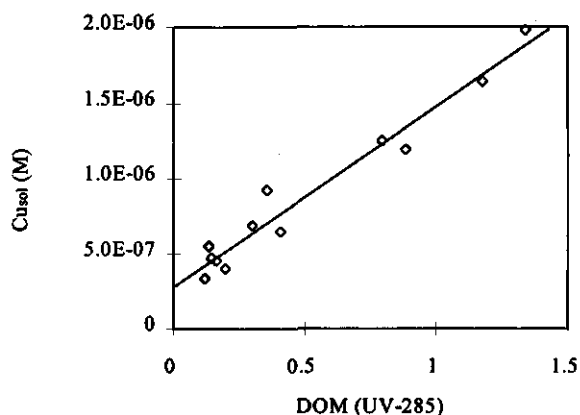


**Figure 7.14**  $\text{Cu}_{\text{sol}}$  as a function of DOM at a Cu(II) loading of  $10^{-5.5} \text{ mol.g}^{-1} \text{ OM}$

The amount of solubilised Cu(II) is linearly correlated to the amount of solubilised humic acid. This result indicates that the Cu(II) binding strength of the soluble humic acid and solid humic acid are equal. This finding is especially remarkable as the data are derived for different particle-sized organic fractions having a different origin of the humic matter. Again Wershaw's representation of humic substances might serve as an explanation (Wershaw, 1989). Increasing pH brings about the release of molecules of the humus aggregates into solution because of the increase in electrostatic repulsion and disruption of hydrogen bonds. Therefore HA increases with a higher content of humic acid (smaller particles) and with increasing pH. The results show that the binding strength of these amphiphilic molecules will not change upon dissolution and the fraction of dissolved Cu(II) will be equal to the fraction of dissolved humic acids.



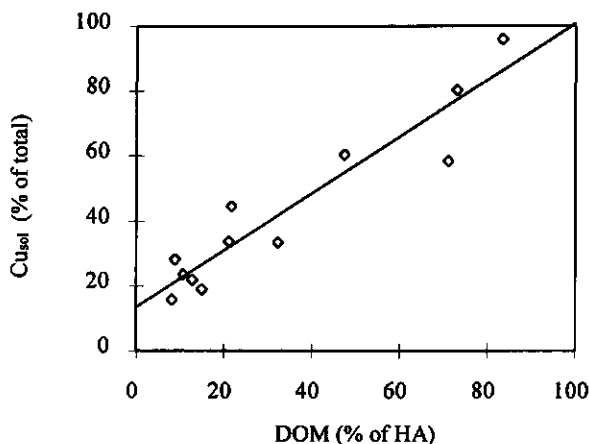


**Figure 7.15** Solid-liquid distribution of Cu(II) as a function of the solid-liquid distribution of humic acid for the particle-sized organic fractions in biowaste

## 7.6. Conclusions

Acid-base titrations were made for humic acid extracted from biowaste and for the five particle-sized fractions in the range 0.05-2 mm. Acid-base titrations of particle-sized organic fractions of biowaste showed that the functional group content increased with decreasing particle size. A comparison of the functional group content of extracted humic acid and the organic particles showed that the functional group of the organic particles can be assigned to the humic acid fraction of these particles.

Various researchers suggest that acid-base properties of humic acids are determined by the origin of the humic acid and the extraction and purification procedures. This study, however, showed that the acid-base properties are also highly dependent on the experimental conditions, i.e. humic acid concentration, ionic strength and drift criterion. It is shown that for short titration times, the adsorption isotherms are not in equilibrium. Moreover, at higher humic acid concentrations the molecules become extremely condensed, preventing the ions from penetrating the gel phase.

The ionic strength effect on acid-base properties of organic particle-size fractions is very small. This is also confirmed by calculations with the NICA-Donnan model which showed that the electrostatic effect is very small due to the small charge density of the particles. Moreover, the small differences in the experimental OH<sup>-</sup> adsorption isotherms are probably obscured by the intrinsic properties of the humic acid fraction of the

particles, i.e. changes in conformation during titrations, and heterogeneity in particle size and composition. Because the titration window is limited from pH 4 to 10, only weakly acidic carboxylic and strong phenolic groups are revealed. Other functional groups, such as strongly acidic carboxyl and sulphonic groups and weakly phenolic sites, cannot be detected in this titration window.

Cu(II) adsorption to the particle-sized organic particles show that the Cu(II) binding strength increases with decreasing particle size. The Cu(II) adsorption isotherms show a linear relationship between the functional group content of the organic particles and the Cu(II) binding strength. The stronger adsorption for the smaller sized organic particles is only partly due to the higher functional group content of the smaller particles. The stronger binding is mainly caused by the higher humification of the smaller organic fractions. Humified organic matter possesses more sites with stronger binding strength for Cu(II), most probably phenolic groups. The OH<sup>-</sup> adsorption isotherms of the organic fractions confirm this hypothesis, a higher number of reactive sites are observed at higher pH values, i.e. phenolic sites, for the smaller particle-sized organic fractions.

In principle, experimental metal and proton titrations can only be compared with the NICA-Donnan model when the experimental adsorption isotherms are made at true equilibrium. A comparison of model and experiments for Cu(II) adsorption, however, showed that the adsorption isotherms are not in equilibrium. It must be borne in mind that the measurements are made in the bulk solution while the reactions take place inside the organic particles or humic acid gel. The reactive sites of the particles can only be reached by diffusion inside the porous particles. Therefore, interpretation of proton metal adsorption isotherms by a chemical equilibrium model should always be regarded with care.

Despite the complexity of humic acids and the organic particles in biowaste, the NICA-Donnan model can adequately describe proton and Cu(II) binding to the particle-sized organic fractions of biowaste. Only carboxylic and phenolic sites have to be considered in order to explain the strong binding at low Cu(II) loadings. No bidentate complexes (e.g. dicarboxylic, phthalic, salicylic and catechol) and N- or S-type of sites have to be considered in order to explain strong adsorption of Cu(II) at low metal loadings to natural organic complexants.

The NICA-Donnan model describes concepts of polyfunctionality, polyelectrolytic effect and competitive binding for natural organic complexants. The model can be seen as a semi-empirical model for which the model parameters are partially fitted on proton and metal ion adsorption isotherms. The model has to be validated at variable ionic strength and in the presence of competing metal ions.

Solubilisation of Cu(II) and humic acids from the organic particles between 0.05-2 mm in the pH range 4-10 showed that both the solubility of Cu(II) and humic acid increase with decreasing particles sizes and increasing pH values. It is shown that the Cu(II) solubility is directly enhanced by the solubilisation of humic acid. Moreover, the Cu(II) reactivity of humic acids in the solid and in the liquid phase are equal, i.e. the Cu(II) binding strength is equal for both types of humic acid. The equal reactivity of the soluble and solid humic acid can only be explained when humic acids, according to Wershaw's model, are regarded as amphiphilic molecules structured in ordered aggregates by hydrogen bonds, electrostatic interactions and hydrophobic forces.

The results show that the mobility of heavy metal ions (e.g. leaching from topsoil to groundwater systems and leaching from landfill sites) can be enhanced when biowaste-derived compost or other organic waste streams are applied.

## References

- Adani, F.; Genevini, P. L.; Gasperi, F.; and Zorzi, G. 1997. Organic Matter Evolution Index (OMEI) as a Measure of Composting Efficiency. *Compost Science & Utilization* 5:53-62
- Aiken, G. R.; McKnight, D. M.; Wershaw, R.L.; and MacCarthy, P. (eds.) 1985. *Humic Substances in Soil, Sediment, and Water: Geochemistry, Isolation and Characterization*. New York, USA: John Wiley & Sons
- Banerjee, S. K.; and Rao, C. V. N. 1981. Studies on Complex Formation Between Clays and Humic Acid of Different Molecular Weights. *Journal of the Indian Society of Soil Science* 29:190-192
- Bartschat, B. M.; Cabaniss, S. E.; and Morel F. M. M. 1992. Oligoelectrolyte Model for Cation Binding by Humic Substances. *Environ. Sci. Technol.* 26:284-294
- Benedetti, M. F.; Milne, C. J.; Kinniburgh, D. G.; Riemsdijk, W. H. van; and Koopal, L. K. 1995. Metal Ion Binding to Humic Substances: Application of the Non-Ideal Competitive Adsorption Model. *Environmental Science and Technology* 29:446-457
- Benedetti, M. F.; Riemsdijk, W. H. van; and Koopal, L. K. 1996. Humic Acids Considered as a Heterogeneous Donnan Gel Phase. *Environmental Science and Technology* 30:1805-1813
- Brannon-Peppas, L.; and Peppas N. A. 1991. Equilibrium Swelling Behavior of pH-sensitive Hydrogels. *Chemical Engineering Science* 46:715-722
- Buffle, J. 1988. *Complexation Reactions in Aquatic Systems: An Analytical Approach*. Chichester, Ellis Horwood Limited
- Burns, R. G.; Dell'Agnola, G.; Miele, S.; Nardi, S.; Savoini, G.; Schnitzer, M.; Sequi, P.; Vaughan, D.; and Visser, S. A. 1986. *Humic substances: Effects on soil and plants*. Italy, REDA
- Chassin, P.; Le Bere, B.; and Nakaya, M. 1978. *Clay Miner.* 13: 1
- Chaney R.; and Ryan J. 1993. Heavy metals and toxic organic pollutants in MSW composts: Research results on phytoavailability, bioavailability, fate, In: *Science and Engineering of Composting: Design, Environmental, Microbiological and Utilization Aspects*, Hoitink A.J. and Keener H.M. (eds.), Ohio, Renaissance Publications
- Choudhry, G. G. 1984. Humic substances. Structural, photophysical, photochemical and free radical aspects and interactions with environmental chemicals. In: *Current Topics in Environmental and Toxicological Chemistry* 7. New York: Gordon & Breach Science Publishers, Inc.
- Greenland, D. J.; and Hayes, M. H. B. (eds.) 1981. *The Chemistry of Soil Processes*. New York: John Wiley & Sons Ltd.
- Hayes, M.H. B.; MacCarthy, P.; Malcolm, R.L.; Swift, R.S. (eds.) 1989. *Humic substances II. In search of structure*. Chichester, John Wiley & Sons Ltd.
- Herrington, T. M.; and Petzold, J. C. 1992a. An Investigation into the Nature of Charge on Surface of Papermaking Woodpulp 1. Charge/pH Isotherms. *Colloids and Surfaces* 64:97-108
- Herrington, T. M.; and Petzold, J. C. 1992b. An Investigation into the Nature of Charge on Surface of Papermaking Woodpulp 2. Analysis of potentiometric titration data. *Colloids and Surfaces* 64:109-118

- Hoop, M. A. G. T. van den; and Leeuwen, H. P. van 1990. Study of the Polyelectrolyte Properties of Humic Acids by Conductometric Titration. *Anal. Chim. Acta* 232:141-148
- Huang, O. M.; and Schnitzer, M. 1986. Interactions of Soil Minerals with Natural Organics and Microbes. *Soil science of America*, Special Publication No 17
- Green, S. A.; Morel, F. M. M.; and Blough, N. V. 1992. Investigation of the Electrostatic Properties of Humic Substances by Fluorescence Quenching. *Environ. Sci. Technol.* 26:294-302
- Kipton, H.; Powell, J.; and Town, R. M. 1992. Solubility and Fractionation of Humic Acid; Effect of pH and Ionic Medium. *Anal. Chim. Acta* 267: 47-54
- Laszlo, J. A. 1987. Mineral Binding Properties of Soy hull. Modelling Mineral Interactions with an Insoluble Dietary Fiber Source. *J. Agric. Food Chem.* 35:593-600
- Livens, F. R. 1991. Chemical Reactions of Metals with Humic Material. *Environ. Poll.* 70:183-208
- Marinsky, J. A.; Gupta, S.; and Schindler, P. 1982. A Unified Physicochemical Description of the Equilibria Encountered in Humic Acid Gels. *J. Colloid Interface Sci.* 89:412-426
- Marinsky, J. A.; Ephraim, J.; 1986. A unified physicochemical description of the protonation and metal ion complexation equilibria of natural organic acids (humic and fulvic acids). 1. Analysis of the influence of polyelectrolyte properties on protonation equilibria in ionic media: fundamental concepts. *Environmental Science and Technology* 20:349-354
- Martell, A. E.; and Smith, R. M. 1977. *Critical Stability Constants, Vol. 3: Other organic Ligands.* New York, Plenum Press
- Martell, A. E.; Motekaitis R. J.; and Smith, R. M. 1988. Structure-Stability Relationships of Metal Complexes and Metal Speciation in Environmental Aqueous Solutions. *Environ. Toxicology and Chemistry* 7:417-434
- Miyajima, T.; 1992. A Donnan Model for the Analysis of Metal Complexation of Weak-Acidic Polyelectrolytes. An Approach to the Quantitative Analytical Treatment of the Metal Complexation Equilibria of Humic Substances. *Sci. Tot. Environm.* 117/118:129-137
- Nederlof, M.M., Van Riemsdijk, W.H. and Koopal, L.K., 1992. Determination of Adsorption Affinity Distributions: A General Framework for Methods Related to Local Isotherm Approximations, *J. Colloid and Interface Sci.* 135:410-426
- Nederlof, M. M.; Riemsdijk, W. H. Van; and Koopal, L. K. 1992. Comparison of Semianalytic Methods to Analyze Complexation with Heterogeneous Ligands. *Environ. Science and Technology* 26:763-771
- Perdue, E. M. 1985. Acidic Functional Groups of Humic Substances. In: *Humic Substances in Soil, Sediment and Water: Geochemistry, Isolation and Characterization*, Aiken, G. R.; McKnight, D. M.; Wershaw, R. L.; and MacCarthy, P. (eds.). New York, John Wiley & Sons
- Schnitzer, M. 1978. In: *Soil Organic Matter*, Schnitzer, M.; and Khan, S. U. (eds.). Amsterdam, Elsevier
- Schnitzer M. 1991. *Soil Organic Matter: The Next 75 years.* *Soil Science* 151:41-58
- Schonherr, J.; and Huber, R. 1977. Plant Cuticles are Polyelectrolytes with Isoelectric Points around Three. *Plant Physiol.* 59:145-150
- Sentenac, H.; and Grignon, C. 1981. A Model for Predicting Ionic Equilibrium Concentrations in Cell Walls. *Plant Physiol.* 68:415-419

- Stevenson, F. J. 1994. *Humic Chemistry: Genesis, Composition, Reactions*. New York, John Wiley & Sons
- Stevenson, F.J. 1993. Stability Constants of Cu(II)-Humate Complexes: Comparison of Selected Models. *Soil Sci.* 155:77-91
- Vaughan, D.; Malcolm, R. E. (eds.) 1985. *Soil Organic Matter and Biological Activity. Developments in Plant and Soil Sciences Vol. 16*. Dordrecht, the Netherlands: Martinus Nijhoff/Dr W. Junk Publishers.
- Vermeer, A. W. P. 1996. *Interactions Between Humic Acid and Hematite and Their Effects on Metal Speciation*. PhD thesis, Wageningen Agricultural University
- Wershaw, R. I.; Thorn, K. A.; Pinckney, D. J.; MacCarthy, P.; Rice, J.A.; and Hemond, H.F. 1986. Application of a membrane model to the secondary structure of humic materials in peat. In *Peat and Water. Aspects of water retention and dewatering in peat*, Fuchsman, C. H. (ed.). Barking, Elsevier Applied Science Publishers Ltd.:133-157
- Wershaw, R.L. 1989. Application of a Membrane Model to the Sorptive Interactions of Humic Substances. *Environmental Health Perspectives* 83:191-203
- Wit, J. C. M de; Riemsdijk, W. H. van; Nederlof, M. M.; Kinniburgh, D. G.; and Koopal, L. K. 1990. Analysis of Ion Binding on Humic Substances and the Determination of Intrinsic Affinity Distributions. *Analytica Chimica Acta* 232:189-207
- Wit, J. C. M de; Riemsdijk, W. H. van; and Koopal, L. K. 1993a. Proton Binding to Humic Substances. 1. Electrostatic Effects. *Environmental Science and Technology* 27:2005-2014
- Wit, J. C. M de; Riemsdijk, W. H. van; and Koopal, L. K. 1993b. Proton Binding to Humic Substances. 2. Chemical heterogeneity and adsorption models. *Environmental Science and Technology* 27:2015-2022

## 8. Kinetics of heavy metal extraction from solid organic particles of biowaste

### 8.1. Introduction

Extraction is one of the technological options to reduce the heavy metal content of solid wastes (Smith et al., 1995). The extraction process involves the transport of the heavy metals from the solid phase to the aqueous phase. The extraction efficiency and rate of extraction are enhanced by the use of water-soluble extracting agents. Traditionally, inorganic acids or complexants have been used, e.g. hydrochloric acid, nitric acid, EDTA and NTA (Wong and Henry, 1988). Recently, interest is growing in the application of microbiological leaching processes, i.e. the water-soluble extracting agents are produced by microorganisms. Promising microbiological extraction processes are extraction with the sulphuric acid produced by *Thiobacilli* strains (Tyagi, 1988) and extraction with the citric acid produced by *Aspergillus niger* (Burgstaller, 1993).

The results of the sequential chemical extraction of Cd, Cu, Pb and Zn from biowaste (presented in Chapter 5) showed that the heavy metal content of biowaste can significantly be reduced by chemical extraction. This study showed that (i) Cd and Zn are less strongly bound to the biowaste particles than Cu and Pb, and (ii) the heavy metals are more strongly bound to the organic fractions of biowaste. The majority of heavy metals in biowaste are bound to the organic matter and organo-mineral aggregates. Dissolution of heavy metal precipitates is believed to play a minor role in this. Organic matter and organo-mineral aggregates exhibit a surface and a porous structure which carry negatively charged, reactive sites to which metal ions are adsorbed. The majority of reactive sites are carboxyl and phenol groups to which heavy metals are bound through covalent or electrostatic interactions (see Chapters 6 and 7). The results of Chapter 7 showed that the Cu(II) binding to the various particle-sized organic fractions of biowaste is regulated by the humic acid fraction.

For an extraction process on a full-scale, both the extraction efficiency and the rate of extraction are important parameters. Low extraction rates will result in high solid retention times and consequently lead to large reactor volumes. This increases the costs of the extraction process. Therefore, it is important to obtain a better understanding of the factors controlling both the rate and the efficiency of an extraction process.

Various models are presented in the literature to describe heavy metal speciation in sewage sludges (Behel et al., 1983; Fristoe and Nelson, 1983; Fletcher and Beckett, 1987). However limited approaches are made to describe the kinetics of heavy metal extraction. The adsorption and desorption kinetics of heavy metals in soil systems were extensively studied to predict the bioavailability and toxicity of heavy metal for plant growth. The results are mostly interpreted by reaction-kinetic models, e.g. zero order, first order, second order, Elovich, or parabolic equations (Sparks and Suarez, 1991; Sparks, 1989). These empirical models are mathematically appropriate to quantify extraction rates but they do not provide an insight into the mechanisms of the extraction process, i.e. the influence of such factors as pH, properties of the solid waste, solids concentration or type of heavy metal.

Identification of the factors controlling the rate and efficiency of heavy metal extraction from solid wastes can be made by experiments and modelling approaches. The extraction of Cu(II) at low pH is studied for several size ranges of the particle-sized organic fractions isolated from biowaste. The experiments are made in batches and the Cu(II) extraction is monitored by Cu(II)-ISE and GF-AAS. The general trends of the Cu(II) extraction for various particle-sized fraction are discussed together with the differences between the two measurement techniques, i.e. continuously monitoring by an ion-selective electrode and periodically sampling for AAS.

Besides the experiments, a mechanistic model is presented which describes the underlying chemical and physical processes for the desorption of heavy metals from solid organic particles. The model is based on approaches used for describing metal adsorption to synthetic ion-exchangers. Ion-exchange materials are analogous to the complexing components in biowaste, in the way that synthetic ion-exchangers, soil minerals and organic particles are all solid particles with a porous structure and reactive sites which bind (heavy) metal ions. It was first observed with synthetic ion-exchangers that diffusion processes play an important role and that reaction-kinetic models were inappropriate to describe metal adsorption and desorption (Sparks and Suarez, 1991; Petruzelli and Helfferich, 1993).

Various models based on film- and particle diffusion have been proposed to describe the adsorption and desorption of metal ions to immobilised biomass and peat (Tsezos, 1988; Trujillo, 1991; Kadlec, 1986). Several models combine diffusion in the film and particle by an overall mass transfer coefficient. For more advanced models the diffusion in the film layer and that inside the particles are described separately by Fick's law, the metal binding to biomass is described by the Langmuir or Freundlich adsorption isotherm, and it is assumed that the partition coefficient of mobile ions at the solid-liquid interface is unity. These concepts are inappropriate for the description of proton-metal exchange in solid organic particles for the following reasons:



1. metal ions are charged species for which mass transport has to be described by the Nernst-Planck equations
2. metal binding inside the particles cannot be described by an overall Langmuir or Freundlich adsorption isotherm because they do not take into account the effect of ionic strength, pH and competing ions. Therefore, the adsorption isotherm changes during the extraction process, depending on the position inside the particle
3. the negative charge density of the inside solid organic particles will generate a concentration jump at the solid-liquid interface (see Chapter 6).

In this chapter, a model will be presented which takes into account the three phenomena described above for the heavy metal extraction from organic particles. The model incorporates chemical reactions of protons and metal ions with the reactive sites of the organic particles and describes film diffusion and diffusion inside the particles. The model adopts an alternating diffusion-reaction approach to describe the extraction process (Hwang and Helfferich, 1987). Chemical equilibrium in the bulk solution, film layer and inside the complexing particles are handled by a standard chemical equilibrium algorithm (see Appendix 6A). The diffusion processes in the film layer and inside the particles are described by the Nernst-Planck equations for charged species.

The model is used to support the interpretation of the Cu(II) extraction experiments. The experiments can only monitor the bulk solution but the model also shows the course of extraction in the film layer and inside the particles. With the model the effect of particle properties (particle size, number and type of reactive sites, porosity), extraction conditions (pH of the aqueous phase, stirring rate) and type of heavy metal ion on the metal extraction can be studied. A combination of model and experiments can thus give additional insight into the extraction process of heavy metals from solid organic particles. As discussed in subchapter 2.2, heavy metal extraction from sewage sludge by inorganic acids showed some peculiar behaviour during in the course of the extraction. In some cases, a lag phase at the start of the extraction and unexpected changes in extraction rate during the course of extraction were observed. The duration of the lag phase and the extraction rate highly depend upon pH, solids concentration and type of heavy metal ion. These phenomena will also be interpreted and explained by the same model.

## **8.2. Model for heavy metal extraction from solid organic particles**

In this subchapter a mechanistic model is developed to describe the metal extraction at low pH from solid organic particles. The model incorporates the underlying physical and chemical processes involved in the extraction process.

### 8.2.1. System definition

Figure 8.1 is a schematic presentation of the heavy metal extraction process at low pH at particle level. For this, the complex nature of the solid organic particles and process conditions are simplified. The solid organic particles are presented as spherical, charged particles of equal size. One type of reactive site is considered and these sites are homogeneously distributed over the particles. The complexity of the pore structure is ignored and is presented as a single quasi-homogeneous, penetrable phase which is water-saturated. The diffusion inside the particles is presented by a single diffusion coefficient, i.e. no distinction is made between pore diffusion, diffusion inside organic matter and surface diffusion. The heavy metal ions are adsorbed to the organic particles through covalent binding with the reactive sites and electrostatic attraction by the net negative charge density of the particles. Heavy metal extraction at low pH with an inorganic acid (e.g. HCl, HNO<sub>3</sub>) involves the establishment of a low pH inside the particles. Two processes which promote the extraction of heavy metals take place inside the particles:

1. heavy metals adsorbed to the reactive sites are exchanged for protons, and
2. the electrostatic attraction of heavy metals by the negative charge density of the particles is reduced because protons will occupy the functional groups.

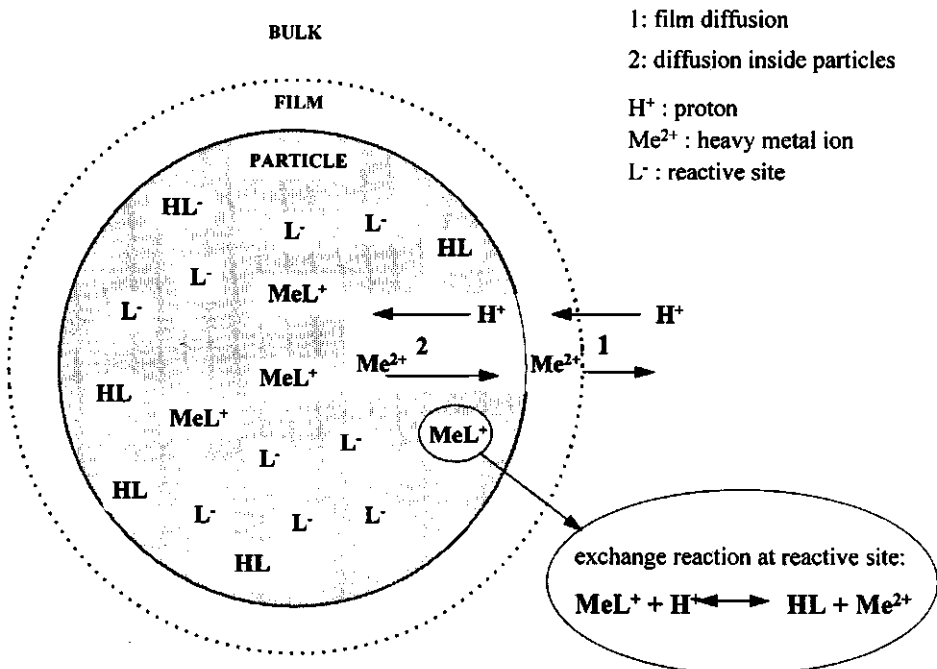


Figure 8.1 Schematic presentation of the heavy metal extraction process at a low pH

Mass transport resistance between the bulk solution and the surface of the particles is represented by the stagnant water layer (or film layer) model through which the solutes can only move by diffusion (Wesselingh and Krishna, 1990; Levenspiel, 1972). In this concept, protons have to diffuse through the film layer and through the porous structure of the particles to reach the reactive sites. The protons occupy the free sites ( $L + H^+ \leftrightarrow HL$ ) and will exchange with  $Me^{2+}$  ions if the protons bind more strongly ( $MeL^+ + H^+ \leftrightarrow HL + Me^{2+}$ ). The  $Me^{2+}$  ions exchanged for protons will diffuse through the porous structure of the particles and through the film layer to the bulk solution.

The reactions of protons and metal ions with the reactive sites are represented by the mass law of action and corresponding equilibrium constant. The model takes into account one complexing site ( $L$ ), one heavy metal ion ( $M^{2+}$ ), an indifferent cation ( $Na^+$ ) and an indifferent anion ( $NO_3^-$ ). Lowering the pH of the solution is brought about by the addition of  $HNO_3$ .

### 8.2.2. Rate-limiting step for the extraction process

The model assumes that local equilibrium for each reaction is maintained at all times at any location inside the particles. This assumption is reasonable if the chemical reactions are fast compared to diffusion in the particles. Here, arguments will be given to show that this assumption is valid.

The chemical reactions taking place inside the particles are exchange reactions between metal ions and protons at the reactive sites:  $MeL^+ + H^+ \leftrightarrow HL + Me^{2+}$ . For complexation reactions in solution, Pankow and Morgan (1981) showed that these reactions are generally very fast (reaction times in the order of microseconds to seconds). On the basis of literature data, Sparks (1989) showed that reaction times for ion exchange and sorption cover a broad range, probably due to mass transport phenomena. When the reactive sites are only accessible by diffusion, the sorption and desorption reactions are limited by mass transfer and establishment of equilibrium can take days or even weeks. Sparks (1986) also showed the effect of agitation of the solution on the kinetics of sorption of potassium by a loamy soil. The apparent rate coefficient of potassium sorption increased steadily with increasing stirring rate, showing that the process is film-diffusion controlled. Metal sorption reactions on oxides, hydroxides and humic substances are in general rapid, ranging from milliseconds to seconds (Bunzl and Schimmack, 1991; Sparks, 1989). Helfferich (1962b) found no experimental evidence for reaction control for cation exchange processes on organic zeolites; the results pointed universally to diffusion control.

The arguments put forward show that the rate constant of reactions are in the order of millisecond to seconds, far less than the half-times for diffusion in the film layer and inside particles.

### 8.2.3. Model description

#### 8.2.3.1. Mass transport processes

The diffusion of ionic species, as carriers of electric charge, generates an electrical potential gradient which influences their diffusion (Helfferich, 1962a). Therefore, the diffusion of ionic species is driven by both a concentration gradient and an electrical potential gradient. Both the chemical and electrical potentials are incorporated in the Nernst-Planck equation for diffusion of ionic species (Wesselingh and Krishna, 1990):

$$J_i = -D_i \left( \nabla C_i + Z_i C_i \frac{F}{RT} \nabla \phi \right) \quad (8.1)$$

where  $D_i$  (in  $\text{m}^2 \cdot \text{s}^{-1}$ ) and  $\nabla C_i$  are the diffusion coefficient and concentration gradient of species  $i$ ,  $Z_i$  and  $C_i$  are the charge and concentration of ion  $i$ , and  $\nabla \phi$  is the electric potential gradient. The Nernst-Planck equation can be considered as a special case of the Maxwell-Stefan equations, all frictional forces are neglected except those between the solvent and ions. It is also assumed that the solvent has zero flux. Kraaijeveld and Wesselingh (1993) studied the ion exchange kinetics for HCl-NaCl and HCl-CaCl<sub>2</sub> Lewatit S100 (strong acid ion-exchanger carrying sulphonic groups). They showed that the Nernst-Planck equation equally well described the ion-exchange process as the Maxwell-Stefan equations.

A system containing ions should remain electrically neutral at all times. Furthermore, in the absence of an external electric field, the net molar flux of the charges of ionic species should be zero at all locations in the system, in order to maintain electroneutrality (Mafe et al., 1988; Aguilera et al., 1987; Hu et al., 1992). These conditions are given by:

$$\sum_i Z_i C_i = 0 \quad (8.2)$$

and

$$\sum_i Z_i J_i = 0 \quad (8.3)$$

Newman (1973) showed that deviations from electroneutrality are very small and the validity of the Nernst-Planck equations is proved in the electrochemistry of dilute and moderately concentrated solutions (Graham and Dranoff, 1982). Substitution of equation 8.3 in equation 8.1 renders the electrical potential  $\nabla\phi$  in terms of concentration:

$$\nabla\phi = -\frac{\sum_i D_i Z_i \nabla C_i}{\sum_i D_i Z_i^2 C_i} \frac{RT}{F} \quad (8.4)$$

Substitution of equation 8.4 in equation 8.1 results in a flux expressed solely as a function of concentration gradients:

$$J_i = -D_i \left( \nabla C_i - Z_i C_i \frac{\sum_j D_j Z_j \nabla C_j}{\sum_j D_j Z_j^2 C_j} \right) \quad (8.5)$$

Equation 8.5 shows that the flux of one ionic species is affected by the fluxes of all other ions.

### 8.2.3.2. Solid-liquid interface

Special attention has to be paid to the mass transport through the solid-liquid interface. The negative charge of the solid organic particles creates an electrical field. Assuming that the negative charge is distributed inside the particles, cations are accumulated in the particles and anions are partially excluded. The negatively-charged sites inside the particles thus create a potential jump at the solid-liquid interface, the so-called Donnan potential (Marinsky, 1982). As described in Chapter 6, the magnitude of this potential depends on the net charge density of the particles sites and the ionic strength of the bulk aqueous solution. The partition coefficient of mobile species at the interface between the charged solids and the liquid is described by the Donnan potential term (Marinsky, 1982):

$$\frac{(C_i)_{\text{particle}}}{(C_i)_{\text{film}}} = \exp\left(-\frac{Z_i \phi}{RT}\right) \quad (8.6)$$

The same type of concentration jump is also encountered at gas-liquid interfaces for which the concentration jump is defined by the Henry constant. Whereas the Henry constant is constant, the Donnan potential term depends on the net charge density of the particles and the ionic strength of the solution, and thus changes during the extraction

process. It is assumed that equilibrium holds at the solid-liquid interface (MacGillivray, 1968). The interface has no capacity and therefore the flux from the film solution to the interface can be set equal to the flux from the interface to the inside of the particle.

### 8.2.3.3. Chemical equilibrium and mass balances

The following species and reactions have to be considered for the defined model system:

1. in the bulk solution and film layer:

- species:  $H^+$ ,  $OH^-$ ,  $Na^+$ ,  $NO_3^-$ ,  $Me^{2+}$
- reactions:  $H_2O \leftrightarrow H^+ + OH^-$

2. inside the particles:

- species:  $H^+$ ,  $OH^-$ ,  $Na^+$ ,  $NO_3^-$ ,  $Me^{2+}$ ,  $L^-$ ,  $HL$ ,  $MeL^+$
- reactions:  $H_2O \leftrightarrow H^+ + OH^-$   
 $LH \leftrightarrow L^- + H^+$   
 $MeL^+ \leftrightarrow L^- + Me^{2+}$

The chemical system in the bulk aqueous phase and the film layer are equal and comprised of 5 ionic species, and is described by 5 equations: one balance for electroneutrality, 3 mass balances for  $Na^+$ ,  $NO_3^-$  and  $M^{2+}$ , and one reaction equation for the dissociation of water. Chemical equilibrium in the bulk and film layer can be solved analytically. The chemical system inside the particles is made up of 8 ionic species and is described by 8 equations: one balance for electroneutrality, 4 mass balances for  $Na^+$ ,  $NO_3^-$ ,  $M$  and  $L^-$  and 3 reaction equations for the dissociation of water, the complexation of  $Me^{2+}$  and  $L^-$  and the association of  $H^+$  and  $L^-$ . Chemical equilibrium inside the particles is computed by EQUILIB, a thermodynamic chemical equilibrium algorithm (see Appendix 6A of Chapter 6).

The material balance equation for species in the bulk solution, film layer and inside the particles is given by:

$$\frac{\partial C_i}{\partial t} = -\nabla J_i + R_i \quad (8.7)$$

where  $\nabla J_i$  is the flux gradient for species  $i$  and  $R_i$  is the reaction term of species  $i$ . Equation 8.7 comprises of two sets of equations: one set relates the fluxes to the concentrations and the other set imposes constraints on the reaction terms. The fluxes are defined by the Nernst-Planck equation 8.5, with  $Z_i=0$  for neutral species and  $D_i=0$  for fixed species (i.e.  $L^-$ ,  $HL$  and  $MeL^+$ ).

Initial conditions:

$$t=0; \quad C_i = C_i(t=0) \quad (8.8)$$

Boundary conditions:

$$x=0; \quad \delta C_i / \delta x = 0 \quad (8.9)$$

$$\text{solid-liquid interface; } J_{\text{liquid-to-interface}} = J_{\text{interface-inside particle}} \quad (8.10)$$

#### 8.2.3.4. Numerical solution

Summarising, the model uses the following assumptions and simplifications:

1. the particles are spherical, of equal size and water-saturated
2. the solids are considered as a single quasi-homogeneous phase, i.e. no distinction is made between diffusion in the free pore water of the interstices and that in the porous structure of organic matter
3. the particles are suspended in a solution for which the bulk liquid is well-mixed
4. transport from the bulk liquid to the particle is assumed to be by diffusion through a stagnant film around the particles
5. transport in the particles is described by diffusion through a stagnant porous sphere
6. film and intraparticle diffusion are described by the Nernst-Planck equations under electroneutrality and zero-current conditions, i.e. coupling of ion fluxes other than by electric diffusion potential are neglected
7. surface diffusion is negligible
8. Donnan equilibrium holds at the solid-liquid interface between particle and liquid of the film
9. sorption and desorption of solvent (water) as well as swelling and shrinking of the particles are not considered
10. osmotic pressure is ignored, i.e. convective transport is ignored (water flux is zero)
11. the flux from the aqueous solution to the interface is equal to the flux from the interface into the particle, i.e. the interface has no adsorbing capacity
12. the reactions at the reactive sites are instantaneous, i.e. the chemical reaction is not rate-limiting
13. the individual diffusivities of ions in the particles are assumed to be constant.

Solutions of mass balance equation 8.7 in combination with the Nernst-Planck equation and the reaction term are not easy to obtain. Therefore, the problem is simplified by assuming that diffusion and reactions are taking place separately; this is the so-called alternating diffusion-reaction approximation (Hwang and Helfferich, 1987). The partial differential equations are solved by discretisation applying central finite difference. Film and particle are each divided into five slices and numerical accuracy is acquired by varying the size of the time step. Local chemical equilibrium is calculated analytically in the bulk solution and the film, and numerically by EQUILIB inside the particle. Diffusion takes place during the whole time interval, new mass balances are calculated and new equilibrium is established. The new concentration distribution of species is used as the initial condition for the diffusion stage of the next time interval.

### 8.2.4. Model calculations

The parameters that determine the extraction process can be divided into three groups:

1. particle properties: particle size, type and density of reactive sites, restriction factor<sup>1</sup>
2. extraction conditions: pH and ionic strength of the extraction, film layer thickness, solids concentration
3. type of metal ion: concentration of the metal, metal affinity for reactive sites.

The heavy metal extraction at a low pH from solid organic particles is simulated for the model presented in the preceding chapter. The heavy metal ion is presented by a divalent metal ion Me(II) (e.g. Cd, Cu, Pb or Zn) and the reactive sites L<sup>-</sup> are presented by carboxylic sites. The extraction is simulated for an instant pH lowering which is equivalent to the addition of solids to a solution of low pH. The pH in the bulk is maintained at a constant level by the addition of HNO<sub>3</sub>. The extraction is extensively discussed for one set of parameters. Next, the course of metal extraction is discussed for varying particle size properties, extraction condition and type of metal ion.

Computer simulations are made for the following standard set of parameters:

- particle size diameter:  $10^{-4}$  m
- film layer thickness:  $10^{-5}$  m<sup>2</sup>
- concentration of organic particles: 100 g.l<sup>-1</sup>
- diffusivities of mobile ions in diluted solutions: from Newman (1973)<sup>3</sup>

#### 8.2.4.1. Detailed interpretation of the metal extraction process

To obtain a clear picture of the extraction process on film- and particle scale, a simulation is extensively discussed for the following set of parameters:

- initial concentrations in bulk and film: pH=3; I=0.01 M; [Me<sup>2+</sup>]=10<sup>-7</sup> M
- initial concentrations in particle: pH=7; [Me]<sub>tot</sub>=10<sup>-3</sup> M; [L<sup>-</sup>]=1 M
- affinity constants: K<sub>HL</sub>=10<sup>4</sup> M; K<sub>MeL<sup>+</sup></sub>=10<sup>2</sup> M
- restriction factor: 1

Figure 8.2 shows the concentration profiles of H<sup>+</sup>, Me<sup>2+</sup> and ML<sup>+</sup> and the potential profile in the film layer and particle at four time moments during the extraction. The pH in the organic particles is neutral at the start of the extraction. The sites are only partially occupied by Me(II) ions (10<sup>-3</sup> M on a total sites concentration of 1 M), and the rest of the

<sup>1</sup> diffusion in the particles is restricted by the high viscosity of water (Buffle, 1988; Peppas and Reinhart, 1983)

<sup>2</sup> found by Kraaijeveld and Wesselingh (1993) for solid particles in a stirred batch reactor

<sup>3</sup> D<sub>H<sup>+</sup></sub>=9×10<sup>-9</sup>, D<sub>OH<sup>-</sup></sub>=5×10<sup>-9</sup>, D<sub>NO<sub>3</sub><sup>-</sup></sub>=2×10<sup>-9</sup>, D<sub>NH<sub>4</sub><sup>+</sup></sub>=2×10<sup>-9</sup> and D<sub>Me<sup>2+</sup></sub>=2×10<sup>-9</sup> m<sup>2</sup>.s<sup>-1</sup>



negative charge density is neutralised by  $\text{Na}^+$  ions. At the solid-liquid interface a discontinuity in concentration is encountered because the electrical field generated by the negatively-charged solids accumulates cations and excludes anions from the solid phase; this is the so-called Donnan exclusion. When the extraction starts, protons diffuse freely through the film layer into the particles.

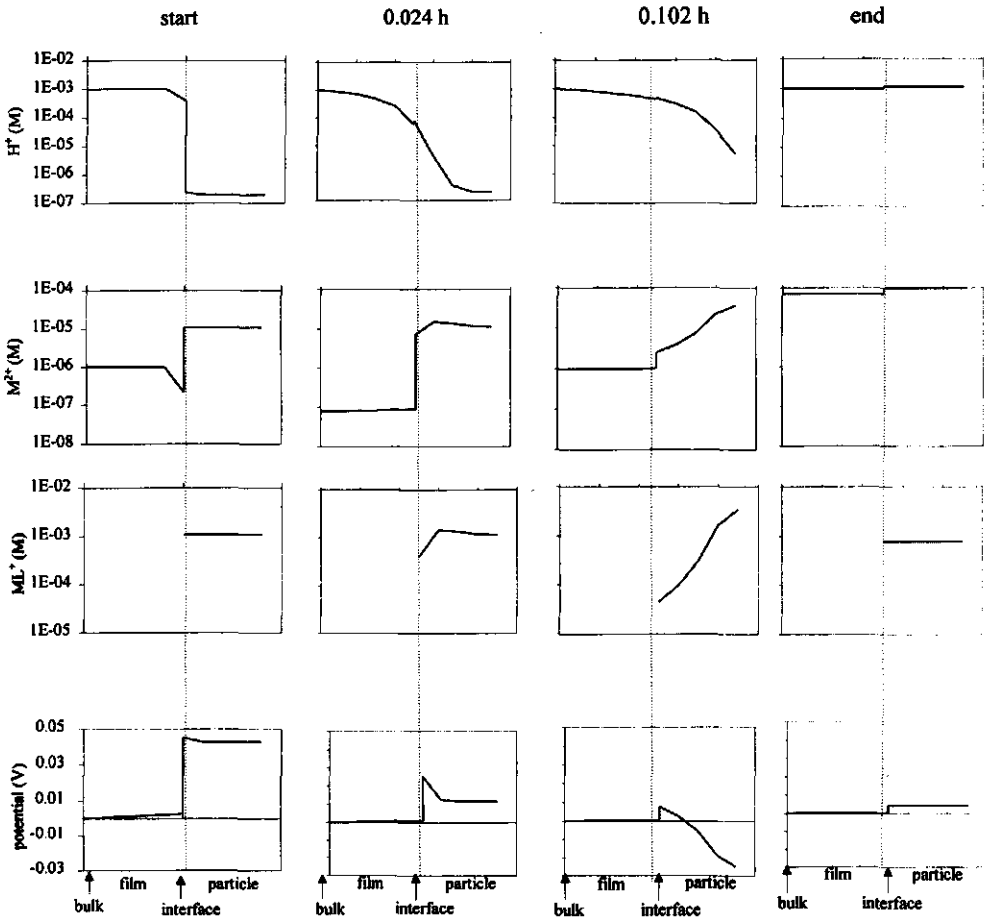


**Figure 8.2** Concentration profiles of proton ( $\text{H}^+$ ), free metal ion ( $\text{M}^{2+}$ ), metal-ligand complex ( $\text{ML}^+$ ) and electrical potential ( $\text{V}$ ) in film and particle for simulation of the metal extraction from solid organic particles (last column: at equilibrium after 0.36 h)

In the particle, protons do not diffuse freely but are bound to carboxyl sites ( $\text{L}^- + \text{H}^+ \leftrightarrow \text{LH}$ ). A dispersed pH front is established which gradually progresses to the centre of the particles over time. The pH in the film layer near the solid surface increases because the proton flux into the particles cannot be compensated by the diffusion of protons from the bulk to the solid-liquid interface.

At the start of the extraction, the free metal ion concentration  $Me^{2+}$  in the particles is higher than in solution. Although the  $Me^{2+}$  concentration gradient at the solid-liquid interface is directed towards the bulk solution,  $Me^{2+}$  starts to move inside the particles. There are two reasons for this unexpected metal flux. Firstly, the pH inside the particles is still neutral to slightly acidic at the initial stage of the extraction. This leads to the adsorption of metal ions from the film and bulk to the solid phase. Secondly, the metal flux is not determined only by the concentration potential but also by an electrochemical gradient, i.e. the electrochemical gradient acting upon  $Me^{2+}$  is determined by a concentration gradient and an electric potential gradient. In some cases this can imply that the metal flux is directed in the opposite direction to the concentration gradient. This phenomenon was also described by other authors. Wesselingh and Krishna (1990) observed that the transport of ions through charged synthetic membranes moves against its concentration gradient. Tyree et al. (1990) proposed that  $Ca^{2+}$  could be accumulated in the leaf cuticles against a concentration gradient under acidic conditions due to an oppositely directed electrical force generated by the diffusion of KCl from the inside to the outside of the leaf cuticles. Theuvenet and Borst-Pauwels (1976) showed that the uptake of divalent cations in yeast can be described by a diffusion process regulated by the surface potential near the cell membrane.

Movement of  $Me^{2+}$  ions against the concentration potential can possibly account for the fact that, at the initial stage of the extraction,  $Me^{2+}$  ions do not flow to the bulk of the solution but move towards the centre of the organic particles. This can be seen from the concentration profiles of  $Me^{2+}$  and  $MeL^+$  inside the particles (Figure 8.2). As the pH front progresses inside the particles, it is expected that  $MeL^+$  gradually decrease at places where pH starts to drop. On the contrary, it is observed that  $MeL^+$  in the particle increases as the pH-front advances inside the particles. This implies that  $Me^{2+}$  ions exchanged for protons ( $MeL^+ + H^+ \leftrightarrow HL + Me^{2+}$ ) are transported further inside the particles where they are bound to unoccupied reactive sites.

Figure 8.3 displays the metal concentration in the bulk solution and the metal flux to the bulk solution as a function of time. Note that both the extraction time and the concentration are plotted on a logarithmic scales. This implies that low metal concentrations at the beginning of the extraction are magnified. Figure 8.3 shows that in the initial stage of the extraction process, the metal flux to the bulk solution is negative and  $Me^{2+}$  is quickly removed from the bulk solution (note the logarithmic concentration and time scale). The flux decreases to zero but does not become positive up to 0.1 h although the pH in the particles continues to drop and  $Me^{2+}$  ions are exchanged for protons at the reactive sites. After 0.1 h the metal flux again becomes positive, reaches a maximum and then drops to zero as the extraction process reaches the end. The time when the flux again becomes positive coincides with the moment the electric potential is reduced to zero over the entire particle (see Figure 8.2). The electrical potential gradient is directed inside the particles as long as the pH front progresses through the particles. As the pH in the particles is

established, the potential gradient fades away, and  $\text{Me}^{2+}$  starts to flux towards the bulk of the solution.

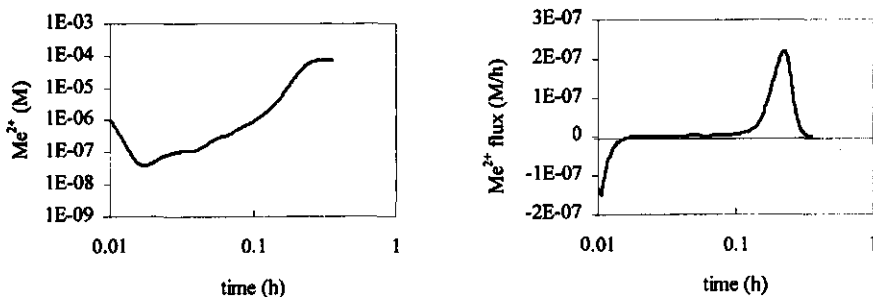


**Figure 8.3** Bulk metal concentration (left) and metal flux to the bulk solution (right)

The course of  $\text{Me}^{2+}$  in the bulk solution can only be explained by processes taking place inside the particles. The simulations show that  $\text{Me}^{2+}$  ions exchanged for protons inside the particles are not directly transported to the bulk solution. On the contrary,  $\text{Me}^{2+}$  can be adsorbed further inside the particles because (1) metal ions can be adsorbed to reactive sites farther inside the particles and (2) the electrochemical gradient is directed towards the inside the particles. As the pH front progresses inside the particles,  $\text{Me}^{2+}$  ions are not directly transported to the bulk solutions. Due to both concentration and electric potential gradients,  $\text{Me}^{2+}$  can be pushed further into the particle. This process continues as the pH front progressively penetrates the particles. As the proton gradient levels out and the potential gradient becomes zero,  $\text{Me}^{2+}$  transport to the bulk phase is completely regulated by the concentration gradient of  $\text{Me}^{2+}$ .

#### 8.2.4.2. Extraction for variable conditions

Figure 8.4 shows the effect of the stability constant of the  $\text{ML}^+$  complex, pH of the bulk solution, sites density of the particles, restricted diffusion inside the particles and particle size on the course of metal extraction.

**Affinity constant** A stronger affinity of  $\text{Me}^{2+}$  for the reactive sites results in a lower minimum in  $\text{Me}^{2+}$ , a lower  $\text{Me}^{2+}$  extraction efficiency and a longer time until equilibrium is reached. A stronger affinity means that metal ions are exchanged to a lesser extent, i.e. they have a lower extraction efficiency. Because  $\text{Me}^{2+}$  ion are more strongly adsorbed to the reactive sites, a higher metal flux directed inside the particles is observed. The time until equilibrium is reached, increases for higher affinity because the concentration gradient is smaller.

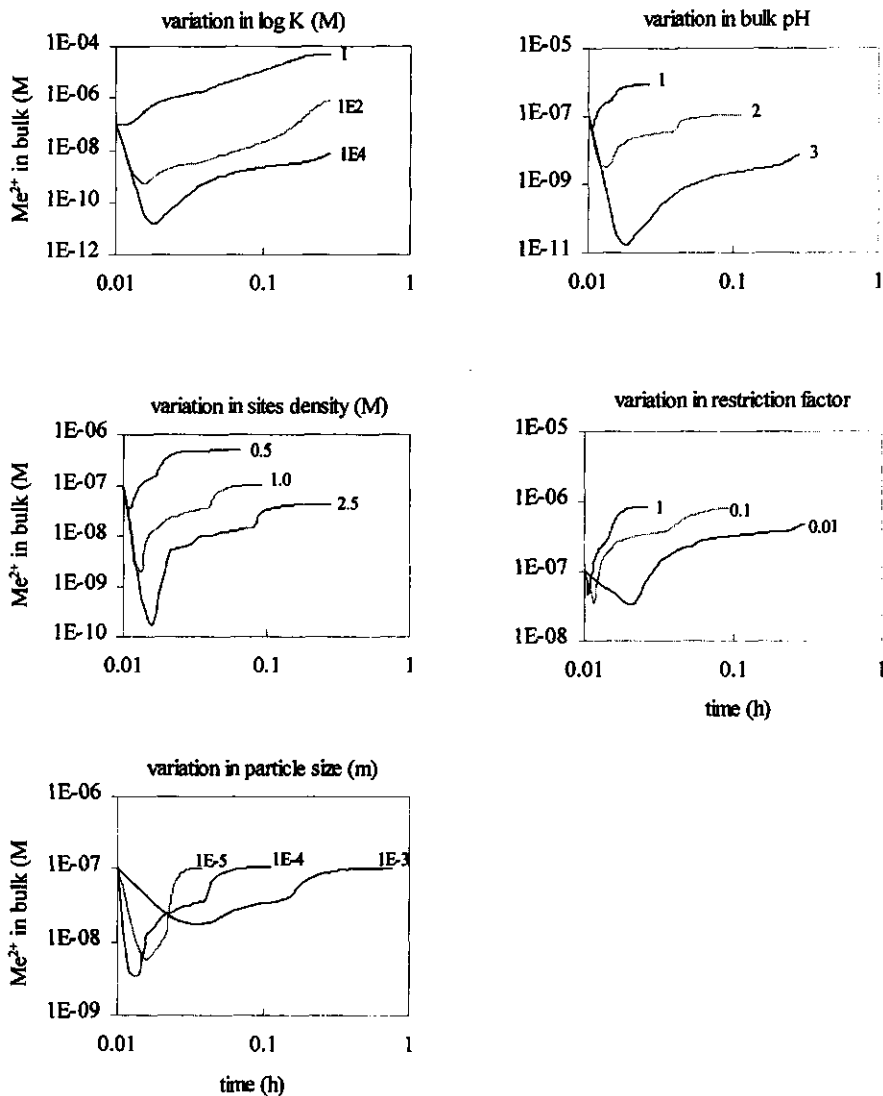


**Figure 8.4** Metal extraction from organic particles for variable extraction conditions and particle size properties

**pH of extraction** Lowering the pH results in a higher  $Me^{2+}$  extraction and shorter extraction times. At lower pH values the  $H^+$  concentration gradient is higher and also the  $Me^{2+}$  concentration gradient is higher because  $Me(II)$  ions are exchanged to a larger extent. This results in faster extraction rates. Besides this,  $Me(II)$  ions are pushed less far back into the particles because the potential gradient effect is less pronounced due to a

fast pH drop in the particles. The final bulk  $\text{Me}^{2+}$  concentration is higher because more  $\text{Me(II)}$  ions are exchanged for protons at lower pH values.

**Sites density** A higher site density results in a lower  $\text{Me(II)}$  extraction and longer extraction times. The higher site density in the particles gives a slower progression of protons in the particles because more protons are bound to the reactive sites. Also less  $\text{Me(II)}$  ions are exchanged for a higher site concentration. Both these effects lead to lower potential gradients and therefore the extraction takes longer.

**Restricted diffusion** Restricted diffusion in the particles leads to a slower diffusivity of ions in the particles. A slower diffusion does not change the extraction profile but the extraction rates proportionally decreases due to the smaller diffusivity of ions in the particle phase.

**Particle size** For particles of larger size, the extraction time increases with size. The initial decrease in the  $\text{Me(II)}$  bulk concentration is larger for smaller particles because of the higher specific surface area of smaller particle sizes. Both a stronger adsorption of the particles and the inwardly directed flux over the solid-liquid interface will increase with a higher specific surface area.

### 8.3. Materials and methods

#### 8.3.1. Particle-sized organic fractions

Biowaste was sampled at VAM, Wijster and physically separated by wet sieving and water elutriation as described in subchapter 3.4. The obtained fractions were stored at 4 °C before use. The characteristics of the organic fractions are given in Table 8.1 (extracted from Tables 3.10 and 3.11)

**Table 8.1 Humic acid content and (heavy) metals content of the particle-sized organic fractions in biowaste**

Fraction (mm)	Humic acid ( $\text{g.g}^{-1}$ OM)	K	Ca	Fe	Cu	Zn
		(g.kg <sup>-1</sup> DM)			(mg.kg <sup>-1</sup> DM)	
1-2	0.11	0.19	5.12	1.24	20	138
0.2-0.5	0.11	0.40	6.11	2.70	28	527
0.05-1	0.21	1.48	14.9	4.83	52	982

### 8.3.2. Extraction experiments

The acid extraction experiments were conducted in a 400-ml polyethylene beaker which was magnetically stirred at approx. 500 rpm. The beaker was placed in a water bath of 20 °C. The solution in the beaker was connected to the computer-controlled titration apparatus as described in subchapter 3.7. The organic particles with a specific particle-size range were suspended in solution. When equilibrium was reached, the pH was brought to 1 with nitric acid and maintained at pH 1 during the extraction. The amounts of dosed acid, pH and pCu and were registered continuously. Total control and monitoring of the experiment was completely computer controlled. The pH and the pCu of the bulk solution were measured with a pH glass electrode (Schott, type N32A) and Cu(II)-ISE (ORION, model 94-29), respectively. The combined glass electrode was calibrated with commercial pH buffers of pH 4.0 and 7.0 (Merck) and the Cu(II)-ISE with  $10^{-3}$  M and  $10^{-5}$  M  $\text{Cu}(\text{NO}_3)_2$  in 0.01 M  $\text{NaNO}_3$ . The electrodes were calibrated before and after the measurement. Changes in slope and intercept should not exceed 1 mV.

At regular time intervals the stirring of the solution was stopped for 1 minute to allow the suspension to settle. A sample of 2 ml was withdrawn from the solution with a micropipet and centrifuged at 10,000 rpm for 1 minute. Total Cu(II) concentration in the supernatant was measured by GFAAS as described in subchapter 3.2 (detection limit approx.  $4 \times 10^{-8}$  M). Two modes of analytical techniques are applied to monitor the Cu(II) extraction from the solid organic particles. Cu(II)-ISE measures the free Cu(II) activity (specified as  $\text{Cu}^{2+}$  in the rest of the text) and GFAAS measures the total Cu(II) in solution (specified as  $\text{Cu}_{\text{sol}}$  in the rest of the text). The advantages and disadvantages of both analytical techniques are presented in Table 8.2.

**Table 8.2 Advantages and disadvantages of the AAS and ISE techniques**

Advantages	Disadvantages
<b>Ion-selective electrode (ISE)</b>	
<ul style="list-style-type: none"> <li>• measurement does not disturb equilibrium because it is carried out in-situ and no phase separation is necessary</li> <li>• activity can be measured continuously; the time interval is in the order of seconds so trends and sudden changes can be monitored clearly</li> <li>• very low free ion concentrations can be measured</li> </ul>	<ul style="list-style-type: none"> <li>• only free ion activities can be measured which, in most cases, is not a measure of the total Cu concentration in solution</li> <li>• poor selectivity of the electrode when interfering metal ions are present</li> <li>• for fast changes the electrode signal is not in equilibrium with bulk phase Cu(II)</li> </ul>
<b>Atomic Absorption Spectroscopy (AAS)</b>	
<ul style="list-style-type: none"> <li>• high selectivity</li> <li>• total Cu(II) content of solution is measured</li> </ul>	<ul style="list-style-type: none"> <li>• fast changes and slow trends cannot be monitored by periodical sampling</li> <li>• suspended solids have to be removed by centrifugation or filtration</li> <li>• solution is seriously disturbed by periodic withdrawal of a sample</li> <li>• Cu(II) speciation in the sample probably changes during withdrawal and centrifugation</li> </ul>

#### 8.4. Results

Cu(II) was extracted at pH 1 from the organic fractions 1-2 mm, 0.2-0.5 mm and 0.05-0.1 mm at a solids concentrations of 21, 17 and 17 g.l<sup>-1</sup>, respectively. Figure 8.5 shows the results of the extraction experiments. The Cu(II) concentration, measured by GFAAS and Cu(II)-ISE, are plotted on the left abscissa and the pH on the right. The pH of the solutions started at approx. 7 and reached its final pH in approx. 0.3 h, as shown for the fraction 1-2 mm. At the start of the extraction no samples were taken for GFAAS because the sampling of the solution had a pronounced effect on the course of the computer-controlled pH lowering.

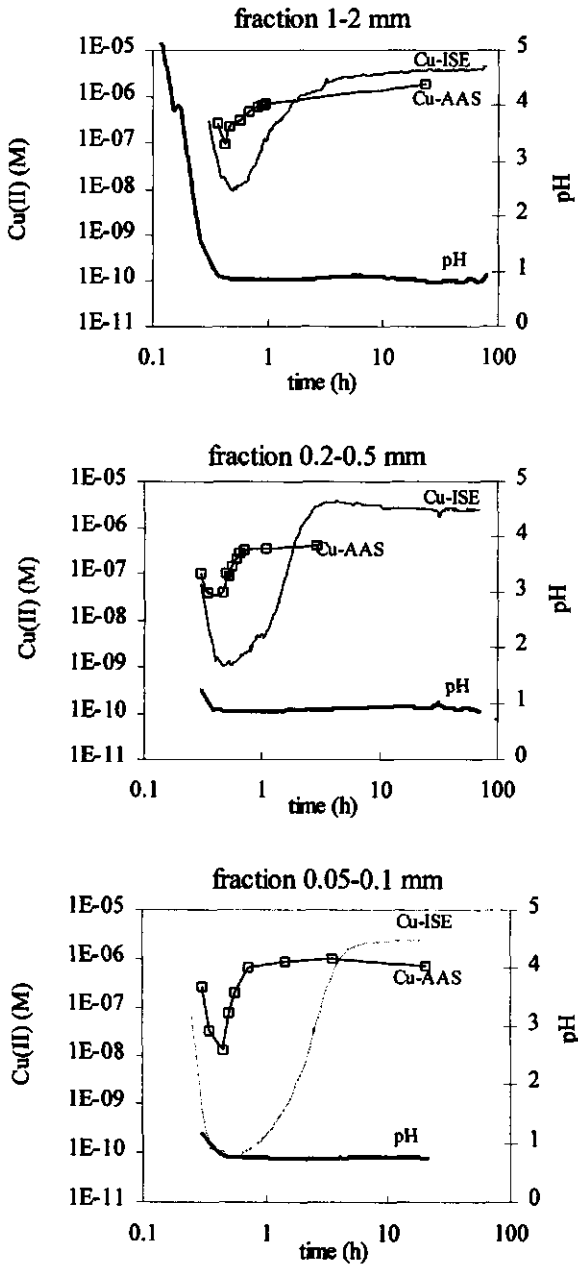


**Figure 8.5** Cu(II) extraction from particle-sized organic fractions of biowaste at pH 1



## 8.5. Discussion

The results of the experiments are qualitatively interpreted; only trends are discussed and no extraction rates and efficiencies are calculated. The experimental results are compared with the simulations of subchapter 8.2.2. The simulations are also employed to interpret the heavy metal extraction from sewage sludge as found in literature. These extractions were discussed in subchapter 2.2.

### 8.5.1. Cu(II) extraction from organic fractions of biowaste

#### 8.5.1.1. Discussion of the experiments

Both Cu-AAS and Cu(II)-ISE show the same trends. As the pH drops, both  $\text{Cu}^{2+}$  and  $\text{Cu}_{\text{sol}}$  decrease. The Cu(II) concentration reaches a minimum and then increases to a constant level, i.e. equilibrium is reached. The Cu(II)-ISE shows the following trends with decreasing particle size: (1) a faster drop in  $\text{Cu}^{2+}$ , (2) the drop in  $\text{Cu}^{2+}$  extends to a lower concentration, and (3) it takes longer before equilibrium is reached. The trends in Cu-AAS are less pronounced with decreasing particle sizes due to the periodic sampling. It can be seen that (1) the drop in  $\text{Cu}_{\text{sol}}$  proceeds to a lower concentration, and (2) time to reach equilibrium does not differ distinctly.

There are also several distinct differences between the course of the extraction as measured by Cu(II)-ISE and Cu-AAS. Theoretically  $\text{Cu}_{\text{sol}}$  should always be larger than  $[\text{Cu}^{2+}]$  because ISE only measures free  $\text{Cu}^{2+}$  ions and Cu-AAS measures the total soluble Cu(II) concentration. However, at the end of the extraction  $\text{Cu}^{2+} > \text{Cu}_{\text{sol}}$ . This is caused by the poor selectivity of the Cu(II)-ISE for several metal ions. Metal ions present in the organic particles are also extracted at low pH and will contribute to the Cu(II)-ISE signal. Especially Fe(III) will interfere with the Cu(II)-ISE (subchapter 3.4.6) because Fe(III) has a high selectivity coefficient at pH 1 and its concentration is approx. 100 times higher than for Cu(II) in the organic fractions (Table 8.1).

For the initial drop in Cu(II), the minimum in Cu(II) is a few orders of magnitude lower for Cu(II)-ISE than for Cu-AAS and the drop proceeds for longer times. This large discrepancy is peculiar because at pH 1 Cu(II) in solution is almost completely present as  $\text{Cu}^{2+}$ . The difference is most probably due to the fact that  $\text{Cu}^{2+}$  measured at the electrode of the Cu(II)-ISE is not in equilibrium with  $\text{Cu}^{2+}$  in the bulk solution (Ammann, 1986).

Differences between Cu(II)-ISE and Cu-AAS are due to the intrinsic properties of both measurement techniques (see Table 8.2). Cu(II)-ISE gives only a qualitative impression of the extraction process because (1) in the initial stage of the extraction the electrode is not in equilibrium with the bulk solution and (2) the contribution of interfering metal ions to the electrode signal is too high to provide a reliable indication of the actual  $\text{Cu}^{2+}$

concentration. However, the question remains whether  $Cu_{sol}$  measured by Cu-AAS is representative for Cu(II) in solution at the time the sample was withdrawn from the bulk solution. During sampling and centrifugation the speciation of Cu(II) is changed, especially at the beginning of the extraction process where changes in Cu(II) are too fast to be clearly pictured by periodical sampling. Moreover, periodical sampling disturbs the solution and will probably have a pronounced effect on the course of the extraction.

#### *8.5.1.2. Comparison of experiments and model simulations*

In comparison with the model calculations of subchapter 8.2.2 we have to bear in mind that the particle-size organic fractions of biowaste are ill defined. The solid organic particles do not have a regular spherical shape, they show a particle size distribution, the composition of the fractions are not exactly known (i.e. the concentration and type of reactive sites are not known), the interior of the organic particles cannot be considered as a single quasi-homogeneous phase, and the diffusivity (or porosity) of the particles is not known. Moreover, in contrast to the model, the solid organic particles contain other (heavy) metal ions which influence the course of the Cu(II) extraction. Therefore, the experiments and simulations are only compared qualitatively. The simulations give a good qualitative description of the experimental Cu(II) extraction from the organic particles in biowaste (compare Figures 8.4 and 8.5). Initially, the Cu(II) concentration in solution decreases. The model indicates that this decrease can be caused by adsorption of Cu(II) to the solid organic particles or by the inwardly directed electrochemical gradient. After the Cu(II) concentration reaches a minimum, Cu(II) diffuses out of the organic particles until equilibrium is reached. Due to the complexity of the organic particles, no correlation was found between the particle size of the organic particles and the course of the extraction.

#### **8.5.2. Heavy metal extraction from sewage sludge**

The extraction of Cd(II), Cu(II) and Zn(II) from sewage sludge at various pH values as found in the literature were discussed in Chapter 2 (see subchapter 2.2 and Figure 2.2). Closer examination of these results revealed some strange phenomena, such as a lag phase at the initial stage of the extraction and sudden changes in extraction rates during the course of extraction. These phenomena were more pronounced for stronger-binding heavy metals and at higher pH values. These phenomena can qualitatively be explained by the model (see Figure 8.4).

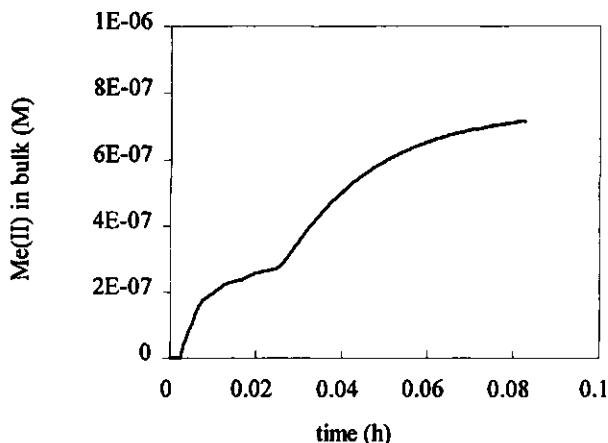


**Figure 8.6** Simulation of the heavy metal extraction from sewage sludge

Figure 8.6 shows the results of one of the model simulation of Figure 8.4 ( $\text{pH}=1$  and  $K_{\text{MeL}^+}=10^4$  M) on linear concentration and time scale. The lag phase and the changes in extraction rate are well described by the model. The extent of the lag phase, the changes in the rate of extraction and the total extraction time depend on the various parameters discussed in subchapter 8.2.4.2 (Figure 8.4). According to the model, the course of heavy metal extraction from sewage sludge can be explained as follows:

- the lag phase is due to the initial adsorption of metal ions by reactive sites on the solid particles or to the inwardly directed electrochemical gradient
- due to the higher affinity of Cu(II) for the reactive sites of sewage sludge biomass (most probably carboxyl sites) compared to Cd(II) and Zn(II) the following differences are observed: (i) Cd(II) and Zn(II) are extracted faster and (ii) the lag phase is shorter for Cd(II) and Zn(II)
- lower pH values result in higher extraction efficiencies and higher extraction rates, as discussed in subchapter 8.2.2
- the sudden changes in metal extraction rates can be explained by the course of the electrical potential gradient
- higher solids concentration will lead to a longer lag phase because the specific surface area is higher.

The observed extraction times for sewage sludge compared to the model results indicate that the diffusivity in the sludge flocs is heavily restricted.

## 8.6. Conclusions

A mechanistic model is presented to describe the extraction of heavy metals from solid organic particles at a low pH. The model uses the Nernst-Planck equations to describe the mass transport processes for charged ions in the film layer and inside the particles. The chemical reactions in bulk, film layer and particle are described by the chemical equilibrium concept which can be computed for multicomponent systems by EQUILIB. A Donnan term is included to account for the discontinuity in cation and anion concentrations at the solid-liquid interface caused by negative charge of the organic particles.

The model shows that heavy metals are not necessarily directly extracted from the solid particles but can be adsorbed to the solid particles during the initial stage of the extraction. As the pH front becomes established in the particles, the exchanged metal ions are not transported to the bulk solution but are pushed back into the particles where the metal ions occupy reactive sites. The direction of transport of the metal ions is determined by the electrochemical gradient. The electrochemical gradient, as described by the Nernst-Planck equations, is composed of a concentration gradient and an electrical potential gradient. The latter is determined by the diffusion of all involved charged ions. When the pH front is established over the entire particles, and the potential gradient is levelled out, metal ions are transported from the particles to the bulk solution according to their concentration gradient.

The model shows the effect of the particle properties (size, type and density of reactive sites, restriction factor), the extraction conditions (pH, ionic strength, film layer thickness, solids concentration) and the type of metal ion on the course of the extraction and the extraction efficiency.

Close monitoring of the Cu(II) extraction from particle-sized organic particles of biowaste at pH 1 by Cu(II)-ISE and GF-AAS showed the same phenomena. During the initial stage of the extraction, Cu(II) is withdrawn from the bulk solution. After a certain period of time, the direction of Cu(II) transport is inverted, after which Cu(II) is extracted from the solid particles to the bulk solution. The model can qualitatively describe the Cu(II) extraction from solid organic particles isolated from biowaste. Quantitative information cannot be extracted from these experiments because both the properties of the organic particles and the extraction conditions in a batch reactor are ill defined.

Also anomalies observed for the extraction of Cd(II), Cu(II) and Zn(II) from sewage sludges can be explained by the model. The lag phase in the extraction of Cu(II), sudden changes in extraction rates and the effects of pH, type of heavy metal, and the solids concentration are explained by the model.

The model is developed for a relatively simple system but is applicable for more complex multicomponent systems. It can also be applied to describe adsorption and desorption to

ion-exchange materials, and to describe the transport of ions through charged membranes, i.e. all processes involving chemical reactions and mass transport. The model can also be applied to model biofilm processes for which biological reactions terms have to be incorporated in the mass balance equation.

The model has to be validated by well-defined compounds and under well-defined extraction conditions. Appropriate model compounds are various types of ion-exchange materials, such as Sephadex (carboxylic group), Chelex 100 (iminodiacetate group) or IRC 50 (sulphonic group). To establish well-defined hydrodynamic conditions around the particles the experiments have to be performed in e.g. a shallow-bed reactor.

## References

- Aguilella, V. M.; Mafe, S.; and Pellicer, J. 1987. On the Nature of the Diffusion Potential Derived from Nernst-Planck Flux Equations by Using the Electroneutrality Assumption. *Electrochimica Acta* 32 483-488
- Ammann, D. 1986. *Ion-Selective Microelectrodes, Principles, Design and Application*. Berlin:Springer-Verlag
- Behel, D.; Nelson, J., Darrell, W.; and Sommers, L. E. 1983. Assessment of Heavy Metal Equilibria in Sewage Sludge Treated Soil. *J. Environ. Qual.* 12:181-186
- Buffle, J. 1988. *Complexation Reactions in Aquatic Systems: An Analytical Approach*. Chichester, Ellis Horwood Limited
- Bunzl, K.; and Schimmack, W. 1991. Kinetics of Ion Sorption on Humic Substances, In: *Rates of Soil Chemical Processes, Soil American Society of America, Special publication 27*, Sparks, D. L.; and Suarez D. L. (eds.):119-134
- Burgstaller, W.; and Schinner, F. 1993. Leaching of metals with fungi, Minireview. *J. Biotechnol.* 27:91-116
- Fletcher, P.; and Beckett, P. H. T. 1987. The Chemistry of Heavy Metals in Digested Sewage Sludge - I. Copper(II) Complexation with Soluble Organic Matter. *Wat. Res.* 21:1153-1161
- Fristoe, B. R.; and Nelson, P. O. 1983. Equilibrium Chemical Modelling of Heavy Metals in Activated Sludge. *Water Res.* 17:771-778
- Graham, E. E.; and Dranoff, J. S. 1982. Application of the Stefan-Maxwell Equations to Diffusion in Ion Exchangers. 1. Theory. *Ind. Eng. Chem. Fundam.* 21:360-365
- Helfferich, F. G. 1962a. *Ion Exchange*, New York: McGraw-Hill Book Company Inc.
- Helfferich, F. G. 1962b. Ion-Exchange Kinetics, III. Experimental Tests of the Theory of Particle-Diffusion Controlled Ion Exchange. *J. Phys. Chem.* 66:39
- Helfferich, F. G. 1983. Ion Exchange Kinetics: Evolution of a Theory. In: *Mass Transfer and Kinetics of Ion Exchange*, Liberti, L. and Helfferich, F. G. (eds.). NATO ASI Series, Series E: Applied Sciences no. 71. The Hague: Nijhoff
- Hu, X.; Do, D. D.; and Yu, Q. 1992. Effects of Supporting and Buffer Electrolytes on the Diffusion of BSA in Porous Media. *Chem. Eng. Sci.* 47:151-164
- Hwang, Y.; and Helfferich, F.G. 1987. Generalized Model for Multispecies Ion-Exchange Kinetics Including Fast Reversible Reactions. *Reactive Polymers* 5:237-253
- Kadlec, R. H.; Keoleian, G. A. 1986, Metal Ion Exchange on Peat. In: *Peat and water. Aspects of Water Retention and Dewatering in Peat*, Fuchsman, C. H. (ed.). Essex, UK:Elsevier Applied Science Publishers Ltd.
- Kraaijeveld, G.; and Wesselingh, J. A. 1993. The Kinetics of Film-Diffusion-Limited Ion Exchange. *Chem. Eng. Sci.* 8:467-473
- Levenspiel, O. 1972. *Chemical Reaction Engineering*. New York:John Wiley & Sons
- MacGillivray, A. D. 1968. Nernst-Planck Equations and the Electroneutrality and Donnan Equilibrium Assumptions. *J. Chem. Physics* 48:2903-2907
- Mafe, S.; Aguilera, V. M.; and Pellicer, J. 1988. Film Control and Membrane Control in Charged Membranes. *J. Membrane Science* 36:497-509

- Marinsky, J. A.; Gupta, S.; and Schindler, P. 1982. A Unified Physiochemical Description of the Equilibria Encountered in Humic Acid Gels. *J. Colloid Interface Sci.* 89:412-426
- Newman, J. 1973. *Electrochemical Systems*. Englewood Cliffs, N.J.:Prentice-Hall, Inc.
- Pankow, J. F.; and Morgan, J. J. 1981. Kinetics for the aquatic environment. *Environ. Science & Technol.* 15:1155-1164, 1306 - 1313
- Peppas, N. A.; and Reinhart, C. T. 1983. Solute Diffusion in Swollen Membranes. Part I. A New Theory. *J. Memb. Sci.* 15:275-287
- Petruzelli, D.; and Helfferich F.G. (eds.) 1989. *Migration and Fate of Pollutants in Soils and Subsoils*, NATO ASI Series. Berlin:Springer-Verlag
- Smith, L.A., Means, J.L., and Chen, A. 1995. *Remedial Options for metals-contaminated sites*. Lewis, Boca Raton Sparks, D.L. 1986. *Soil Physical Chemistry* Boca Raton: CRC Press Inc.
- Sparks, D. L.; 1989. *Kinetics of Soil Chemical Processes*. San Diego: Academic Press, Inc.
- Sparks, D. L.; and Suarez D. L. (eds.) 1991. *Rates of Soil Chemical Processes*, Soil American Society of America, Special publication 27
- Theuvenet, A.; and Borst-Pauwels, G. 1976. The Influence of Surface Charge on the Kinetics of Ion-Translocation Across Biological Membranes. *J. Theor. Biol.* 57:313-329
- Trujillo, E.; Jeffers, T. H.; Ferguson, C.; Stevenson, H. Q. 1991. Mathematically Modeling the Removal of Heavy Metals from a Wastewater Using Immobilized Biomass. *Environ. Sci. Technol.* 25:1559-65
- Tsezos, M.; Noh, S. H.; and Baird, M. H. I. 1988. A Batch Reactor Mass Transfer Kinetic Model for Immobilized Biomass Biosorption. *Biotechnol. Bioeng.* 32:545-553
- Tsezos, M.; and Deutschmann, A. A. 1992. The Use of a Mathematical Model for the Study of the Important Parameters in Immobilized Biomass Biosorption. *J. Chem. Tech. Biotechnol.* 53:1-12
- Tyagi, R. D.; Couillard D.; and Tran, F. 1988. Heavy Metals Removal from Anaerobically Digested Sludge by Chemical and Microbiological Methods. *Environ. Poll.* 50:295-316
- Tyree, M. T.; Tabor, C. A.; Wescott, C. R. 1990. Movement of Cations Through Cuticles of *Citrus Aurantium* and *Acer Saccharum*: Diffusion Potentials in Mixed Salt Solutions. *Plant Physiol.* 94:120-126
- Wesselingh J.A.; and Krishna R. 1990. *Mass Transfer*. Chichester, Ellis Horwood Limited
- Wong, L. T. K.; and Henry, J. G. 1988. Bacterial Leaching of Heavy Metals from Anaerobically Digested Sludge. In: *Biotreatment Systems*, Vol. III, Wise, D. L. (ed.), Boca Raton, CRC Press, Inc.

## 9. Pilot plant study for the valorisation of biowaste

### 9.1. Introduction

**B**iwaste-derived compost can be applied as soil improver or organic fertiliser if the compost meets the quality standards for composts derived from organic matter. In the first place, the heavy metal content of the compost has to meet the legal criteria as laid down in the law concerning the quality and use of other organic fertilisers, the BOOM decree (SDU, 1991). Two types of composts are defined in the BOOM decree: compost and clean compost (see Table 1.2). The dosage of compost is fixed at a maximum amount, while the dosage of clean compost is only limited as regards the maximum phosphate dosage (see Table 1.3). As discussed in Chapter 1, heavy metals in biowaste-derived compost are critical for some heavy metals with respect to legal standards for compost and the standards for clean compost cannot be met for most heavy metals (see Table 1.4).

As described in Chapter 2, there are two technological approaches to reduce the heavy metal content of solid wastes: (1) physical wet-separation of the contaminated fractions from the solid waste and (2) solid-to-liquid extraction of the heavy metals from the solid waste. Based upon the results of Chapters 4 and 5 a new process for the valorisation of biowaste is proposed. The main goal of the process is the production of compost which complies with the BOOM decree for compost, or possibly with the standards for clean compost.

As discussed in Chapter 4, the composition of biowaste varies widely, depending on the time and place of collection. Therefore, large variations in biowaste composition can lead to large fluctuations in the quality of the compost; this concerns, among other things, heavy metal content and maturity of the compost. Moreover, the organic matter content of biowaste-derived compost is low, generally ranging from 25 to 35% (see Table 1.4). The low organic matter content is largely due to the presence of soil components in outdoor-collected biowaste. Due to the low organic matter content and fluctuations in maturity of biowaste-derived compost, the marketing of biowaste-derived compost can encounter serious problems. Therefore, the second goal of the new valorisation process is the production of biowaste-derived compost which has a constant, high quality independent of the quality and composition of the incoming biowaste. In this way, the sales of compost will be facilitated and compost can become competitive with other soil improvers and fertilisers, such as animal manure and peat.



The major criteria for the selection of a new valorisation process for biowaste are:

- extraction or separation efficiency: the compost has to meet the legal demands for heavy metals as laid down in BOOM
- prevention or minimisation of the amount of residual and environmentally-hazardous waste streams, i.e. residual solid waste, air emissions and wastewater
- costs of the process: costs of the process are set to an upper limit because the process has to compete with other treatment processes, such as incineration and gasification
- the heavy metal removal process should not have negative effects on subsequent biological treatment processes, e.g. composting/digestion of the biowaste, aerobic/anaerobic wastewater treatment. Microorganisms are very sensitive to a deficiency in nutrients and the toxicity of heavy metals.

Physico-chemical fractionation of heavy metals (Cd, Cu, Pb and Zn) in biowaste showed that heavy metals accumulate in the organic fractions <1 mm and the organo-mineral fraction <0.05 mm (see Chapter 5). Physical separation on a lab-scale indicate that separation of the physical entities of biowaste is possible when the processes take place under wet conditions. Sequential chemical extraction of integral biowaste showed that Cd, Cu, Pb and Zn are extractable for 90, 35, 80 and 75%, respectively, with a strong complexing agent or at low pH. It was also found that heavy metals are more strongly bound to the organic fraction <1 mm and the organo-mineral fraction <0.05 mm. Both physical wet-separation and chemical extraction can reduce the heavy metal content of biowaste-derived compost to below the standards for compost.

A comparison has to be made between physical wet-separation and chemical extraction in order to choose the best option for the removal of heavy metals. The main advantages of the physical wet-separation process are:

- relatively simple processes
- no chemical modification of the process streams
- no hazardous waste streams are produced.

The major disadvantages of the process are:

- leaching of readily-degradable organic matter and salts from the biowaste, which will end up in the wastewater stream
- production of a relatively large, residual solid waste stream.

The main advantage of chemical extraction is the fact that the residual solid organic waste stream is limited. Moreover, all incoming biowaste is treated and suitable for the production of compost. The major disadvantages of the extraction process are:

- the total process is complex and the costs of the process are relatively high
- production of hazardous waste streams such as excess extraction liquid, heavy metal sludge and wastewater with high salt loadings

- chemical modification of the process streams (e.g. EDTA, inorganic acids) will most probably have negative effects on subsequent biological treatment processes.

On the basis of these considerations, the following valorisation scheme for biowaste is proposed:

1. physical separation of biowaste in three fractions:
  - organic fraction >1 mm
  - sand fraction
  - residual fraction, composed of the organic particles <1 mm and the organo-mineral fraction <0.05 mm
2. the organic fraction >1 mm can directly be composted and will reach the BOOM standard for compost
3. the sand fraction is very low in heavy metals and can directly be reused in the construction of roads and buildings
4. the residual fraction can be landfilled, or the heavy metals can be extracted from the residual fraction in order to reach the BOOM standards for compost.

## **9.2. Process scheme for valorisation of biowaste**

A process was designed and tested on pilot-plant scale to produce the following streams: (1) an organic fraction >1-2 mm suitable for composting, (2) a sand fraction, and (3) a residual fraction.

### **9.2.1. Introduction**

Physical separation of biowaste without the addition of water is impossible because the physical entities of the waste are stuck together. Therefore, physical separation on a large-scale is possible only when the processes are performed under wet conditions. The water should be recycled in order to reduce consumption and the costs of wastewater treatment. A valorisation process was designed, which produces three streams:

1. **fraction for composting:** organic particles larger than 1-2 mm can be composted to produce a compost or a clean compost; the ultimate goal is the production of a compost which can replace peat compost; substitution of peat compost means that peat soils do not need to be excavated and the biowaste-derived compost can be sold for a significantly higher price
2. **sand fraction:** sand with a low organic matter content (<1 %) and a very low heavy metal content can be reused in road and building construction
3. **residual fraction:** the heavy metal content of this fraction is too high; for now it has been decided to treat this waste stream anaerobically and to landfill the residue; an

additional advantage of the anaerobic process is the production of energy in the form of biogas.

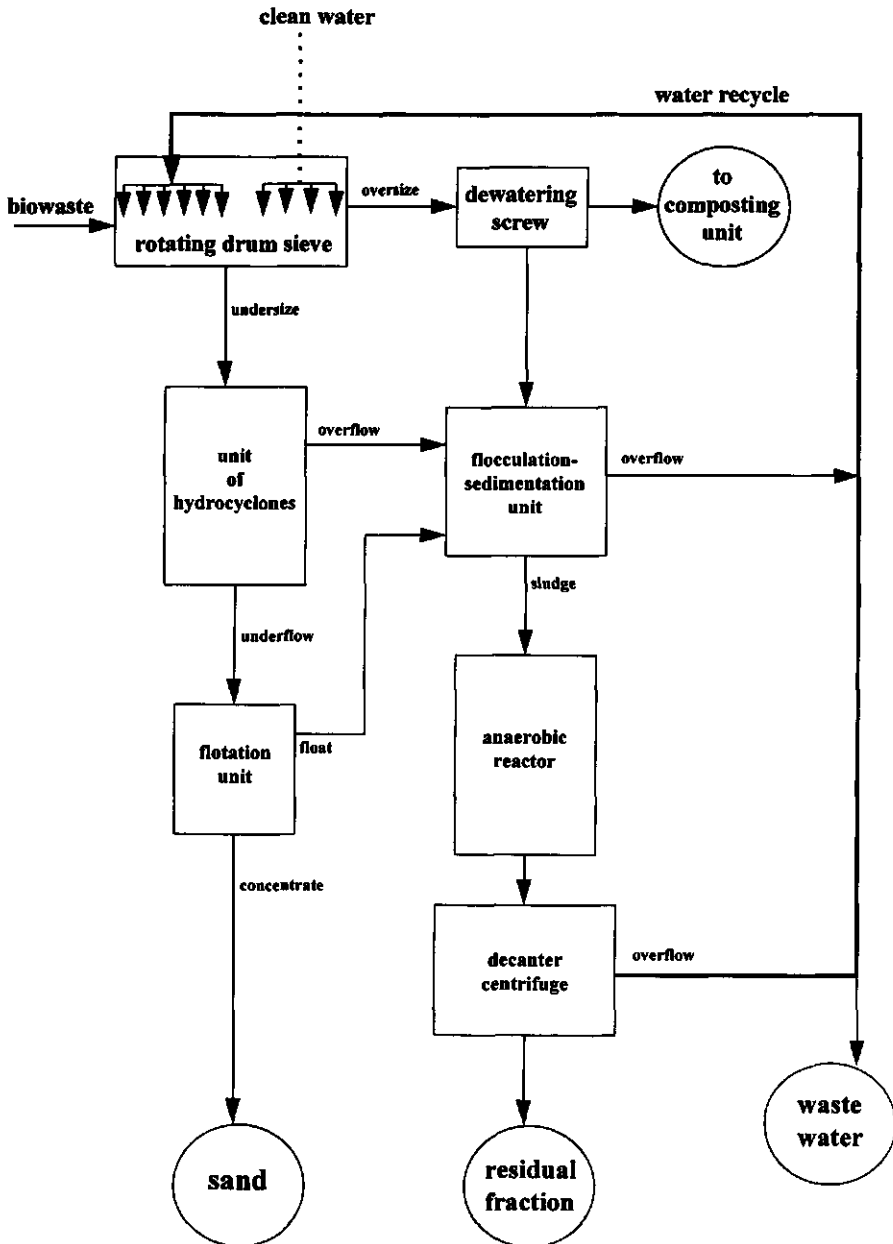


Figure 9.1 Flow chart of the VECOTECH<sup>®</sup> process for valorisation of biowaste

A valorisation process was designed to achieve these goals. The process is built up of several physical wet-separation steps, together with an anaerobic reactor to reduce the residual fraction and degrade the soluble organic matter. Figure 9.1 shows a schematic presentation of the valorisation process.

The biowaste enters a rotating drum screen with holes of 1-2 mm in diameter in order to separate the larger-sized organic material from the rest of the biowaste. In the first part of the screen, the waste is thoroughly sprinkled with recycling water. Large amounts of soluble organic matter and salts will accumulate in the recycling water which could end up in the oversize of the drum screen. Therefore, a sprinkling step with clean water is performed at the end of the drum screen to reduce the salt content of the oversize stream. The oversize of the drum screen is dewatered in a dewatering screw before entering the composting plant. The undersize of the drum screen is passed through a set of hydrocyclones in order to separate the sand fraction from the organic fraction. Large-sized organic particles ending up in the undersize of the hydrocyclone are separated from the sand by a flotation device.

The streams from the dewatering screw, the overflow from the hydrocyclone and the floating layer from the flotation cell are thickened in a sedimentation tank. The sludge of the sedimentation tank is anaerobically digested in a one-phase slurry digester and the effluent of the reactor is dewatered by a decanter centrifuge.

A large part of the water from the sedimentation tank and decanter centrifuge is recycled to the drum screen. A small part of the water has to be discharged because there is a net production of water for the total valorisation process. The wastewater can be treated anaerobically to remove the organic matter.

### 9.2.2. Pilot plant study and objectives

The valorisation process was tested on pilot-plant scale. The following topics were studied:

1. performance of the physical separation units
2. aerobic composting of the oversize of the rotating drum screen
3. anaerobic digestion of the residual fraction.

The following solid-solid and solid-liquid units were tested on pilot-plant scale:

- rotating drum screen
- hydrocyclone
- flotation
- flocculation-sedimentation unit
- decanting centrifuge.

The performance of the units was quantified by mass balances of dry matter, organic matter and heavy metals.

Soluble organic matter and soluble salts are washed from the biowaste in the rotating drum screen. Especially the washout of soluble organic matter (e.g. fats, carbohydrates, hemicellulose) and the increased water content of the oversize of the drum screen will effect the composting process. The aerobic composting of the oversize of the rotating drum screen was studied on a pilot-plant scale.

The organic fraction <1-2 mm is flocculated and thickened in a sedimentation unit. The sludge is anaerobically digested in a one-phase slurry reactor. The performance of the one-phase slurry digestion is studied on bench scale in a 100-l reactor. The biodegradability of the organic matter of the various solid and liquid fractions is studied in 5-l batch reactors.

### **9.3. Materials and methods**

The separation units were tested at VAM Wijster or contracted out to specialised companies. Composting on pilot-plant scale was carried out at VAM Wijster and analysis took place at Wageningen. Bench-scale digestion and digestion test in 5-l reactors were performed at Wageningen. Characterisation of the various solid and liquid streams was carried out at Wageningen Agricultural University.

#### **9.3.1. Physical separation units**

The performance of the rotating drum screen to separate the organic fraction >1-2 mm from biowaste was tested by a rotating drum screen in series with screen bends of 2 and 0.25 mm. The rotating drum screen was 3.4 m in length and 1.2 m in diameter, and the separation was achieved by battens mounted 5-7 cm apart. The drum screen was equipped with six sprinklers and rotated at 12 rpm. The first three sprinklers used recycled water and the last sprinklers groundwater. The undersize of the drum screen was led over the 2 mm screen bend and the undersize of this screen bend was led over a 0.25 mm screen bend. The undersize of the 0.25 mm screen was used as recycling water in the first step of the rotating drum screen.

The hydrocyclone unit (cut size of 63 mm), dispersed air flotation (with surface active agents to increase particle hydrophobicity) and flocculation-sedimentation units were tested on site by contractors. The performance of the decanter centrifuge was tested at laboratories of specialised companies.

### 9.3.2. Composting

Composting on pilot-plant scale was performed by the aerated static pile method (Haug, 1993). The piles were set up over an aeration pipe under a covering. The piles were 5 m wide and 2.5 m high and contained approx. 20 m<sup>3</sup> of the oversize from the rotating drum screen. The composting process was based on the Rutgers strategy (Finstein et al., 1983; Robinson and Stentiford, 1993), air was blown into the pile and the aeration rate was controlled in conjunction with a temperature feedback control system (set-point temperature of 55 °C). The feedback system was controlled by the average of 6 thermocouple readings, equally distanced on both sites of the pile. The piles were turned over and remixed once a week. After 6-7 weeks the material was sieved through a drum screen with a cut size of 15 mm.

### 9.3.3. Digestion

Batch digestion experiments were carried out in 5-l batch reactors at 30 °C. The reactors were filled with mixtures of the biowaste fractions and inoculum at a total solids concentration of 50-100 g.l<sup>-1</sup>. The substrate-inoculum ratio varied from 1.8-2.3 on the basis of organic matter. Digested biowaste (SMB, Tilburg) was used as inoculum and substrates were taken from the pilot plant separation units. During the experiment pH and volatile fatty acids (VFA) of the solution, biogas production and biogas composition (CH<sub>4</sub>, CO<sub>2</sub> and H<sub>2</sub>) were determined periodically, as described by Ten Brummeler (1993). At the initial stage of the digestion tests, pH was maintained at 7 by the addition of NaOH to prevent inhibition of the methanogenic activity by undissociated VFA.

The one-phase digestion was performed for a total solids concentration of 60-80 g.l<sup>-1</sup> at 30 °C in a 96.5-l cylindrical reactor (1.45 m in height and 0.29 m in diameter) continuously stirred at 20 rpm. The effective reactor volume was 87.5 l, and a head space of 0.13 m was reserved to prevent clogging of the gas collection system. The reactor was started up with 10% digested pig manure (Promest, Helmond) as inoculum. The reactor was fed with the undersize of the 2 mm screen bend from which sand was first removed by sedimentation. After a start-up period of 30 days, the reactor was semi-continuously fed every 1 or 2 days. The total suspended solids, total volatile solids, total nitrogen and total COD of influent and effluent were analysed according to Standard Methods (APHA, 1992). Ammonia nitrogen and VFA were analysed as described by Ten Brummeler (1993). Biogas was lead through a 5 M NaOH solution and the outcoming methane was registered continuously by a digitised wet gas meter coupled to a data taker.

## 9.4. Results

### 9.4.1. Physical separation units

Table 9.1 presents the average mass distribution of the fractions over the rotating drum screen, 2 mm screen bend and 0.2 mm screen bend, together with the organic matter content and the content of Cu, Pb and Zn.

**Table 9.1 Performance of the rotating drum screen and two screen bends (4 measurements)**

Fraction	Contribution (% of DM)	OM content (% of DM)	Heavy metal content (mg.kg <sup>-1</sup> DM)		
			Cu	Pb	Zn
total	-	32 - 58	8 - 15	22 - 44	46 - 80
>5 mm	30 - 45	80 - 89	6 - 10	6 - 29	27 - 128
2-5 mm	5 - 10	70 - 80	11 - 15	29 - 94	80 - 147
0.2-2 mm	30 - 40	15 - 25	7	32 - 39	38 - 44
<0.2 mm	15 - 25	57 - 75	35-40	39 - 106	130 - 193

Table 9.2 gives the performance of the hydrocyclone and flotation cell with respect to the OM content and levels of some heavy metals. No detailed mass balances were available for these experiments; approx. 58% of the mass ends up in the sand fraction and 42% in the overflow.

**Table 9.2 Performance of the hydrocyclone and flotation unit (7 measurements)**

Stream	OM (% of DM)	Heavy metal content (mg.kg <sup>-1</sup> DM)					
		Cd	Cr	Cu	Ni	Pb	Zn
<u>hydrocyclone:</u>							
feed	26 - 40	0.19 - 0.29	12 - 15	16 - 31	5 - 9	51 - 69	101 - 169
overflow	56 - 71	0.27 - 0.54	13 - 22	35 - 48	6 - 11	84 - 115	175 - 267
underflow	5 - 7	0.07 - 0.17	4 - 5	2 - 4	<5	17 - 28	22 - 35
<u>flotation cell:</u>							
float	30 - 51	0.21 - 0.35	19 - 28	22 - 95	8 - 20	125 - 250	155 - 290
sand	0.3 - 0.6	0.05 - 0.09	2 - 4	<0.1 - 2	<5	<15 - 22	11 - 18

Lab-scale tests demonstrated that a cationic polyelectrolyte dosed at 1:1000 on DM basis gave the best settling rate and sludge volume index (results not shown here). The results of sedimentation tests on lab-scale and pilot-plant scale are given in Table 9.3. No complete mass balances were available for these experiments.

The suppliers of the decanter centrifuge tested the thickening of the effluent of the pilot plant digester on a lab-scale. Dewatering of sludge to 30-40% DM was possible and the overflow contained 0.5% DM (no results given here). No characteristics of dewatered sludge and overflow after centrifugation were available.

**Table 9.3 Performance of sedimentation units for the residual fraction**

Flow	DM	OM	heavy metal concentration in slurry (mg.l <sup>-1</sup> )					
			Cd	Cr	Cu	Ni	Pb	Zn
<b>lab-scale:</b>								
feed	0.5 - 1.6	50 - 60	6.4	875	1100	750	1600	900
sludge	7 - 10	40 - 55	-	-	-	-	-	-
overflow	0.2 - 0.4	70	2	200	300	150	100	250
<b>pilot-plant scale:</b>								
feed	2 - 3	49	24	750	260	90	240	2600
sludge	8 - 12	37	48	1280	400	240	350	10400
overflow	0.5 - 0.7	60	8	180	205	30	60	1100

#### 9.4.2. Composting

Composting on a pilot-plant scale was carried out for static piles of 15 to 30 m<sup>3</sup> without application of air recirculation. In practice, control of the composting process based on the the Rutgers strategy was very difficult to accomplish for these piles. The control of composting was very sensitive to cooling down, configuration of the piles and placing of the thermocouples. A compilation of the results is given in Table 9.4.

**Table 9.4 Results of composting on pilot-plant scale (5 experiments)**

Parameter	Starting material	Compost
DM content (%)	22 - 24 (23) <sup>1</sup>	31 - 50 (40)
OM content (% of DM)	70 - 86 (79)	58 - 72 (66)
pH <sup>2</sup>	5.0 - 6.5 (5.5)	7.9
OM degradation (%)	23 - 55 (40)	
composting time (d)	43 - 59 (45)	
temperature (°C)	47 - 53 (51)	
screen yield <15 mm (%)	47 - 61 (59)	

<sup>1</sup> average between brackets; <sup>2</sup> pH of material determined after shaking with demiwater at a liquid-solid ratio of 5 for 20 minutes



### 9.4.3. Digestion

#### Batch experiments

Batch digestion experiments were performed for various fractions obtained from the pilot plant separation units. Figure 9.2 shows a typical result of the methane production and VFA in solution. The gas production was recalculated to standard temperature and pressure (NI: 0 °C, 1 bar).

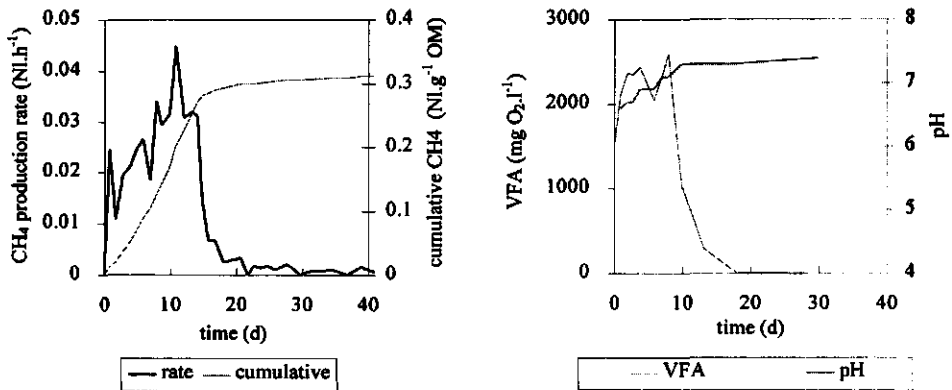


**Figure 9.2** Methane production and VFA concentration in solution for a typical batch digestion experiment

The course of methane production, VFA and pH are typical for a batch digestion. The anaerobic degradation of complex organic substrates to carbon dioxide and methane is the result of the activity of several groups of anaerobic consortia (Gujer and Zehnder, 1980). For the anaerobic degradation of particulate and colloidal organic matter, four subsequent steps can be distinguished: (1) hydrolysis, (2) acidogenesis, (3) acetogenesis and (4) methanogenesis. When the methanogenic activity is high enough, hydrolysis of complex organic matter is the rate-limiting step (Parkin and Owen, 1986). Hydrolysis can generally be described by first-order hydrolysis kinetics (Pavlostathis and Giraldo-Gomez, 1991). The cumulative production of VFA and methane can then be expressed by:

$$CUM(t) = CUM_0 + (CUM_{max} - CUM_0) \cdot (1 - \exp(-k_h \cdot t)) \quad (9.1)$$

where  $CUM(t)$  is the cumulative production of VFA and methane at time  $t$  (in g O<sub>2</sub>),  $CUM_0$  CUM at time is zero (in g O<sub>2</sub>),  $CUM_{max}$  the maximum CUM production (in g O<sub>2</sub>),  $k_h$  the first-order hydrolysis rate (in d<sup>-1</sup>) and  $t$  time (in d). Figure 9.3 shows the course of production of VFA and  $CUM(t)$  for the experiment of Figure 9.2.  $CUM(t)$  is fitted to equation 9.1 by non-linear least squares fitting (Doucet and Sloep, 1992) and yield the

first-order hydrolyse rate constant  $k_h$  and the maximal methane yield  $CUM_{max}$ . Table 9.5 shows the results for the studied fractions.

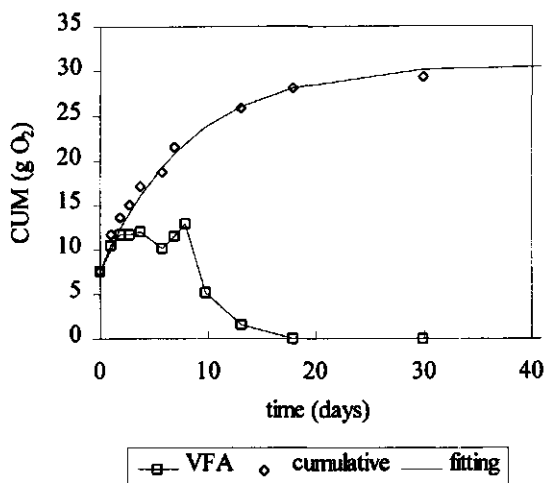


**Figure 9.3** Cumulative production of VFA and methane and first-order hydrolysis rate fitting

Addition of flocculation agents (to improve the sludge settlement) and surface active agents (used for flotation) did not have negative effects on the digestion process (results not shown here).

**Table 9.5** Fitted maximum methane yield and first-order hydrolysis rate constant for various fractions of the residual fraction of biowaste

Fraction	No of expt	DM (%)	OM (% DM)	Maximum methane yield (NI.g <sup>-1</sup> OM)	$k_h$ (d <sup>-1</sup> )
liquid	1	0.5	74	0.63	0.12
solids 0.2-2 mm	3	5.8	43	0.37	0.11
sludge <2 mm <sup>1</sup>	2	6.7	53	0.34	0.08

<sup>1</sup>undersize of 2 mm screen bend from which sand is removed by a fast sedimentation step

#### 9.4.3.1. Semi-continuous experiments

At the end of the start-up period the reactor was semi-continuously, non-periodically fed for 12 days (0 to 300 h) at an organic loading rate of 0.07 g OM.l<sup>-1</sup>.h<sup>-1</sup>. In this period VFA dropped to 100 mg O<sub>2</sub>.l<sup>-1</sup> and the CH<sub>4</sub> content of the biogas was 60-70%. Between 300 and 700 hours the reactor was fed semi-continuously and periodically at a hydraulic retention time of 21 days. From 700 to 1200 h at a HRT of 15 days and after 1200 h the

HRT was decreased to 8 days. Figure 9.4 shows the influent and effluent VFA composition and the methane production ( $\text{NI}\cdot\text{h}^{-1}$ ) for this period.

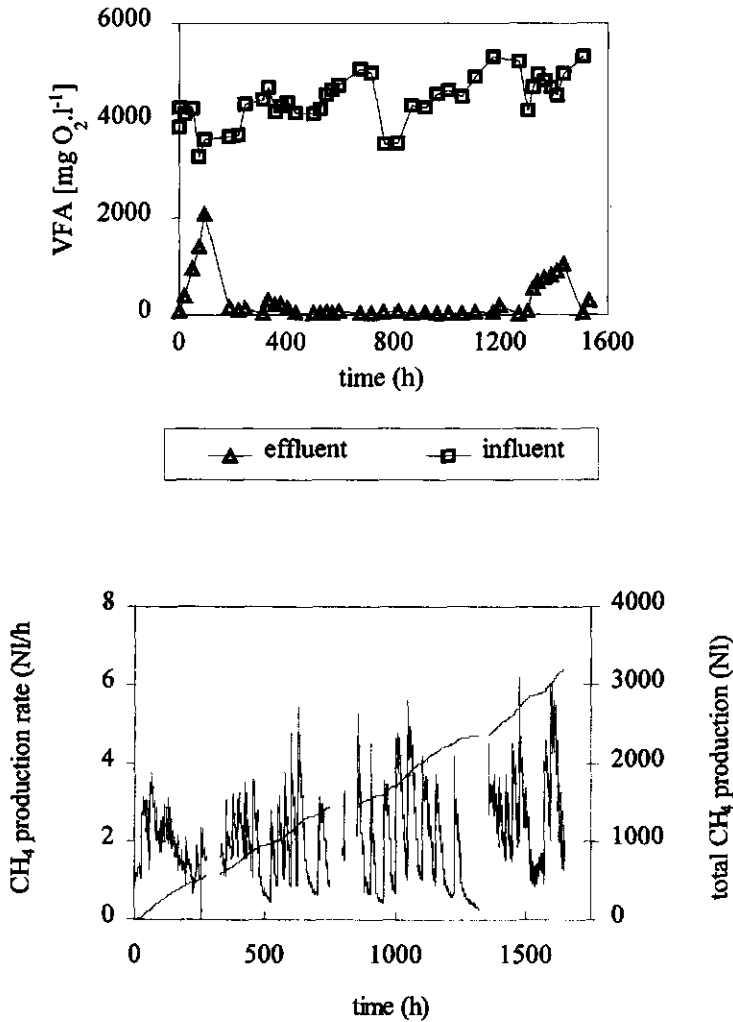


**Figure 9.4** Performance of the semi-continuous slurry digester: influent and effluent concentration of VFA (top) and gas production (bottom)

At a HRT of 21 and 15 days, VFA in the reactor remains low ( $<100 \text{ mg O}_2\cdot\text{l}^{-1}$ ) and pH is constant at 7.3-7.5. When the HRT of the reactor is decreased to 8 days, VFA in the effluent increases from 20 to  $1000 \text{ mg O}_2\cdot\text{l}^{-1}$  in 5 days and pH decreases to 6.8. In Table 9.6 the average characteristics of the influent and effluent and the average reactor performance are presented.

**Table 9.6** Influent and effluent characteristics and performance of the semi-continuous slurry reactor at variable hydraulic retention time

parameter	21 days		15 days		8 days	
	influent	effluent	influent	effluent	influent	effluent
VS concentration (g.l <sup>-1</sup> )	33	17	37	23	29	21
total COD (g O <sub>2</sub> .l <sup>-1</sup> )	39.8	27.9	42.5	36.9	41.3	36.7
COD soluble <sup>1</sup> (g O <sub>2</sub> .l <sup>-1</sup> )	7.2	0.9	-	1.2	-	-
VFA (g O <sub>2</sub> .l <sup>-1</sup> )	4.40	0.04	4.42	0.05	4.86	0.52
total N (g.l <sup>-1</sup> )	1.2	1.5	1.0	1.8	1.1	1.7
total N soluble <sup>1</sup> (g.l <sup>-1</sup> )	0.28	0.64	0.33	0.51	0.26	0.39
pH	4.9	7.4	4.9	7.2	5.0	7.1
OLR <sup>2</sup> (g OM.l <sup>-1</sup> .h <sup>-1</sup> )	0.075		0.098		0.151	
CH <sub>4</sub> production (Nl.g <sup>-1</sup> OM)	0.48		0.27		0.18	
OM degradation (% of OM)	43		33		23	

<sup>1</sup> filtered through 0.45 µm membrane filter; <sup>2</sup> organic loading rate

## 9.5. Discussion

### 9.5.1. Physical separation units

The fractionation of biowaste into the three major fractions by various physical separation steps can be achieved on pilot-plant scale by combining various physical separation units. The mass balances of dry matter and organic matter are in good agreement with the results of the lab-scale separation tests (compare Tables 4.1 and 9.1). The rotating drum screen and screen bend of 2 mm returned 35-55% of the biowaste to the fraction >2 mm and this fraction is very high in organic matter (80-85%). The hydrocyclone divided the fraction <2 mm into an organic overflow and inorganic underflow. The small percentage of organics in the underflow (5-7%) of the hydrocyclone was completely removed in the flotation cell. The overflow of the hydrocyclone and float of the flotation cell can be thickened in a settling tank to a dry matter content of 10% by addition of a cationic polyelectrolyte. The overflow of the settling tank was clear with a dry matter content of 0.5%, composed of inorganic salts and solubilised organic matter. After digestion of the sludge, a decanter centrifuge thickened the sludge to a dry matter content of 30-40%, thereby producing a clear overflow.

The Cu content of the fraction >5 mm is constant but the results show a broad distribution for Pb and Zn (Table 9.1). The low values correspond well with the contents found for indoor waste on lab-scale and the upper values with the contents found for integral waste (Table 4.3). The average values for Cu, Pb and Zn in the fraction >5 mm are substantially lower than values found for lab-scale experiments of integral waste (see Table 4.3). This is due to the more complete physical separation of the physical entities of biowaste on pilot-plant scale compared to the lab-scale sieving devices. As seen with the lab-scale experiments (Table 4.2), also the pilot-plant scale tests show that the heavy metals are concentrated in the small organic fractions (overflow of the hydrocyclone and float of the flotation cell, Table 9.2). The heavy metal content of these streams is of the same order as found for the smaller particle-sized organic fractions and organo-mineral fraction <50 mm after sieving and elutriation on lab-scale. The heavy metal content of sand (Table 9.2) is very low and is in good agreement with values measured on a lab-scale (Table 4.2). Table 9.7 shows the average organic matter and heavy metal content of the three major streams of the VECOTECH process, fraction >2 mm, sand fraction and residual fraction together with the values for integral biowaste.

**Table 9.7 Characterisation of streams from the VECOTECH process**

Parameter	Integral biowaste <sup>1</sup>	Fraction >2 mm	Residue	Sand
contribution (% of DM)	-	33-55	25 - 35	20 - 30
OM (% of DM)	45	80	59	0.5
Cd (mg.kg <sup>-1</sup> DM)	0.6	0.3	1.1	0.06
Cr	9	8	22	3
Cu	47	9	75	1
Ni	4	5	7	<5
Pb	70	26	110	15
Zn	110	95	370	13

<sup>1</sup> average OM and heavy metal content as determined by VAM at Wijster in 1992-1993

The heavy metals are accumulated in the residual fraction. The residual fraction, composed of the organic particles <1 mm and the organo-mineral fraction <0.05 mm, shows a strong affinity for heavy metals. This is due to the high humic acid content of these fractions (subchapter 3.9.2). The residual fraction acts as a heavy metal sink: heavy metals which are solubilised and washed out in the physical separation steps of the process are adsorbed to the organic and organo-mineral particles. In this way the heavy metal content of the recirculating water stream is kept low. Heavy metals adsorbed to the sand particles are washed out together with other impurities. The heavy metal content of sand is therefore lower than background levels found in sandy soils (see Table 4.4).

The heavy metal content found in the fraction >2 mm indicates that the heavy metal content of compost produced from that fraction is significantly lower than the heavy metal content of compost from integral biowaste. The compost can comply with legal demands for compost with respect to Cd, Cr, Cu, Ni, Pb and Zn. The compost from the fraction >2 mm can easily meet the BOOM standards for compost and could possibly meet the BOOM standards clean compost with respect to Cd, Cr, Cu, Ni and Pb. Only Zn is too high to meet the legal demands for clean compost. As discussed in Chapter 4, it will never be possible to produce clean compost from fresh plant material with respect to Zn without treatment.

### 9.5.2. Composting

Due to the washout of soluble and readily degradable organic matter in the rotating drum screen, biowaste has a relatively low oxygen uptake rate (OUR). The OUR is a measure of the microbial degradation of the organic matter and is directly related to the heat production of the composting process (Hamelers, 1990). Due to the low OUR of biowaste, the aerated static pile composting process was very difficult to control on a pilot-plant scale. Moreover, for small piles with high surface-volume ratios the heat loss at the surface is high. On the average 40% of the initial organic matter is degraded but the initial low DM content made it impossible to produce compost with a DM content of 60% or more.

### 9.5.3. Digestion

#### Batch experiments

Biowaste is made up of various types of organic substrates. According to Ten Brummeler, the organic fraction of biowaste comprises 54% cellulose and hemicellulose, 21% lignin, 15% proteins, 5% starch, 3% lipids and 7% cell solubles (Ten Brummeler, 1993). During the wet-sieving steps of the physical separation, part of the degradable organic matter of biowaste is washed out and ends up in the liquid phase. The solubilised organic matter is composed of lipids, proteins, carbohydrates, hemicellulose and other cell-soluble compounds. These substrates are readily accessible to enzymes and microorganisms and can easily be degraded.

Table 9.5 gives the maximum methane yield and first-order hydrolysis rate for various fractions of the separation process. The high methane yield of the liquid fraction indicates that the lipid and protein contribution to the soluble fraction is high. The first-order hydrolysis constant of  $0.12 \text{ d}^{-1}$  is in agreement with values found for lipids, proteins and hemicellulose at 30-35 °C (Pavlostathis and Giraldo-Gomez, 1991).

The solid organic fraction of biowaste in the fraction <2 mm is composed of humified organic matter (Chapter 4). It is generally accepted that lignin and humic substances are recalcitrant towards anaerobic degradation (Schlegel, 1993). Therefore, the solids will make only a minor contribution to the total methane yield of the fraction <2 mm. The methane yield from the solid fractions mainly originates from the soluble organic matter in these fractions. This is also confirmed by the high methane yield of 0.35 NL.g<sup>-1</sup> VS. The methane yield for municipal solid waste and yard waste normally ranges from 0.15 to 0.22 NL.g<sup>-1</sup> VS (Chynoweth et al., 1992; Tong et al., 1990).

### Semi-continuous

The course of the methane production rate for the semi-continuous CSTR reactor shows that two types of substrate are present in the feeding. The sharp increase in methane production directly after the feeding is due to the degradation of VFA and readily-degradable soluble organic matter, such as proteins and carbohydrates. The particulate organic compounds that degrade more slowly give rise to a base line in the methane production rate. At high organic loading rates, VFA accumulates in the reactor because the acidifying rate is faster than the methanogenic activity of the reactor system.

Although it is recognised that the influent contains several types of organic substrates, the methane production as a function of the solids retention time ( $\tau$ ) can adequately be described by a single, first-order hydrolysis constant. The semi-continuous reactor can be approximated by a CSTR and the average methane production (in NL.g<sup>-1</sup> OM) is then described by:

$$\text{CH}_4(\tau) = \text{CH}_{4, \text{max}} \left( 1 - \frac{1}{1 + k_h \cdot \tau} \right) \quad (9.2)$$

where  $\text{CH}_{4, \text{max}}$  is the maximum methane yield of the substrate (in NL.g<sup>-1</sup> OM),  $k_h$  is the first-order hydrolysis rate constant (in d<sup>-1</sup>) and  $\tau$  is the solids retention time (in d). The average methane production and organic matter degradation as a function of the OLR can be fitted by a hydrolysis rate constant of 0.09 d<sup>-1</sup>. This value is in good agreement with results of the batch experiments and literature values found for the organic fraction of municipal solid waste, leaves, grass and branches (Chynoweth et al., 1992; Tong et al., 1990).

### 9.5.4. Conclusions

The pilot-plant study shows that physical separation of biowaste is possible by a combination of physical separation units operated under wet conditions. The pilot plant achieves the goals which were formulated on basis of the results of Chapters 4 and 5:

1. physical separation of biowaste into three fractions:
  - organic fraction >1-2 mm
  - sand fraction
  - organic/organo-mineral fraction <1 mm
2. the organic fraction >1-2 mm can be aerobically composted and the compost reaches the BOOM demands for compost and meets the BOOM requirements for clean compost except for Zn
3. the sand fraction is very low in organic matter and heavy metals and can directly be utilised in road and building construction
4. heavy metals are accumulated in the organic/organo-mineral fraction <1 mm for which the heavy metal content does not reach BOOM qualities for compost.

Aerobic composting on a pilot-plant scale showed that the oxygen uptake rate is significantly lower compared to total biowaste (results not shown here). This is due to the washout of readily degradable organic matter from biowaste in the wet-sieving steps. The aerated static pile composting process was difficult to control on a pilot-plant scale. On the average 40% organic matter is degraded but the heat production is insufficient to produce compost with a dry matter content of 60% or more. The required dry matter content of 60% can be reached when the fraction >1-2 mm is dewatered to 30% before composting.

The compost produced from the fraction >1-2 mm is low in heavy metals and high in organic matter. The high quality of this compost makes it possible to compete with other soil improvers and possibly means that it can replace peat compost for horticultural applications. Another important advantage of the process is the fact that the quality of the compost does not depend on the quality of the incoming biowaste: the components originating from the litter layer and soil are separated from the fresh plant material and end up in the sand and the residual fraction.

The organic/organo-mineral fraction <1-2 mm can be digested in a one-phase slurry reactor, after thickening in a settling tank. The results show that the major part of the methane production comes from the soluble organic matter. The particulate organic matter is composed of non-biodegradable humified organic matter with a very low methane yield. Therefore it is more appropriate to separate the solids and treat the liquid fraction in an upflow anaerobic sludge blanket (UASB) reactor with a high biomass retention time. In this way the hydraulic retention times can significantly be increased.

The solid organic matter of the fraction <1 mm is high in humified organic matter (approx. 15-20%, Table 3.11) and could be an excellent compost product. Unfortunately, the heavy metal content of this fraction is too high to produce compost which can meet the BOOM demands. Therefore, the residual fractions must be landfilled. However, since 1996 new landfill regulations in the Netherlands have prohibited the landfilling of solid wastes with an organic matter content higher than 5% (Stax, 1995). The only option for



the disposal of the residual fraction is incineration. An attractive alternative could be the chemical extraction of heavy metals from the residual fraction in order to reach the BOOM quality levels for compost.

## References

- APHA 1992. Standard Methods for the Examination of Water and Wastewater. 18th ed., part 2540D. Washington D.C.: American Public Health Association
- Brummeler, E. ten; 1993. Dry Anaerobic Digestion of the Organic Fraction of Municipal Solid Waste. Ph.D. Thesis. Wageningen, The Netherlands: Wageningen Agricultural University
- Chynoweth, D. P.; Owens, J.; O'Keefe, D.; Earle, J. F. K.; Bosch, G.; and Legrand, R. 1992. Sequential Batch Anaerobic Composting of the Organic Fraction of Municipal Solid Waste. *Wat. Sci. Technol.* 25:327-339
- Doucet, P.; and Sloep P.B. 1992. *Mathematical Modeling in the Life Sciences*. Chichester:Ellis Horwood Limited
- Finstein, M. S.; Miller, F. C.; Strom, P. F.; MacGregor, S. T.; and Psarianos, K. M. 1983. Composting Ecosystem Management for Waste Treatment. *Biotechnology* 1:347-353
- Gujer, W.; and Zehnder, A. J. B. 1983. Conversion processes in Anaerobic Digestion. *Wat. Sci. Tech.* 15:127-167
- Hamelers, H. V. M.; Koster, I. W.; and Wilde V. de 1990; A Simulation Device for the Composting Process and its Ammonia Emission. In: *Agricultural Biotechnology In Focus in the Netherlands*, Dekkers J. J. (ed.). Wageningen: Pudoc
- Haug, R. T. 1993. *The Practical Handbook of Compost Engineering*. Boca Raton: Lewis
- Parkin, G. F.; and Owen, W. F. 1986. Fundamentals of Anaerobic Digestion of Wastewater Sludges. *J. Environ. Engn.* 112:867-920
- Pavlostathis, S. G.; and Giraldo-Gomez, E. 1991. Kinetics of Anaerobic Treatment: A Critical Review. *Critical Reviews in Environmental Control* 21:411-490
- Robinson, J. J.; and Stentiford, E. I. 1993. Improving the Aerated Static Pile Composting Method by the Incorporation of Moisture Control. *Compost Science & Utilization* 1:52-69
- Schlegel, H. G. 1993. *General Microbiology*. Cambridge:University Press
- SDU 1991. Besluit Overige Organische Meststoffen (BOOM). *Staatblad* 613:1-45 (in Dutch)
- Stax, A. B. M. 1995. Landfill guidelines in the Netherlands. *Proceedings of the Fifth International Landfill Symposium Calgliari, Italy*
- Tong, X.; Smith L. H.; and McCarty, P.L. 1990. Methane Formation of Selected Lignocellulosic Materials. *Biomass* 21: 239-255

# 10. General discussion

## 10.1 Introduction

This closing chapter will discuss the development of new technologies for the removal of heavy metals from organic solid wastes. It will also evaluate the mechanistic models describing the binding of heavy metals to biowaste and kinetics of heavy metal extraction from biowaste. These models can provide a better understanding of the parameters determining the extraction efficiency and extraction rate of heavy metals from biowaste. This understanding will support the development of new technological approaches to optimise the extraction of heavy metals from biowaste. This work focuses on the reduction of heavy metals in biowaste, but the results can be extended to other solid (organic) waste streams. The research can be divided into three parts:

1. physico-chemical characterisation of heavy metals in biowaste:
  - distribution of heavy metals in biowaste
  - binding strength of heavy metals to biowaste
2. modelling aspects:
  - development of a mechanistic model to describe the heavy metal binding to natural organic complexants
  - development of a mechanistic model to describe the rate and efficiency of heavy metal extraction from solid organic particles
3. technological aspects:
  - development of a physico-chemical fraction scheme for heavy metals in biowaste for assessing the physical separation and chemical extraction processes
  - development of a physical separation process for the valorisation of biowaste
  - proposal for a chemical extraction process to reduce the heavy metal content of solid waste streams.

These aspects will briefly be discussed in this chapter.

## 10.2 Physico-chemical characterisation of heavy metals in biowaste

To explore the application of the heavy metal removal technologies for biowaste, the first step was the full characterisation of the waste, i.e. its chemical composition and the distribution of physical entities within the waste. A large part of biowaste is composed of organic matter with variable particle sizes. Surprisingly, a large part of biowaste is

composed of inorganic material, i.e. sand, silt and clay minerals. The inorganic part of biowaste originates from the collection of garden waste, especially the top layer of garden soil. A comparison of the natural background content of heavy metals in the various components of biowaste with the heavy metal content of these components in biowaste indicates that biowaste is not contaminated with heavy metals. Based on these results it can be stated that prevention of contaminated components in biowaste by changing the collection criteria does not offer a solution. In fact, it has been shown that the heavy metal standards for clean compost in the BOOM decree are in conflict with the natural background concentration of heavy metals in fresh organic matter.

An analytical fractionation scheme is presented to determine the physico-chemical distribution of heavy metals in biowaste. First, the distribution of heavy metals over the physical entities of biowaste was determined. Subsequently, the binding strength of the heavy metals to the various physical entities was determined by the application of a sequential chemical extraction scheme. From the results of the physical distribution of heavy metals in biowaste, the use of a physical separation process can be considered to separate a fraction with elevated heavy metals from biowaste. The results of the sequential chemical extraction provide information on the binding strength and extraction efficiency of heavy metals from total biowaste and fractions of biowaste. These results can be used to assess the employment of a chemical extraction reagent to reduce the heavy metal content of biowaste.

### **10.3 Modelling aspects**

Mechanistic models were developed in order to gain more insight into factors controlling the extraction efficiency and rate of extraction of heavy metals from biowaste.

Knowledge of the distribution of the chemical forms of heavy metals (= heavy metal speciation) provides more insight into the behaviour of heavy metals in natural systems. In multicomponent systems, the distribution of chemical species is calculated with so-called chemical equilibrium models. The NICA-Donnan model was presented which describes the binding of protons and Cu(II) to organic particles of biowaste. The model takes into account the complex binding characteristics of humic substances, i.e. polyfunctional and polyelectrolytic behaviour. The NICA-Donnan model was validated for Sephadex CM-25, an ion-exchanger with well-defined chemical and physical properties. The model was also applied to interpret the proton and Cu(II) binding to particle-sized organic particles of biowaste. Despite the complexity of the particle-sized organic fractions of biowaste, the NICA-Donnan model can adequately describe the proton and Cu(II) binding. The model should be considered as a semi-empirical one: the parameters have a thermodynamic basis but the parameters are fitted on proton and metal

### ion adsorption isotherms.

The chemical equilibrium model gives insight into the extraction efficiency but does not provide any information on the factors controlling the kinetics of the extraction process. The kinetics of metal extraction are often interpreted by reaction-kinetic models but these empirical models do not provide an insight into the mechanisms of the extraction process. A mechanistic model was developed which describes the chemical and transport processes which determine the course of the acid extraction of heavy metals from solid organic particles. The solid organic particles were presented as spherical, charged particles of equal size. One type of reactive site was considered, and these sites are homogeneously distributed over the particles. The mechanistic model made use of the Donnan concept for charged complexants. The extent of the proton-metal exchange is determined by the affinity of the heavy metal ion and the proton affinity for the reactive sites of the organic particles. Diffusion in the film layer around the particles and diffusion inside the particles was described by the Nernst-Planck equations for charges species. This model is able to give a qualitatively interpretation of the acid extraction of Cu(II) from the isolated particle-sized organic fractions in biowaste at pH 1. The model can also explain the anomalies observed during the extraction of Cd, Cu and Zn from sewage sludge at low pH, i.e. lag phase in extraction, changes in extraction rates and the differences for the type of heavy metal and variations in pH.

The kinetic model has been developed for a relatively simple system but could easily be modified for the description of more complex multicomponent systems, i.e. the presence of different metals, different reactive sites, variations in particle size, etc.. The model can also be applied to model biofilm processes for which biological reactions terms have to be incorporated in the mass balance equation.

## **10.4 Technological aspects**

The development of a process to reduce the heavy metal content of solid waste streams depends on the status of the available removal technologies and the characteristics of the solid waste stream. For biowaste, additional conditions are set by the legal demands for heavy metals in compost, subsequent biological processes (i.e. composting of biowaste, wastewater treatment), and demands for the minimisation of residual solid and liquid waste streams. The available technologies for the removal of heavy metals from solid waste streams are (1) physical separation of fractions contaminated with heavy metals and (2) extraction of the heavy metals by water-soluble extractive reagents. No full-scale plants exist for the treatment of solid organic waste streams. Chemical extraction of heavy metals from sewage sludge with inorganic acids and complexing agents is only applied on a lab-scale. Physical separation processes have only been employed for the removal from soils and sediments of fractions contaminated with heavy metals.

On the basis of the results of the physical distribution of heavy metals in biowaste, a physical separation process was designed to valorise biowaste. A pilot plant study showed that physical separation of the biowaste is possible by a combination of physical wet separation units operated under wet conditions. The pilot plant achieved the goals formulated on the basis of the lab-scale results. The biowaste was separated into three fractions:

1. organic fraction >1 mm
2. sand: inorganic fraction 0.05-0.5 mm
3. organic/organo-mineral fraction <1 mm

The organic fraction >1 mm can be aerobically composted and the compost reaches the BOOM demands for compost and meets the BOOM requirements for clean compost except for Zn. The sand fraction is very low in organic matter and heavy metals and can directly be utilised in road and building construction. The heavy metals are accumulated in the organic/organo-mineral fraction <1 mm for which the heavy metal content does not reach BOOM qualities for compost; therefore this fraction has to be landfilled. However, as from 1996 it has been forbidden to landfill solid waste streams which have an organic matter content higher than 5%. This means that the residue from the valorisation process has to be treated in another way which is economically and environmentally acceptable. The following possibilities are qualified for the treatment of the residual fraction:

1. incineration
2. reduction of heavy metals by chemical extraction.

Incineration is a very expensive treatment technology which produces contaminated slags and fly ashes which also have to be landfilled. Chemical extraction can only be applied when heavy metals can be reduced to values below the BOOM standards. The results of the sequential chemical extraction indicate that this is possible. From a discussion of the advantages and disadvantages of the chemical extraction by inorganic acids and complexing agents it was concluded that these extracting reagents are not applicable on a practical scale due to the costs of the process and the negative environmental impacts of the discharged solid and liquid waste streams. Another extracting agent, citric acid, is proposed which does not have serious drawbacks. The main advantages of citric acid are:

- heavy metal extraction is partly due to the acidic character but for the greater part to the complexing behaviour of the citrate anion; therefore extractions can be performed at mildly acidic conditions, i.e. pH 3-5
- citric acid is readily degraded under aerobic and anaerobic conditions; this implies that the 'cleaned' waste does not have to be conditioned, leading to a substantial reduction of wastewater; moreover, wastewater can be treated (an)aerobically
- heavy metals can be removed from the citric acid solution; in this way the extraction liquid can be recycled, reducing the costs of the process.

The citric acid extraction process has been applied successfully on a lab-scale to remove heavy metals from sewage sludge (Boots, 1995) and soils (Braspenning and Dijkhuizen, 1996). The extraction with citric acid can be integrated into the total physical wet-separation process as shown in Figure 10.1.

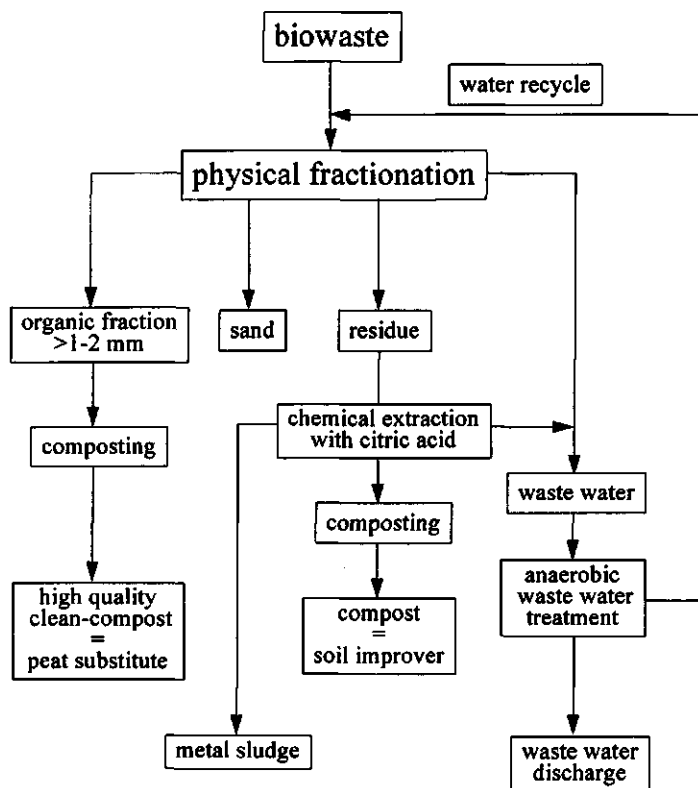


**Figure 10.1** Integrated process scheme for the valorisation of biowaste

The processes for the reduction of heavy metals in biowaste and production of biowaste-derived compost can involve several types of processes, i.e. physical separation processes, chemical extraction processes and biological treatment processes. For biowaste a combination of processes can lead to more optimal conditions with respect to cost aspects and the minimisation of waste streams. An important boundary condition for the total process is the fact that the processes have to be tuned to the subsequent biological process, i.e. the composting of cleaned biowaste and the (an)aerobic treatment of the wastewater.

Summarising, the processing of biowaste to compost involves several steps for which the following conditions have to be met:

- the production of residual waste streams has to be minimised
- the costs of the process should be economically acceptable
- treated biowaste should be suitable for further biological conversion steps
- biowaste-derived compost has meet the standards of BOOM for compost.

The valorisation scheme for biowaste as presented in Figure 10.1 may meet these conditions.



## References

- Boots, E. (1995).** Heavy metal extraction from sewage sludge using citric acid. MSc thesis Wageningen Agricultural University, Department of Environmental Technology series no. 95-67
- Braspenning, J.; and Dijkhuizen, C. (1996).** Removal of heavy metals from sewage sludge. MSc thesis Wageningen Agricultural University, Department of Environmental Technology series no. 96-32 (in Dutch)

# Summary

The title of this thesis shows that the research covers a wide field of interest. On the one hand work is being done to develop practical and applicable technologies in order to reduce the heavy metal content of fruit, vegetable and yard waste (so-called biowaste). On the other hand, physico-chemical models are being developed to gain more insight into the behaviour of heavy metals. In this summary an overall view will be given of the research which was covered by this dissertation.

## Recycling of biowaste as compost

The Dutch government policy on treatment of solid wastes is aimed at prevention and recycling. In the National Environmental Policy Plan preference is given to these methods above incineration and landfilling. The recycling of municipal solid waste can be promoted by means of separate collection of the individual components, amongst others paper, glass and the organic fraction. Approximately 50% of municipal solid waste in the Netherlands is composed of organic matter which can be re-used as a soil improver and organic fertiliser after aerobic composting or anaerobic digestion.

The use of compost as a fertiliser is regulated by the BOOM decree (Dutch abbreviation for 'Besluit Overige Organische Meststoffen'). BOOM is part of the Dutch governmental policy concerning soil protection. This policy aims to prevent the accumulation of heavy metals in the soil. The BOOM criteria are formulated and based on the recommendations of the 'Technische Commissie Bodembescherming'. Two types of compost can be distinguished: 'compost' and 'clean compost'. The dosage of compost to arable land is limited to a maximum while the dosage of clean compost is limited by the amount of dosed phosphate.

Both the compost derived from municipal solid waste and the compost derived from municipal solid waste after mechanical separation contain levels of heavy metals exceeding the BOOM standards. However, the heavy metal content of compost obtained from the source separated organic fraction of municipal solid waste is considerably lower. This is the reason behind the separate collection of the organic fraction of the municipal solid waste in the Netherlands. At this moment about 80% of the total municipal waste is collected separately. However, the heavy metal content of biowaste-compost is critical with respect to some heavy metals to meet the BOOM standards for compost and the heavy metal content of biowaste-compost is too high with respect to most heavy metals to meet the BOOM standards for clean compost. This shows that in the Netherlands there is a conflict between two governmental policies. On the one hand, the recycling of municipal solid waste is propagated through the separate collection of

biowaste whilst on the other hand it is attempted to prevent the accumulation of heavy metals in the soil in order to protect the natural ecosystems and safeguard public health.

This dissertation will describe the different possibilities of biowaste recycling and at the same time prevent the accumulation of heavy metals in the soil. A reduction of the heavy metal content in compost can be achieved in two ways. Firstly, the criteria for biowaste collection can be modified in order to avoid those components in the biowaste with a high heavy metal content. Secondly, utilising a technological method, the heavy metals in biowaste can be removed. This study will primarily focus on the second approach, the reduction of heavy metals from biowaste in order to reduce the contents in compost and meet the BOOM criteria for compost or clean compost.

Two feasible methods can be applied in order to remove heavy metals from biowaste: physical separation and solid-to-liquid extraction. The physical separation process is aimed at the selective removal of a specific fraction from the solid waste in which the heavy metals are concentrated. Various techniques which can be applied in order to achieve this are sieving, elutriation, hydrocycloning and flotation. These processes have been largely developed by the mining industry and are already being used for remediation of soils and sediments. Solid-to-liquid extraction is based on the transfer of the heavy metals from the solid phase to the aqueous phase. To promote this transfer acids or complexants are added.

The development of a particular technology to remove heavy metals from solid waste depends on the intrinsic character of the technology and the type of waste. Apart from this the removal technology has to satisfy certain boundary conditions. First of all, the separation efficiency has to be sufficiently high. Secondly, especially for organic waste streams, the applied technology should not have negative effects on the composting process or the quality of the compost. Thirdly, the removal technology should be chosen in such a way as to minimise the emissions to the environment, i.e. air emissions, waste water and solid residual waste.

### **Sources of heavy metals in biowaste**

Biowaste is composed of the organic waste products collected indoors and outdoors. The indoor fraction is mainly composed of food remainders, coffee filters, flowers, indoor plants and the like. The outdoor fraction of biowaste is collected in gardens and consists of amongst others grass, leaves, branches and topsoil. Studies conducted in the Netherlands and Germany indicate that only 20% of the total collected biowaste originates from indoor collection. However, no indication of the composition of the biowaste or the contribution from the various components to the total heavy metal content is given.

The contribution to the total heavy metal content from the various components collected from indoor and outdoor organic waste was studied. First of all the composition of the biowaste was examined by physically separating the waste on the basis of particle size and specific gravity in individual components. The experimental set-up was comprised of a wet-sieving process followed by a water-elutriation step. Although biowaste is regarded as an organic waste stream, it was found that around 40% consists of mineral constituents. The mineral part is largely made up of sand (85%) and silt-lutum (15%). For biowaste collected indoors, the mineral fraction is very small (10%) but this fraction can amount to 60-70% in biowaste collected outdoors. The mineral components are introduced in the biowaste due to the collection of topsoil of gardens and potting compost. On the basis of visual inspection and insight in the place of origin of the original components, the biowaste can be classified into the following fractions:

1. organic fraction >1 mm: organic material with intact cell wall structure; this fraction originates from indoor and gardens, e.g. grass, leaves, branches, vegetables, fruit
2. mineral fraction >1 mm: fraction made up of mineral impurities such as pieces of broken glass and small stones
3. organic fraction between 0.05 and 1 mm: spongy, dark brown organic material without cell wall structure; this fraction originates from potting compost and the top soil of gardens
4. mineral fraction between 0.05 and 1 mm: fraction is composed of sand from the top soil of gardens
5. fraction <0.05 mm: fraction made up of silt, lutum and humic material; the mineral and organic material are present as soil aggregates; the fraction originates from potting compost and the top soil of gardens

The heavy metal content (Cd, Cu, Pb and Zn) in the various fractions in the biowaste were determined and compared with the natural background concentration of heavy metals in the original constituents of biowaste. The natural background concentrations of heavy metals in the original components were retrieved from literature. The measured heavy metal content in the five fractions corresponds well with the natural background concentration of the original components. The heavy metal content in the organic fraction >1 mm corresponds to the natural background concentration of plant material, the levels in the mineral fraction 0.05-1 mm corresponds to the natural background concentration in sandy soils, the levels in the organic fraction 0.05-1 mm is comparable to the natural background concentration in the humified topsoil in forests and the level in the fraction <0.05 mm is comparable to the natural background concentration of soils containing humus and clay.

### **Assessment of the quality of biowaste-compost**

To get an indication of the heavy metal content in biowaste-compost, it must be kept in mind that organic matter is partly degraded during composting. Due to the degradation of organic matter heavy metals are concentrated and the heavy metal content in the compost increases. The degradability of organic matter depends on the structure and composition of the organic matter. Organic compounds such as lipids, proteins and carbohydrates are easily biodegradable, whereas lignin and humic compounds are very recalcitrant. The degradation of cellulose, a compound which is normally readily degradable, is partly inhibited when incorporated in the lignocellulosic complex. Therefore, heavy metals are more strongly concentrated in compost derived from biowaste which consists of food remainders (e.g. lettuce, cabbage, potatoes) than in compost from biowaste collected outdoors (e.g. branches, leaves, grass and flowers). Compost derived from fresh plant material and food remainders complies with the BOOM standards for compost but the standards for clean compost are exceeded for a number of heavy metals (assuming 50% of organic matter is degraded). Even though the humified organic matter, originating from potting mix and topsoil from gardens hardly degrades during the composting process, the BOOM standards are exceeded. In general, biowaste-compost complies with the BOOM standards for compost because biowaste contains about 30% sand. Sand reduces the heavy metal content in biowaste-compost due to the low natural background concentration and the fact that sand is not degraded during composting. However, the presence of sand in the compost results in a low organic matter content, in this way lowering the quality of compost.

Preventive measures to reduce the heavy metal content of biowaste do not offer any perspective due to the fact that the collection of garden waste would have to be prohibited, a fraction comprising 80% of the total collected biowaste. Due to such a change the recycling of municipal solid waste would decrease by 30-40%.

It is worthwhile to note that the application of compost derived from biowaste is bound by strict standards where heavy metals are concerned whereas the application of animal manures as soil fertiliser is not restricted although the levels of copper and zinc in animal manure are much higher. The dosage of animal manure is limited only with respect to the phosphate dosage. At this moment, fertilisers are used abundantly by the agricultural industry in the Netherlands. A more balanced and precise dosage of nutrients and organic matter can prevent the negative effects of nutrients and heavy metals on the environment while still achieving good crop yields. A sustainable agricultural policy can only be achieved if effort is made to close the mineral and organic matter cycle. It is recommended that the different legislations concerning the dosage of various organic and artificial fertilisers have to be combined in a single legislative framework.

### **Physico-chemical fractionation of heavy metals in biowaste**

The feasibility of the removal technology, physical separation or chemical extraction, can initially be assessed by determining to which fraction(s) of the biowaste the heavy metals are adsorbed and by determining the binding strength of heavy metals to these fractions. An analytical method was developed to determine the physico-chemical forms of heavy metals in biowaste. Firstly, the biowaste is fractionated by particle size using a wet-sieving process. The fractions between 0.05 and 1 mm are subsequently separated into a mineral and an organic fraction by a water-elutriation step. The binding strength is determined for each separate mineral and organic fraction using a sequential chemical extraction (SCE) scheme. The SCE approach can determine one specific chemical form of the metal by the use of a selective extracting agent. The five-step Tessier SCE scheme is used as the basis for biowaste. An additional step is introduced to differentiate between metals adsorbed to organic matter and metals incorporated in organic matter. Evaluation of the SCE procedure indicates that the supposed selectivity of the individual extraction steps is not attainable. The chemical character of a natural system (like biowaste) is too complex to fully extract each metal speciation in one single extraction step. The SCE does however give a clear insight into the binding strength of metals to the solid matrix.

The physical fractionation showed that the heavy metals are predominantly bound to the fraction <0.05 mm and to the organic particles in the range 0.05-1 mm. The heavy metal distribution is a logical result of the origin of the components in biowaste which was already discussed. On the basis of physical fractionation of biowaste, the following physical separation process can be proposed:

1. compost fraction, the organic fraction >1 mm: contribution 40-50% on dry matter basis; this fraction can be composted and complies with the BOOM standards for compost; the quality of this compost is higher than compost from integral biowaste due to the high organic matter content
2. sand fraction, the mineral fraction between 0.05-1 mm: contribution 20-30%; this fraction is composed of sand with a very low heavy metal content and can be used directly in road construction
3. residual fraction, the organic fraction 0.05-1 mm and the fraction <0.05 mm: contribution 20-30%; this fraction makes a good soil improver due to the high levels of silt, clay and humus

The residual fraction does not meet the BOOM standards but could possibly be used as a compost after extraction of the heavy metals. The feasibility of the extraction can be assessed on basis of the SCE scheme. The sum of the first four steps of the SCE scheme indicate the fraction of heavy metals which are potentially available for extraction. The rest of the heavy metals is not available for extraction because these metals are bound too strongly to or incorporated in the solid matrix. The results of the SCE scheme show

that Cu and Pb are bound more strongly to biowaste than Cd and Zn. On the basis of the sum of the first four extraction steps, extractive removal is possible for the metals mentioned above.

### **Modelling of the heavy metal adsorption to the organic fraction of biowaste and the role of humic acids in the binding of heavy metals**

In order to develop new techniques for the extraction of heavy metals from biowaste and to predict the bioavailability and toxicity of heavy metals in biowaste and biowaste-compost, more insight needs to be gained into the physical-chemical behaviour of heavy metals. The physical-chemical behaviour is directly related to the heavy metal speciation. The distribution of the different chemical forms of a metal ion (= speciation) in a natural system can be determined using a so-called 'chemical equilibrium model'. The modelling approach has several advantages. For example, the toxicity of heavy metals is determined by the activity of the free metal ion. The free metal ion activity is very difficult to determine experimentally but can be calculated using a chemical equilibrium model. Additionally, more insight can be gained into the intrinsic properties of an extracting agent as the equilibrium model gives insight into the metal binding competition between the extracting agent and the solid matrix of the system. The chemical equilibrium model assumes that the chemical system is at thermodynamic equilibrium.

Biowaste contains natural complexants like clay-minerals, metal hydroxides, fresh organic matter and humic substances. It is proposed that the organic complexants (plant fibres and humic substances) dominate the metal speciation in biowaste. The chemical equilibrium model is reasonably accurate when it is known which components are present and which reactions can take place. However, heavy metal speciation is more difficult to model in natural systems. This is due to the fact that the adsorption behaviour of natural complexants is difficult to model because the composition, chemical structure, size of molecules and the number and type of functional groups are not exactly known. Moreover, it is not exactly known which reactions can take place between metal ions and the natural complexants on molecular scale. Apart from this, natural organic complexants can be present in the aqueous and solid phase and accordingly have a considerable effect on the mobility of heavy metals.

Natural organic complexants like humic substances contain multiple functional groups to which heavy metals can adsorb. Besides, humic substances under natural conditions are negatively charged which increases the adsorption of positively charged, heavy metals. As a result of this polyfunctional and polyelectrolytic character, the binding strength of heavy metals depends on metal loading, pH, ionic strength and the competition with other metal ions. The properties can be described by the NICA-Donnan model. The model consists of two parts: (1) the binding to the polyfunctional complexant is described by the NICA (Non-Ideal Competitive Adsorption) model and (2) the polyelec-

trostatic effect is described by the Donnan formalism. The model is validated for the proton- and copper adsorption to a model compound, the synthetic weak-acid cation-exchanger Sephadex CM-25. The model gives a good description of the proton- and copper binding to Sephadex CM-25. The non-ideality of the local adsorption of the metal ions to the functional groups can be assigned to the high ionic strength in the gel phase.

To study the role of humic acid in the adsorption of copper to the organic fractions in biowaste, acid-base titrations and Cu(II) titrations were carried out and the humic acid content was determined of five isolated particle-sized fractions in the range 0.05-2 mm. The acid-base titrations showed that the functional group content increases with decreasing particle size. The functional group content can be assigned to the humic acid fraction in the organic particles. The carboxyl content remains more or less constant with decreasing particle size while the phenolic group content increases. Additionally, the Cu(II) binding strength increases with decreasing particle size. This stronger adsorption cannot only be due to the higher functional group content of the smaller organic fractions. It is more likely that the increasing phenol group content with a stronger affinity for Cu(II) is responsible for the stronger adsorption.

The acid-base titrations and Cu(II) adsorption isotherms to the organic fraction in the range 0.05-0.1 mm can be described satisfactorily by the developed NICA-Donnan model. The binding properties of the organic fraction were assigned to the humic acid fraction in the organic particles. It is assumed that the humic acid contains two types of functional groups, the carboxyl and the phenol group. The model calculations reveal that the polyelectrostatic effect for the charged particles on the acid-base titrations is small. This is also confirmed by the experiments. Noticeable, however, is the fact that the model calculations show that the Cu(II) adsorption is strongly influenced by the ionic strength. The NICA-Donnan model with two types of functional groups, the carboxyl- and phenol groups, turned out to be a satisfactory semi-mechanistic approach to describe the binding of protons and Cu(II) to humic substances.

A comparison of the model and experimental Cu(II) adsorption isotherms showed that during the experiments the adsorption isotherms were not in equilibrium. This was revealed by the non-linear course of the experimental isotherms while the model calculations show a linear course. Deviation from linearity increased at lower Cu(II) activity, i.e. high pH values, lower Cu(II) loading and for smaller particle size. The non-equilibrium is caused by the diffusion limitation of the Cu(II) ions in the solid particles. The Cu(II) ions must diffuse through the organic particles in order to reach the available reactive sites. The diffusion of Cu(II) ions inside the particles is restricted by the adsorption of Cu(II) to the reactive sites. It can take years before equilibrium is reached for these experiments! This indicates that the fitting of the parameters using experimen-



tally determined acid-base titrations and metal adsorption isotherms must be regarded with care and can result in totally wrong interpretations.

The strong metal adsorption of the humic substances can enhance the mobility of heavy metals in soil systems and landfill sites when the humic substances become mobile. The experimental Cu(II) titrations are a measure of the adsorption of Cu(II) to the organic particles but no distinction is made between Cu(II) adsorbed to dissolved humic acids and Cu(II) adsorbed to solid humic acid (measurement of free  $\text{Cu}^{2+}$  activity with a Cu(II) ion specific electrode). Therefore, the total Cu(II) in solution and the total dissolved humic acid is measured at the end of each experiment to determine the relationship between dissolved Cu(II) and the amount of dissolved humic acid. These analysis were carried out for the five isolated organic fractions in the range 0.05-2 mm between pH 4 and 10. The amount of dissolved humic acid increased with decreasing particle size as the smaller fractions contain more humic acid. As can be expected, the fraction of dissolved humic acid also increased for higher pH values. The results indicated that the amount of dissolved Cu(II) increases linearly with increasing dissolved humic acid. Besides, the data showed that the Cu(II) binding strength of the soluble and solid humic acid are equal. The results indicate that humic acids can not be regarded as polymers with different molecule size but that humic acids behave more in accordance with Wershaw's model for humic acids instead. According to Wershaw's model, humic acids are regarded as aggregates of amphiphilic molecules, structured by hydrogen bonds and van der Waals forces. At higher pH the electrostatic repulsion increases and the hydrogen bonds are broken resulting in subaggregates and finally individual molecules.

### **Modelling of the course of extraction of heavy metals from solid organic particles**

The disadvantage of the chemical equilibrium model is the assumption that the system is at equilibrium, i.e. the chemical reactions take place instantly. However, for extraction of heavy metals from solid particles, diffusion processes play a major role. Apart from the extraction efficiency, the kinetics of the extraction process is an important factor because the rate of extraction determines the hydraulic retention time and thus the size of the reactor. A mechanistic model has been developed which describes the acid extraction of heavy metals from solid organic particles. With this model more insight is gained into the factors which play an important role in the extraction process. The model is tested for the experimental extraction of Cu(II) from organic particles in biowaste and the course of the extraction of cadmium, copper and zinc from sewage sludge.

In the model the solid organic particles are regarded as a homogeneous phase in which the heavy metal ions are adsorbed to functional groups. The adsorbed metal ions are

exchanged for protons during the acid extraction. The assumption is made that the exchange reaction between protons and metal ions proceeds quickly in comparison with the rate of diffusion. The resistance to mass transport from the bulk solution to the film layer is described by the film layer model, i.e. the transport takes place by diffusion through a stagnant water film present around the solid particles. The transport inside the solid particles is described by diffusion through a stagnant porous gel phase.

Because ions are charged particles which create an electric potential during diffusion, the diffusion can not be described by Fick's law but instead have to be described on the basis of the Nernst-Planck diffusion equation. This equation describes the diffusion by combining a concentration gradient and an electric potential gradient. The Nernst-Planck equation states that the diffusion of an ion is not only determined by the concentration gradient of the particular ion but also by the concentration gradient of the other cations and anions present. The chemical equilibrium in the bulk solution, the film layer and inside the particles is described by a standard chemical equilibrium model.

The model simulations of the metal extractions at low pH indicate that during the initial stage of the extraction the metal ions from the solution are adsorbed to the solid phase instead of being extracted from the solid particles. In spite of the fact that during the initial stage of the extraction the protons are transported into the particles and exchange with metal ions bound to the functional groups, the metal ions do not diffuse to the bulk solution but are pushed back into the particles where the metal ions occupy reactive sites. The direction of transport is determined by a combination of the concentration gradient and the electric potential gradient. The concentration gradient dominates when the pH of the bulk solution is fully established over the particles. The model is used to study the course of the metal extraction as a function of the particle size, the pH of the extraction agent, the type of metal ion, the type and concentration of the functional group and the magnitude of ion diffusivity inside the particles.

The Cu(II) extraction at pH 1 is determined experimentally for three isolated organic fractions from biowaste: the organic fractions in the ranges 0.05-0.1, 0.2-0.5 and 1-2 mm. The course of the extraction is represented by periodic measurement of the total copper concentration using atomic adsorption spectrometry and by continuous measurement of the free copper activity using a copper ion-selective electrode. No quantitative interpretation of the extraction was made as the properties of the organic particles are not well defined. On a qualitative basis the experiments confirm the model simulations. In the initial stage of the extraction the remaining copper is removed from the solution. After reaching a minimum concentration the copper concentration in the bulk solution increases until after a certain amount of time an equilibrium is reached.

The extractions of Cd, Cu and Zn from sewage sludge as stated in the literature show a unusual course of extraction. In some cases it takes a certain amount of time before the

extraction will start off (lag phase) and a number of maxima can be observed in the extraction rate. The duration of the lag phase and the rate of extraction depends on the type of metal ion, the solids concentration and the pH of the extraction. This behaviour can be described well by the developed model. According to the model, the lag phase lengthens with increasing pH, higher solids concentrations and for metal ions which adsorb more strongly to the sludge. The occurrence of two maxima in the extraction rate can also be explained by the developed kinetic model.

### **Pilot plant study of technologies for the removal of heavy metals from organic wastes**

On the basis of the laboratory results a pilot plant was designed for the physical separation of biowaste in three fractions: the organic fraction for composting, the sand fraction and the residual fraction. The separation was performed using several wet-separation units: i.e. rotating drumsieve, screen bend, hydrocyclone, flotation cell, sedimentation and decanting centrifuge. The results from the pilot plant study confirm the laboratory experiments. The composting fraction (organic fraction >1 mm) complies with the BOOM standards for compost easily but also with the standards for clean compost except for Zn. The sand fraction, separated from the organic fraction by a hydrocyclone, is further cleaned from organic matter by flotation. The organic matter content in the sand amounts to less than 0.5% and the heavy metal content is very low. The wash water used in the physical separation process is largely recycled. Accumulation of dissolved organic matter in the wash water is prevented by incorporating an anaerobic digestion step in the process. The produced biogas can be used for the production of energy. The residual fraction cannot be re-used as compost because the BOOM standards for compost are exceeded. The main advantage of the physical separation process is the production of biowaste-compost of a constant and high quality which is independent of the composition of the collected biowaste. The biowaste-derived compost has a high organic matter content and complies (except for Zn) with the BOOM standards for clean compost.

After the physical separation process it is not possible to use the residual fraction for composting because it does not meet the BOOM standards. Landfilling was up till now an option but is prohibited for solid organic wastes with an organic matter content exceeding 5% since 1996. Incineration of the residual fraction is an expensive option and is not very attractive in terms of sustainability. The residual fraction makes a good quality soil improver due to the high humic acid and clay content. An alternative is to remove the heavy metals by chemical extraction in order to reach the BOOM standards. A number of different extracting reagents were reviewed. The choice of extracting agent is limited for organic wastes which are to be re-used as compost because the extraction process is not allowed to negatively influence the composting process and the quality of the compost. Inorganic acids and complexants are not a possibility for removal of heavy

metals from biowaste as these extracting agents render the composting process impossible. This negative effect could be reduced by conditioning the remediated waste stream, i.e. washing out the extracting agent from the cleaned waste with water. However, the large amount of wastewater produced by this method means that the costs of this process will be too high. A possible alternative is the use of an organic acid. On the basis of the strength of the extracting agent and the conditions described above, citric acid is a possible extracting agent for the remediation of organic solid wastes. Citric acid is a strong acid and the citrate ion has strong complexing properties. As a result the extraction can be conducted under mild acid pH conditions. Due to these mild extracting conditions and the fact that citric acid is biologically degradable, the remediated waste stream does not need to be conditioned because citric acid is readily degraded during composting. The costs of citric acid usage can be reduced by recycling of the acid. Additionally, the recycling of the extracting agent will reduce the amount of wastewater. Any excess water from the process can easily be treated aerobically or anaerobically. The citric acid extraction has already shown to be successful on laboratory scale for the extractive removal of heavy metals from soils and sewage sludges. Research has indicated that the heavy metals can be removed from the recirculation stream by combination of sulphide precipitation and adsorption to selective ion exchangers.

A integrated process scheme was presented which describes the valorisation of biowaste. The process consists of several linked physical separation units, chemical extraction and biological treatment steps. Using this approach, the biowaste can be turned into three streams: (1) a high quality clean compost, (2) a compost with a high humic substance, lutum and (3) sand. At the moment, the process is not feasible for biowaste as the costs of treatment of biowaste have to remain relatively low. The process can possibly be applied for the treatment of contaminated sewage sludge and polluted soils and sediments. The largest part of the sewage sludge produced in the Netherlands does not meet the BOOM standards and may not be landfilled either since 1996. The only alternative is incineration, an expensive process with several environmental drawbacks. In addition, essential organic matter and nutrients are withdrawn from the cycle by this method. A good alternative for this waste stream can be chemical extraction followed by composting. Also, soils and sediments polluted with heavy metals can possibly be cleaned in this way against nominal costs.

# Samenvatting

De titel van het proefschrift geeft aan dat het onderzoek een breed gebied bestrijkt. Enerzijds wordt gewerkt aan het ontwikkelen van praktisch toepasbare technologieën om het zware metalengehalte in groente-, fruit- en tuinafval (GFT-afval) te reduceren. Anderzijds worden fysisch-chemische modellen ontwikkeld ten einde meer inzicht te verkrijgen in het gedrag van zware metalen in GFT-afval. In deze samenvatting wordt een overzicht gegeven van het onderzoek dat in dit proefschrift is beschreven.

## Hergebruik van GFT-afval als compost

Het Nederlandse beleid met betrekking tot de verwerking van vaste afvalstoffen richt zich op preventie en hergebruik. In het Nationale Milieubeleidsplan wordt hieraan de voorkeur gegeven boven verbranden en storten. Het hergebruik van huishoudelijk afval kan worden bevorderd door het gescheiden inzamelen van o.a. papier, glas en de organische fractie. Het Nederlandse huishoudelijk afval bestaat voor 40-50% uit organisch afval dat na een compostering of vergisting kan worden hergebruikt als compost.

Gebruik van compost is vastgelegd in het "Besluit Kwaliteit en Gebruik van Overige Organische Meststoffen", afgekort als BOOM. BOOM maakt onderdeel uit van het Nederlandse bodembeschermingsbeleid. Dit beleid is erop gericht de accumulatie van zware metalen in de bodem te voorkomen. De BOOM normen zijn vastgesteld op advies van de Technische Commissie Bodembescherming. Er worden in BOOM twee soorten compost onderscheiden, "compost" en "schone-compost". De dosering van compost is aan een maximum gebonden terwijl de toepassing van schone-compost slechts is gebonden aan een maximale fosfaatdosering.

Compost bereid uit huishoudelijk afval en compost bereid uit de mechanisch gescheiden organische fractie van huishoudelijk afval bevatten gehalten aan zware metalen die ver boven de BOOM normen liggen. Daartegenover is het gehalte aan zware metalen in de compost die geproduceerd wordt uit de gescheiden ingezamelde organische fractie van huishoudelijk afval aanzienlijk lager. Daarom is in Nederland gekozen voor het gescheiden inzamelen van de organische fractie van het huisvuil. Op dit moment wordt ongeveer 80% van het totale aanbod aan huishoudelijk afval gescheiden ingezameld. Het blijkt echter dat in sommige gevallen voor meerdere zware metalen het gehalte in compost uit de gescheiden organische fractie van huishoudelijk afval de BOOM normen toch worden overschreden. Dit betekent dat er in Nederland een conflict heerst tussen

twee beleidsstrategieën van de overheid. Enerzijds wordt het hergebruik van huishoudelijk afval gepropageerd door het gescheiden inzamelen van de organische fractie van huisvuil maar anderzijds wordt beoogd de accumulatie van zware metalen in de bodem te voorkomen om het natuurlijke ecosysteem en de volksgezondheid te beschermen.

In dit proefschrift wordt beschreven welke mogelijkheden er zijn om toch te komen tot hergebruik van GFT-afval zonder dat dit leidt tot de verdere accumulatie van zware metalen in de bodem. Verlaging van zware metalen in compost kan op twee manieren worden bereikt. Ten eerste kunnen preventieve maatregelen genomen waarbij de inzamelingscriteria worden veranderd en componenten met een hoog zware metalengehalte in het GFT-afval worden vermeden. Ten tweede kan door het verwijderen van zware metalen uit het GFT-afval door middel van technologisch ingrijpen het gehalte in GFT-compost worden verlaagd. In deze studie wordt de nadruk gelegd op de tweede benadering, het verwijderen van zware metalen uit GFT-afval om de gehalten in compost te verlagen zodat de compost aan de BOOM normen voldoet.

Voor het verwijderen van zware metalen uit GFT-afval komen twee methoden in aanmerking: fysische scheiding en extractieve reiniging. De fysische scheidingstechnologie beoogt de fractie in een afvalstroom die het zwaarst is verontreinigd, selectief uit de totale afvalstroom te verwijderen. Hiervoor worden scheidingstechnieken zoals zeven, sedimentatie, hydrocyclonage en flotatie toegepast. Deze technieken zijn voornamelijk ontwikkeld in de mijnbouw en worden ook toegepast voor het reinigen van bodems en sedimenten. Bij extractieve reiniging worden de zware metalen van de vaste fase naar de waterfase overgebracht. De overdracht wordt bevorderd door het toevoegen van bijvoorbeeld een zuur of complexvormer.

De ontwikkeling van een technologie voor de verwijdering van zware metalen uit vaste afvalstromen wordt bepaald door het intrinsieke karakter van de technologie en de aard van de afvalstroom. Dit betekent dat een technologie niet zonder meer kan worden losgelaten op elk type afvalstroom. Daarnaast moet de verwijderingstechnologie aan een aantal randvoorwaarden voldoen. Ten eerste moet het vereiste verwijderingsrendement voldoende hoog zijn. Ten tweede geldt specifiek voor organische vaste afvalstromen dat de gebruikte verwijderingstechnologie geen nadelige effecten mag hebben op het composteringsproces en de kwaliteit van de compost. Ten derde moet bij de keuze van de verwijderingstechnologie gestreefd worden naar minimalisering van schadelijke emissies naar de omgeving, zoals luchtmissies, vrijkomen van verontreinigd afvalwater en de produktie van verontreinigde vaste reststromen.

### **Bronnen van zware metalen in GFT-afval**

GFT-afval bestaat uit de organische fractie van huishoudelijk afval dat binnenshuis en buitenshuis wordt verzameld. Het binnenshuis ingezamelde huisvuil bestaat voornamelijk uit etensresten, koffiefilters, bloemen, planten, e.d.. Het buitenshuis ingezamelde

GFT-afval is afkomstig uit de tuin en bestaat uit o.a. gras, bladeren, takken en de strooisellaag van de tuin. Eerder onderzoek in Nederland en Duitsland wijst uit dat slechts 20% van het totale aanbod aan GFT-afval binnenshuis wordt ingezameld. In deze onderzoeken is echter niet gekeken naar de samenstelling van het GFT-afval en de bijdrage van de verschillende componenten in GFT-afval aan het totale zware metalengehalte. Daarom is in deze studie de bijdrage van verschillende componenten uit binnenshuis en buitenshuis ingezameld organisch aan het totale zware metalengehalte in GFT-afval onderzocht.

Eerst is de samenstelling van het GFT-afval onderzocht door het afval fysisch te scheiden op basis van deeltjesgrootte en soortelijk gewicht van de verschillende bestanddelen. De scheiding vond plaats door middel van natzeven en waterelutriatie. Alhoewel GFT-afval als een organische afvalstroom wordt aangemerkt bestaat gemiddeld 40% uit minerale bestanddelen, voor het grootste gedeelte zand (34%) en een silt-lutum fractie van ongeveer 6%. De minerale fractie is klein (10%) in binnenshuis GFT-afval maar kan 60-70% bedragen in buitenshuis ingezameld GFT-afval. De minerale bestanddelen worden in het GFT-afval geïntroduceerd doordat bij de inzameling van organisch afval uit de tuin een deel van de strooisellaag wordt meegenomen. Op basis van visuele inspectie en inzicht in de herkomst van de oorspronkelijke componenten in GFT-afval, kan het GFT-afval in de volgende fracties worden ingedeeld:

1. organische fractie >1 mm: organisch materiaal met een intacte celwandstructuur; deze fractie is afkomstig uit de tuin en van binnen, bv. gras, bladeren, takken, groenten, sinaasappelschillen
2. minerale fractie >1 mm: deze fractie bestaat uit minerale verontreinigingen zoals kattebakgrit, glasscherven en steentjes
3. organische fractie tussen 0.05 en 1 mm: sponsachtig, donkerbruin organisch materiaal zonder celwandstructuur; deze fractie is afkomstig uit o.a. potgrond, en de strooisellaag van de tuin
4. minerale fractie tussen 0.05 en 1 mm: deze fractie bestaat uit zand afkomstig uit de strooisellaag van de tuin
5. fractie <0.05 mm: deze fractie bestaat uit silt, klei en humus; de minerale en organische fracties zijn aanwezig in aggregaten en niet van elkaar te scheiden; de fractie is afkomstig van o.a. potgrond en de strooisellaag van de tuin

Het zware metalen gehalte (Cd, Cu, Pb en Zn) in de verschillende fracties van GFT-afval is gemeten en vergeleken met het natuurlijke achtergrondgehalte van de oorspronkelijke bestanddelen in GFT-afval. Hiervoor zijn de natuurlijke achtergrondgehalten aan zware metalen in de oorspronkelijke componenten van GFT-afval door middel van een literatuurstudie vastgesteld. Het gemeten zware metalengehalte in de vijf fracties komt goed overeen met de natuurlijke achtergrondgehalten van de oorspronkelijke componenten. Het zware metalen gehalte in de organische fractie >1 mm komt overeen met het

natuurlijke achtergrondgehalte in plantaardige materiaal, het gehalte in de minerale fractie 0.05-1 mm komt overeen met de gevonden natuurlijke achtergrondgehalten in zandgronden, de gehalten in de organische fractie 0.05-1 mm is te vergelijken met de natuurlijke achtergrondgehalten in de gehumificeerde strooisellaag in bossen en het gehalte in de fractie <0.05 mm komt overeen met het natuurlijke achtergrondgehalte in lutum- en kleihoudende bodems. Deze studie toont dus aan dat het zware metalengehalte in GFT-afval van natuurlijke oorsprong is en niet is verontreinigd met zware metalen vanuit andere bronnen.

### **Beoordeling van compost uit GFT-afval**

Om een indruk te krijgen van het zware metalen gehalte in de compost moet rekening gehouden worden met het feit dat een gedeelte van de organische stof wordt afgebroken tijdens het composteren. Door de afbraak van organisch materiaal worden de zware metalen geconcentreerd en neemt het zware metalengehalte in GFT-compost toe. De afbreekbaarheid van organisch materiaal is afhankelijk van de samenstelling. Organische verbindingen zoals vetten, eiwitten en koolhydraten kunnen gemakkelijk worden afgebroken terwijl lignine en humuszuurverbindingen zeer moeilijk afbreekbaar zijn. De afbraak van cellulose, een verbinding die in principe volledig afbreekbaar is, wordt verhinderd door de inbouw in het lignocellulose complex. Daarom worden de zware metalen sterker geconcentreerd in compost die afkomstig is van GFT-afval uit voedselresten dan in compost van GFT-afval dat verzameld is in de tuin.

Compost uit vers plantaardig materiaal en voedselresten voldoet aan de BOOM normen voor compost maar de normen voor schone-compost worden niet gehaald voor enkele zware metalen. Hierbij is uitgegaan van een organische stof afbraak van 50%. Alhoewel gehumificeerd organisch materiaal, afkomstig van o.a. potgrond en de strooisellaag van de tuin nauwelijks afbreekt tijdens het composteren, worden de BOOM normen voor compost ruim overschreden. Compost uit GFT-afval voldoet niet aan de BOOM normen voor schone-compost. Compost uit GFT-afval voldoet wel aan de BOOM normen voor compost omdat GFT-afval voor ongeveer 30% uit zand bestaat. Zand verdunt het zware metalengehalte in GFT-compost omdat het zware metalengehalte in zand zeer laag is en zand niet afbreekt tijdens composteren. Door het hoge gehalte aan zand heeft de compost echter een laag organisch stofgehalte, een eigenschap die als kwaliteitsverlies van compost moet worden beschouwd.

Het nemen van preventieve maatregelen om de zware metalengehalten in GFT-afval te verlagen biedt geen perspectief omdat hiervoor de inzameling van tuinafval moet worden verboden, de fractie die 80% van GFT-afval uitmaakt. Door deze verandering zou het hergebruik van huishoudelijk afval echter met 30-40% afnemen.

Het is opmerkelijk dat aan het gebruik van compost uit GFT-afval strenge normen gesteld worden met betrekking tot de zware metalengehalten terwijl het gehalte aan



koper en zink in dierlijke meststoffen aanzienlijk hoger zijn. Voor toediening van dierlijke meststoffen aan de bodem wordt echter alleen de fosfaatnorm gehanteerd. Op dit moment wordt in Nederlandse landbouw nog te kwistig gebruikt gemaakt van meststoffen. Een meer evenwichtige, precieze dosering van nutriënten en organische stof kan voorkomen dat nutriënten en zware metalen schadelijke gevolgen hebben voor het milieu terwijl tegelijkertijd toch goede oogstresultaten bereikt kunnen worden. Een duurzaam landbouwbeleid kan alleen tot stand komen als gestreefd wordt naar een sluitende kringloop van mineralen en organische stof. Daarbij wordt aanbevolen om de regelgeving voor het toedienen van meststoffen in één wettelijk kader vast te leggen.

### **Fysisch-chemische fractionering van zware metalen in GFT-afval**

De haalbaarheid van de verwijderingstechnologie, fysische scheiding of extractieve reiniging kan in eerste instantie worden beoordeeld door te bepalen aan welke fracties van het GFT-afval de zware metalen gebonden zijn en hoe sterk de zware metalen aan GFT-afval gebonden zijn. Er is een analytische methode ontwikkeld waarmee de fysisch-chemische vormen van zware metalen in GFT-afval kunnen worden bepaald. Allereerst is GFT-afval gefractioneerd op deeltjesgrootte door een natzeefopstelling. De fracties tussen 0.05 en 1 mm zijn verder gescheiden in een minerale en organische fractie met een wateropstroomkolom. Voor de afzonderlijke minerale en organische deeltjesgrootte fracties is de bindingssterkte bepaald met een sequentieel chemisch extractie (SCE) schema. Met SCE wordt beoogd in opeenvolgende extractiestappen, één bepaalde chemische vorm uit de vaste fase te extraheren met een selectief extractiemiddel. Als basis voor GFT-afval wordt het vijfstaps Tessier SCE schema gebruikt. Er wordt een extra stap ingepast om onderscheid te maken tussen zware metalen die zijn geadsorbeerd aan het organisch materiaal en zware metalen die zijn ingebouwd in het organische materiaal. Een nadere beschouwing van de SCE procedure geeft aan dat de veronderstelde selectiviteit van de extractiestappen niet haalbaar is. De chemie van een natuurlijk systeem (zoals GFT-afval) is te complex om elke metaalvorm in één enkele stap volledig te kunnen extraheren. Het SCE schema geeft wel een goed inzicht in de bindingssterkte van de zware metalen aan de vaste matrix.

De fysische fractionering geeft aan dat de zware metalen voor het grootste gedeelte gebonden zijn aan de fractie  $<0.05$  mm en de organische deeltjes tussen 0.05 en 1 mm. De zware metalenverdeling is een logisch gevolg van de herkomst van de componenten van GFT-afval. Op basis van de fysische fractionering van GFT-afval kan het volgende fysische scheidingsproces worden opgesteld:

1. compostfractie, de organische fractie  $>1$  mm: bijdrage 40-50% op droge-stofbasis; deze fractie kan worden gecomposteerd en voldoet aan de BOOM normen voor compost; door het hoge organische stofgehalte van deze compost is de kwaliteit van de compost aanzienlijk hoger dan van compost uit integraal GFT-afval

2. zandfractie, de minerale fractie tussen 0.05-1 mm: bijdrage 20-30%; deze fractie bestaat uit zand met een zeer laag zware metalengehalte dat direct kan worden hergebruikt in de wegenbouw
3. residufractie, de organische fractie 0.05-1 mm en de fractie <0.05 mm: bijdrage 20-30%; deze fractie vormt een goede bodemverbeteraar door het hoge gehalte aan silt, klei en humus; helaas voldoet de fractie niet aan de BOOM normen

De residufractie voldoet niet aan de BOOM normen maar kan mogelijk na extractieve reiniging als compost worden aangewend. De haalbaarheid van de extractie kan worden beoordeeld aan de hand van het SCE schema. De som van de eerste 4 stappen van het SCE schema geeft de fractie zware metalen weer die potentieel beschikbaar is voor extractie. De rest van de zware metalen is niet beschikbaar voor extractie omdat deze metalen te sterk zijn gebonden aan of opgesloten zijn in de vaste matrix. De resultaten van het SCE schema geven aan dat Cu en Pb sterker gebonden zijn aan GFT-afval dan Cd en Zn. Op basis van de som van de eerste vier extractiestappen is extractieve reiniging mogelijk voor de onderzochte vier zware metalen.

### **Modellering van de zware metaalbinding aan de organische fractie van GFT-afval en de rol van humuszuurverbindingen in de binding van zware metalen**

Om nieuwe technieken voor de extractie van zware metalen uit GFT-afval te kunnen ontwikkelen en om de biobeschikbaarheid en toxiciteit van zware metalen in GFT-compost beter te kunnen voorspellen moet meer inzicht verkregen worden in het fysisch-chemisch gedrag van zware metalen. Het fysisch-chemisch gedrag is direct gerelateerd aan de speciatie van de zware metalen. Met het zogenaamde "chemisch evenwichtsmodel" kan de distributie van de verschillende chemische vormen van een metaalion (= speciatie) in een natuurlijk systeem berekend worden. Zo wordt bijvoorbeeld de toxische werking van zware metaalionen bepaald door de activiteit van het vrije metaalion. De vrije metaalionactiviteit kan echter moeilijk experimenteel bepaald worden maar deze kan wel met een chemisch evenwichtsmodel berekend worden. Ook kan meer inzicht verkregen worden in de werking van een extractiemiddel doordat het evenwichtsmodel inzicht geeft in de competitie van metaalbinding tussen het extractiemiddel en de vaste fase. Het chemisch evenwichtsmodel heeft als belangrijk uitgangspunt dat er thermodynamisch evenwicht geldt in het chemisch systeem.

Het GFT-afval bevat natuurlijke complexvormers zoals kleimineralen, metaalhydroxides, organisch materiaal en humuszuurverbindingen. Er wordt verondersteld dat de aanwezige organische complexvormers, plantaardig materiaal en humuszuurverbindingen, de metaalspeciatie in het totale GFT-afval domineren. Voor goed gedefinieerde systemen is het chemisch evenwichtsmodel redelijk betrouwbaar omdat bekend is welke componenten in het systeem aanwezig zijn en welke reacties kunnen optreden. Het

bindingsgedrag van metalen aan de natuurlijke organische complexvormers is echter moeilijk te beschrijven omdat de samenstelling, chemische structuur, molecuulgrootte, en het aantal en type functionele groepen niet bekend zijn. Hierdoor is het minder duidelijk welke reacties kunnen optreden tussen de metaalionen en de natuurlijke organische complexvormers. Daarnaast kunnen organische complexvormers aanwezig zijn in opgeloste vorm en als vaste fase waardoor deze verbindingen een groot effect hebben op de mobiliteit van zware metalen.

Natuurlijke organische complexvormers zoals humuszuurverbindingen bezitten een veelvoud aan functionele groepen waaraan zware metaalionen kunnen binden. Daarnaast bezitten humuszuurverbindingen onder natuurlijke condities een netto negatieve lading die de adsorptie van zware metalen versterkt. Als gevolg van dit polyfunctionele en polyelectrolytische karakter van de complexvormers is de bindingssterkte van zware metalen afhankelijk van de metaalbezetting, de pH, de ionsterkte en de competitie met andere metaalionen. Deze eigenschappen kunnen worden beschreven met het NICA-Donnan model. Het model is uit twee onderdelen opgebouwd: (1) de binding aan de polyfunctionele complexvormer wordt beschreven door het NICA (Niet-Ideale Competitieve Adsorptie) model en (2) het polyelectrostatische effect van de negatief geladen complexvormer wordt beschreven door het Donnan model. Het model is gevalideerd voor de proton- en koperbinding aan een modelverbinding, de zwakzure ionenwisselaar Sephadex CM-25. Het model geeft een uitstekende beschrijving van de proton- en koperbinding aan Sephadex CM-25. De niet-idealiteit van de lokale adsorptie van metaalionen aan de functionele groepen kan worden toegeschreven aan de hoge ionsterkte in de gelfase.

Om de rol van humuszuur in de koperbinding aan de organische fractie in GFT-afval te bestuderen zijn aan vijf geïsoleerde deeltjesgrootte fracties van GFT-afval tussen 0.05 en 2 mm zuur-base titraties en kopertitraties uitgevoerd en is het humuszuurgehalte van de vijf fracties bepaald. De zuur-base titraties geven aan dat het gehalte aan functionele toeneemt met afnemende deeltjesgrootte. Het gehalte aan functionele groepen kan worden toegeschreven aan de humuszuurfractie in de organische deeltjes. Het carboxylgehalte blijft nagenoeg gelijk met afnemende deeltjesgrootte maar het gehalte aan fenolgroepen neemt toe. De bindingssterkte van koper neemt ook toe met afnemende deeltjesgrootte. De sterkere binding kan echter niet alleen toegeschreven worden aan het hogere functionele groepgehalte van de kleinere organische fracties. Waarschijnlijk is het toenemende gehalte aan fenolgroepen met een sterkere affiniteit voor koper verantwoordelijk voor de sterkere binding.

De zuur-base titraties en koper adsorptie-isothermen aan de organische fractie 0.05-0.1 mm kunnen goed beschreven worden met het ontwikkelde NICA-Donnan model. De bindingseigenschappen van de organische fractie worden hierbij toegeschreven aan de humuszuren in het organisch materiaal. Er is aangenomen dat het humuszuur twee typen

functionele groepen draagt, de carboxyl- en de fenolgroep. De modelberekeningen tonen aan dat het polyelectrostatisch effect voor de geladen organische deeltjes op de zuur-base titraties klein is. Dit wordt tevens bevestigd door de experimenten. Opvallend is echter dat de modelberekeningen aangeven dat de koperadsorptie wel sterk beïnvloed worden door de ionsterkte. Het NICA-Donnan model met twee typen functionele groepen, de carboxyl- en fenolgroepen, blijkt een goede semi-mechanistische benadering om de binding van protonen en koper aan humuszuurverbindingen te beschrijven.

Vergelijking van de gemeten en gemodelleerde koperadsorptie isothermen geeft aan dat gedurende de experimenteel bepaalde adsorptie isothermen niet in evenwicht zijn. Dit blijkt uit het niet-lineair verloop van de experimentele isothermen terwijl de modelberekeningen een lineair verloop voorspellen. De niet-lineariteit neemt toe voor lagere vrije koperactiviteit, optredend bij hogere pH, lagere koperbezettingen en kleinere deeltjesgrootte. Het niet-evenwicht wordt veroorzaakt door de diffusielimitatie van koperionen in de vaste deeltjes. De koper ionen moeten de organische deeltjes binnendringen om de beschikbare adsorptieplaatsen te bezetten. De diffusie van koper ionen in de deeltjes wordt sterk vertraagd door de koperbinding aan de adsorptieplaatsen. Het kan het jaren duren voordat er evenwicht wordt bereikt voor deze experimenten! Dit geeft aan dat het fitten van parameters van adsorptiemodellen met experimenteel bepaalde zuur-base titraties en metaaladsorptie isothermen met grote voorzichtigheid moet worden betracht omdat deze anders tot totaal verkeerde interpretaties kan leiden.

De sterke metaaladsorptie van humuszuurverbindingen kan de mobiliteit van zware metalen in bodemsystemen en stortplaatsen bevorderen als de humuszuurverbindingen oplossen. De gemeten kopertitraties, meting van vrije koperactiviteit met een koperionspecifieke elektrode, geven een maat voor de binding van koper aan de organische deeltjes maar er wordt geen onderscheid gemaakt tussen koper dat gebonden is aan opgeloste humuszuren en koper dat gebonden is aan humuszuren in de vaste fase. Om de relatie tussen opgelost koper en de hoeveelheid opgeloste humuszuren te bepalen wordt aan het einde van elke kopertitratie de totale opgeloste koperconcentratie en het opgeloste humuszuur bepaald. Deze bepalingen zijn uitgevoerd voor de vijf geïsoleerde organische fracties tussen 0.05 en 2 mm tussen pH 4 tot 10. De opgeloste hoeveelheden koper en humuszuur nemen beide toe met toenemende pH en met afnemende deeltjesgrootte van de organische fracties. De hoeveelheid opgelost humuszuur neemt toe voor kleinere deeltjesgrootte omdat de kleinere fracties meer humuszuur bevatten. Zoals mag worden verwacht neemt de opgeloste fractie humuszuur ook toe met stijgende pH. Uit de resultaten blijkt dat de fractie opgelost koper lineair toeneemt met de hoeveelheid opgelost humuszuur. Uit de gegevens kan bovendien worden afgeleid dat het opgeloste humuszuur en het humuszuur in de vaste fase dezelfde bindingssterkte vertonen voor koper. De resultaten geven aan dat humuszuren niet als polymeren met verschillende molecuulgrootte kunnen worden gezien maar dat humuszuren zich meer gedragen

volgens Wershaw's model voor humuszuren. In Wershaw's model worden humuszuur-moleculen beschouwd als aggregaten van amfifiele moleculen die door waterstofbruggen en van der Waalskrachten worden gevormd. Bij hogere pH neemt de electrostatische repulsie toe en worden waterstofbruggen verbroken waardoor de aggregaten uiteenvallen in subaggregaten en uiteindelijk in afzonderlijke moleculen.

### **Modellering van het extractieverloop van zware metalen uit organische vaste deeltjes**

Het nadeel van het chemisch evenwichtsmodel is het feit dat wordt aangenomen dat het systeem in evenwicht is, d.w.z. de chemische reacties vinden instantaan plaats. Bij de extractieve reiniging van zware metalen uit vaste afvalstromen vinden de reacties echter niet instantaan plaats en spelen reactiekinetiek maar vooral diffusieprocessen een belangrijke rol. De kinetiek van het extractieproces is naast het extractierendement een belangrijke factor omdat deze de verblijfstijd en dus de grootte van de extractiereactor bepaald. Er is een mechanistisch model ontwikkeld dat het verloop van de zuurextractie van zware metalen uit vaste organische deeltjes beschrijft. Met het model wordt meer inzicht verkregen in de factoren die een belangrijke rol spelen in het extractieproces. Het model is getoetst aan de experimentele koperextracties uit organische deeltjes van GFT-afval en het extractieverloop van cadmium, koper en zink uit zuiveringslib.

Het model beschouwd de vaste organische deeltjes als een homogene fase waarin de zware metaalionen zijn gebonden aan functionele groepen. Bij de zuurextractie worden de gebonden metaalionen uitgewisseld tegen protonen. Er wordt aangenomen dat de uitwisselingsreactie tussen protonen en metaalionen snel verloopt in vergelijking met de optredende diffusieprocessen. De transportweerstand van bulkvloeistof naar grensvlak van de deeltjes wordt beschreven met het filmlaagmodel, d.w.z. transport vindt plaats via diffusie door een stagnante waterlaag die zich rond de vaste deeltjes bevindt. Het transport in de vaste deeltjes wordt beschreven door diffusie in een stagnante poreuze gelfase. Omdat ionen geladen deeltjes zijn die een elektrische potentiaal creëren tijdens diffusie, kan de diffusie niet beschreven worden door de wet van Fick maar moet de Nernst-Planck diffusievergelijking uit de kast worden gehaald. Deze vergelijking beschrijft de diffusie door een combinatie van een concentratiegradient en een elektrische potentiaalgradiënt. De Nernst-Planck vergelijking geeft aan dat de diffusie van een ion niet alleen bepaald wordt door de concentratiegradient van het desbetreffende ion maar ook door de concentratiegradient van de andere aanwezige kationen en anionen. Het chemische evenwicht in de bulkvloeistof, de filmlaag en in de deeltjes wordt beschreven door het standaard chemisch evenwichtsmodel.

De modelsimulaties van de metaalextractie bij lage pH geven aan dat in de eerste fase van de extractie de metaalionen niet uit de vaste deeltjes worden geëxtraheerd maar de resterende metaalionen uit de vloeistof in de vaste fase worden geadsorbeerd. Ondanks

het feit dat in de eerste fase van de extractie de protonen de deeltjes binnendringen en uitwisselen met metaalionen die gebonden zijn aan de functionele groepen diffunderen de metaalionen niet naar de bulkvloeistof toe maar zetten zich verderop in de deeltjes vast aan de functionele groepen. De drijvende kracht wordt gevormd door een combinatie van de concentratiegradient en de elektrische potentiaalgradiënt. De concentratiegradient overheerst pas op het moment dat de pH van de bulkvloeistof zich volledig heeft ingesteld in de deeltjes. Daarna diffunderen de metaalionen onder invloed van de concentratiegradient naar de bulkvloeistof. Met het model is het metaalextractieverloop bestudeerd als functie van de deeltjesgrootte, pH van de extractievloeistof, type metaalion, type en concentratie van de functionele groep en de grootte van de diffusiecoëfficiënt in de deeltjes.

De koperextractie bij pH 1 is experimenteel bepaald voor drie geïsoleerde organische fracties uit GFT-afval: de organische fracties tussen 0.05-0.1, 0.2-0.5 en 1-2 mm. Het extractieverloop is gevolgd door periodieke meting van de totale koperconcentratie met atomaire absorptie spectrometrie en door continue meting van de vrije koperactiviteit met een koperion-selectieve electrode. Er is geen kwantitatieve interpretatie van de extractie gemaakt omdat de eigenschappen van de organische deeltjes en de extractiecondities slecht gedefinieerd zijn. Kwalitatief bevestigen de experimenten de modelsimulaties. In de eerste fase van de extractie verdwijnt het resterende koper uit de oplossing. Na het bereiken van een minimum koperconcentratie neemt de koperconcentratie in de bulk toe tot na een bepaalde tijd evenwicht wordt bereikt.

De in de literatuur beschreven extracties van Cd, Cu en Zn uit zuiveringsslib vertonen een merkwaardig verloop. In sommige gevallen duurt het een bepaalde periode voor de extractie van start gaat (lagfase) en vertoont de extractiesnelheid meerdere maxima gedurende de extractie. De duur van de lagfase en de extractiesnelheid is afhankelijk van het type metaalion, de vaste stofconcentratie en de pH van de extractie. Dit gedrag kan kwalitatief uitstekend worden verklaard met het ontwikkelde model. Volgens het model neemt de lagfase ook toe met toenemende pH, hogere vaste stofconcentratie, en voor metaalionen die sterker binden aan het slib. Het optreden van twee maxima in de extractiesnelheid kan tevens verklaard worden met het ontwikkelde kinetiekmodel.

### **Praktijkontwerp van technologieën voor de verwijdering van zware metalen uit organische afvalstromen**

Op basis van de verkregen resultaten op labschaal is een praktijkontwerp gemaakt voor de fysische scheiding van GFT-afval in de drie beoogde fracties: de compostfractie, zand en de residufractie. De scheiding wordt uitgevoerd door een reeks van natte scheidingseenheden: natzeefrommel, zeefbogen, hydrocyclonage, flotatie, sedimentatie en decanteercentrifuge. De resultaten van een pilot plant studie bevestigen de experimenten op labschaal. De compostfractie (organische fractie >1 mm) voldoet ruim aan de

BOOM normen voor compost en aan de normen voor schone-compost behalve voor Zn. De zandfractie wordt na scheiding met een hydrocycloon verder ontdaan van organisch materiaal met een flotatie-eenheid. Het organisch stofgehalte in het zand bedraagt minder dan 0.5% en het zware metalengehalte is zeer laag. Het spoelwater in het fysische scheidingsproces wordt grotendeels hergebruikt. Accumulatie van opgelost organisch materiaal in het spoelwater wordt voorkomen door een anaerobe waterzuiveringsstap in te bouwen. Het daarbij geproduceerde biogas kan weer worden omgezet in energie. De residufractie kan niet worden hergebruikt als compost omdat de BOOM normen voor compost worden overschreden. Het grote voordeel van het fysische scheidingsproces is de produktie van GFT-compost met een constante en hoge kwaliteit die onafhankelijk is van de samenstelling van het aangeleverde GFT-afval. De GFT-compost heeft een hoog organisch stofgehalte en voldoet (behalve voor Zn) aan de BOOM normen voor schone-compost.

De residufractie is niet te aan te wenden als compost omdat het niet voldoet aan de BOOM normen. Storten van de residufractie was tot op heden een optie maar sinds 1996 is het storten van vaste afvalstromen met een organisch stofgehalte boven de 5% verboden. Verbranding van de residufractie is een dure optie en verdient niet de voorkeur omdat de residufractie een hoogwaardige bodemverbeteraar vormt door het hoge humuszuur- en kleigehalte. Mogelijk is door middel van extractie van zware metalen de residufractie op te waarderen tot compost. Er zijn daarom verschillende extractiemiddelen onder de loep genomen. Voor organische afvalstromen die als compost hergebruikt moeten worden is de keuze van het extractiemiddel beperkt omdat de extractiestap de compostering en de kwaliteit van de compost niet nadelig mogen beïnvloeden. Anorganische zuren en complexvormers voldoen niet als extractiemiddel voor de verwijdering van zware metalen uit GFT-afval omdat deze extractiemiddelen het composteringproces onmogelijk maken. Dit nadelig effect zou beperkt kunnen worden door de gereinigde vaste afvalstroom te conditioneren, d.w.z. door het uitspoelen van het extractiemiddel uit de gereinigde afvalstroom met water. Hierbij komt echter zoveel verontreinigd afvalwater vrij dat de kosten van het proces te hoog worden. Een mogelijk alternatief is het gebruik van een organisch zuur. Op basis van de sterkte van het extractiemiddel en de hierboven beschreven randvoorwaarden wordt citroenzuur als een mogelijk extractiemiddel gezien om organische vaste afvalstromen te reinigen. Citroenzuur is een sterk zuur en het citraat anion heeft sterke complexerende eigenschappen. Hierdoor kan de extractie worden uitgevoerd onder mild zure pH condities. Door deze milde extractiecondities en het feit dat citroenzuur biologisch afbreekbaar is, hoeft de gereinigde afvalstroom niet geconditioneerd te worden. Het citroenzuur wordt tijdens de compostering gemakkelijk afgebroken. De kosten van het citroenzuurgebruik kunnen sterk gereduceerd worden door het citroenzuur te recyclen. Tevens blijft door hergebruik van de extractievloeistof de hoeveelheid afvalwater beperkt. Eventueel spuiwater uit het extractieproces kan gemakkelijk aerob of anaerob gezuiverd worden.

De citroenzuurextractie is op labschaal reeds succesvol gebleken voor de extractieve reiniging van verontreinigde bodems en zuiveringsslib. Onderzoek heeft ook aangetoond dat de zware metalen uit de recirculatiestroom kunnen worden verwijderd door een combinatie van sulfideprecipitatie en adsorptie aan selectieve ionenwisselaars.

Er is een geïntegreerd processchema gepresenteerd dat de valorisatie van GFT-afval beschrijft. Het proces bestaat uit op elkaar afgestemde fysische scheidingsstappen, extractieve reiniging en biologische zuiveringsprocessen. Met deze aanpak kan GFT-afval worden omgezet in (1) een hoogwaardige schone-compost, (2) een compost met een hoog gehalte aan humus en lutum en (3) zand. Het proces is op dit moment niet haalbaar voor GFT-afval door een combinatie van factoren: er worden nog geen hoge eisen gesteld aan de kwaliteit van GFT-compost en het proces te duur omdat de verwerkingskosten van GFT-afval relatief laag moeten blijven. Het proces is mogelijk geschikt voor de reiniging van zuiveringsslib en verontreinigde bodems en sedimenten. Het overgrote deel van het geproduceerde zuiveringsslib in Nederland voldoet niet aan de BOOM normen en mag sinds 1996 ook niet meer gestort worden. Het enige alternatief is verbranden, een duur proces met meerdere nadelige milieu-effecten. Ook wordt op deze manier waardevolle organische stof en nutriënten aan de kringloop onttrokken. Extractieve reiniging gevolgd door compostering kan voor deze afvalstroom een goed alternatief vormen. Ook kunnen zware metaalverontreinigde bodems en sedimenten mogelijk tegen acceptabele kosten gereinigd worden.



## Curriculum vitae

Adrie Veeken werd op 30 september 1960 geboren in het plaatsje Noordhoek, gelegen in de West-Brabantse klei. Na een lange schoolweg via MAVO, HAVO, Atheneum-B en HBO-B Analytische Chemie leek het hem in 1983 tijd om deze kleine gemeenschap te verlaten en zich naar de grote stad te begeven om Scheikunde te studeren aan de Katholieke Universiteit Nijmegen. Alvorens deze stap te nemen verruilde hij in 1983 het burgerleven voor 12 maanden om bij de Nederlandse Landmacht zijn militaire dienstplicht te vervullen. In 1989 studeerde hij af aan de Katholieke Universiteit na omzwingingen op verschillende Nederlandse universiteiten waarbij hij afstudeervakken afrondde bij de vakgroep Molecuulspectroscopie van de Katholieke Universiteit Nijmegen, de vakgroep Macromoleculaire Chemie en Materiaalkunde aan de Universiteit Twente en de vakgroep Bodemkunde en Plantevoeding aan de Landbouwwuniversiteit Wageningen. Tijdens een verder niet afgerond afstudeervak bij de toenmalige vakgroep Waterzuivering van de Landbouwwuniversiteit Wageningen werd hem een AIO-plaats aangeboden die hij vanaf 1990 tot 1994 innam. De resultaten van deze periode en latere werkzaamheden aan de vakgroep Milieutechnologie zijn neergelegd in dit proefschrift. Vanaf 1994 is hij als wetenschappelijk onderzoeker verbonden aan de vakgroep die sinds 1998 onder de naam sectie Milieutechnologie van het Departement Agro-, Milieu- en Systeemtechnologie door het leven gaat. Zijn voornaamste werk- en onderzoeksgebieden zijn de verwerking van vaste afvalstromen en alles wat met zware metalen te maken heeft.